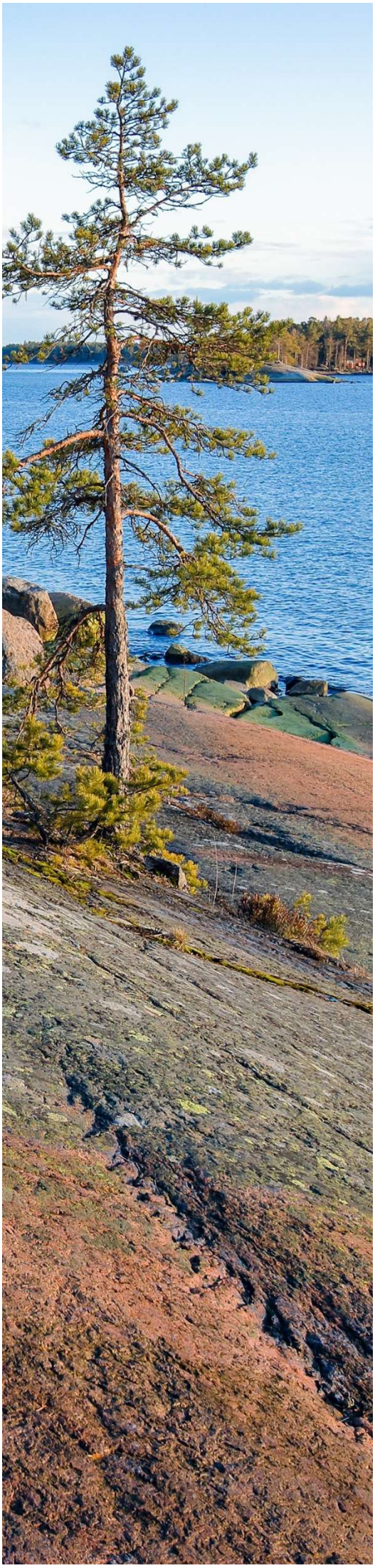

Technical Report

Generic Safety Assessment for the Norwegian National Facility

Authors:

Nuria Marcos (ed.)
Bernt Haverkamp
Niklas Bertrams
Henrik Nordman
Pirjo Hellä
Toivo Wanne

Vantaa, Finland,
November, 2022

Mitta **Engineering Oy**
www.mitta.fi
Business ID FI3268431-2

Project name: Technical Assistance “National Facility”

Report title: Generic Safety Assessment for the Norwegian National Facility

Version: Final, November 30th, 2022

Date: 30.11.2022

Additional information:

Authors: N. Marcos, H. Nordman, P. Hellä, Mitta Engineering Oy B. Haverkamp, N. Bertrams, T. Wanne, BGE TEC	Approved by Timo Saanio, AINS Group	Accepted by the Teemu Laurila, Mitta Engineering Oy
Date 29.11.2022	Date 30.11.2022	Date 30.11.2022
Reviewed by Hellä, P., Mitta Engineering Oy		
Date 29.11.2022		

ABSTRACT

NND is studying several concepts for how to update the Norwegian infrastructure for the management of radioactive waste. One concept consists of combining different types of repositories into a National Facility for the management of radioactive waste. In this concept, the radioactive waste will be disposed of in a single disposal location. The disposal concepts aim at long-term isolation of the nuclear waste from the biosphere. This report focuses on the development of the methodology of a generic safety case and on a preliminary safety assessment for two repositories, one for high level waste and another for low and intermediate level waste.

In this report, the assumed repository concept for spent nuclear fuel is a deep borehole, the maximum depth of which is about 3500 m, the disposal zone being between 3000 m and 3500 m. The repository concept for low and intermediate level waste is a series of chambers at about 100 m depth. The disposal site is assumed to be in crystalline rock and to have a low topography to avoid adverse hydraulic gradients.

In the analyses of both the deep borehole repository for spent nuclear fuel and the intermediate depth repository for the LLW and ILW, the same principles were applied. The engineered barriers were assumed to perform as expected at the time of closure of the repositories. During evolution, these barriers were assumed to fail gradually or suddenly due to various features, events, and processes (FEPs). The resulting scenarios were analysed to evaluate the consequences of barrier failures and of potential radionuclide releases. The analyses used conservative assumptions, models, and data. At the present stage, the site has not yet been selected and the details of the repository designs are yet to be defined. Consequently, many features and processes were implemented in a simplified way. Nonetheless, the developed models allow updating once more advanced technical planning of the disposal concepts, engineered barriers, and site-specific data become available.

The scenarios for deep borehole disposal addressed uncertainties in the timing of failure of the barriers, in the radionuclide transport paths including the occurrence and position of potential fractures in the geosphere, along with uncertainty in the parameter values of sorption, solubility limits and hydraulic conductivity. In addition, impact of the position of the different wastes (metallic uranium and spent nuclear fuel) on the results was considered.

The scenarios for repository for the LLW and ILW addressed the potential consequences of human activity assuming a construction of a well close to the repository. The potential consequences of human intrusion were addressed assuming a drilling event that hits the waste package with the highest activity in the repository.

The radionuclide release and transport models for the deep borehole repository and for the intermediate depth repository were developed and implemented in GoldSim. The doses to human were calculated by applying a dose conversion factor to ingestion from a drinking water well. The results from the analyses of the deep borehole disposal show that the maximum doses remain below the proposed dose limit of 0.1 millisievert per year. The results suggest that deep borehole disposal is a potentially suitable solution for the disposal of the Norwegian HLW. Similarly, the assessed intermediate depth repository would be suitable for the disposal of the expected amounts of LLW and ILW.

For future safety assessments, emphasis should be put on an update of the radionuclide inventory, on the integrity and performance of the engineered barriers, and adaptation of the layout of the repositories to in-situ conditions, when an appropriate site is selected.

Keywords: Norwegian National Facility, long-term safety assessment, deep borehole disposal, LILW repository, HLW, spent nuclear fuel

TABLE OF CONTENTS

ABSTRACT

1 Introduction

1.1 Background

Norwegian Nuclear Decommissioning (NND) is working with the Finnish Mitta Group together with subconsultants AINS Group of Finland, VTT Technical Research Centre of Finland, and BGE Technology GmbH of Germany. The group assists NND with the concept development and technical design for their disposal solutions for radioactive waste in Norway.

Norway's inventory of radioactive waste is characterised by high-level waste from the research reactors in Halden (HBWR) and Kjeller (JEEP I, N0RA, and JEEP II), which have been taken out of operation. In addition, there is and there will be low and intermediate level waste from the planned decommissioning of the research reactors and other nuclear facilities. Norway also has other radioactive waste generated by, e.g., the medical sector and industry.

NND is studying several concepts for how to update the Norwegian infrastructure for the management of radioactive waste. One concept consists of combining different types of repositories into a National Facility for management of radioactive waste. In this, the radioactive waste will be disposed of in a single disposal location. This nuclear waste facility, called Norwegian National Facility, may consist of underground repositories as well as a landfill repository and auxiliary facilities above ground.

The National Facility may contain the following repository types for the different radioactive wastes:

- Intermediate depth repository for very low, low- and intermediate-level waste,
- Deep geological repository (DGR) for high-level waste,
- Deep borehole repository for high-level waste as an alternative to the DGR, and
- Landfill-type repository as an option for non-radioactive decommissioning waste, mainly soil and concrete.

A key element in the development of the disposal programme is a safety case, which demonstrates the safety of the disposal concept, identifies the remaining uncertainties, and provides feedback on the further research and development needed in the following programme steps. A safety case is typically issued for key decision points and licencing steps. There is an internationally widely approved consensus on the elements of the safety case for disposal of radioactive waste (Section 1.2) and safety assessment being part of the safety case (Section 1.3).

This work focuses on the process, methodology, and example of tools to develop a generic post-closure safety assessment that can be applied to future safety assessments by NND. The repositories considered in this work are an intermediate depth repository for low and intermediate level waste (LLW and ILW), and a deep borehole repository for high-level waste (HLW). An illustration of the Norwegian National Facility with surface and underground infrastructure with the option of deep borehole for HLW disposal is shown in Figure 1-1.

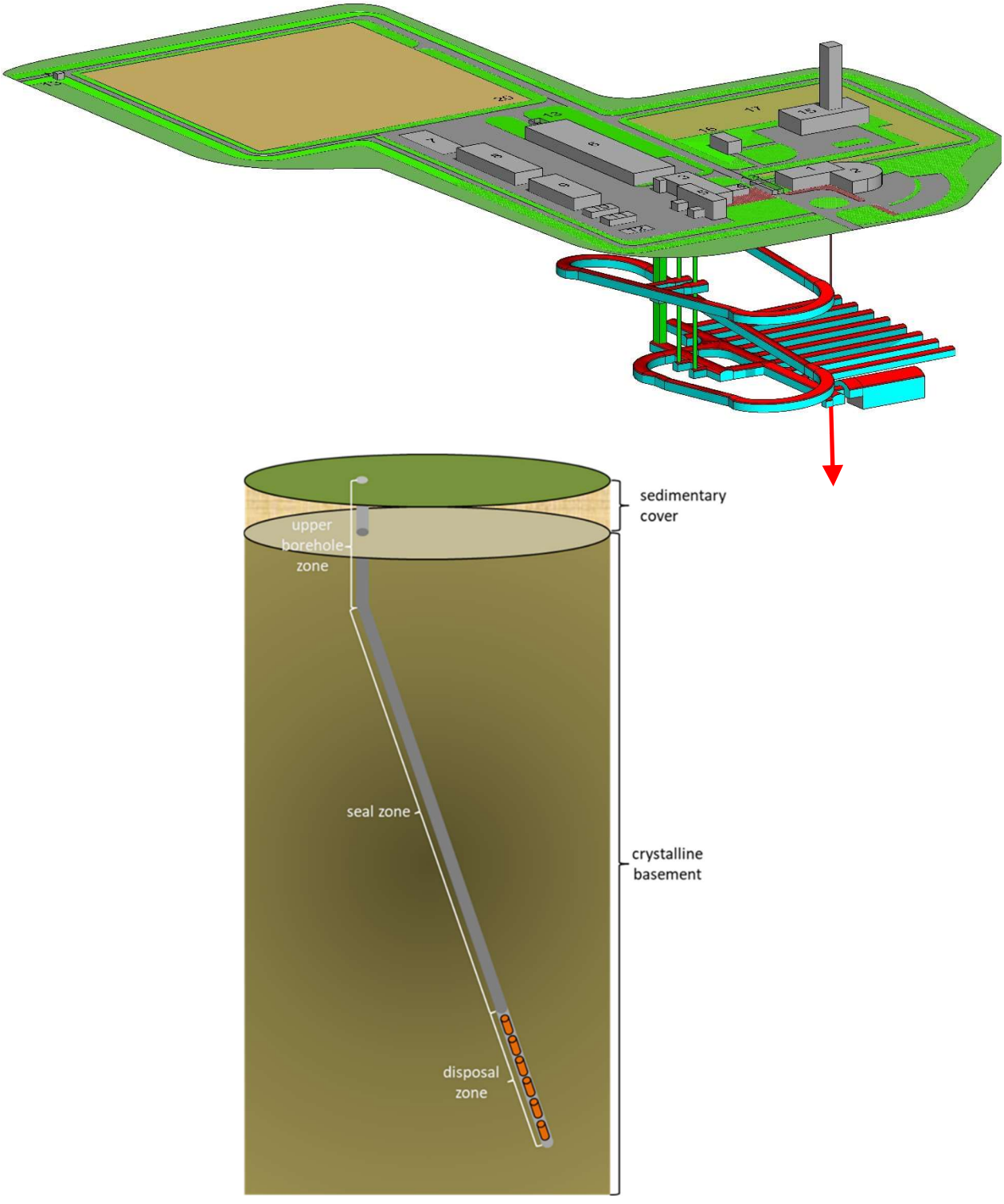

Figure 1-1. Illustration of the Norwegian National Facility (above) with surface and underground infrastructure with the option of deep borehole for HLW disposal. The borehole is the thin black line below building 15, and it continues out of the figure with the red arrow. Below – a schematic view of borehole disposal, based on Fischer et al (2020).

For this work, several assumptions are made due to the pending decisions on the disposal concept and disposal site, and they account for uncertainties in the available data or lack of data. The most important ones are presented below:

- The facility considered in this work is assumed to consist of an intermediate depth repository for low and intermediate level waste at an approximate depth of 100 m and a deep borehole repository for high-level waste where canisters containing the waste are emplaced at a depth between 3000 and 3500 m.
- The intermediate depth repository for LLW and ILW and the HLW repository are assumed to be located at a single site in crystalline rock. However, no interaction between the two repositories is considered. As no site has yet been selected for the facility, generic site properties are assumed.
- The design of the repositories is according to Fischer et al. (2020) and Ikonen et al. (2020).
- The available information on the radioactive wastes in Norway is considered, but assumptions are made on the waste characteristics based on data from similar types of radioactive waste that has been generated and characterised in other countries to arrive at representative radioactive waste inventories.

1.2 Safety case methodology

According to NEA (2004, 2013), a safety case is an integration of arguments and evidence that describe, quantify, and substantiate the long-term safety, and the associated level of confidence, of a geological disposal facility. In a safety case, the results of safety assessment – i.e., the calculated numerical results for safety indicators – are supplemented by a broader range of evidence that gives context to the conclusions or provides complementary safety arguments, either quantitative or qualitative. A safety case is the compilation of underlying evidence, models, designs, and methods that give confidence in the quality of the scientific and institutional processes as well as the resulting information and analyses that support safety. The elements of the safety case are presented in Figure 1-2.

The NEA report on post-closure safety case for geological repositories (NEA 2004) describes the essential elements of a safety case as follows:

- A clear *statement of purpose* provides context for the safety case.
- The *safety strategy* is the high-level approach adopted for achieving safe disposal, including an overall management strategy, a siting and design strategy and an assessment strategy. It incorporates good management and engineering practice and provides sufficient flexibility to cope with new information and technical advances. Strategies favour robustness and minimise uncertainty by selecting a site with assessable features and by tailoring repository design to its geological setting.
- The *assessment strategy* ensures that events and processes relevant to safety are identified and guides how their consequences will be quantified. The *assessment* strategy involves the definition of conceptual models and mathematical approaches to be used to evaluate them and is an integral part of the *assessment basis*.
- The *assessment basis* is the collection of information and analysis tools supporting the safety assessment. This includes an overall description of the disposal system that consists of the chosen repository and its geological setting; the scientific and technical data and understanding relevant to the assessment of safety; and the assessment methods, models, computer codes and databases for analysing system performance. The quality and reliability of a safety assessment depends on the quality and reliability of the assessment basis. The definition of the assessment basis should be tailored to provide the necessary information supporting *evidence, analyses, and arguments for safety.* The description of the process that leads from evidence to a safety evaluation is an important part of the safety case.

- *Evidence, analyses, and arguments for safety* must be compiled into a safety case. Results of analyses are typically compared against safety criteria, often in terms of radiological dose and/or risk, but there may also be other performance measures applied either for regulatory compliance or as indicators of performance that provide insights into system behaviour. The evaluation of these performance measures or indicators, using mathematical analyses (i.e., *safety assessment*) is typically accompanied by more qualitative arguments that provide a context or support for the performance-calculation results. A series or range of appropriate evolution scenario*s may be address*ed for the disposal system. Evaluating system performance under various scenarios may provide an opportunity to optimise the system to increase the robustness of the case for safety. Robustness of the safety case may also be strengthened using multiple lines of evidence, leading to complementary safety arguments, to compensate for any shortcomings in confidence in any single argument.

- The *synthesis* of available evidence, arguments, and analyses, supported by the quality and reliability of the assessment basis, supports a safety case statement of confidence. It should explicitly state that sufficient confidence exists in the safety of the system to justify a positive decision to proceed to the next stage of planning or implementation of a disposal system.

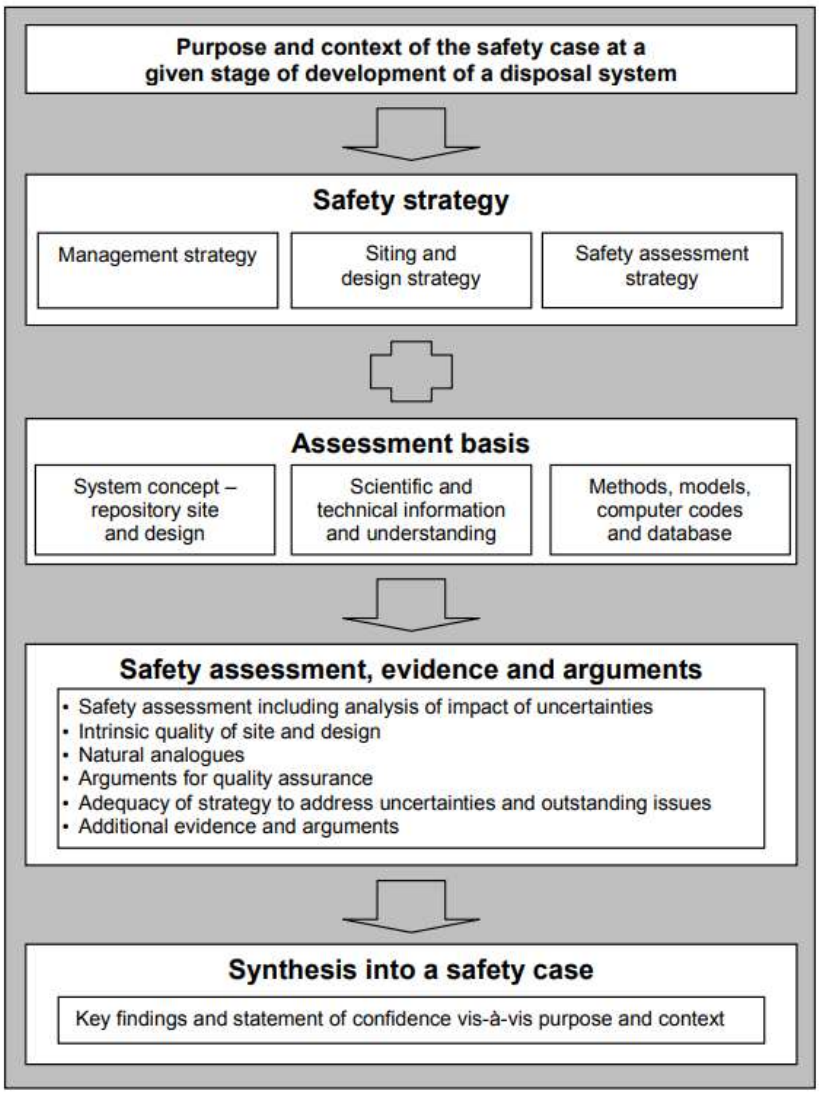

Figure 1-2. Elements of the safety case (NEA 2013, modified from Figure 1 in NEA 2004).

1.3 Safety assessment in the safety case

It can be noted that *safety assessment*, per se, is an "element" of a safety case in Figure 1-2. Its essential role in the safety case means that aspects of safety assessment relate to numerous elements of the safety case. Based on the figure from the 2004 NEA report (Figure 1-2), the safety assessment involves elements of the safety strategy, the assessment basis, and the evidence and arguments for safety.

The safety case methodology, along with the safety case elements can be simplified as presented in Figure 1-3 to highlight the role of the safety assessment in the safety case.

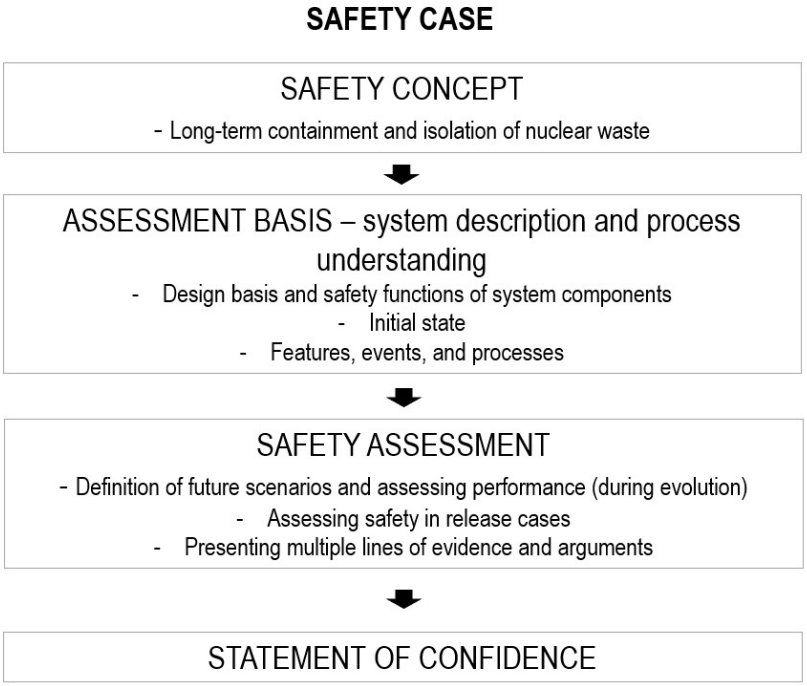

Figure 1-3. Simplified safety case methodology.

A safety assessment considers the performance of a disposal facility in terms of radiological impact or some other measure(s) of impact on safety. Differences may exist from programme to programme concerning the time frame(s) considered relevant, the level of detail, the range of issues considered, and the degree of precision required for input data and in resulting calculations. The purpose of the safety case and the programme development phase often dictate the scope and degree of detail needed in safety assessment.

In addition to the waste type to be disposed of, the time frame over which the safety indicators must be evaluated varies considerably between national regulations and sometimes has to be determined and justified by the proponent. Cut-off times specified in national regulations are derived from the declining radiological toxicity of the waste, from peak radiological consequences (which depend on the chosen host rock), from increasing uncertainty with time, or from the need for adequate coverage of transient or perturbing processes.

The selection of the time frame influences many aspects of safety assessment, including the range of scenarios that might occur and the level of uncertainty that must be accommodated. Furthermore, the time frame under consideration has a significant effect on how the results of safety assessment can be interpreted. In this context, it is important to note this caution in the IAEA/NEA safety requirements (IAEA 2006, Section 2.12):

> "*It is recognized that radiation doses to people in the future can only be estimated and the uncertainties associated with these estimates will increase for times further into the future. Care has to be exercised in applying the criteria for periods beyond the time where the uncertainties become so large that the criteria may no longer serve as a reasonable basis for decision making*".

Given that this is a generic safety case, the time frame selected for well dose constraints is 1,000,000 years for both repositories. For future updates of the safety case, different time frames may be selected for dose and release constraints and for the different repositories.

According to the recommendations of the IAEA (2006), the post-closure safety assessment shall be based on the evaluation of the radiological impact derived from the expected radionuclide inventory to be disposed of in the repositories for the set of selected scenarios.

At this stage of the project, and as noted in Chapter 2, there are no final data on the radioactive waste to be disposed of in the deep borehole disposal (DBD) facility. However, the results of the calculations will give an estimate of the potential radiological impact even if future determinations of the inventory may deviate from the data used here.

Another significant aspect in a safety assessment is to define the range of scenarios and how they will be addressed. The assessment strategy typically establishes conditions that define a base case representing "expected performance," meaning that it addresses a range of conditions and evolutionary lines that are reasonably likely to occur over the time frame of interest. The safety assessment also takes account of disruptive events and scenarios of low probability. Lastly, safety cases include "what-if" scenarios/cases that are considered implausible, but they can provide information regarding, for example, the robustness of the disposal system (see definition of scenarios for this report in Chapters 8 and 9).

Scenarios are commonly used to study different outcomes of the future. Scenarios are applied in various fields like strategic planning in the military and in companies, municipal and land-use planning, in climate changes, just to mention a few examples (e.g., Schweizer & Kurniawan 2016).

In the context of radioactive waste disposal, a scenario is defined as "*A postulated or assumed set of conditions and/or events*" (IAEA, 2018) and used in analysis or assessment to represent possible future evolution of a disposal facility and its surroundings. A scenario may represent the conditions at a single point in time or a single event, or a time history (i.e., evolution) of conditions and/or events (including processes) (IAEA 2018).

1.4 Objectives and methodology of this generic safety assessment

1.4.1 Objectives of this safety assessment

The objective of this generic safety assessment at this stage of the project is to give a first – generally conservative – estimate of the performance of the system to allow a first assessment of the safety of the disposal concept. In addition, the boundary conditions and parameters used in the models aim to identify which of them have the largest impact on the performance of the system and should, therefore, be in the focus of future R&D work for the disposal project.

The model of the disposal facility used to simulate the release of radionuclides assuming different evolutions of the system as well as the associated potential radiological impact has been prepared to achieve these objectives. It is important to keep in mind that, at the present stage, there is uncertainty in the assumptions and data used, which will be reduced when data on a selected site become available. While a high level of uncertainty is generally the case for projects at this stage of planning, it is probably even more so for a deep borehole disposal facility. The uncertainties about hydrogeological and chemical conditions at DBD emplacement depths are particularly high because experience from disposal facility projects at this depth is very limited.

In this case, NND also expressed its wish to use the study to get an overview of the typical steps to be taken during the preparation of a long-term safety assessment and in the development of a respective mathematical model. Accordingly, the mathematical implementation of the disposal concept, the functionality of the different processes describing release of radionuclides and their transport through the model are described in Chapters 8 and 9 in more detail than what is usually expected.

1.4.2 Methodological steps of this safety assessment

The performance assessment methodology followed by the group to analyse the long-term safety of the planned disposal facility for the Norwegian radioactive waste has been based on the international best practices, standards and recommendations described above.

As the concept for the deep borehole disposal is still at a very general level and, so far, no site has been selected, in many aspects, this safety assessment is bound to be limited to simplifications and assumptions, which partly have a high degree of uncertainty. Also, the radionuclide inventory is a preliminary one. The following paragraphs describe the essential steps in conducting the safety assessment.

As the future inventory governs the disposal concepts as well as the layout of the repositories, the estimation of the future inventory based on the available data is the first step for this generic safety assessment. Then, the engineered and natural safety-relevant components (barriers) for the two repositories are identified.

Considering the conceptual layout of the repositories and their barrier systems, safety relevant Features, Events and Processes (FEPs) have been identified, which are also listed for the two repositories. Based on a selection of FEPs, different scenarios were developed to consider the initial state of the repositories as well as future evolutions, specifically regarding potential pathways for release and migration of radionuclides.

For both repositories, one scenario has been selected to represent the normal or expected evolution, and in addition, less likely alternative scenarios have been defined, which are essentially characterised by different transport pathways. At the present state of the project and in the framework of this study, these scenarios have mostly exemplary character and are strongly simplified, but they give a reasonable estimate about the expected potential radiological impact and other consequences.

Analysis of the different scenarios was done by performing deterministic simulations over the assessment period of one million years. In addition to simulations using the reference data set for the different scenarios, also certain calculation cases were defined to address uncertainties in system evolution as well as “what-if” scenarios to illustrate robustness of the repository system. The robustness and general sensitivity of the model towards changed parameters or boundary conditions were further addressed by a comprehensive sensitivity analysis for specific scenarios and parameters.

The compliance of the results with expected regulatory limits was examined. Finally, a general evaluation of the long-term safety was carried out based on the calculated results and the uncertainties that exist in the data and assumptions underlying the assessment at this stage of the project.

1.5 Scope and structure

This report focuses on the development of the methodology of a generic safety assessment and on a preliminary safety assessment. The methodology can be applied in future safety assessments, and current results will serve to provide information on the long-term safety of the currently assumed disposal concept and give feedback on the needs for research and development for the subsequent phases of the Norwegian disposal programme.

The report is structured as follows:

Chapter 1 presents the background and introduction to the safety case and safety assessment and gives the main objectives of the report.

Chapter 2 presents the amounts and characteristics of the nuclear waste to be disposed of.

A schematic presentation of the disposal concepts for high-level waste and for low and intermediate level waste is given in Chapter 3.

A suggestion for the regulatory criteria to be applied is presented in Chapter 4.

Chapter 5 presents the characteristics of a generic site.

Chapter 6 deals with FEPs that affect evolution and radiological consequences.

Chapter 7 presents the evolution of the engineered barrier system (EBS) and host rock along time.

Chapter 8 presents the scenarios and calculation cases, along with conceptual model and modelling results of the safety assessment (i.e., radiological consequences), for DBD. An analysis of the results and discussion on uncertainties is also presented.

Chapter 9 presents the scenarios and calculation cases, along with conceptual model and modelling results of the safety assessment (i.e., radiological consequences), for the LILW disposal concept. An analysis of the results and discussion on uncertainties is also presented.

Chapter 10 presents a summary and conclusions, along with recommendations for future work.

Finally, Appendices I to VI present the data and assumptions used in the safety assessment for the repositories.

2 Nuclear wastes to be disposed of

2.1 Amounts and characteristics of high-level waste (HLW)

The high-level waste considered in this work consists of UO_2 spent nuclear fuel (including instant release fraction (IRF)), metallic uranium (MU), Zircalloy and other metal parts. The types and characteristics of UO_2 spent nuclear fuel and metallic uranium considered in this work are presented in Table 2-1; see also Appendix I.

*Table 2-1. Fuel types and characteristics (Loukusa & Nordman (2020) based on data from Bennett (2020). *: Bennett (2020a), **: calculated based on other values in the table.) HBWR = Halden boiling water reactor.*

Reactor	**JEEP I in Kjeller**	**HBWR in Halden, 1st charge**	**JEEP II in Kjeller**	**HBWR, 2nd to 4th charge / 5th charge**	**HBWR, Booster / +experimental**
Fuel	U metal	U metal	UO_2	UO_2	UO_2 /+ MOX, ThO_2
^{235}U enrichment (%)	0.72	0.72	3.5	≤ 10	≤ 20 / + higher
Cladding material	Al	Al	Al	Zircalloy	Zircalloy / + zirconium
U mass per rod (kg)	19	22	1	0.6–0.9	0.2–0.9
Burn-up (MWd/kg_U)	≤ 1	≤ 0.021	≤ 15	≤ 79.4	≤ 79.4 / + higher
Rod length (m)	2.4	2.8	1.5	~ 1.8 /1.1	≤ 1.1
Rod diameter (mm)	25	40	15	12.25–14.3	6.25 – 9.5 /+ 14.3
Number of rods (ca.)	170	300	1500	700 /4500	2000
Assembly or single rods*	Assembly	Rods	Assembly	Assembly/rods	Rods and assemblies/ + mostly rods
Assembly length (m)	2.8	2.8	1.5	2nd charge: 2.83, 3rd & 4th charge: 3.66, 5th charge 1.1	1.2
Assembly diameter (m)	70	40	90	≤ 70	≤ 70
Number of rods per assembly	2*	1*	11*	7*	
Number of assemblies (-)	85**	300**	136**	100**	
Mass (kg)	3000	7000	1500	3600	1400
Mass per assembly (kg)	35.29	23.3	11.03	4.2–6.3/0.4–0.9	0.2–0.9

2.2 Burnups and cooling time(s) for HLW

As the burnups of the high-level waste are not known with accuracy, the following assumptions on the burnups are used to define the inventory according to Equation 2-1 (see Section 2.3):

- JEEP I: Waste generated is aluminium cladded rods, 3 tonnes of metallic uranium with typical burnup of 0.2-–0.4 MWd/kg according to Bennet & Larsen (2013). 0.3 MWd/kg is a chosen for this work.
- HBWR 1st charge: Waste generated is aluminium cladded rods, 7 tonnes of metallic uranium with burnup of only 0.012 MWd/kgU according to Bennet & Larsen (2013).
- JEEP II: Waste generated is 1.5 tonnes of UO_2 with aluminium cladding and burnup 15 MWd/kgU.
- HBWR 2nd to 5th charge: Waste generated is 3.6 tonnes of UO_2 experimental fuel with zirconium cladding. Burnup is assumed to be 40 MWd/tU.
- HBWR booster/experimental: Waste generated is Zircalloy cladding 1.4 tonnes of UO_2 experimental with zirconium cladding. Burnup is assumed to be 80 MWd/tU.

2.3 Activity inventory for HLW

The activity inventory for the UO_2 fuel and metallic uranium is presented in Table 2-2. This inventory has been arrived at by applying a simplified methodology presented in Appendix I and using the information of the amount and burnups for the different waste types (see Section 2.1 and 2.2).

Inventory of the spent fuel is defined based on a known inventory of a commercial spent fuel, such as those presented by Posiva (Anttila 2005) or SKB (SKB 2010). This data has been used for normal burnup fuel of NND (Appendix I, Table I.2-5). The inventory for lower burnup NND fuel has been estimated from a simple linear extrapolation according to Equation 2-1 below.

$$INV_{NND} = INV_{comm} \cdot BU_{NND} / BU_{comm} \cdot M_{NND} / M_{comm} \qquad \textit{(Equation 2-1)}$$

where

INV_{comm} is activity inventory of commercial fuel (Bq) per a given amount of charged U,
M_NND is the mass of relevant NND fuel and isotopes with burnup of BU_{NND}
M_{comm} is the given amount of charged U (tU or kgU),
BU_{comm} is the burnup of the commercial fuel (MWd/kgU), and
BU_{NND} is the burnup of the NND fuel (MWd/kgU).

Equation 2-1 is not valid for actinides like Pu-239 in low burnup fuel, for their treatment see Appendix I.A2.

The estimation of the inventory is based on a number of assumptions to account for lack of data on the actual waste characteristics. The presented inventory can be considered a reasonable approximation for the purposes of the generic safety assessment presented in this report, e.g., in terms of coverage of the nuclides. However, a more realistic inventory based on the actual characteristics of the radioactive waste in Norway will need to be developed for the licensing purposes during the next steps of the disposal programme.

Table 2-2. Activity inventory for spent nuclear fuel in Bq.

Radionuclide	Name	Metallic uranium*	UO_2	Half-life (years)
Ac-227	Actinium 227	0.00E+00	5.20E+06	2.18E+01
Ag-108m	Silver 108m	2.10E+04	1.70E+07	4.38E+02
Am-241	Americium 241	0.00E+00	6.90E+14	4.33E+02
Am-242m	Americium 242m	0.00E+00	1.00E+12	1.41E+02
Am-243	Americium 243	0.00E+00	1.00E+13	7.36E+03
C-14	Carbon 14	1.80E+09	5.80E+11	5.70E+03
Cl-36	Chlorine 36	2,10E+08	5.80E+10	3.01E+05
Cm-245	Curium 245	0.00E+00	3.50E+11	8.42E+03
Cm-246	Curium 246	0.00E+00	2.30E+11	4.71E+03
Cs-135	Cesium 135	6.70E+08	1.40E+11	2.30E+06
Cs-137	Cesium 137	6.50E+13	1.40E+16	3.00E+01
I-129	Iodine 129	3.10E+07	8.30E+09	1.60E+07
Mo-93	Molybdenum 93	3.00E+01	1.40E+05	4.00E+03
Nb-93m	Niobium 93m	1.80E+09	4.00E+11	1.60E+01
Nb-94	Niobium 94	1.30E+05	5.30E+07	2.03E+04
Ni-59	Nickel 59	5.00E+07	1.10E+10	7.60E+04
Ni-63	Nickel 63	5.10E+09	1.30E+11	1.01E+02
Np-237	Neptunium 237	0.00E+00	8.40E+10	2.14E+06
Pa-231	Protactinium 231	1.90E+05	9.90E+06	3.28E+04
Pb-210	Lead 2010	0.00E+00	2.30E+05	2.22E+01
Pd-107	Palladium 107	5.20E+07	3.60E+10	6.50E+06
Pu-238	Plutonium 238	0.00E+00	8.10E+14	8.80E+01

Radionuclide	Name	Metallic uranium*	UO_2	Half-life (years)
Pu-239	Plutonium 239	1.60E+12	6.80E+13	2.40E+04
Pu-240	Plutonium 240	2.10E+11	1.20E+14	6.56E+03
Pu-241	Plutonium 241	4.30E+12	5.00E+15	1.40E+01
Pu-242	Plutonium 242	0.00E+00	7.30E+11	3.75E+05
Ra-226	Radium 226	0.00E+00	8.10E+05	1.60E+03
Ra-228	Radium 228	0.00E+00	2.90E+01	5.75E+00
Se-79	Selenium 79	8.10E+07	2.00E+10	3.27E+05
Sm-151	Samarium 151	7.70E+11	6.90E+13	9.30E+01
Sn-126	Tin 126	2.50E+08	1.40E+11	2.30E+05
Sr-90	Strontium 90	5.50E+13	9.00E+15	2.90E+01
Tc-99	Technetium 99	1.80E+10	3.70E+12	2.10E+05
Th-228	Thorium 228	0.00E+00	0.00E+00	1.91E+00
Th-229	Thorium 229	0.00E+00	1.20E+05	7.88E+03
Th-230	Thorium 230	0.00E+00	1.10E+08	7.54E+04
Th-232	Thorium 232	0.00E+00	1.20E+02	1.40E+10
U-233	Uranium 233	0.00E+00	1.70E+07	1.59E+05
U-234	Uranium 234	1.20E+11	5.90E+11	2.50E+05
U-235	Uranium 235	5.70E+09	7.60E+09	7.00E+08
U-236	Uranium 236	0.00E+00	6.70E+10	2.30E+07
U-238	Uranium 238	1.20E+11	8.00E+10	4.50E+09
Zr-93	Zirconium 93	2.50E+09	5.10E+11	1.50E+06
All	**Total**	**1.27E+14**	**2.98E+16**	
All	**Total alpha**	**2.05E+12**	**1.70E+15**	

*****As metallic uranium has a very low burnup, it does not contain heavy actinides. Some simplifications are made in the inventory of the metallic uranium, e.g., the Th-230 and Ra-226 inventories should present the same fraction of the total inventory as in UO_2 spent fuel. However, this simplification doesn't affect the modelling results as the vast majority of Th-230 and Ra-226 is produced after tens of thousands of years in the repository as a result of the parent nuclide U-238. The radionuclide decay process is included to Goldsim model. At the time of disposal, in UO_2 spent fuel, Ra-226 inventory is only 8.10E+05 Bq, whereas the inventory of the parent nuclide U-238 is five orders of magnitude higher, 8.00E+10 Bq. In the far future, the Ra-226 inventory will reach the U-238 inventory. The same phenomenon will take place in metallic uranium. Anyway, a better estimate should be produced with more detailed data on reactor operational history and using a reactor physics model.

2.4 Low and intermediate level waste (LLW and ILW)

The low and intermediate level waste considered in this work consists of decommissioning waste of reactors, civil waste (from hospitals and industry – mostly low-level waste included in the total amount of waste around 10,000 tonnes), legacy waste considered to be intermediate level waste (including disused sealed radioactive sources DSRS), operational waste from HBWR and JEEP reactors, contamination of materials and activity in, e.g., ion exchange resins, and reprocessing waste from Himdalen. An estimate on the number of drums of legacy waste is 13 at Kjeller and 166 at KLDRA.

2.5 Activity inventory for ILW/LLW

In a generic safety assessment, as it will follow in the next chapters, the used inventories should be as realistic and credible as possible. Especially, the relation between different isotopes should be as correct as possible. This is an important factor in risk and dose evaluation, as dose potential differs between isotopes. Currently, there is lack of information of the characteristics of the waste. Therefore, the inventory of the ILW and LLW is derived taking into account the existing information on the amount of the waste to be disposed and scaling it based on a known inventory of a similar type of waste. Details of derivation of the inventory is presented in Appendix II.

The LILW inventory used in the present safety assessment for most scenarios in Chapter 9 is presented in Table 2-3; for details, see Appendix II. In addition, there are several waste packages containing, among

others, radium needles (Ra-226) and (un)sealed sources (e.g., Co-60). According to the classification scheme in IAEA (2009, Fig.III-1, Table III-1), these nuclides are classified as ILW for the purpose of dose/release calculations for the human intrusion scenario in Chapter 9. The inventory of these waste packages is presented in Table 2-4.

Table 2-3. Activity inventory for low and intermediate level waste in Bq as derived in Appendix II.

Radionuclide	Name	LLW	ILW	Half-life (years)
H-3*	Tritium	1.50E+06	1.99E+10	1.13E+01
Be-10	Beryllium 10	5.60E+01	4.55E+04	1.50E+06
C-14 org	Carbon 14	8.00E+07	6.50E+10	5.73E+03
C-14 inorg	Carbon 14	1.90E+08	2.06E+11	5.73E+03
C-14 tot	Carbon 14	2.70E+09	2.71E+11	5.73E+03
Cl-36	Chlorine 36	7.20E+04	6.80E+07	3.00E+05
Ca-41	Calcium 41	0.00E+00	7.02E+07	1.00E+05
Fe-55	Iron 55	2.90E+08	2.32E+12	2.73E+00
Ni-59	Nickel 59	3.70E+08	7.22E+11	7.60E+04
Ni-63	Nickel 63	4.60E+10	7.83E+13	1.00E+02
Co-60	Cobalt 60	2.50E+09	6.26E+12	5.27E+00
Se-79	Selenium 79	3.40E+04	4.77E+07	3.27E+05
Sr-90	Strontium 90	3.30E+08	6.12E+11	2.90E+01
Mo-93	Molybdenum 93	1.40E+06	6.16E+08	4.00E+03
Nb-93 m	Niobium 93m	2.20E+07	6.86E10	1.60E+01
Nb-94	Niobium 94	9.20E+05	1.19E+09	2.00E+04
Zr-93	Zirconium 93	3.30E+05	8.67E+07	1.53E+06
Tc-99	Technetium 99	3.50E+07	1.58E+10	2.10E+05
Ru-106	Ruthenium 106	2.20E+02	5.96E+07	1.10E+00
Pd-107	Palladium 107	8.60E+03	1.19E+07	6.50E+06
Ag-108m	Silver 108m	2.90E+07	4.35E+09	4.38E+02
Cd-113m	Cadmium 113m	7.40E+05	1.30E+09	1.41E+01
Sb-125	Antimony125	2.10E+07	8.67E+10	2.73E+00
I-129	Iodine 129	2.20E+04	3.79E+07	1.57E+07
Ba-133	Barium 133	1.20E+05	1.21E+08	1.05E+01
Cs-134	Caesium 134	1.70E+06	3.63E+10	2.06E+00
Cs-135	Caesium 135	1.40E+05	1.95E+08	2.30E+06
Cs-137	Caesium 137	3.40E+09	5.23E+12	3.00E+01
Pm-147	Promethium 147	7.00E+06	7.04E+10	2.62E+00
Sm-151	Samarium 151	1.90E+07	2.67E+10	9.00E+01
Eu-152	Europium 152	7.50E+07	1.81E+09	1.35E+01
Eu-154	Europium 154	5.20E+07	1.03E+11	8.59E+00
Eu-155	Europium 155	5.60E+06	2.28E+10	4.76E+00
Ho-166	Holmium 166	1.20E+06	3.37E+08	1.20E+03
U-232	Uranium 232	4.10E+01	3.18E+04	6.89E+01
U-234	Uranium 234	2.10E+03	1.30E+06	2.54E+05
U-235	Uranium 235	3.00E+07	1.73E+07	7.00E+08
U-236	Uranium 236	6.20E+02	5.26E+05	2.30E+07
U-238	Uranium 238	9.90E+07	2.24E+08	5.50E+09

Radionuclide	Name	LLW	ILW	Half-life (years)
Np-237	Neptunium 237	1.90E+03	5.96E+06	2.14E+06
Pu-238	Plutonium 238	3.30E+06	5.02E+11	8.80E+01
Pu-239	Plutonium 239	9.10E+05	3.14E+10	2.40E+04
Pu-240	Plutonium 240	1.80E+06	1.21E+11	6.56E+03
Pu-241	Plutonium 241	3.40E+07	1.60E+13	1.43E+01
Pu-242	Plutonium 242	6.20E+03	3.34E+08	3.73E+05
Am-241	Americium 241	3.50E+06	1.90E+10	4.32E+02
Am-242m	Americium 242m	1.70E+04	1.14E+07	1.41E+02
Am-243	Americium 243	6.20E+04	4.12E+07	7.37E+03
Cm-243	Curium 243	1.60E+04	1.08E+07	2.90E+01
Cm-244	Curium 244	1.50E+06	3.79E+08	1.81E+01
Cm-245	Curium 245	6.20E+02	3.95E+05	8.50E+03
Cm-246	Curium 246	1.70E+02	1.03E+05	4.73E+03
Total	-	5.30E+10	1.11E+14	-

*HBWR in Halden is a heavy-water reactor so the inventory of H-3 is relatively higher than in light-water reactors, which has been used as a basis for this estimate. Thus, the inventory of H-3 in above table should be re-evaluated for the next safety assessment.

Table 2-4. Inventory of the most important radionuclides in GBq in other waste packages according to IFE (see Appendix IV, Table IV-1 for further information).

Radionuclide	Name	Unit GBq	Half-life (years)
Ra-226	Radium 226	176	1.60E+03
Co-60	Cobalt 60	100	5.27E+00
Ba-133	Barium 133	0.037	1.05E+01
Cs-137	Caesium 137	0.006	3.00E+01
U-234	Uranium 234		2.54E+05
U-238	Uranium 238		5.50E+09
Pu-239	Plutonium 239	9.6	2.40E+04
Am-241	Americium 241		4.32E+02
Cm-244	Curium 244	18.5	1.81E+01

3 Disposal concepts and repository designs

In this chapter, the disposal concepts for the high-level waste repository and for the intermediate-depth repository for the low and intermediate level waste are presented. For both repositories, the disposal concept including the different barriers, the safety concept including the safety functions of the components and key design information relevant for the safety assessment are presented.

3.1 Repository for HLW

The deep borehole disposal concept for Norway has been described in Fischer et al. (2020). In this concept, a deep borehole (of a few kms) is drilled into crystalline rock. The deep borehole is divided into three zones: disposal zone (diameter 775 mm), seal zone (later called sealing zone, diameter 1050 mm) and upper borehole zone (later called backfilling zone, diameter 1350 mm) (see Figure 3-1). In this concept, the radioactive waste is emplaced in canisters. The canisters surrounded by bentonite buffer are installed in the disposal zone. After completion of waste disposal in the disposal zone, the sealing zone and backfilling zone above the disposal zone is sealed and backfilled with a barrier system expected to last long periods. Safety is mostly ensured by the great depth of disposal, which ensures that the waste remains isolated from the surface environment (i.e., accessible biosphere).

For this work, the depth of the borehole was selected to be about 3500 metres, of which the lowest 500 metres are used for disposal of the waste packages (88 canisters according to Wunderlich et al. 2021).

A schematic view of the deep borehole disposal concept is presented in Figure 3-1.

The components of the deep borehole repository are the spent nuclear fuel (SNF, UO_2 SNF and metallic uranium), the engineered barrier system (steel canister, bentonite buffer around the canisters and as a plug between the canister layers, sealing and backfill consisting of one or different materials at different depths) and the host rock around the disposal and sealing zones. According to Hagros et al. (2021), the host rock should provide a rock volume large enough to act as a containment providing rock zone.

At this stage of the concept development, the detailed design, and materials to be used, especially in the sealing and backfilling zone are not yet decided. Therefore, assumptions on the materials and their properties needed for this work are made, that is, bentonite buffer in the disposal zone with bentonite plugs between canister layers, bentonite in the sealing zone and crushed rock in the backfilling zone (see Chapter 8).

According to Hagros et al. (2021), in the deep borehole concept, the main barrier and isolation function is provided by the geological formation and the distance between the environment and the disposal zone. Additionally, the engineered barrier system provided by sealing and backfilling measures is important for the efficiency of the repository. The canisters are used mainly as a tool to safely dispose the waste into the borehole and provide additional secondary safety.

Hagros et al. (2021) define the safety functions and related performance targets for the host rock of a deep borehole repository. Safety functions for the canister are defined by Wunderlich et al. (2021). The safety functions for the other components are not defined in detail. The safety functions for the deep borehole components applied in this work are presented in Table 3-1. For the host rock and canister, they are modified from Hagros et al. (2021) and Wunderlich et al. (2021), respectively, and for the other components they are derived from the safety concept of the deep borehole disposal described above. In line with the scope of this generic safety assessment, the safety functions applied in this work focus on long-term containment of radioactive waste and especially on limiting release and transport of radioactive waste. Table 3-1 also presents the periods during which the respective safety functions are assumed to be fulfilled in the normal evolution scenario of this safety assessment (for further information, see Chapter 8).

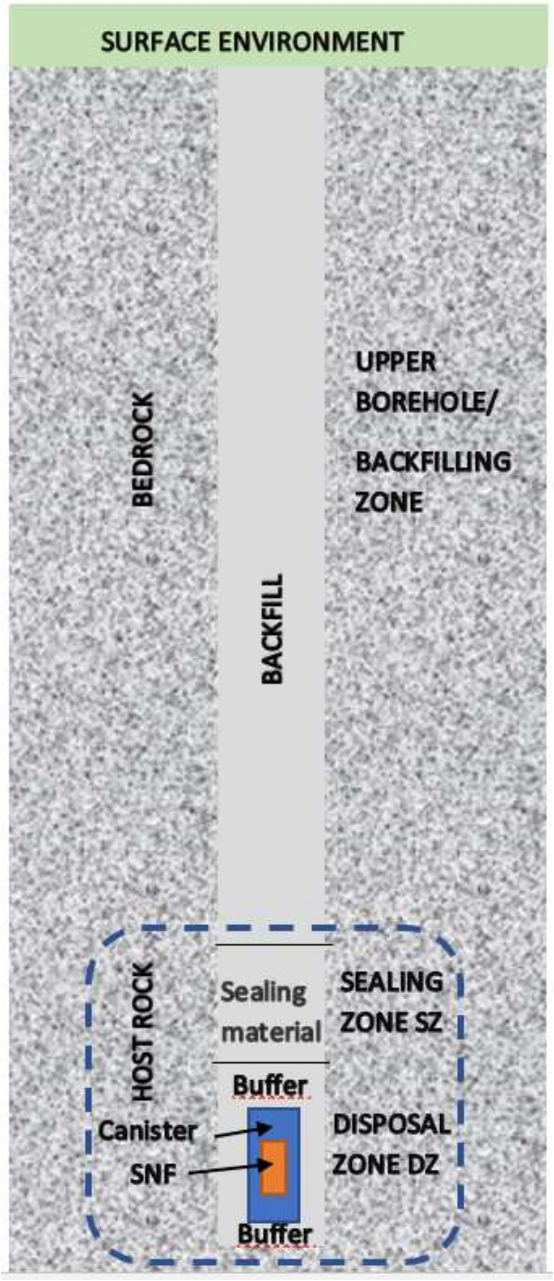

Figure 3-1. Schematic view of the deep borehole disposal concept. Not to scale.

As said above, the host rock is considered as a main barrier of the deep borehole repository. The large distance from the disposal zone to the surface environment delays radionuclide migration. The expected low hydraulic conductivity of the host rock around the disposal zone provides retardation of radionuclide migration by minimizing advective transport. Another important component is the sealing material in the sealing zone, which minimizes flow along the borehole and has large sorption capacity, both leading to strong retardation of radionuclides. Further retardation of radionuclides is provided by sorption in the backfill material in the backfilling zone. A canister is expected to contain the radionuclides for appr. 30,000 years until failure by general corrosion (see Wunderlich et al. 2021; Sections 4.2 and 4.6, where it is assumed that the canister loses its containment when the corrosion depth is 30 mm and the corrosion rate is 1 mm in 1,000 years). Release of radionuclides from the waste occurs according to release rates specific to waste form.

Table 3-1. Deep borehole components and associated safety functions. Safety functions for the host rock defined by Hagros et al. (2021) and for canister by Wunderlich et al. (2021) are presented in italic and complemented by the factors considered in this work. The column "Time scale" presents the time over which the safety functions are expected to be fulfilled (normal evolution scenario). Yellow marked safety functions are not dealt with in this generic safety assessment.

Repository component	Safety function	Time scale
Canister and waste form	*Containment, limiting corrosion:* Minimising access of water to waste	Fulfilled until general corrosion of canisters and degradation of waste form. In the normal evolution scenario, expected canister lifetime is ca. 30,000 years.
	Containment: Minimising diffusion and advection	
	Containment: Retention of radioactive substances inside the waste form	Fulfilled until failure of the canisters due to general corrosion. Release of radionuclides from waste form according to waste form specific degradation (release rate depends on waste type), ca. 99% release for Metallic uranium, after 450 a, Other metal after 4600 a, SNF after 198,000 a, Zircalloy after 106,000 a
	Guaranteeing *sub-criticality*	Assumed to be fulfilled over the whole assessment period.
	Limiting temperature	Assumed to be fulfilled over the whole assessment period.
Bentonite buffer around canisters and between canister layers (in the disposal zone DZ)	Minimising contact of infiltrating water with the waste	Sensitivity and what-if cases address consequences of not fulfilling these safety functions.
	Mechanical stability	
	Retention of radioactive substances inside the repository (sorption) and time needed to travel along the borehole	Over the whole assessment period
	Limiting transport by advection and diffusion	
	Reduction of radionuclide release due to dispersion, filtration of colloids	

Repository component	Safety function	Time scale
Host rock - Depth of disposal zone	*Isolation:* Minimising the likelihood of human intrusion	Over the entire assessment period
	Containment: Large distance to the surface environment, which increases transport times of radionuclides	
	Containment: Minimising potential groundwater flow	
Sealing material (sealing zone SZ)	Minimising potential advective flow through the borehole	Over the entire assessment period (may degrade with time or fail)
	Retention of radioactive substances inside the disposal facility (sorption) and time needed to travel through borehole zone	Over the entire assessment period
	Reduction of radionuclide release due to dispersion, filtration of colloids	
Backfill material (backfilling zone BZ)	Retention of radioactive substances inside the disposal facility (sorption) and reduce the time needed to travel through borehole zone.	Over the entire assessment period
	Reduction of radionuclide release due to dispersion, filtration of colloids	
Host rock/Geosphere	*Containment:* Long groundwater retention times	Over the entire assessment period
	Containment: Low hydraulic conductivity	
	Containment: Low groundwater flow	
	Containment: Low fracture density	
	Containment: Absence of large water-conducting fractures	
	Containment: Low hydraulic gradients	
	Mechanically stable conditions	

3.2 Repository for LLW and ILW

The repository concept for the low and intermediate level waste (LILW) repository has been presented in Ikonen et al. (2020). A schematic representation of a disposal facility with an intermediate depth repository for LILW is presented in Figure 3-2.

The components of the disposal facility are as follows:

- low-level waste – disposed in chamber(s) without any other engineered barriers than the backfill around and on top to waste containers.
- intermediate level waste – disposed in hall/chamber in waste containers, with additional engineered barriers consisting of concrete; backfill can be added to fill the waste chamber to avoid rock fallings. In this work, the backfill is assumed to be crushed rock.
- concrete barriers – structures around the intermediate level waste packages. These are engineered barriers including reinforced-concrete vaults.
- waste chambers: halls excavated in the bedrock hosting the waste packages.
- closure – structures or engineered barriers designed to separate the repository from the surface environment and to provide mechanical support for the overall repository. It may consist of concrete or rock plugs to limit groundwater flow and inadvertent human intrusion and of backfill material for otherwise empty spaces.
- bedrock – bedrock is the natural barrier at the disposal site hosting the repository.
- surface environment – the living environment that may receive radionuclide releases from the repository.

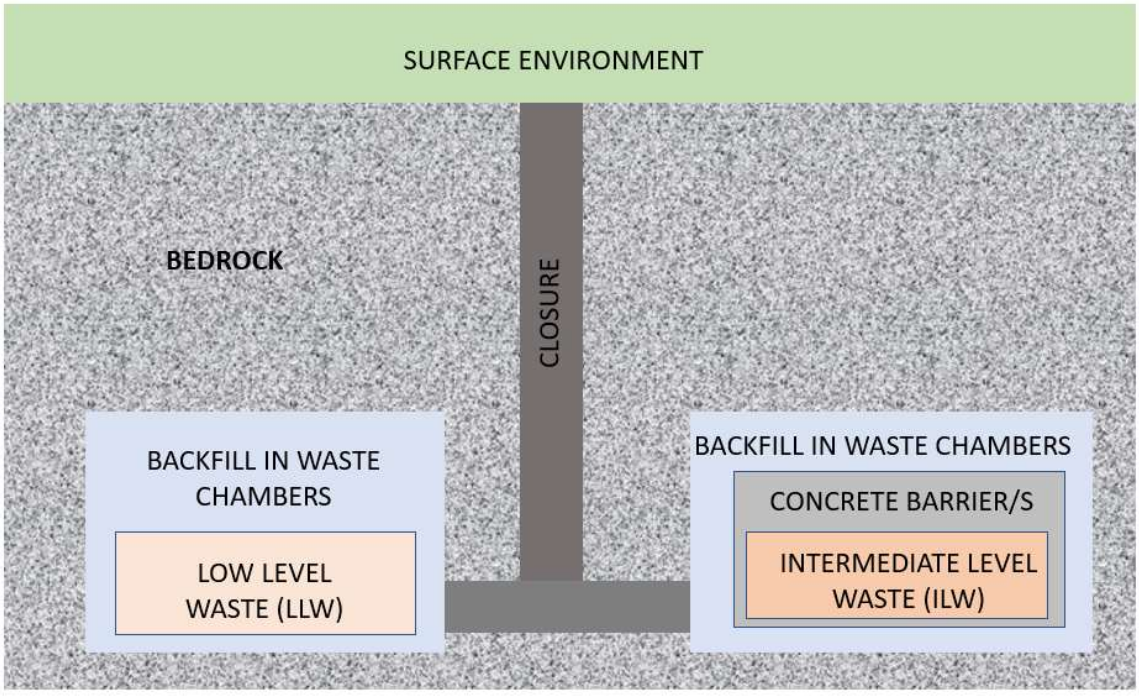

Figure 3-2. Schematic representation of an intermediate depth repository for LLW and ILW (after Nummi 2018 and Ikonen et al. 2020).

At this stage of concept development, the detailed design, and materials to be used other than concrete are not yet decided. Therefore, assumptions on the material and their properties needed for this work are made (see Chapter 9).

Safety functions for the barriers of an intermediate depth repository containing LILW are presented in Ikonen et al. (2020). According to Ikonen et al. (2020), the safety functions are to confine, limit or retard the release and transport of radionuclides, and protect other barriers by supporting them in meeting their safety functions. A more detailed definition of the safety functions and related performance targets for the host rock is presented in Hagros et al. (2021).

The safety functions considered in this work for components of the LILW repository are presented in Table 3-2. For the host rock, they are modified from Hagros et al. (2021) and for the other components from Ikonen et al. (2020). In line with the scope of this generic safety assessment, the safety functions applied in this work focus on long-term containment of radioactive waste and especially on limiting release and transport of radioactive waste. Table 3-2 also presents the periods during which the respective safety functions are assumed to be fulfilled in the reference scenario of this safety assessment (for further information, see Chapter 9).

Table 3-2. LILW repository components and associated safety functions with time. Safety functions for the host rock defined by Hagros et al. (2021) and for other components by Ikonen et al. (2021) are presented in italics and complemented by the factors considered in this work. The column time scale presents the time over which the safety functions are expected to be fulfilled (reference scenario). Yellow marked safety functions are not dealt with or accounted for in this generic safety assessment.

Repository component	Safety function	Time scale
Waste form and container	*Contain waste (ILW only):* Retarding access of water to waste	Fulfilled until failure of the waste container
	Limit and retard release (ILW only): Limiting advection and diffusion	
	Limit and retard release (ILW only): Chemical control – retention of constant chemical properties of the wastes (microbiology).	
	Limit and retard release (ILW only): Retention of radioactive substances inside the waste form/container	Sorption in concrete over safety assessment period
Concrete structure of ILW disposal vault	*Limit groundwater flow:* Minimising contact of infiltrating water with the waste	Over the entire assessment period; general use of degraded concrete parameters
	Limit groundwater flow, limit and retard transport: Limiting advection and diffusion	
	Protect chemically: Limiting penetration of chemical substances and microbes	
	Limit and retard transport: Filtration of colloids	
	Limit and retard transport: Retention of radioactive substances inside the EBS	Over the entire assessment period; general use of degraded concrete parameters
	Protect mechanically: Mechanical stability (e.g., seismic loads)	
	Reduce likelihood of inadvertent human intrusion	
Bedrock (host rock)	*Mechanically stable conditions*	Over the whole assessment period
	Favourable hydrogeological conditions with limited transport of solutes: Minimising radionuclide release and transport along release pathway	Over the whole assessment period
	Chemically favourable and stable conditions	Assumed to be fulfilled over the whole assessment period

4 Regulatory criteria

The requirements table by Hagros et al. (2021b) presents the connection between the regulatory requirements and the design solutions. However, long-term safety is addressed only to a limited extent. In a document by the IAEA (2018), the relevant regulatory criteria set by the Norwegian Radiation and Nuclear Safety Authority (Direktoratet for strålevern og atomsikkerhet, DSA) with respect to long-term safety at the storage facility at Himdalen (KLDRA) are as follows:

- For the most likely scenarios, based on realistic calculations, doses to the most exposed individuals should not exceed 1 μSv per year.
- For other scenarios, a dose of 100 μSv per year to the potentially most exposed individuals should not be exceeded.

The regulatory criteria above are specifically set to KLDRA and seen stricter than those used and recommended internationally (IAEA 2018). Therefore, in this work, the dose criteria applied is based on the regulations on radiation protection Section 6 (Strålevernforskriften FOR-2016-12-15-1659), specifically on the following two criteria:

- *"The effective dose to the public and non-occupationally exposed workers shall not exceed 1 mSv/year for ionising radiation."*
- *"The undertaking shall plan the use of radiation and protective measures to ensure that exposure of the non-occupationally exposed workers and the public, shall not be exposed to an effective dose exceeding 0.25 mSv/year."*

Consequently, the recommended dose criteria to be applied are as follows:

- For the most likely scenarios, based on realistic calculations, doses to the most exposed individuals should not exceed 0.25 mSv per year (note that this limit in the Finnish regulatory criteria is 0.1 mSv per year). Note that in this work 0.1 mSv has been used regardless of the recommendation, because 0.1 mSv is a stricter limit.
- For other scenarios, a dose of 1 mSv per year to the potentially most exposed individuals should not be exceeded.

5 Site

Following the site selection criteria and site selection process (see IAEA, 2011, 2015 and Hagros et al., 2021) the main characteristics of a generic site for a disposal facility are low topography to avoid unfavourable hydraulic gradients and undue erosion rates, crystalline rock, as it is the most abundant to accommodate the repositories given a thorough characterisation of faulting and fracturing and the absence of natural resources. The hydrogeology and hydrogeological features at the site should not form a straightforward path between the repository and the living environment. Hydrogeochemistry should be favourable for the long-term durability of the engineered barriers.

The development of technical site selection criteria and process for a disposal site in Norway has been presented in Saanio et al. (2021a) and the siting strategy and criteria in Saanio et al. (2021b).

The site selection criteria are listed below according to Saanio et al. (2021) first for deep borehole disposal (DBD) and then for the intermediate depth repository (IDR):

- The DBD site should not include significant groundwater resources.
- The disposal zone (DZ) should be possible to locate at a minimum depth of 1500 m below the current ground surface.
- It should be possible to place the DZ so that it does not intersect large fractures or faults that form a potential flow path to the ground surface.
- It should be possible to identify a rock volume large enough to act as a containment providing rock zone (CRZ), including the placement of seals.
- The deep disposal borehole should not be drilled in the Oslo Rift zone.
- The DBD location should be in such groundwater regime that groundwater discharge does not take place through the borehole or in its immediate vicinity.
- The chemical conditions at the depth of the DZ should be favourable for the engineered barriers of the DBD concept.
- The deep borehole should not be located in a region known for high seismic activity. The deep borehole should not intersect faults that could possibly host large movements in a seismic event.
- The rock at the DBD site should have rock mechanical conditions that allow for wellbore stability during construction and disposal. There should be favourable conditions for drilling and operation in the DBD host rock.
- The intermediate depth repository (IDR) site should not contain a significant risk for early permafrost development. Current permafrost areas should be avoided.
- The IDR should be possible to locate in rock mass with an average hydraulic conductivity of less than 10^{-8} m/s. The natural (undisturbed) hydraulic gradient at the disposal site should be 0.01 or less.
- The IDR should be possible to locate so that it does not intersect fractures with a transmissivity of 10^{-7} m^2/s or more. The natural (undisturbed) hydraulic gradient at the disposal site should be 0.01 or less.
- The IDR location should be in such groundwater regime that groundwater discharges does not take place through the repository or in its immediate vicinity.
- The groundwater in the IDR host rock should have reducing conditions in natural (undisturbed) conditions. The IDR should be possible to construct without intersecting a transmissive fracture zone that could transport oxygen-rich water into the repository.
- The groundwater in the IDR host rock should have the following ranges of composition in natural (undisturbed) conditions: pH > 5.5, SO_4^{2-} < 600 mg/L, free CO_2 < 30 mg/L, NH^{4+} < 30 mg/L, Mg^{2+} < 300 mg/L and Cl^- < 1000 mg/L, unless the unfavourable composition can be compensated for by the design of the engineered barriers.
- The construction and operation should be possible without using materials that would have a long-term effect on the groundwater composition so that the required composition could not be reached.

Even if all the criteria are fulfilled, for the purpose of a generic safety assessment and to demonstrate the robustness of the disposal system, it can be, and it is, assumed that one criterion or more than one is not fulfilled. Some assumptions can be scientifically backed up but not all of them. The ones that cannot be scientifically backed up are mostly used in what-if cases.

6 Features, events, and processes (FEPs)

FEPs have a dual service in the safety case, some of them being used to describe/assess the behaviour/performance of the system along time (i.e., performance assessment), but FEPs are also used to define and select the scenarios to be analysed in the safety assessment for radionuclide transport and dose assessment calculations (i.e., safety assessment; see Sections 8.1 and 8.2 for deep borehole disposal and Section 9.1 and 9.2 for LILW disposal). As an example of this dualism, the FEP groundwater flow serves for both.

Potentially relevant FEPs for deep borehole disposal, as well as for LILW disposal at intermediate depth, have been screened in from the general FEP list for Posiva's disposal facility at Olkiluoto (including a KBS-3V type repository for spent nuclear fuel and a LILW repository) reported in Hjerpe et al. (2021). Regardless of the differences between the design of a KBS-3V disposal facility located at a depth of less than 500 m and of deep borehole disposal (DBD), the FEPs related to HLW disposal are adopted as a reasonable starting point for the current generic safety assessment.

The adopted FEPs are listed in Tables 6-1 for DBD disposal and 6-2 for LILW disposal. They are assigned to the respective components of the disposal system. The processes that are accounted for in the safety assessment calculations are in bold.

Table 6-1. FEPs associated to deep borehole disposal. In bold, the processes that are accounted for in the safety assessment calculations.

Deep borehole disposal components				
HLW (UO_2, metallic U)	**CANISTER**	**BUFFER/SEALING (bentonite)**	**BACKFILL (crushed rock)**	**GEOSPHERE**
Alteration	Advection	**Advection**	**Advection**	Alteration
Aqueous solubility and speciation	Aqueous solubility and speciation	Alteration	Alteration	Aqueous solubility and speciation
Criticality	Colloid transport	**Aqueous solubility and speciation**	**Aqueous solubility and speciation**	Colloid transport
Deformation	Deformation	Colloid transport	Colloid transport	Deformation
Diffusion	**Diffusion**	Deformation	Deformation	Diffusion
Heat generation	Gas generation	Desiccation	**Diffusion**	**Dispersion**
Heat transfer	Heat transfer	**Diffusion**	Erosion	Erosion
Metal corrosion	**Metal corrosion**	Erosion	Freezing and thawing	Freezing and thawing
Microbial activity	Microbial activity	Freezing and thawing	Gas generation	Gas generation
Precipitation and co-precipitation	Precipitation and co-precipitation	Gas transport	Gas transport	Gas transport
Radioactive decay (and in-growth)	Radiation attenuation	Heat transfer	Heat transfer	**Groundwater flow**
	Radioactive decay (and in-growth)	Microbial activity	Microbial activity	Heat transfer
	Radiolysis	Precipitation and co-precipitation	Precipitation and co-precipitation	**Matrix diffusion**
	Sorption	**Radioactive decay (and in-growth)**	**Radioactive decay (and in-growth)**	Microbial activity
	Stress redistribution	Radiolysis	**Sorption**	Precipitation and co-precipitation
	Thermal expansion	**Sorption**	Water exchange	**Radioactive decay (and in-growth)**
		Water exchange		**Reactivation-displacement**
		Water uptake and swelling		**Rock damage**
				Sorption
				Stress redistribution
				Thermal expansion
				Water exchange
				Water-rock interaction
				Well

Table 6-2. FEPs associated to LILW disposal. In bold, the processes that are accounted for in the safety assessment calculations.

LILW repository system components				
Concrete basin(s)	**Chamber backfill**	**Geosphere (LILW repository host rock)**	**LILW (and containers)**	**Closure/Infrastructure**
Advection	**Advection**	Aqueous solubility and speciation	**Advection**	**Advection**
Aqueous solubility and speciation	Alteration	**Diffusion**	Aqueous solubility and speciation	Aqueous solubility and speciation
Deformation	Aqueous solubility and speciation	Dispersion	Deformation	Deformation
Degradation	Deformation	Drillhole	**Degradation**	**Degradation**
Desiccation	Degradation	Land uplift and depression	**Diffusion**	Desiccation
Diffusion	**Diffusion**	**Groundwater flow**	Freezing and thawing	**Diffusion**
Freezing and thawing	Freezing and thawing	Microbial activity	Gas generation	Freezing and thawing
Gas generation	Microbial activity	Precipitation and co-precipitation	Gas transport	Gas generation
Gas transport	Precipitation and co-precipitation	Reactivation-displacement	**Metal corrosion**	Gas transport
Metal corrosion	Sorption	Rock damage	Microbial activity	Metal corrosion
Microbial activity		Rock-water interaction	Precipitation and co-precipitation	Microbial activity
Precipitation and co-precipitation		Sorption	Sorption	Precipitation and co-precipitation
Radiation attenuation		Stress redistribution		Radiation attenuation
Sorption		Water exchange		Sorption
		Well		

7 Evolution of the EBS and host rock

The evolution of canister/casks, buffer, sealing (bentonite) and backfill (crushed rock) depend on the initial conditions of the components and on the evolving hydrogeological and hydrogeochemical conditions. The small amounts of HLW are not likely to make heat generation a process to be considered, not even in the early evolution, though better knowledge on the burnup of the waste would be needed to assert this claim. HLW and LILW will evolve according to radioactive decay (and in-growth) and will further depend on the evolving conditions in the engineered barriers and the host rock.

It must be noted that the potential consequence of a seismic event is not dealt with in detail in this report, as that would require either a detailed hydrogeological or hydrogeochemical evolution. It is assumed that canister and the LLW and ILW waste package failures occur either due to corrosion, degradation, or as the consequence of a seismic event. The selection of parameters values for calculation cases in the subsequent chapters cover these possibilities.

The evolution of hydrogeology and hydrogeochemistry depends on climate evolution (factors like precipitation, temperature, evapotranspiration, etc., will affect the amount of rainwater able to infiltrate in the bedrock). At depth groundwater flow and transport depend mostly on the configuration of water-conducting fractures in the geosphere, on groundwater chemistry, and to some extent on heat transfer. Groundwater flow rates around the repository or repositories also depend on the depth of disposal.

Assumptions on the characteristics of potential release pathways for DBD and for LILW disposal are detailed in Chapters 8 and 9.

Though for this work the impact of climate evolution is not assessed as such, the parameter values, especially for groundwater flow, are selected to address a level of conservatism to demonstrate the robustness of the system. Selecting parameter values outside of the expected or of what could be plausible cover uncertainties in the extent of the FEPs that will act during the evolution of the disposal site and disposal system.

7.1 The evolution of DBD

After closure of the disposal facility, which is assumed to be constructed as planned and the waste and barriers also emplaced with no fails, it is expected that the clay component at the disposal and sealing zones will saturate through water uptake and swelling, thus providing a tight barrier for potential release of radionuclides and for the entrance of corrosive substances to the canister. The crushed rock in the backfilling zone is also assumed to limit groundwater flow upward and downward the borehole.

For the purposes of the present safety assessment for DBD, and according to assumed corrosion rates, canisters will fail after the closure of the deep borehole making able the release of radionuclides. Assumed transport paths to the biosphere (drinking well) are through the EBS (buffer and seals) or through the excavation damaged zone (EDZ) upwards. Also, an undetected feature (a water-conducting fracture) crossing the borehole could be assumed as a transport path, though such a fracture is highly likely to be detected during site investigations.

Several lines of evolution can be defined. The so-called normal evolution (see scenario Sc-1 in Ch. 8) is developed assuming that the external FEPs are constant (note that climate evolution is not constant but influences groundwater flow rates, the changes accounted for in most of the alternative evolutions/scenarios; see below), construction, operation, and closure of the facility has been implemented according to plan and no disturbing events take place during post-closure.

In the normal evolution scenario, it is expected that metallic uranium (MU), uranium dioxide (UO_2/SNF) other metal (OM) and zircalloy (ZA) will degrade according to certain fractional release rates defined for the different wastes. For certain radionuclides from the UO_2 inventory an initially released fraction (instant release fraction, IRF) has been defined (see Ch.8).

The canisters containing the waste will corrode with time. Once general corrosion of the canister walls has reduced their thickness below a certain value, the walls will fail. From that failure the void volume of the canister is assumed to be filled with water. The released radionuclides will be dissolved in the water

accounting for the specific solubility limits for the different radionuclides. Transport of radionuclides from the interior of the canisters into the surrounding bentonite buffer is assumed to take place by diffusive transport only. Upon failure of the canister, diffusion is assumed to take place across the full original surface area of the canister.

Essentially during the normal evolution (see scenario Sc-1 in Ch. 8) it is assumed that radionuclide transport is limited to diffusive transport through the borehole itself and the surrounding EDZ for the whole post-closure period.

In the DZ of the borehole, in the near-field zone around a disposal canister, in addition to the diffusive transport between canister interior and buffer volume the following diffusive flows are considered:

- horizontally between the buffer volume enclosing the canisters and the surrounding EDZ of the borehole sequence containing the canister,
- vertically between the buffer volume surrounding the canister and the buffer volumes enclosing the canisters emplaced above and below, and
- vertically between the EDZ and the respective EDZs of the borehole area above and below.

In the SZ, diffusive transport is considered

- horizontally between the sealed part of the borehole and the surrounding EDZ,
- vertically along the sealed borehole, and
- vertically along the borehole but within the EDZ volume.

In the BZ, diffusive transport is considered as for the SZ

- horizontally between the sealed part of the borehole and the surrounding EDZ,
- vertically along the sealed borehole, and
- vertically along the borehole but within the EDZ volume.

At its uppermost part, the borehole is assumed to be intersected by an aquifer, so that radionuclides that have been transported to the top of the borehole will be transported by advection into the aquifer, from which a drinking water well draws its water.

The radiological impact from the release of radionuclides from the deep borehole repository is estimated by calculating the annual dose rate that result from a simple drinking water scenario that assumes a person drinking 3 litres of contaminated water per day (see Ch. 8).

As seen in Table 3-1, the fulfilment of the safety functions defined for the repository components vary in time.

Alternative lines of evolution considering advection, the occurrence of undetected fractures/fracture systems at different depths, etc., leading to alternative scenarios are dealt with in detail in Chapter 8.

7.2 The evolution of the LILW repository

If the location of the repository is selected in a relatively unfractured bedrock, it will take time before the chambers are filled with groundwater. After that, it is assumed that the waste packages containing the LLW will slowly degrade, and the radionuclides will be first released to the chamber and then to the surrounding environment. The concrete vaults will degrade with time after the chamber(s) are filled with groundwater before the waste emplaced degrades and releases start.

For the current safety assessment of the LILW repository, releases from the LLW are assumed to start soon after closure, whereas release from the ILW will be delayed by the concrete in the concrete vault, which is assumed to perform as expected or to be degraded due to desiccation of the cement/concrete or corrosion

of the reinforcement bars and present fissures/fractures undetected by inspection during post-construction verification.

The evolution of the concrete vault(s) containing the ILW will depend on its initial conditions at the time of closure and on the hydrogeological and hydrogeochemical evolving conditions affecting also the backfill surrounding the concrete. The evolution of the waste will further depend on the evolving conditions in the waste packages and the concrete vaults.

If the engineered barriers perform as expected, then transport through them is assumed to be diffusive, but if not, then transport is assumed to be advective.

The line of evolution selected as the reference scenario in Chapter 9 is a credible one, but not necessarily expected or normal. It is based on a relatively credible assemblage of assumptions and simplifications to illustrate the safety assessment methodology.

For the biosphere/surface environment the existence of a well, used to draw drinking water, is assumed. In Chapter 9, it is called the “drinking water scenario”, where the radiological exposure is limited to the ingestion of 3 litres of contaminated water per day.

The safety functions of the repository components shown in Table 3-2 are assigned the periods during which they are fulfilled in the reference scenario.

A simplified and conservative approach has been used to model the reference scenario (Chapter 9). For this purpose, a simplified conceptual model has been chosen as well as mathematical models describing the migration of radionuclides from the waste to drinking well to finally calculate the potential radiological impact to the critical individual.

Variations in the parameter values used in analysing the reference scenario are used in sensitivity analysis (Ch. 9). Alternative lines of evolution consider the possibility of human activities in form of a well drilled near to the shaft area. Human intrusion assumes a drilling event and hitting one of the special waste packages having the highest activity (see inventory in Table 2-4 and Section 2.5).

8 Long-term safety – Modelling and calculations for DBD

A generic safety assessment for a disposal project that is at a very early stage of technical development, follows to a large extent a top-down approach focussing on the integration and coupling of all system components. The controlling processes are typically initially represented by approximate high-level (i.e., less detailed or “abstracted”) models and parameters. Input parameters and boundary conditions are usually taken either from other safety assessments or represent educated guesses and assumptions.

During subsequent development of the project, the model can be developed by adding detail (and reducing uncertainty) for specific components, as more is learned about the system. With time, more details are added to the total system model and the degree of reliance on expert judgment will be reduced.

8.1 Scenario development and definition of calculation cases

As described above in Section 3.1, the deep borehole repository will consist of a multi-barrier system designed to isolate and confine the HLW from the environment in a safe manner. To demonstrate long-term safety and the robustness of the facility to contain and limit radionuclide releases to the environment, a set of scenarios are defined, bearing in mind that this is a post-closure safety assessment, that is, no operation is any longer in force.

8.1.1 Identification of safety relevant post-closure scenarios

The identification of scenarios is performed by considering the Features, Events and Processes (FEPs) derived from the characteristics of the disposal system, including FEPs external to the system (see Chapter 6).

The identified scenarios are all release scenarios that assume failure of the containment of radionuclides in the canisters due to corrosion or another unspecified reason. The main differences are in the assumed time and extent of canister failure.

Scenarios related to human intrusion have not been depicted and not addressed. Due to the large depth of the disposal zone and the small footprint, inadvertent human intrusion is highly unlikely.

First radionuclides will be released from their waste form and the canisters inside the disposal zone. Once the radionuclides have migrated into the near field surrounding the canisters, essentially two main pathways for further transport through the far field exist. Released radionuclides could be transported towards the surface either along the borehole and/or its surrounding EDZ or through fractures in the fracture network in the surrounding host rock.

As further pathway to the biosphere, it is assumed that all contaminated flow from the borehole will enter either directly or via some fracture network an aquifer near to the surface, where a drinking water well is assumed to exist.

Based on the discussion above, the following potential transport pathways for radionuclides are considered in definition of the scenarios:

- Transport along the borehole and/or its surrounding EDZ, and
- Transport through a fracture or fracture network.

Transport along the borehole and/or its surrounding EDZ

Transport along the borehole or the EDZ can take place as advective transport or as diffusive transport. Diffusive transport takes place as long as there is fluid as transport medium and a difference in radionuclide concentration.

Radionuclide transport from inside the canisters to the near field (i.e., bentonite surrounding the canisters and EDZ) has been modelled exclusively as diffusive transport, which is well suited to model the release from the canister. Compared to the release from the canister, diffusive transport through the sealing zone or the crystalline rock from the disposal zone towards the surface is a very slow process, because diffusive areas are smaller and radionuclide concentrations are low. Under reasonable assumptions concerning the parameters of the host rock or the material inside the borehole, most radionuclides will not reach the surface. Some authors therefore exclude diffusion in crystalline rock and in the sealing zone as a significant process for radionuclide transport in safety assessment analyses for DBD (Brady et al. 2009).

In contrast to diffusive transport, advective transport will take place only if there is some physical driving force. For most theoretical scenarios, advective transport would be either:

- Thermally driven, or
- Driven by a hydraulic gradient.

Thermally driven advective transport through a borehole would most probably be caused by thermal energy from heat-generating waste. Freeze et al. (2013) refer to hydrological modelling of a generic set of nine 5000 m boreholes. Each borehole was assumed to contain 400 commercial used fuel assemblies for pressurized water reactors (ca. 150 tonnes of uranium) in a 2000 m long disposal zone in crystalline rock. Using expected permeability values of 10^{-19} m² for the undisturbed host rock and 10^{-16} m² for the borehole including EDZ, the model resulted in an upward flow through the borehole and EDZ of ca. 50 L/a for the first 100 years decreasing towards 0.1 L/a at 10,000 years and to 0.001 L/a at 1,000,000 years.

For the NND nuclear waste conditions, significant thermally induced vertical flow seems to be very unlikely considering the small amounts of heat-generating waste. In addition, even if the thermal energy for the NND waste was to lead to a certain upward flow, at the end of the expected lifetime of the canisters of ca. 30,000 years (see Section 8.2.4 and Wunderlich et al. 2021; Sections 4.2 and 4.6), thermally induced flow would not occur, because heat generation would have declined to insignificant rates by then.

Alternatively, hydrological conditions could lead to a hydraulic gradient between the disposal zone and the surface, which would be a driver for vertical transport. The order of magnitude of such flow will depend on the:

- Potential hydraulic gradient,
- Quality of sealing, and
- Density stratification of saline fluids

Figure 8-1 visualizes a groundwater flow concept that could lead to hydraulic gradients in a crystalline host rock. The example was given in relation to potential groundwater flow at the location of a geological disposal facility in a depth of several hundred metres, but a similar situation could also be present at the disposal depth of a deep borehole repository.

Advective transport for deep disposal boreholes driven by a hydraulic gradient has been considered by Freeze et al. (2013) as unlikely, because the order of magnitude of such vertical flow would depend on the hydraulic gradient, the quality of sealing, and density stratification of saline fluids. According to them, it is expected that the probability of existing significant hydraulic gradients in the disposal zone is very low, being demonstrated by the usually long residence times of deep groundwater in crystalline rock below 3000 m depth and their low flow rates. They further expect that geological characterization during site selection will exclude any site, where such conditions are probable. Therefore, they exclusively consider thermally driven transport for their DBD model.

Based on the usually long residence times of deep groundwater and low flow rates in crystalline rock below 3000 m depth, the existence of significant hydraulic gradients in the disposal zone does not seem likely. Freeze et al. (2013) consider thermally driven transport exclusively, because of density stratification of saline fluids and the great disposal depth.

For the Norwegian case, significant thermally driven transport seems very unlikely due to the small amount of heat generating waste compared with the model calculations referred to by Freeze et al. (2013).

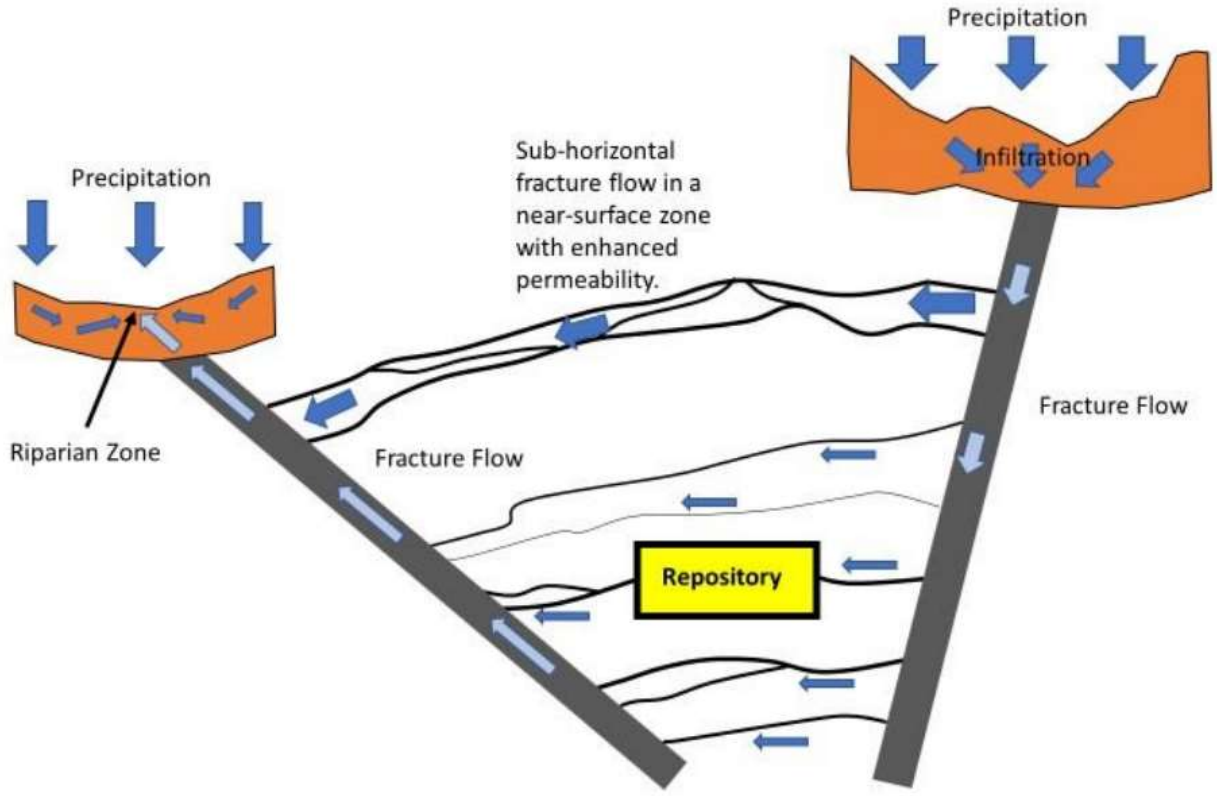

Figure 8-1. Conceptualization of general groundwater flow model (from Walke et al. 2018).

Another source for upward flow through the borehole and surrounding EDZ could be thermo-chemical reactions, e.g., corrosion of waste canisters that release water or gas within the disposal zone (e.g., Brady et al. 2009). At the present state of the project, analyses of gas related processes, like gas transport or two-phase flow have not been accounted for. If the gas production rate is low or the gas quantity small, the gas can be dissolved and removed by diffusion. In the opposite situation, a separate gas phase will be formed, and then a two-phase flow could be possible. At disposal depth, gas production and gas production rate due to corrosion of e.g., metallic uranium (more prone to corrosion than UO_2 spent fuel) is low due to the high lithostatic pressure, so that gas is expected to be dissolved and removed by diffusion. The same reasoning applies to gas generated or otherwise occurring in the geosphere.

Transport through a fracture network

Transport through a fracture network in the surrounding geosphere could either take place via:

- Many small borehole fractures leading to a bulk hydraulic conductivity of the geosphere, or
- Borehole intersection by a highly transmissive fracture.

Transport through a number of small fractures intersecting the borehole is rather probable, as minor fractures will always exist, but the total water flow is expected to be very small. In contrast, transport through a highly transmissive fracture intersecting the borehole is considered less probable. During site investigation and characterization of the site, the main effort will be directed towards finding a site with a low number of fractures and with the absence of strongly water-conducting fractures particularly in the disposal zone or the sealing zone of the borehole. However, with time and changing geological or hydrogeological conditions, previously existing closed fractures might be reactivated, or new fractures might develop.

Transport through a fracture network would also require some driving force, in addition to the existence of transmissive fractures. In the same was as for the potential advective transport through borehole and EDZ, for advective transport through fractures, the most probable driver would be hydrological conditions that lead to a hydraulic gradient.

Scenarios identified

For this generic safety assessment, it has been assumed that there will be no pre-closure events with negative impact on the multi-barrier disposal concept. It is further assumed that the borehole will be in the planned condition at the time of closure of the facility. This means that, for example, potential scenarios such as that of emplacement of a canister with reduced quality or a disposal canister stuck somewhere above the sealing zone that cannot be retrieved, are not considered in this generic safety assessment.

Accounting for the potential release pathways, several scenarios have been identified (see Table 8-1) that cover three main areas:

- Release of radionuclides from the canister to the near field (buffer inside the disposal zone or EDZ around disposal zone),
- Transport from the near field and through the far field to near surface, and
- Transport from near surface to biosphere.

Table 8-1. Summary of scenarios for deep borehole disposal. In yellow, scenarios screened out from further analyses. See Section 8.1.2.

Summary of safety relevant scenarios												
№	Release into near field			Transport through far field					Transport to biosphere			
	Expected corrosion and failure of canisters and release from waste form	Premature failure of individual canisters or localised corrosion	Direct failure of all canisters	Diffusive flow through borehole (and EDZ)	Advective flow through borehole (and EDZ)	Advective transport through horizontal small-fracture system	Advective transport through horizontal highly transmissive fracture	Advective transport through highly transmissive vertical fracture	Intersec-tion of near surface aquifer with vertical fracture system and borehole	Existence of drinking water well drawing from aquifer	Use of drinking water by members of the public
A											
B											
C											
D											
E											
F											
G											
H											
I											
J											
K											
L											

This matrix is not assumed to be complete but comprehensive enough. For the transport from the far field to the biosphere in each combination, it is assumed that there will be a direct connection and fast pathway between the disposal zone to the surface. It is uncertain that there will be a vertical fracture system allowing fast transport of radionuclides from the disposal level to the surface, as is the presence of near-surface aquifer, from which a drinking water well will draw water.

It is remarked that the option of a sudden failure of all canisters at a specific time is unrealistic and, thus, considered as a bounding or worst-case scenario.

For the most hypothetical scenarios, advective transport would be either thermally driven, or driven by a hydraulic gradient. As pointed out in the early part of this section, any thermally driven transport caused by heat-generating waste would not lead to significant transport in the case of a potential Norwegian deep borehole disposal, as the amount of heat-generating waste is far too small to sustain any significant vertical flow. In any case, vertical flow associated with the decay heat of the waste would be limited to a few hundred years, a time interval for which the canisters are assumed to confine the activity disposed of in the borehole.

An alternative driver for vertical transport could be a hydraulic gradient between the disposal zone and the surface. The order of magnitude of such a flow will depend on the hydraulic gradient, the quality of sealing, and density stratification of saline fluids.

The probability of such significant hydraulic gradients in the disposal zone is very low. The usually long residence times of deep groundwater and low flow rates in crystalline rock already below a few hundred of metres support this. Moreover, it is expected that geological characterization during site selection will exclude any site where such conditions could be possible.

At this stage of the general Norwegian disposal programme, there is no site-specific information. Thus, it is not possible to derive any reasonable vertical flows through the borehole that might be realistic. The approach chosen here is to simply assume that a vertical flow does exist and consider it as a potential alternative scenario.

For the associated flow rate, values have been used that are in the same order as flow rates assumed for potential flow through fractures intersecting the disposal borehole (see Sc-3 below).

This scenario is included as a typical “what-if scenario”, which aims to provide some insight of the consequences in case a vertical flow through the borehole would occur. It also shows the robustness of the system.

GoldSim (see Appendix III) allows the definition of a constant vertical flow as well as a time-dependent one. As it is considered very unlikely that time-dependent heat production will cause any significant flow through the borehole, only the impact of constant vertical flow rates has been assessed.

8.1.2 Selection of scenarios and calculation cases

Based on the scenarios (Table 8-1) for the release of radionuclides into the biosphere a few scenarios and calculation cases have been selected to give a comprehensive overview of the potential radiological impact that might be related to the disposal of the HLW in a deep borehole.

As mentioned above, not each scenario for the release of radionuclides is addressed. We have assumed very pessimistic conditions for certain areas, especially for the transport from the geosphere at the disposal level to the surface and for the pathway from the near surface area to the biosphere.

The selected scenarios are scenario A (see Table 8-1), considered as the normal evolution scenario (Sc-1), representing the expected evolution of the deep borehole repository. Scenario B is not addressed here as there is little difference to the normal evolution scenario (Sc-1). Scenario C is addressed as a calculation case within the normal evolution scenario (Sc-1; see Section 8.5.1). The scenarios assuming vertical flow through the borehole are D, E, and F. Scenario D (called Sc-2; see Section 8.5.2) addresses the normal evolution of the technical barriers, and the calculation cases for Sc-2 address an individual early failure of a canister or localised corrosion (Scenario E), and an instantaneous failure of all canisters after closure of the borehole (Scenario F). The scenarios G, H, and I are related to the advective transport via many small

fractures will be addressed in principle, analysing the expected flowrate through such a fracture network, but is not implemented in the GoldSim model of the deep borehole disposal and will not be analysed in detail (see Figure 8-8). The potential radiological impact from these scenarios is conservatively covered by the scenarios assuming an intersection of the borehole by a “highly” transmissive fracture (Scenarios J, K, and L, called Sc-3). Scenario Sc-3 includes several variants; each of them assumes a different location for the intersection of transmissive fracture and borehole (see Section 8.5.3).

Thus, the list of scenarios selected for analysis are:

- Sc-1 Normal evolution – Diffusive transport along the borehole (see Section 7.1),
- Alternative scenario: Sc-2 Vertical flow – Advective transport through the borehole and EDZ, and
- Alternative scenario: Sc-3 Fracture – Intersection by a transmissive fracture.

The normal evolution scenario Sc-1 is described in Section 7-1. Further assumptions for model development (see Section 8.2) are given below.

The main assumptions that form the basis for the normal evolution scenario Sc-1 are:

- Hydrogeological conditions remain constant over the entire assessment period, regardless that groundwater flow rates may change in different calculation cases.
- Length of borehole will be 3460 m with a disposal zone of 460 m length, a sealing zone of 500 m length and a backfilling zone of 2500 m length.
- In the disposal zone, bentonite will be placed around canisters and as a 1-m plug between consecutive canisters.
- Metallic uranium (MU) fuel elements will be disposed of in the lower part of the disposal zone.
- The sealing zone will be properly sealed with bentonite, and conditions will not change with time.
- The backfilling zone will be backfilled by crushed rock.
- The backfill material (crushed rock) and bentonite will have sorption capacity and retard most radionuclides.
- The borehole will be surrounded by annular EDZ over its whole length.
- Corrosion of canisters will be limited to general corrosion with an expected rate of 1 µm/a.
- Canisters will fail, once thickness of canister walls has been corroded from the 80 mm initial thickness to 50 mm.
- Concentration of radionuclides in fluid are governed by solubility limits.
- Radionuclides will be released from the different waste forms according to constant fractional release rates.
- There will be no significant horizontal groundwater flow through the borehole or parts of it with exception of the near-surface aquifer.
- There will be no vertical groundwater flow through the borehole or parts of it.

Deviations from these assumptions especially regarding the hydrogeological conditions and to the corrosion of canister and degradation of waste form are considered by sensitivity analyses or in alternative scenarios.

To model the potential radiological impact resulting from the alternative scenarios, Sc-2 Vertical flow and Sc-3 Fracture, the same conceptual model is used as for the normal evolution scenario Sc-1. Deviating from the description given in the bullet list above, certain parameters are changed to account for alternative evolutions of the deep borehole disposal as detailed below.

For Sc-2 it is assumed that a constant hydraulic gradient exists between the DZ and the near surface aquifer. Therefore, a certain flowrate is assumed to pass through the borehole and EDZ from the bottom part of the borehole to its top part. Advective transport of radionuclides is assumed towards the surface area, where it enters an aquifer as in the normal evolution scenario Sc-1. Diffusive flows are considered in the same way as in Sc-1 but depending on the assumed vertical flow rates they have significantly less relevance.

For Sc-3 and its variants, no vertical flow along the borehole is assumed, but a water-conducting sub-horizontal fracture intersects the borehole at varying locations along the borehole (see Figure 8-9).

Water from the fracture enters the EDZ and the inner part of the borehole. After mixing with the contaminated water inside EDZ and borehole it travels further through the fracture by advection transporting radionuclides until intersecting with a vertical fracture system that is connected to the near surface aquifer. Transport through the fractures is assumed to be advective driven by a hydraulic gradient.

Diffusive flow in Sc-2 and Sc-3 are considered in the same way as for Sc-1.

8.2 Conceptual model of DBD

8.2.1 Conceptual model of DBD for the normal evolution scenario Sc-1

The conceptual model of the deep borehole differentiates between the main components in the near field (i.e., disposal zone and EDZ) from those in the far field (i.e., sealing zone SZ, backfilling zone BZ, geosphere). The biosphere model defines the transfer of radioactivity to potentially exposed members of the public.

The near-field model describes the release of radionuclides from their respective waste forms, either MU or UO_2 SNF, and their transport through the engineered barrier system to the immediate surroundings, which is the saturated bentonite buffer filling the borehole outside the canister and the EDZ.

The principal components in the near field in the conceptual model are:

- the waste matrix,
- the stainless-steel canister,
- the bentonite surrounding the canister, and
- the surrounding EDZ.

The different waste forms are assumed to degrade according to a constant fractional release rate. Once the waste form is dissolved, the radionuclides may be mobilised in the water phase if water is in contact with the material. Radionuclides might also be immobilised through processes like precipitation/dissolution and sorption.

The solubility limits of radionuclides in the disposal zone define the maximum concentrations of radionuclides within the water phase of the materials in the near field, which, in turn, governs sorption within the bentonite and diffusive transport to neighbouring areas of the borehole, i.e., the surrounding bentonite layer and EDZ as well as the borehole segments of the disposal zone above and below a canister.

To model radionuclide transport through the far field, the following processes have been considered:

- advection/groundwater flow,
- dispersion,
- sorption,
- matrix diffusion,
- radioactive decay (and ingrowth), and
- dilution.

Other processes, such as colloid transport, gas generation, etc., may also play a role in radionuclide migration but have not been considered in this generic safety assessment.

For Sc-1, the only possible pathway through the far field is diffusive transport along the borehole, as advective flow through or along the borehole is not expected. Alternative scenarios consider also advective flow.

There has been no final recommendation regarding the casing of the disposal zone and sealing zone (Fischer et al. 2021). For modelling purposes, it is assumed that the disposal zone will not be cased. The sealing zone is also assumed to be without casing before sealing. The backfilling zone is also modelled assuming the same diameter as the sealing zone above and without casing. This is a simplified assumption, but at the

present stage of the DBD concept there is little basis for a more realistic model and deviations in the diameter of the upper part of the borehole are considered to have little influence on the results of the safety assessment calculations. For model calculations, the thickness of the EDZ has been set to the same value as the borehole diameter (Engelhardt & Fischer 2021). Figure 8-2 shows the dimensions of the borehole for a cross section through a canister in the disposal zone.

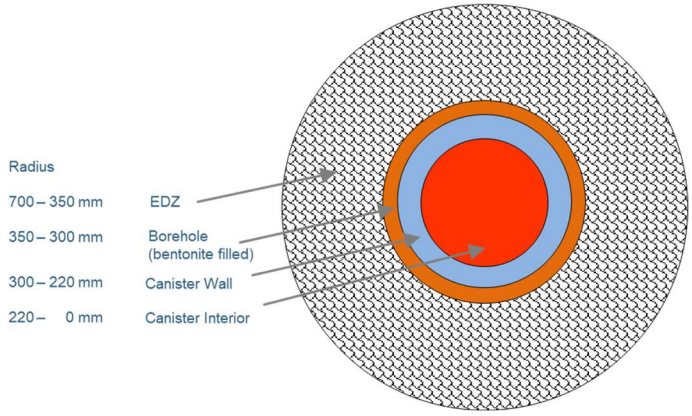

Figure 8-2. Schematic concept of borehole in DZ at canister location. Between canisters the borehole is filled by a 1-m plug of bentonite.

The canisters are separated by a 1-m plug of bentonite. In the sealing zone and the backfilling zone, the borehole is modelled as filled by bentonite and crushed rock, respectively.

The vertical cross section for a canister segment of the disposal zone is shown in Figure 8-3.

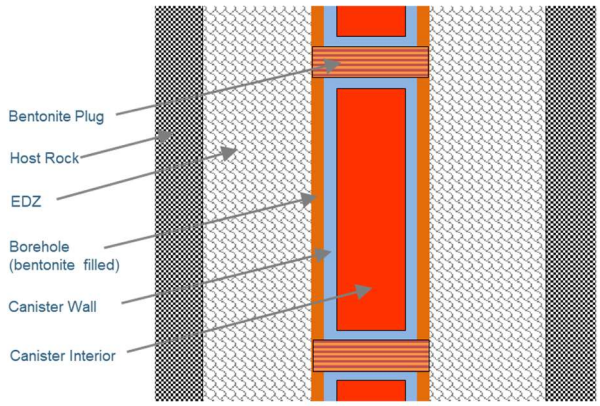

Figure 8-3. Schematic concept of the disposal zone (DZ) in the borehole. Vertical cross section of canister segment. Dimensions of the different components are not to scale.

The EDZ volume as well as the bentonite volume and the canister interior are modelled as compartments that are completely mixed during each step of the calculation. Concentration of radionuclides in the fluids inside the compartments will depend on volume of fluids and mass of solids as well as on solubility limits and the sorption capacity of the solids inside.

For the disposal zone, radionuclide solubility limits were applied, which are representative of geochemically reducing conditions in brine and were based on assumed isothermal conditions at 100 °C (Brady et al. 2009). The sealing zone is assumed to provide the same conditions regarding solubility as the disposal zone. Therefore, the same solubility values were chosen for both zones. However, there is only transport of radionuclides into the sealing zone by diffusive transport if radionuclide concentrations inside the sealing zone are lower than in the disposal zone. Solubility limits are not assumed to be exceeded inside the sealing zone.

Radionuclide concentrations in the backfilling zone are significantly smaller, so that solubility limits are not reached.

Radionuclide sorption is modelled in all three zones. Data for radionuclide-specific partition coefficients (k_{ds}) are taken from Freeze et al. (2013), who used data selected to comply with the expected conditions in the disposal zone and the sealing zone of a deep borehole in crystalline rock.

Partition coefficients for the backfilling zone were also taken from Freeze et al. (2013), not from their DBD model data but from their model for a mined geological disposal facility in crystalline rock. These are assumed to better represent the backfilling zone with crushed rock.

The canisters are assumed to fail, once corrosion has degraded the canister walls so far that the isostatic pressure expected at the depth of the disposal zone cannot be carried any longer by the remaining wall thickness. General corrosion is the process to lead to canister failure in scenario Sc-1. After failure, the canisters are assumed to be immediately filled with groundwater.

Dissolution of radionuclides from the waste into the water is governed by solubility limits. Transport of radionuclides out of the interior of the canister into the surrounding bentonite layer is modelled by diffusion between the water filling the inner volume of the canister and the saturated bentonite. To calculate the diffusive transport, the total outer surface of the canister is considered as diffusive area, equivalent to completely “disappeared” canister. Sorption to waste or canister material is omitted in the model.

The diffusive transport taking place after canister failure is schematically illustrated in Figure 8-4.

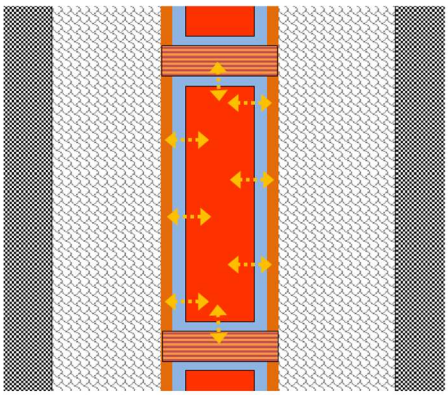

Figure 8-4. Diffusive transport between the inner volume of the canister and the surrounding bentonite layer after failure of the canister.

For the conceptual model, the disposal zone is subdivided into disposal zone segments between which diffusive fluxes take place. Diffusive transport takes place within the disposal segments between the bentonite layer and the surrounding EDZ as well as between EDZ volumes and bentonite volumes of adjacent disposal zone segments (Figure 8-5).

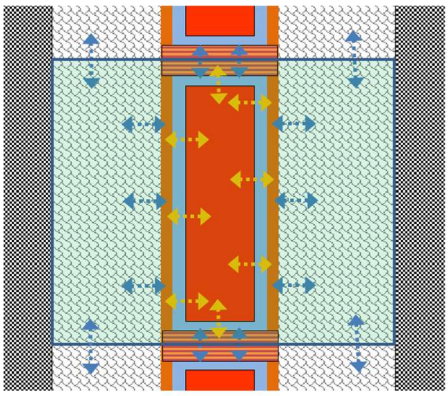

Figure 8-5. Diffusive transport within disposal zone segment and between adjacent segments that are considered for the conceptual model.

The two other zones of the borehole, the sealing zone above the disposal zone and the upper backfilling zone are also subdivided into segments. Diffusive transport also takes place internally between the material inside the borehole and the surrounding EDZ and between the EDZ and borehole volumes of adjacent segments as illustrated in Figure 8-6.

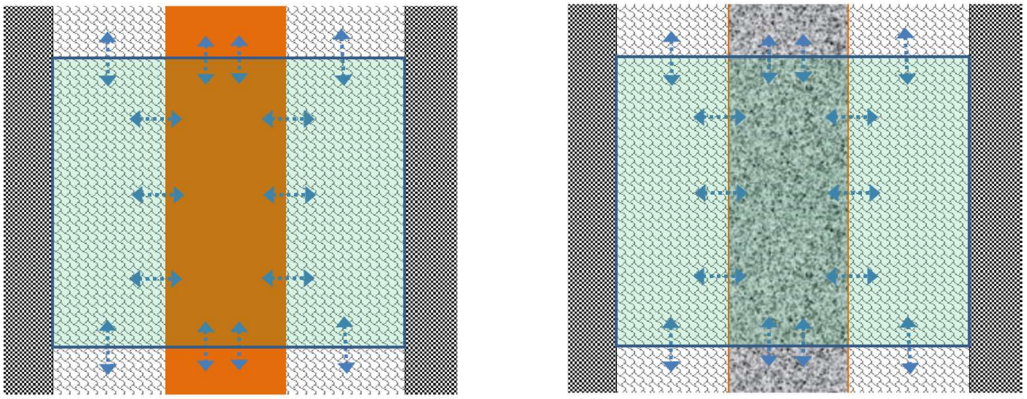

Figure 8-6. Conceptual model of diffusive fluxes within bentonite-filled sealing zone segment (left) and backfilling zone segments filled with crushed rock (right) and between adjacent segments.

Figure 8-7 shows the conceptual model of the complete disposal borehole. The schematic view is not to scale. It differentiates the main borehole zones and the surrounding EDZ and indicates the diffusive and advective transport that is considered for the normal evolution scenario Sc-1.

The uppermost backfilling zone segment is assumed to intersect a near-surface aquifer or transmissive fracture system. Based on the expected groundwater flow and the cross section of the borehole within the aquifer layer, a certain water flow is assumed to enter the EDZ and the inner part of the borehole and leaving it on the other side. Both the EDZ volume of the segments and the borehole volume of the segments are modelled as compartments that are completely mixed at each time step of the safety assessment calculations.

Concentration of radionuclides in the fluid in the compartments that are expected to be fully saturated will depend on the mass of radionuclides inside the compartments and on the volume and mass of liquids and solids as well as the sorption capacity of the solids.

The aquifer is conceptually modelled as a 5-m-thick layer of higher transmissivity, and it is assumed that the width of the aquifer, which will potentially contain the released radionuclides, will be limited to 10 m until it reaches the intersection of the drinking water well at a 100-m distance. The flowrate of the aquifer through this area of 50 m² is set to the expected minimum production rate of the drinking water well of 600 L/h. According to this conservative conceptual model the total mass of radionuclides released from the upper part of the borehole per time will be diluted by the minimum realistic production rate of the drinking water well only. The resulting radionuclide concentration then directly leads to the estimated dose rates resulting from drinking the water.

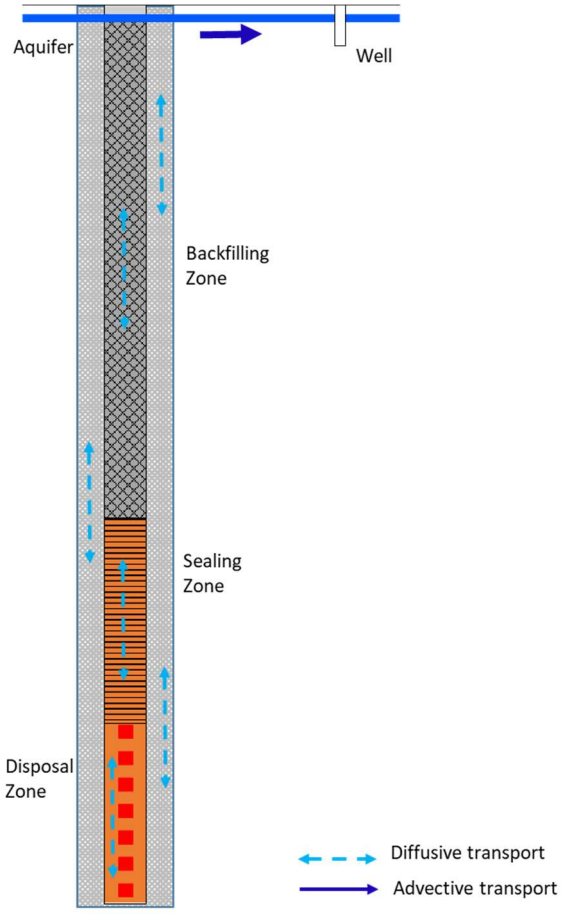

Figure 8-7. View of the conceptual deep borehole model (not to scale).

The biosphere model

To assess the radiological impact of the deep borehole repository, a very simple biosphere model has been used to calculate doses. It is assumed that a member of the public will drink 3 litres of water per day from a drinking water well either directly connected to the disposal borehole or through a fracture.

This simple biosphere model has been chosen because it is considered to give a good estimate of what might be the radiological impact under unfavourable conditions. Another advantage compared with more sophisticated biosphere models is that it is easily understandable and reproducible.

Depending on the details of a chosen biosphere model, a small farm biosphere model including the drinking water well and ingestion of contaminated meat, milk, vegetables etc. would probably lead to maximum doses that are 2 to 4 times higher than the drinking water doses. Investigations carried out in the framework of the IAEA BIOMASS project (IAEA, 2003) indicate that more sophisticated biosphere models might lead to individual dose rates that are higher than those for a simple drinking water scenario by up to a factor of 5.

It needs to be kept in mind therefore that this simply biosphere model might not be strictly conservative. On the other hand, this simple model includes a number of conservative assumptions. It is assumed that all radionuclides released to the biosphere will enter the aquifer to which the well is connected, and the amount of drinking water drawn from that well will contain all the radionuclides that have entered the aquifer. Moreover, it is assumed that the aquifer flow rate is equal to the capacity of the well, for which the usual minimum amount has been chosen. Consequently, the potential dose resulting from drinking the water from the contaminated well is considered rather pessimistic. At least it is a well-suited yardstick to assess the order of magnitude of the potential radiological impact and to compare the radiological impact for different scenarios and calculation cases.

To calculate the potential radiological impact that potential future release of radionuclides from the repository might have on members of the critical group, it has been assumed that all members of the critical group are adults, that is, the dose conversion factors for adults have been applied. This has been done following the line of argument as given in the IAEA document on the BIOsphere Modelling and ASSessment (BIOMASS) project (IAEA, 2003). This is in accordance with the ICRP (1998), where it is concluded that it is reasonable to calculate the annual dose/risk averaged over the lifetime of the individuals, which means that it is not necessary to calculate doses to different age groups. In particular, it is suggested that the lifetime average annual dose can then be adequately represented by the annual dose/risk to an adult.

Calculation of Potential Dose Rates

The dose due to ingestion of water is expressed as:

$$D_{ing\_water} = Q_{water} \cdot C_{water} \cdot DF_{ing} \qquad \textit{(Equation 8-1)}$$

where

D_{ing_water} is the dose due to water ingestion ($Sv \cdot y^{-1}$),
Q_{water} is the intake rate of drinking water ($m^3 \cdot y^{-1}$)
C_{water} is the concentration of radionuclides in water ($Bq \cdot m^{-3}$), and
DF_{ing} is the dose factor for ingestion ($Sv \cdot Bq^{-1}$).

In the GoldSim model, radionuclide concentration of the water inside the aquifer C_{water} is calculated based on the model for simulating radionuclide migration through the near field and the geosphere described above.

Calculation cases for the normal evolution scenario Sc-1

Calculation cases considered for the normal evolution scenario Sc-1 are mainly related to the assumptions regarding the emplacement sequence of canisters containing UO_2 spent fuel or metallic uranium inside the disposal zone, the release of radionuclides from the near field and transport conditions inside the borehole and the EDZ. While all parameters considered as having a significant impact on the results have been addressed in the framework of sensitivity assessment, certain features have been assessed as calculation cases.

For the normal evolution scenario Sc-1, the following changes to the initial assumptions have been considered in the calculation cases:

- Sc-1-C1 Changed canister sequence in borehole
- Sc-1-C2 No solubility limits
- Sc-1-C3 No sorption
- Sc-1-C4 Direct failure of all canisters

8.2.2 Conceptual model for the alternative scenarios

Sc-2 is the alternative scenario that assumes vertical upward flow of water along the borehole and its surrounding EDZ. Consequently, advective transport of radionuclides along the borehole takes place.

In Sc-3, it is assumed that the disposal borehole will be intersected by a transmissive fracture. Radionuclides inside the borehole segment intersected by the fracture will be advectively transported from the borehole segment through a fracture system all the way to the aquifer near to the surface.

Alternative scenario Sc-2 Vertical flow

As mentioned in Section 8.1.1, inside the borehole and its surrounding EDZ diffusive transport will take place because of differences in radionuclide concentration. In this scenario, also advective transport along the borehole driven by a hydraulic gradient is considered to take place.

In the model, the defined total flowrate along the borehole is distributed into flow through the borehole itself and through its surrounding EDZ. The respective values have been calculated based on the assumed hydraulic conductivity within the borehole and EDZ and their respective cross sections:

$$Flow_{EDZ} = Flow_{total} \cdot (CS_{EDZ} \cdot HC_{EDZ}) / (CS_{EDZ} \cdot HC_{EDZ} + CS_{BH} \cdot HC_{BH}) \quad \textit{(Equation 8-2)}$$

$$Flow_{BH} = Flow_{total} \cdot (CS_{BH} \cdot HC_{BH}) / (CS_{EDZ} \cdot HC_{EDZ} + CS_{BH} \cdot HC_{BH}) \quad \textit{(Equation 8-3)}$$

where

$Flow_{total}$ = Total vertical flow through borehole and surrounding EDZ (L/a),
$Flow_{EDZ}$ = Vertical flow through EDZ (L/a),
$Flow_{BH}$ = Vertical flow through borehole (L/a),
CS_{EDZ} = Cross section of EDZ (m^2),
CS_{BH} = Cross section of borehole (m^2),
HC_{EDZ} = Hydraulic conductivity of EDZ (m/s), and
HC_{BH} = Hydraulic conductivity of borehole (m/s).

Alternative scenario Sc-3 Fracture

There are two possible variations of scenario Sc-3. If the extreme variants are considered, inflow of groundwater into the borehole and its surrounding EDZ through a fracture or fracture systems in the underground could either take place via a system of many tiny fractures or via one highly transmissive fracture. In the first case the inflow could be simulated as groundwater flow through a quasi-porous system. In the second case inflow could be simulated to occur at the intersection between the fracture and the borehole. Of course, intermediate conditions between these two extreme variants are possible.

The potential conditions that include the location of the fracture intersection and flow rates are discussed in the following sections.

Crystalline rock with equally distributed hydraulic conductivity with depth

A conceptual model of the scenario with a large number of tiny fractures that could be modelled as a surrounding host rock with equally/homogeneously distributed hydraulic conductivity, or a porous host rock is shown in Figure 8-8. Homogenous distribution is indicated by a group of parallel tiny fractures intersecting the disposal zone of the borehole. These are connected to an aquifer at the surface by a sub-vertical highly transmissive fracture.

Lacking hydraulic conductivity data from an actual selected site in Norway, representative data for crystalline rock from other sites are used.

SKB (2006) carried out investigations in the Oskarshamn area and found that in crystalline bedrock hydraulic conductivity decreases strongly with depth. Banks et al. (2010) give a simple empirically based model to estimate the average bulk hydraulic conductivity (K_d) with depth based on that work by SKB (2006):

$$K_d = K_0 \cdot 10^{-d/D} \qquad \textit{(Equation 8-4)}$$

where

- d is the depth below the surface (m),
- K_0 is the surficial average bulk hydraulic conductivity at d=0, set to 1.134×10^{-7} m/s, and
- D is the increase in depth that leads to the decrease of hydraulic conductivity by a factor 10, for Oskarshamn = 380 m

To estimate the expected advective transport that would relate to this equally distributed hydraulic conductivity model, it has been assumed that Equation 8-5 can be appropriately used to estimate flow through the borehole and its surrounding EDZ.

$$Q = K \cdot A \cdot gr_{hydr} \qquad \textit{(Equation 8-5)}$$

where

- Q is the flow rate through the borehole (L/a),
- K is the hydraulic conductivity (m/s),
- A is the cross section of the borehole and EDZ (m^2), and
- gr_{hydr} is the hydraulic gradient (-).

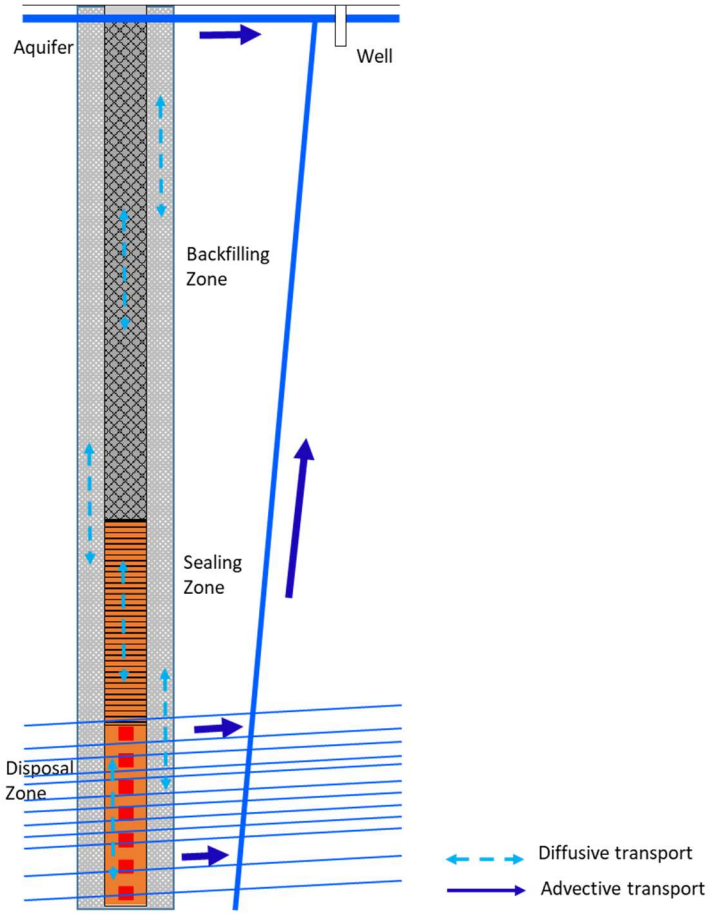

Figure 8-8. View of the conceptual deep borehole model (not to scale) and potential release pathway via "homogeneously" fractured rock and a sub-vertical fracture connecting disposal zone area and the near-surface aquifer in Sc-3.

It has further been assumed that the values derived from data for Oskarshamn (SKB, 2006) can be used as representative values for hydraulic conductivity and its logarithmic decrease in Norway (K_0 = 1.134×10^{-7} m/s, D = 380 m) and that the empirical Equation 8-4 would also give reasonable results for a depth larger than 1000 m, up to which it has been tested.

According to the target values developed for site selection purposes for NND (Hagros et al. 2021), a maximum hydraulic gradient of 0.01 is a realistic target value for 200 m depth. As minimization of hydraulic gradients will be one of the targets during site selection, it is assumed that the hydraulic gradient at depths of more than 2000 m will not exceed that value.

For the uppermost part of the disposal zone at the depth of 3000 m, an approximate rock hydraulic conductivity is 1.44×10^{-15} m/s. For the lowest part of the disposal zone at 3460 m depth the estimated hydraulic conductivity would be 8.9×10^{-17} m/s. For the calculations here, an average value of 4.9×10^{-16} m/s has been used.

The total flow through the disposal zone of the borehole (Q_{DZ}) would then be:

$$Q_{DZ} = 5\times10^{-16}\ \text{m/s} \times 1.4 \times 460\ \text{m}^2 \times 0.01 = 3.16\times10^{-15}\ \text{m}^3\text{/s} = 9.96\times10^{-5}\ \text{L/a}$$

For this safety assessment, to avoid too optimistic results, pessimistic or conservative parameter values are selected. Therefore, for a generic site a significantly slower decrease of hydraulic conductivity with depth has been chosen. It has been assumed that the hydraulic conductivity would decrease by a factor 10 for each increase of 600 m depth. The respective results are:

K_{3000} = 1.13×10^{-12} m/s and K_{3460} = 1.94×10^{-13} m/s for upper and lower disposal zone, respectively, leading to a mean value of K_{DZ} = 5.32×10^{-13} m/s. The total flow through the disposal zone resulting from this mean hydraulic conductivity would be 0.11 L/a.

Freeze et al. (2016) give typical values of hydraulic conductivities between 1.0×10^{-10} m/s and 1.0×10^{-15} m/s for scarcely fractured crystalline rock between 500 and 5000 m depth. This supports the assumption that the values calculated above using 600 m as depth interval for reducing the hydraulic conductivity are considered pessimistic given the fact that site selection will be targeted to find locations where hydraulic conductivities are low.

Similar calculations for the sealing zone give mean hydraulic conductivities of 6.57×10^{-14} m/s and 3.44×10^{-12} m/s for 380 m and 600 m stepwise decrease, respectively. The associated total flow through the sealing zone would be 2.07×10^{-3} L/a for the 380 m interval and 0.76 L/a for the more pessimistic assumption of a decrease by a factor 10 for each 600-m-interval.

Implementation of advective transport equivalent to flow through porous media by assuming a continuous conductivity and groundwater flow becomes less realistic with increasing depth in crystalline rock. At the present stage of model development, this approach has not been implemented. The values given here for the total expected or typical bulk conductivities are used to develop a feeling for realistic flow rates for groundwater at depths below 2000 m.

Sc-3 Fracture

Alternative scenario Sc-3 Fracture considers the intersection of the borehole by a highly transmissive fracture. The model allows to simulate such an intersection at different depths and in different borehole zones.

Figure 8-9 shows the conceptual model of the scenario, where a transmissive fracture intersects the disposal borehole. The figure indicates the locations at which potential intersections have been implemented in the model. In any case, the intersecting fracture is assumed to be connected to the aquifer near the surface by a sub-vertical highly transmissive fracture.

For scenario Sc-3, the following pessimistic boundary conditions have been chosen to maximise the release of activity to the biosphere:

- Existence of (sub-)horizontal fracture or fracture system with a significant flow rate,
- Existence of a nearby (sub-)vertical fracture system with a significant flow rate connected to the sub-horizontal fracture,
- Existence of a nearby suitable aquifer to supply a drinking water well,
- Direct connection between the vertical fracture (system) and surface (aquifer).
- Existence of hydraulic gradient between the intersection of the borehole and the surface (aquifer)
- Existence of a drinking water well,
- Hydrogeological conditions that allow all contaminated fracture to enter the well,
- Creation of connection between sub-horizontal and vertical fractures, which takes place after facility closure,
- Insignificant retardation along the fracture pathway.

It must be noted that these assumptions represent an accumulation of very pessimistic boundary conditions.

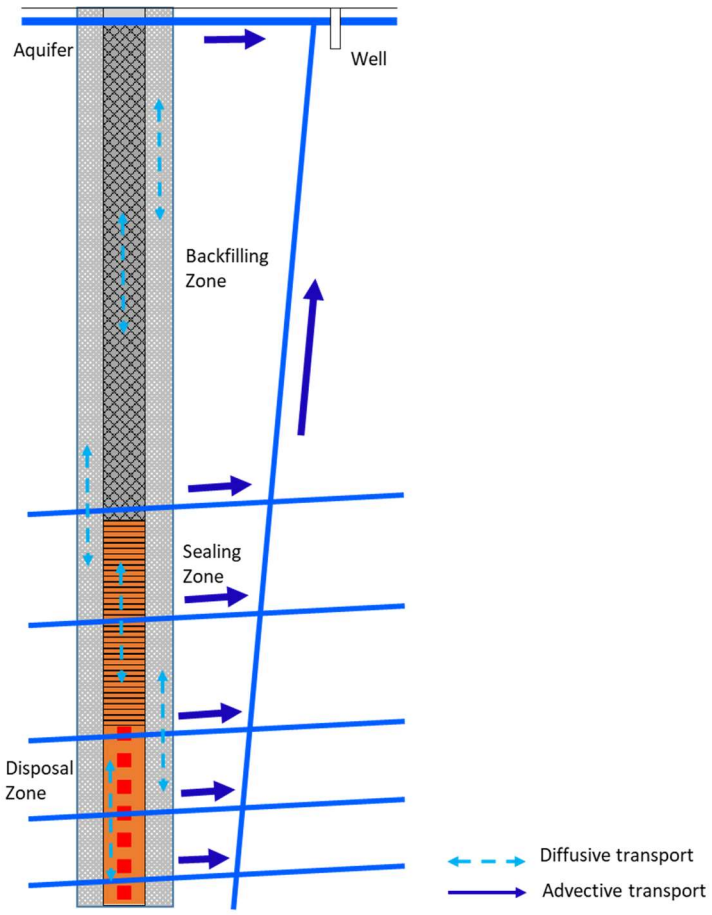

Figure 8-9. View of the conceptual deep borehole model (not to scale) and potential release pathway via a sub-horizontal transmissive fracture at different locations along the borehole and a sub-vertical fracture connecting disposal zone area and near-surface aquifer.

The site selection process will aim to avoid such water-conducting fractures and hydrogeological conditions as described above. If such conditions were to develop after closure, it would be much more likely that they would develop after at least several thousands of years than soon after closure.

The assumption that all contaminated water from the intersecting fracture will enter an existing drinking water well is another strongly pessimistic assumption.

Variants of the alternative scenario Sc-3 cases have been selected that include intersection of fractures with the borehole within the backfilling zone, the sealing zone, and the disposal zone. It is worth noting that most assumptions listed above become more unrealistic with increasing depth: the existence of transmissive fractures and especially the existence of a fracture system with connection to the vertical fracture and the drinking well.

In the GoldSim model, calculation cases for the following variants have been implemented:

- Sc-3.1 Fracture at the bottom of the backfilling zone
- Sc-3.2 Fracture in the middle of the sealing zone
- Sc-3.3 Fracture at the top of the disposal zone
- Sc-3.4 Fracture in the middle of the disposal zone
- Sc-3.5 Fracture at the bottom of the disposal zone

For an individual simulation run of the model, any or all the fractures can be selected and to each of them a specific flow rate can be assigned. As, in general, a vertical connection between the disposal depth and the surface will not be provided by one large straight fracture but by a fracture network, the length of the fracture can be adjusted by choosing a factor that represents the assumed tortuosity of the pathway.

In the GoldSim model, the intersection of the borehole by a transmissive fracture is simulated by defining half of the fracture flow as inflow into the EDZ and the other half as inflow to the borehole. From there the same flow leaves again into the fracture connected to the vertical fracture system, which feeds into the aquifer.

This is a conservative approximation: Provided that there will be no vertical flow through the borehole, radionuclides would have to diffuse towards the location of the fracture. In the model, water flowing into the borehole and EDZ will be completely mixed for each time step with the content of the whole compartments representing – in case of the disposal zone – 21 m disposal zone length and 4 waste canisters.

Flow rates of intersecting fractures

In Hagros et al. (2021) flow rates of less than 1 L/a and m width for fractures have been identified as target property for a disposal site at about 400 m depth. This is a reasonable target property, which can be fulfilled in suitable crystalline host rock formations. Taking this into account, this value is conservatively selected as the flow rate in the fracture, at more than 2000 m depth.

Considering the estimates about the expected bulk conductivity described above leading to flow rates through the entire sealing zone length or disposal zone length of 0.76 L/a and 0.11 L/a as pessimistic values, a value of 1 L/a for a fracture intersecting the sealing zone and 0.1 L/a for fractures crossing the disposal zone seem to be overly pessimistic. In this regard, it is also referred to Freeze et al. (2013) who expect no significant horizontal transport in a carefully selected site for a deep borehole.

For the alternative scenario Sc-3, the flow rates for the intersecting fractures have, therefore, been selected as 1 L/a for the lower part of the backfilling zone and the middle part of the sealing zone and as 0.1 L/a for the fractures intersecting the disposal zones. Larger flow rates will be considered in sensitivity analyses.

Fracture aperture

To estimate the aperture of the fracture intersecting the borehole, the relationship used by Joyce et al. (2010) for SR-Site safety assessment for SKB is used:

$$e_t = 0.5 \cdot \sqrt{T} \qquad \textit{(Equation 8-6)}$$

where

e_t is the effective transport aperture (m), and
T is the transmissivity (m^2/s).

The transmissivity is being calculated from:

$$Q_{Frac} = T_{Frac} \cdot W_{Frac} \cdot gr_{hydr} \qquad \textit{(Equation 8-7)}$$

where

Q_{Frac} is the flowrate through the fracture (L/a),
T_{Frac} is the transmissivity of the fracture (m^2/s),
W_{Frac} is the width of the fracture (m), and
gr_{hydr} is the hydraulic gradient (-).

Based on the assumption that acceptable flow rates would be in the order of 0.1 or 1 L/a, the width of the fracture would be equal to the diameter of the EDZ, and the hydraulic gradient would be 0.01, the resulting transmissivities would be $2.26 \cdot 10^{-9}$ m²/s and $2.26 \cdot 10^{-10}$ m²/s for the assumed flow rates of 1 L/a and 0.1 L/a, respectively.

According to Equation 8-6, the estimated effective transport apertures would be 0.0239 mm and 0.0075 mm, respectively, for flow rates of 1 L/a, and 0.1 L/a. As the effective transport aperture is assumed to be smaller than the average aperture and the assumed hydraulic gradient of 0.01 represents the upper limit of expected values, a value of 0.15 mm has been chosen for the average aperture of the fracture. In the model, this value is later used to define the volume of water inside the fracture(s).

For the vertical transport, a system of ten vertical fractures is assumed that intersects with the horizontal fracture at about 50 m from the borehole. Each of the fractures is assumed to have the same aperture and the same flowrate. The width of the vertical fracture system through which the contaminated flow from the horizontal fracture is transported upwards to the aquifer is assumed to be 5 m.

It is further assumed that the vertical pathway has a strong tortuosity. Consequently, a value of 5 is chosen as multiplier of the vertical distance. From considerations presented in SKB (2010), this should represent a conservative estimate.

Calculation cases for alternative scenarios

For scenario Sc-2 Vertical flow, the calculation cases selected are similar to those for the normal evolution scenario Sc-1. The impact the potential uncertainty in other parameters values than those considered in the calculation cases is addressed in sensitivity cases/analyses.

For Sc-2, the following changes of the initial assumptions have been considered as calculation cases:

- Sc-2-C1 Reverse order of canister emplacement in borehole
- Sc-2-C2 No solubility limits
- Sc-2-C3 No sorption
- Sc-2-C4 Localised corrosion
- Sc-2-C4 Direct failure of all canisters

To assess the impact of potential localised corrosion in a canister, the uppermost canister in the disposal zone has been selected to develop a pit-hole leak. It is the nearest canister to the surface and therefore considered to have the largest impact on the calculated dose rates.

For each of the variants of the alternative scenario Sc-3 Fracture, the reference calculation case concerns the location of the intersection of fracture and borehole. As mentioned above, five different intersection locations have been considered as variants of Sc-3. In addition to these calculation cases, for the variant Sc-3.3 with a fracture intersection at the top of the disposal zone, the same calculation cases as for the normal evolution scenario Sc-1 and the alternative scenario Sc-2 have been analysed to demonstrate the impact of the respective boundary conditions for this alternative scenario.

- Sc-3.1 Fracture at the bottom of the backfilling zone
- Sc-3.2 Fracture in the middle of sealing zone
- Sc-3.3 Fracture at the top of disposal zone
    - C1 Changed canister sequence in borehole
    - C2 No solubility limits
    - C3 No sorption
    - C4 Localised corrosion
    - C5 Direct failure of all canisters
- Sc-3.4 Fracture in the middle of disposal zone
- Sc-3.5 Fracture at the bottom of disposal zone

The variant Sc-3.3 with a fracture in the disposal zone has been chosen to assess the impact of other boundary conditions, because for the other variants with a fracture in the sealing zone or in the backfilling zone, many radionuclides significantly decay before reaching the respective locations.

8.3 Mathematical model for long-term safety calculations

The computer code used to carry out the long-term calculations is GoldSim Simulation Environment extended by the Radionuclide Transport Module.

Despite GoldSim's ability to run probabilistic calculations, for the purpose of this generic safety assessment, the calculations are focused on deterministic calculations and sensitivity analysis to investigate the influence of changing parameter values. Compared to probabilistic calculations, deterministic calculations are easier to understand and interpret and to reproduce in case of an independent review is made using a different software code.

A brief description of the main features of GoldSim Simulation Environment is given in Appendix III. It is aimed to allow an easier understanding of the following description of the computer model for the generic safety assessment of a deep borehole disposal for NND.

The implementation of the conceptual model for the normal evolution scenario Sc-1 into a GoldSim model is visualized in the figures below using certain sections from the GoldSim user interface that indicates the relations between the main compartments of the deep borehole model.

The same model, however, with different parameter sets, will be used for the normal evolution scenario Sc-1 and for alternative scenarios and related calculation cases. Therefore, this description of the model includes certain features that are not considered in the normal evolution scenario Sc-1.

The GoldSim model has been divided into several main parts to increase transparency of the model and its comprehensiveness. Figure 8-10 displays a simplified version of the main parts, where the transport calculations are carried out. Arrows have been added to indicate the direction of diffusive and advective transport that is considered between the different parts or areas of the deep borehole. Potential advective transport pathways refer to alternative scenarios or calculation cases. The detailed models for the different parts are described below.

For the normal evolution scenario Sc-1, diffusive fluxes will be calculated between the different borehole zones and advective fluxes within the aquifer intersecting the top part of the backfilling zone. The activity concentration within the aquifer will then be used to calculate potential dose rates for people using this aquifer as a source of drinking water.

For alternative scenarios/calculation cases, in addition to the diffusive fluxes, also advective transport by vertical flow through the borehole and EDZ are considered as well as advective transport through fractures or fracture systems connecting certain locations of the different borehole zones with the aquifer.

In GoldSim, the different potential pathways from the waste to the biosphere is simulated using different types of pathway cells. For each time step and pathway cell, the computer model calculates the distribution according to which radionuclides are either associated with the solid media inside the cell or with the liquid media to determine the radionuclide concentration in the water inside the pathway cell. For both types of transport, diffusive as well as advective, the concentration is an important parameter to define the transport rates.

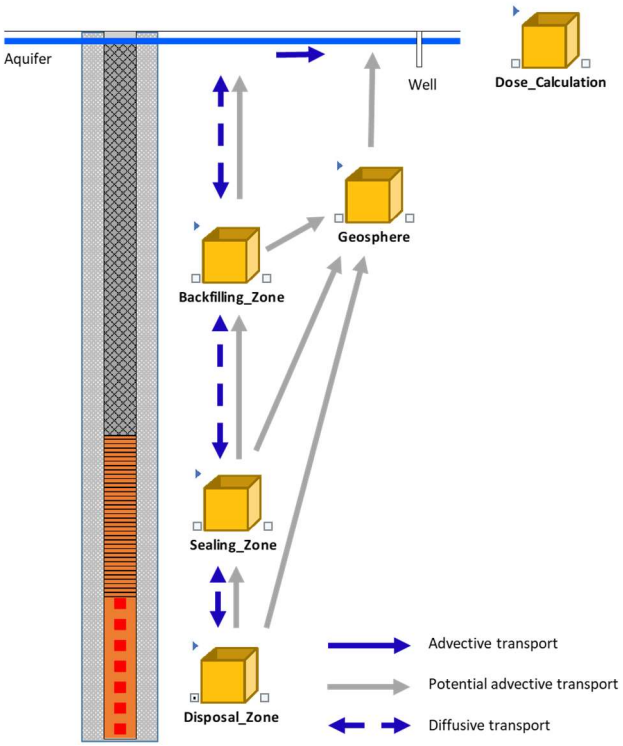

Figure 8-10. Upper level of GoldSim user interface showing the main model parts where transport calculations are carried out. Arrows indicate diffusive and advective transport pathways considered for the normal evolution scenario Sc-1. In case of potential advective transport, those possible transport pathways are indicated, which are considered additionally for some of the alternative scenarios and calculation cases.

8.3.1 GoldSim disposal zone model

To keep the model in a reasonable size and calculation times, the disposal zone has been divided into 22 segments. Each of the segments represents 4 disposal canisters, their combined inventory, void volume inside the canisters (respectively water volume after canister failure), the associated bentonite volume and its water content and the surrounding EDZ including its water content.

To model the disposal zone, which is the source term of the model, each disposal zone segment has an associated source element, which allows to define the properties of the conditioned waste. It defines the number of waste packages inside the segment, technical barriers with their associated failure modes, the inventory of the waste form and rates for release of radionuclides from the waste form. Inventories and related release rates can be defined separately for different waste forms inside the source element.

The waste content of the source elements (representing 4 disposal canisters) for the individual disposal zone segments is entered into the model from the Excel input data file. There are two different possibilities. The canisters contain either UO_2 SNF or metallic uranium. The sequence of the different types of canisters (containing either UO_2 SNF or metallic uranium) is also defined by the input data file and can be freely chosen.

The inventory of the UO_2 SNF canisters is divided into the three waste forms UO_2, other metals and Zircalloy. In addition, a certain amount of instant release fraction (IRF) of the activity has been defined. The other canisters contain exclusively metallic uranium.

A compartment or mixing cell is associated with each source element into which the released inventory (exposed waste) is being transferred. For this cell the volume of fluids and masses of solid are defined to allow application of sorption capacities and solubility limits.

The time of failure of the canister, is fed into the model from an Excel data file. For the normal evolution scenario Sc-1, the failure time assumes general corrosion rates for stainless steel. The four canisters of one segment are not assumed to fail at the same time but their failure time is distributed over a certain defined period. This leads to a smoother and more natural release of activity. This smoothing effect can be further increased by multiplying the number of waste packages by a respective factor.

For alternative scenarios/ calculation cases, the time of canister failure can be changed individually for the different segments. An alternative localised corrosion process has been implemented to simulate a pit hole. The faster formation of a pit hole leads to early releases, although through a smaller area.

As mentioned above, each disposal zone segment represents four disposal canisters. According to Wunderlich et al. (2021), it is expected that the total waste to be disposed of in the borehole can be conditioned in 88 canisters. Accordingly, the disposal zone has been modelled as a sequence of 22 source elements that are distributed over the disposal zone from 3000 to 3460 m depth.

Figure 8-11 shows a detail of the GoldSim model of the disposal zone. On the left side the GoldSim elements of three subsequent segments are shown, which form a part of the 22-segment chain modelling the complete disposal zone. For each segment there are three GoldSim elements: the source representing the canister, and two more mixing cells that represent the bentonite buffer around the canister and the EDZ surrounding the borehole in this depth section.

Each mixing cell contains certain amounts of solids and water, which are used to calculate sorption of radionuclides inside the cells and solubility limits. Data for both partition coefficients as well as solubility limits are used that are typical for saline groundwater. For the EDZ mixing cells, sorption to fracture fillings or fracture wall coatings have conservatively been omitted. For the interior of the canister, any sorption has been omitted as well.

The sketched figure at the right side visualizes the different fluxes that are calculated to simulate the release and transport of radionuclides within the near field. The broken arrow lines symbolize diffusive fluxes that can occur in both directions between the different mixing cells. The following fluxes are modelled:

- Diffusive transport between a mixing cell with exposed waste inside the source element and the surrounding buffer mixing cell (yellow arrows).
- Diffusive fluxes between buffer and surrounding EDZ mixing cell (light blue arrows).
- Diffusive fluxes between an EDZ cell of the segment and the EDZ cells of the segments directly above and below (light blue arrows).
- Diffusive fluxes between a buffer cell of the segment and the buffer cells of the segments directly above and below (light blue arrows).

For alternative scenarios and calculation cases, in addition to diffusive fluxes, upwards directed advective fluxes have been considered for the simulation. Vertical flow is assumed to be divided into flow through the column of EDZ cells and flow through the column of buffer cells. In Figure 8-11 this potential advective transport is indicated by the dark blue arrows. The relation between the two flows can be freely chosen. For the existing model, the relative share of vertical flow through the different pathways is calculated based on the respective cross sections and assumed hydraulic conductivities of the EDZ and buffer columns.

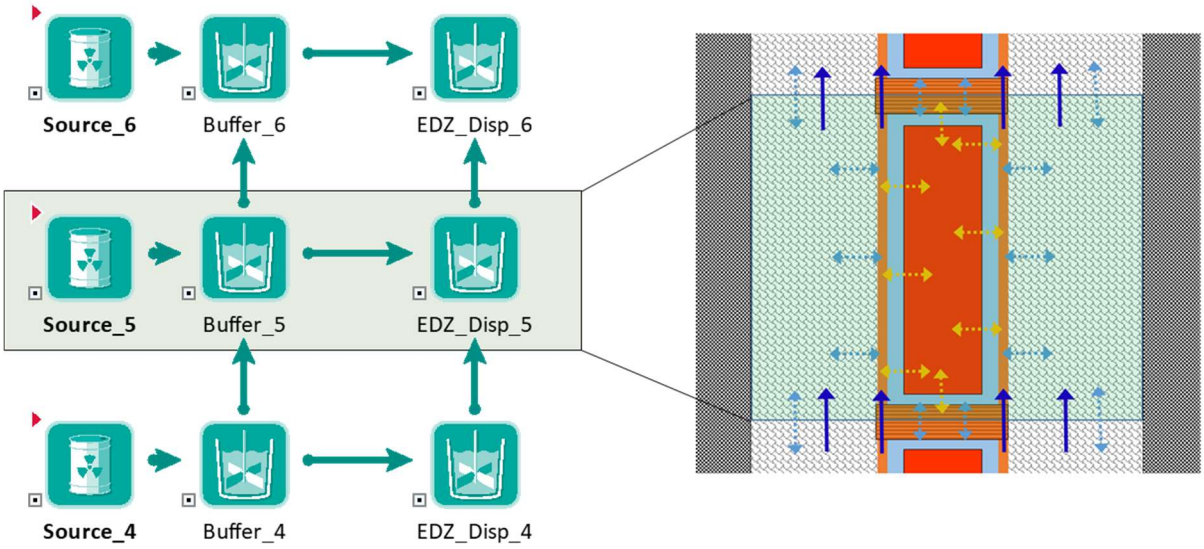

Figure 8-11. Left: Detail of disposal zone model in GoldSim. Right: the conceptual model of a disposal zone segment is shown together with diffusive transports (light blue arrows) that are considered. The vertical dark blue arrows indicate potential advective transport for alternative scenario Sc-2 with vertical flow through borehole.

8.3.2 GoldSim sealing zone model

In the GoldSim model, the sealing zone above the disposal zone has been divided into 25 segments. For the existing DBD concept, the total length of the sealing zone is assumed to be 500 m. Each of the segments represents a 20-m-section of the sealing zone.

Figure 8-12 shows a detail of the GoldSim model of the sealing zone. On the left side, the GoldSim elements of three subsequent segments are shown, which form a part of the 25-segment chain. For each segment, there are two mixing cells, one representing the bentonite sealing inside the borehole and the other the EDZ surrounding the sealing segment. Each mixing cell contains certain amounts of solids and water, which are used to calculate sorption of radionuclides inside the cells and solubility limits. Data typical for saline groundwater are used for partition coefficients and solubility limits. For the EDZ mixing cells, sorption to fracture fillings or fracture wall coatings is conservatively omitted. This is a simplified model compared with system of sealing elements that would be developed for a specific hydro-geological situation, but for this generic safety assessment it is justified

The borehole in the sealing zone is assumed to be sealed with compacted bentonite with low hydraulic conductivity and high sorption capacity.

As for the disposal zone segment discussed above, the sketched figure at the right side of Figure 8-12 visualizes the different fluxes that are calculated to simulate the transport of radionuclides within the sealing zone. The following fluxes are considered:

- Diffusive fluxes between sealing bentonite and surrounding EDZ mixing cell (light blue arrows),
- Diffusive fluxes between EDZ cell of the segment and the EDZ cells of the segments directly above and below (light blue arrows), and
- Diffusive fluxes between sealing cell of the segment and the sealing cells of the segments directly above and below (light blue arrows).

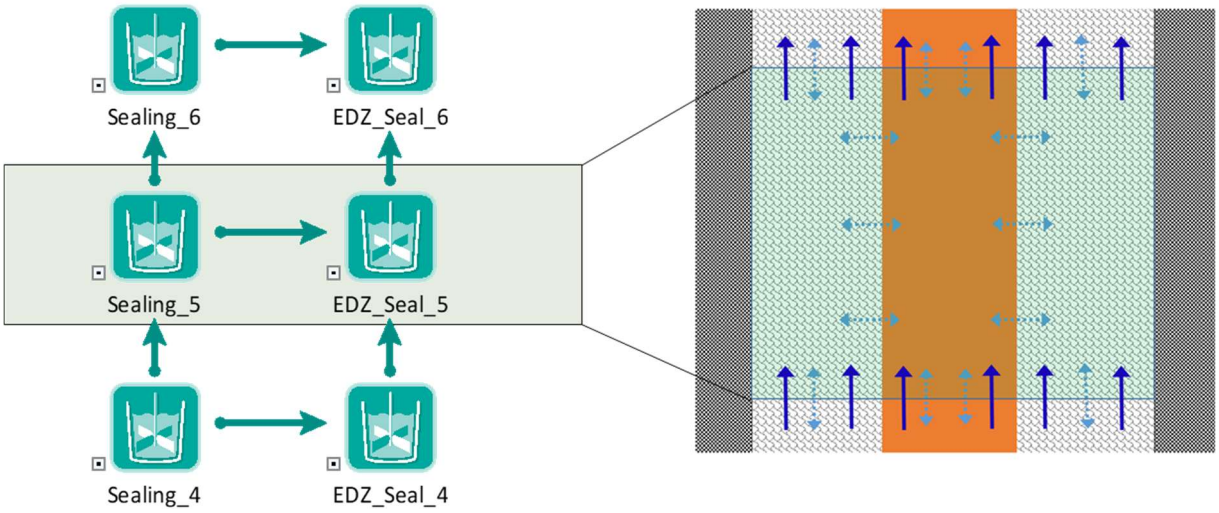

Figure 8-12. Left: Detail of sealing zone model in GoldSim. On the right, the conceptual model of a sealing zone segment is shown together with diffusive transport that are considered (light blue arrows). The vertical dark blue arrows indicate potential advective transport for alternative scenario Sc-2 with vertical flow through borehole.

For alternative scenarios and calculation cases, in addition to diffusive fluxes, upwards directed advective fluxes are considered for the simulation. Vertical flow is assumed to be divided into flow through the column of EDZ cells and flow through the column of sealing cells. In Figure 8-12, this potential advective transport is indicated by the dark blue arrows. The relation between the two flows is calculated again based on the respective cross sections and assumed hydraulic conductivities of the EDZ and the borehole with its sealing material.

8.3.3 GoldSim backfilling zone model

The backfill zone extends from the top of the sealing zone at 2500 m depth to the surface. In the GoldSim model, the backfilling zone has been divided into 25 segments. Consequently, each of the segments represents a 100-m-section of the backfilled borehole.

Figure 8-13 shows a detail of the GoldSim model of the backfilling zone. On the left side, the GoldSim elements of three subsequent segments are shown, which form a part of the 25-segment chain modelling the complete backfilling zone. In the same way as for the sealing zone, for each segment there are two mixing cells, one representing the backfilled borehole and the other one the EDZ surrounding the borehole at this depth section. Each mixing cell contains certain amounts of solids and water, which are used to calculate sorption of radionuclides inside the cells and solubility limits. Data used as partition coefficients is assumed to be typical for crystalline bedrock. For solubility limits the same data have been used as for the sealing zone, but concentrations in this pathway will not come near to any realistic solubility limits. For the EDZ mixing cells, sorption on fracture fillings or fracture wall coatings has conservatively been omitted.

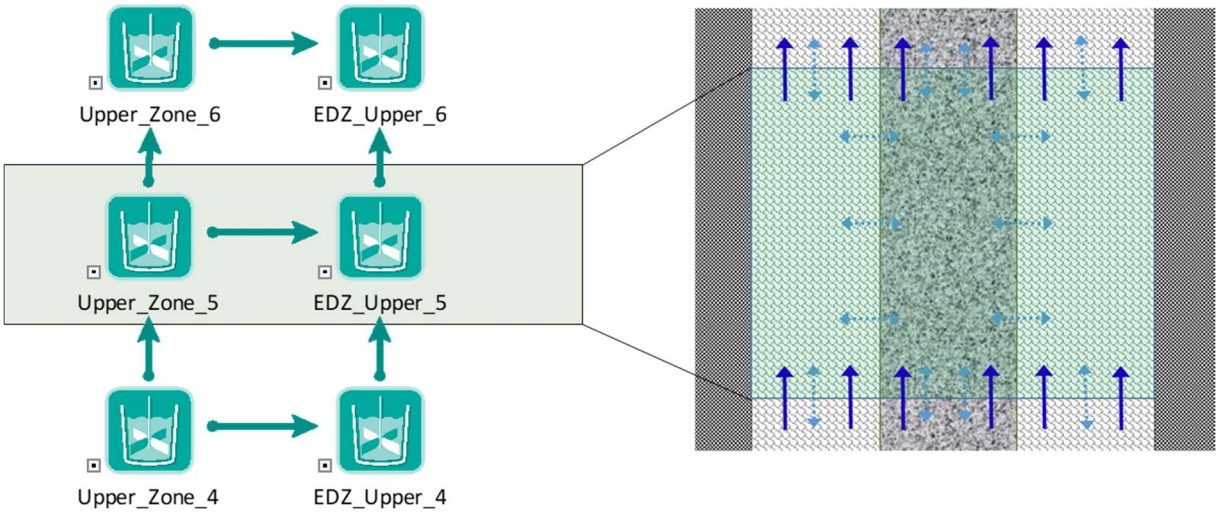

Figure 8-13. Left: Detail of backfilling zone model in GoldSim. Right: The conceptual model of a backfilling zone segment is shown together with diffusive transport arrows (light blue). The vertical dark blue arrows indicate potential advective transport for alternative scenario Sc-2 with vertical flow through the borehole.

The borehole in the backfilling zone is assumed to be filled with crushed rock over the total length. As for the sealing zone segment discussed above, the sketched figure at the right side of Figure 8-13 indicates the different fluxes that are considered in calculating the transport of radionuclides within the backfilling zone:

- Diffusive fluxes between crushed rock backfilling and surrounding EDZ mixing cell (light blue arrows),
- Diffusive fluxes between EDZ cell of the segment and the EDZ cells of the segments directly above and below (light blue arrows), and
- Diffusive fluxes between backfill cell of the segment and the backfill cells of the segments directly above and below (light blue arrows).

For alternative scenarios and calculation cases, in addition to the diffusive fluxes, upwards advective fluxes have been considered for the simulation. Vertical flow is assumed to be divided into flow through the column of EDZ cells and flow through the column of backfilled borehole segments. In **Error! Reference source not found.**, this potential advective transport is indicated by the dark blue arrows. The relation between the two flows is calculated again based on the respective cross sections and assumed hydraulic conductivities of the EDZ and the backfilled borehole.

8.3.4 GoldSim model for fracture simulation

As mentioned above, the intersection of the disposal borehole by a transmissive fracture has been considered as an alternative scenario (Sc-3) with variants for different locations of the fracture intersection along the borehole sequence.

The model to simulate the intersection is shown in Figure 8-14. It is similar to the backfilling zone model in Figure 8-13**Error! Reference source not found.**, but with the additional GoldSim elements simulating the existence of a fracture and the respective fracture flow.

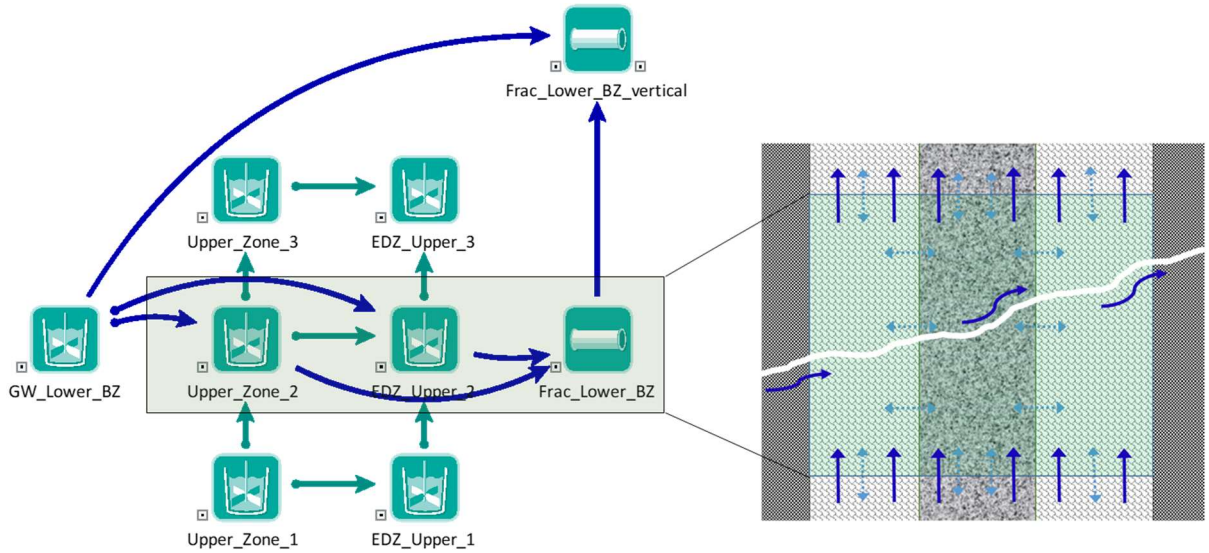

Figure 8-14. Left: Detail of backfilling zone model in GoldSim. In addition to the general transport links inside the backfilling zone, advective groundwater flow into the backfilled borehole and its surrounding EDZ is modelled. The additional inflow leaves via two fractures towards the surface. Right: The conceptual model of a backfilling zone segment is shown with the additional fracture for alternative scenario Sc-3.

In addition to the diffusive and advective transport links considered in the backfilling zone model, advective transport along a fracture is modelled by defining an inflow into one segment of the backfilling zone and its surrounding EDZ.

For modelling purposes, the flow rate in such a horizontal fracture is assumed to be divided equally between the inner borehole and surrounding EDZ. For each time step, this inflow is mixed with the content of these compartments and an outflow with the same flowrate is calculated into a system of an assumed horizontal fracture, intersecting a vertical fracture connected to the aquifer near the surface. A similar sub-model is implemented in the model at other fracture locations in the borehole.

8.3.5 Transport of radionuclides towards drinking water well

The GoldSim model for the deep borehole foresees a direct connection between the uppermost part of the backfilling zone and a near-surface aquifer consisting either of a permeable near surface layer or a near-surface fracture system with higher transmissivity.

In the model (see Figure 8-15), it is assumed that a certain amount of aquifer flow will enter the backfilling zone and its surrounding EDZ. For each time step the content of these two compartments will be mixed and depending on radionuclide content, solid content, water volume and sorption coefficients, flow out of the compartments will advectively transport radionuclides to the aquifer. Conservatively, no sorption is assumed within the aquifer. The length of the aquifer is equal to the distance towards the assumed drinking water well in the near vicinity of the borehole.

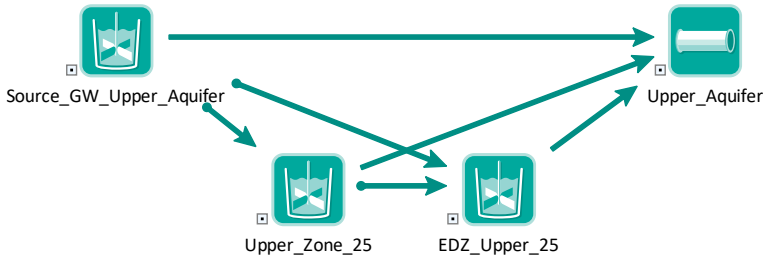

Figure 8-15. Detail of GoldSim model showing the transport links between the near-surface aquifer and the uppermost part of the borehole.

The flow rate of the aquifer is set to the minimum value that is considered reasonable for a drinking water well in Norway. Consequently, the dilution of the potentially contaminated sub-flow from the uppermost borehole segment is at the very low end of the potential range.

The radionuclide concentration of the water flowing out of the aquifer element is used to calculate the dose rate resulting from daily consumption of 3 litres water from that aquifer.

8.4 Mass transport through GoldSim model

The GoldSim model of the deep borehole considers the following processes and steps for mass transport:

- Decay and ingrowth of daughter nuclides (Section 8.4.1)
- Release of activity from the waste form (Section 8.4.2)
- Release of activity from the canisters (Section 8.4.3)
  - Canister failure by general corrosion
  - Localised corrosion – pit hole development
- Solubility limits for elements (Section 8.4.4)
- Sorption of radionuclides on solids (Section 8.4.5)

In the following, examples are given to show how these processes are considered in the GoldSim model.

Subsequently, the main parts of the GoldSim model dealing with transport are described:

- Transport of radionuclides within the near field (Section 8.4.6)
- Transport of radionuclides along the borehole (Section 8.4.7)
  - Transport through borehole and EDZ
  - Transport through fractures

8.4.1 Decay and ingrowth of daughter nuclides

GoldSim considers decay and ingrowth of daughter nuclides. Decay chains have been simplified to only include daughters with a half-life greater than 1 year. The radiation effects of other, shorter-lived daughters have been considered together with those of the immediate parent by adding DCFs (dose conversion factors) of daughters to those of parents and assuming secular equilibrium within each medium.

For the generic DBD safety assessment model, the following decay chains have been considered:

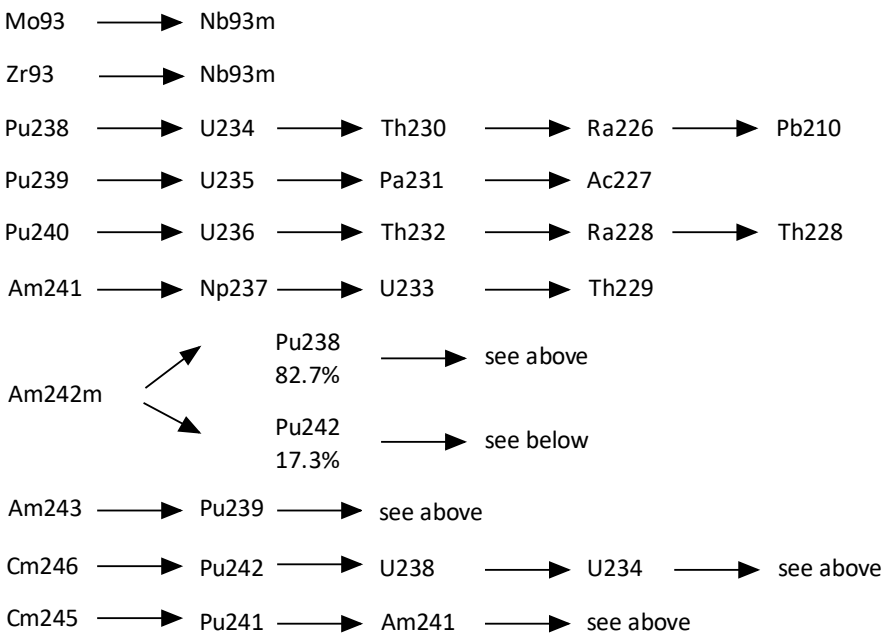

An explicit list of short-lived radionuclides and how they are considered in DCFs is given in the Excel sheet summarizing the data used for the model that has been submitted to NND together with the GoldSim model file.

GoldSim calculates the decay and ingrowth of daughter nuclides automatically based on the defined decay chains and half-lives. For the total inventory of metallic uranium, Figure 8-16 shows the decay and ingrowth of activity for the period of 10 to 1,000,000 years.

The curves for radionuclides that are initially present in the metallic uranium typically start horizontally at the y-axis with their initial activity and then decrease towards lower activity values depending on their respective half-lives. Curves for those radionuclides that are not present in the initial inventory but are produced as daughter products of decaying initial activity start from the bottom line and increase with time. In addition, there are some radionuclides such as Am-241 that are part of the initial inventory and are also daughter products of other radionuclides.

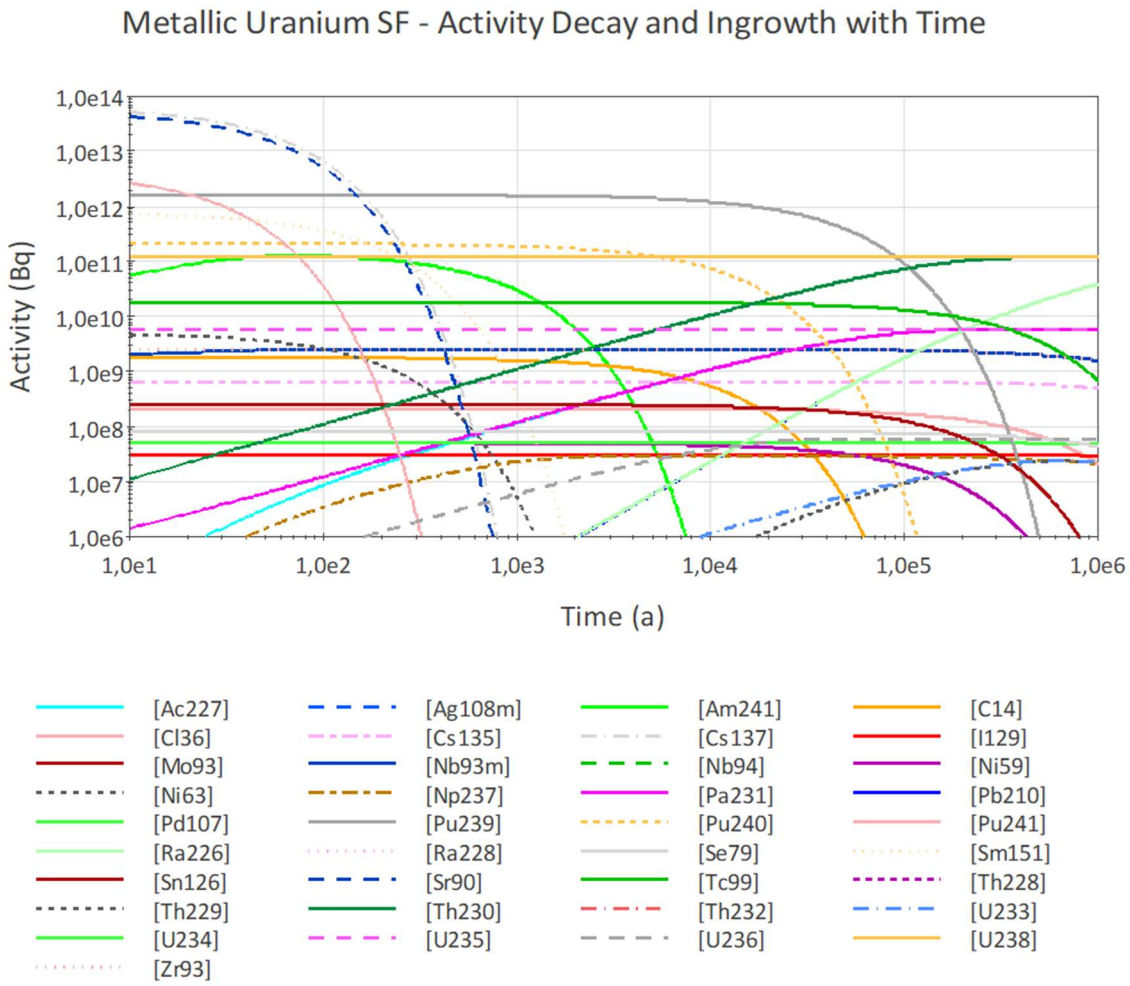

Figure 8-16. Decay and ingrowth of activity along time for the total inventory of metallic uranium (MU).

A typical example of the relative activity development of parent and daughter radionuclide for the case that the daughter radionuclide has a shorter half-life than the parent is given in Figure 8-17**Error! Reference source not found.** for the example of U-235 and Pa-231. In the case of a relatively short-lived daughter nuclide, the activity of both radionuclides is balanced.

The respective example for a situation where the daughter product has a longer half-life than the parent radionuclide is given for the example of Pu-241 and Am-241 in Figure 8-18. As there is also an initial activity of Am-241 in the metallic uranium, the Am-241 curve does not start from zero.

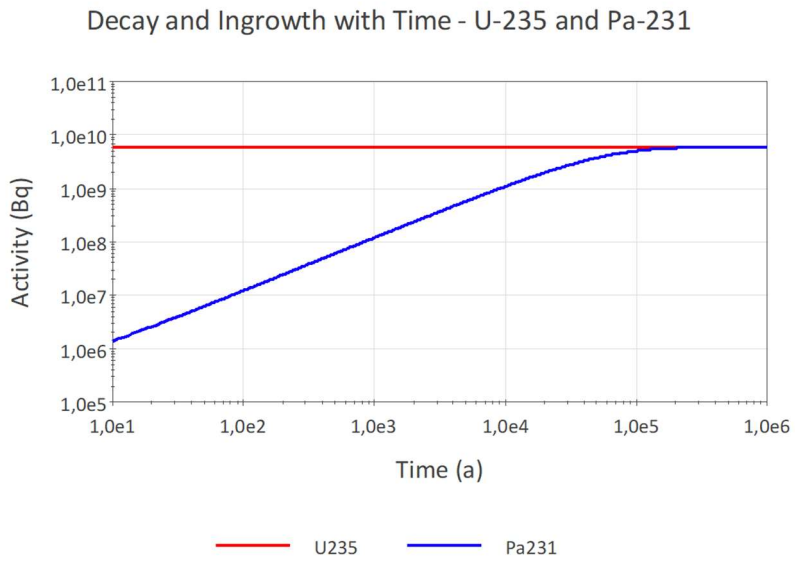

Figure 8-17. Decay and ingrowth of activity along time for U-235 content of MU and Pa-231 as daughter radionuclide.

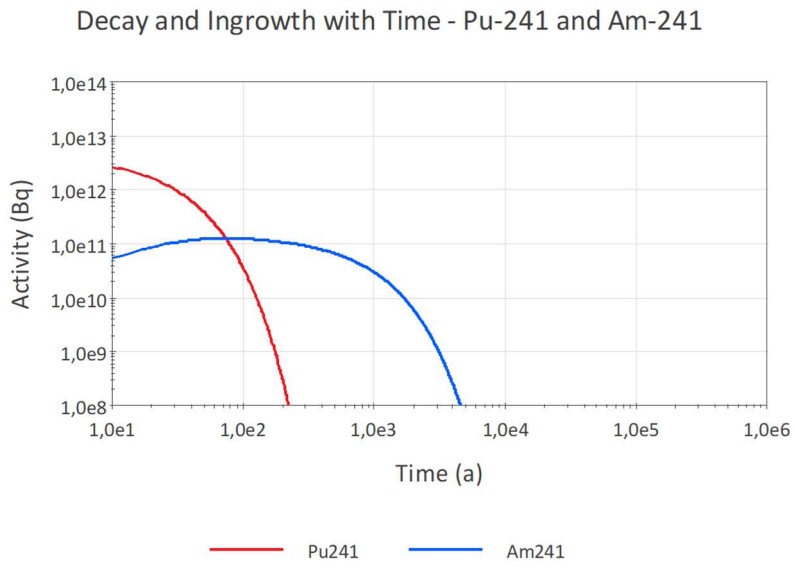

Figure 8-18.0 Decay and ingrowth of activity along time for Pu-241 content of MU and Am-241 as daughter radionuclide.

8.4.2 Release of radionuclides from the waste form

The release of radionuclides from the waste for the different waste streams considered for this generic safety assessment is calculated by the model based on the defined fractional release rates. The fractional release rates have been assumed as listed below (see Appendix I):

Metallic uranium (MU)	0.01/a
Other metal	0.001/a
Zircalloy	0.00004/a
UO_2	0.00002/a

Figure 8-19 visualizes the release of radionuclides with time that results from application of these fractional release rates.

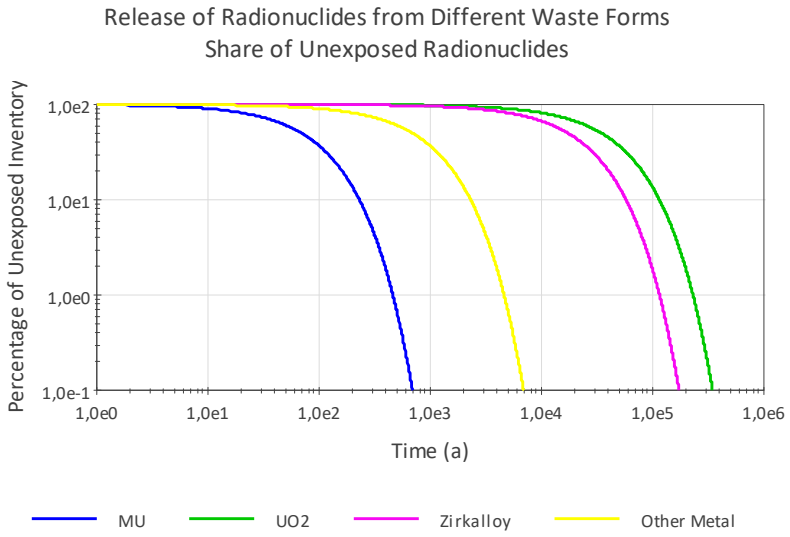

Figure 8-19. Release of radionuclides from the different waste forms according to fractional release rates.

The curves have been calculated by dividing the unexposed mass of a non-radioactive substance by its initial value to demonstrate the consequences from the application of fractional release rates. To model the release of radioactive substances, especially from the waste forms with slow degradation and radionuclides with relatively short half-lives, a major part of the initial activity will have decayed before being released.

Figure 8-20 and Figure 8-21 demonstrate the effect of fractional release and radioactive decay. For Tc-99 with its long half-life of 2.11×10^5 years, the curves look nearly identical to those for non-radioactive release. Only for the very slowly degrading Zircalloy and UO_2, a slightly earlier decrease of non-released activity is observed.

For Sr-90 with its short half-life of 2.88×10^1 years, the decrease of unexposed activity is governed practically exclusively by the radioactive decay. The amount of unexposed mass decreases to zero because the initial mass of Sr-90 has already decayed. The curves for the waste forms with smaller fractional release rates (Zircalloy and UO_2) superimpose each other in Figure 8-21.

Consequently, for the waste forms with slow degradation and release of activity, a large amount of activity is never released from the waste form but decay inside the waste. For Sr-90 the total released activity does not exceed 0.1 % for UO_2 SNF, while about 86% of the initial activity of Tc-99 is being released from the waste form into the surrounding near field.

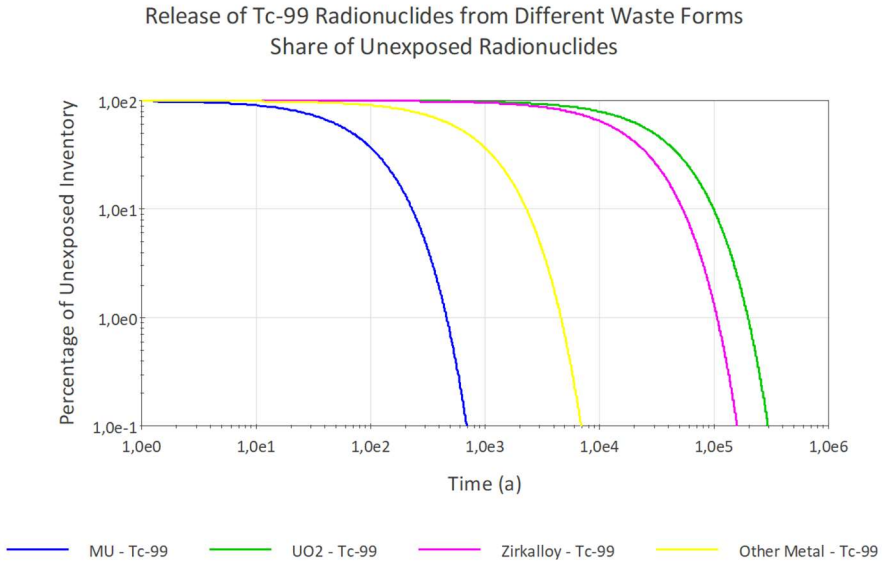

Figure 8-20. Release of Tc-99 (half-life = 2.11×10^{5} years) from the different waste forms according to fractional release rates.

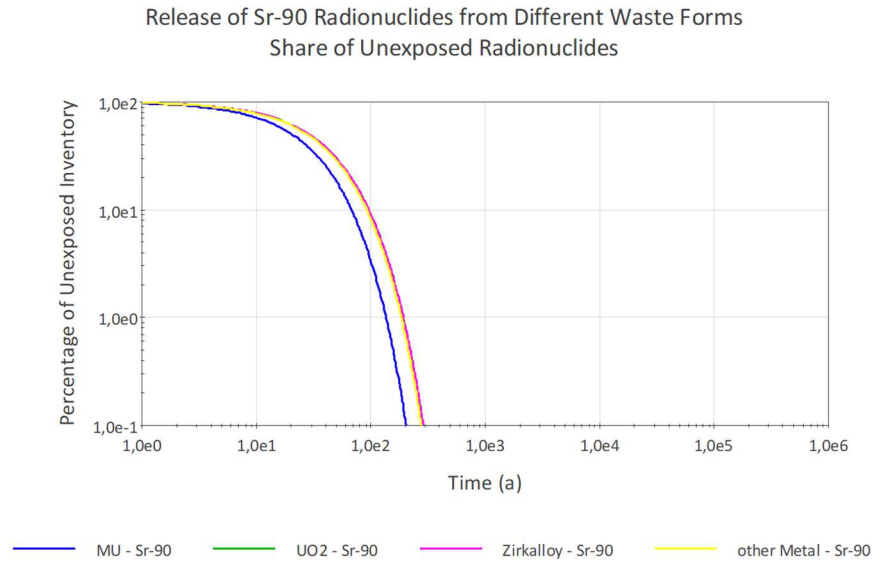

Figure 8-21. Release of Sr-90 (half-life = 2.88×10^{1} years) from the different waste forms according to fractional release rates.

8.4.3 Release of activity from canisters

Canister failure by general corrosion

The canister provides a technical barrier against the release of activity from its interior to the near field surrounding the canister, represented by the bentonite filling the voids between borehole and canister, the surrounding EDZ and the bentonite plugs above and below each canister.

Degradation of the canister is considered in the model by defining a specific time for total canister failure for each canister based on a general corrosion rate of 1 µm/a. A minimum thickness of 50 mm is expected to be required for the canister walls to withstand the mechanical stresses at the bottom of the borehole. Together with the initial thickness of the canister walls of 80 mm this leads to a defined failure time of 30,000 years according to the corrosion rates and mechanical stability investigated in Wunderlich et al. (2021; Sections 4.2 and 4.6). For the model 30,000 years have been assumed for the canisters in the lowermost disposal segment. The lifetimes of the canisters in the disposal zone segments above have been increased in steps of 100 years. This assumes a certain decrease in the expected maximum stress and potentially less aggressive conditions with decreasing depth. Another reason for implementing this stepwise failure is to avoid the failure of all canisters at the same time, which could create a non-realistic release peak.

The model allows the input of any failure time for individual canisters, especially also the definition of immediate failure of all canisters as a worst-case calculation case, that is, as a what-if case.

In addition to general corrosion leading to complete failure of the canister, for alternative evolution, also localised corrosion (creation of a pit hole) has been simulated.

The model allows to define up to 4 pit holes per disposal cell. The localised corrosion rate is assumed to be 0.5 mm/a. The final cross section of the pit hole in the canister is chosen as 1 cm². Once the depth of the pit hole has reached the inner surface of the canister wall, another period of 20 years is assumed for the cross section of the pit hole to develop from 0 to 1 cm².

The chosen values for canister degradation are simple estimates to demonstrate the potential impact of corrosion on the release of radionuclides from the near field for this generic safety assessment and to allow the evaluation of individual parameter for the outcome of the safety calculations by parameter variations.

If immediate failure of the canister is assumed, release of activity is governed exclusively by the release rate of the respective waste form as shown in Figure 8-22**Error! Reference source not found.**.

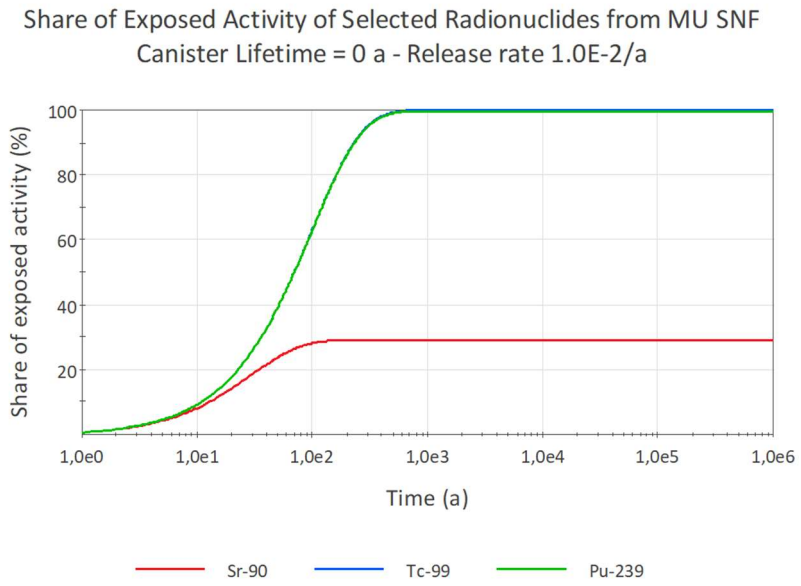

Figure 8-22. Release of Sr-90 (half-life = 2.88×10^{1} years), Pu-239 (half-life = 2.41×10^{4} years) and Tc-99 (half-life = 2.11×10^{5} years) from metallic uranium in case of immediate failure of the canister.

The curves for Pu-239 and Tc-99 are superimposed as both radionuclides have long half-lives so that no significant percentage decays before the waste form has completely degraded. For Sr-90, approximately 70% of initial activity decays before being released from the waste form. If the canister is added as a technical barrier, the release of activity is retarded, as shown in Figure 8-23.

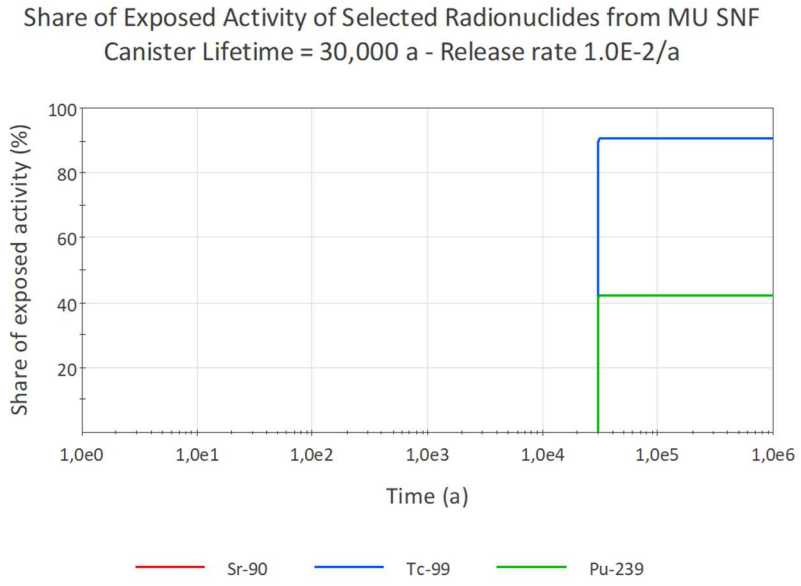

Figure 8-23. Release of Sr-90 (half-life = 2.88×10^{1} years), Pu-239 (half-life = 2.41×10^{4} years) and Tc-99 (half-life = 2.11×10^{5} years) from metallic uranium, canister lifetime is set to 30,000 years.

Because the release rate from the degradation of metallic uranium is very fast, all activity has already been released from the waste form when the canister fails. Accordingly, the total amount of activity that has not already decayed is released at the time of canister failure. Relatively short-lived radionuclides such as Sr-90 decay completely within the canister so that no activity for these radionuclides is being released into the near field.

For other waste forms and radionuclides, the curves vary between the extreme examples shown in Figure 8-22 and Figure 8-23 above.

Each pathway cell represents a disposal borehole segment containing four individual waste canisters. In the model, the respective inventory is assigned to 40 waste packages. This has been done to smooth the failure of the canisters in a specific disposal borehole segment cell and prevent the occurrence of unrealistically sharp release events. The hypothetical 40 packages representing the 4 canisters fail equally distributed over a period of 200 years once the canister lifetime has been reached. Figure 8-24 below shows the failure of these hypothetical packages with time.

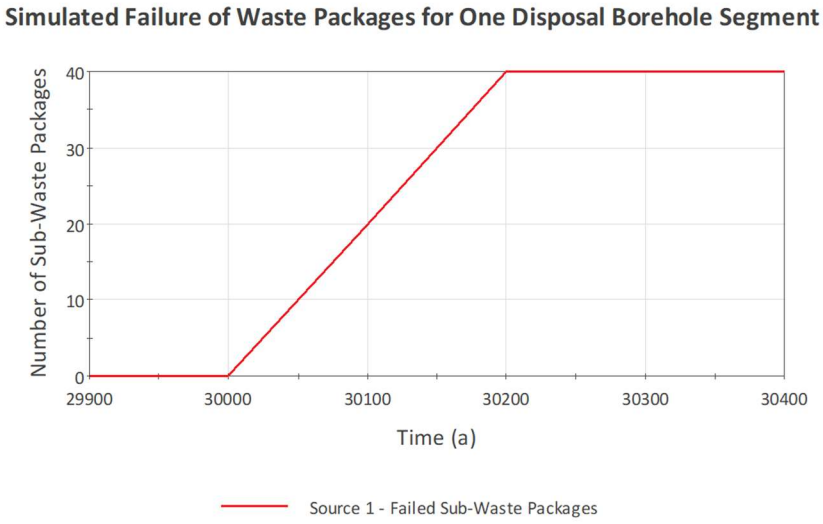

Figure 8-24. Failure of waste packages allocated to one disposal borehole segment.

Localised corrosion

As mentioned above, for alternative scenarios and calculation cases, also the development of a pit hole has been considered and implemented in the model. The effect of a pit hole on the release of activity from the canister is visualized in Figure 8-25 and Figure 8-26. Both figures show the mass of three typical radionuclides with different half-lives that accumulate in a bentonite plug above an assumed canister with metallic uranium due to diffusive fluxes between the bentonite surrounding the canister and the plug.

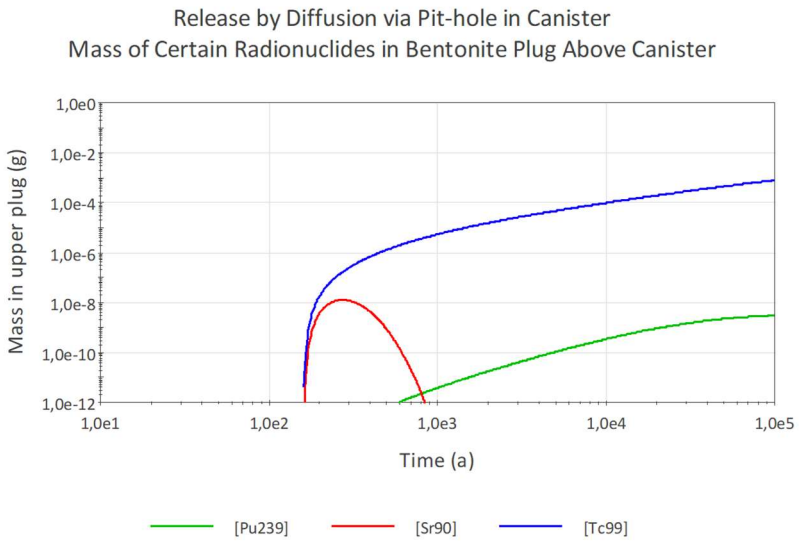

Figure 8-25. Release of Sr-90 (half-life = 2.88×10¹ years), Pu-239 (half-life = 2.41×10⁴ years) and Tc-99 (half-life = 2.11×10⁵ years) from MU. Release by diffusion through pit hole.

The curves have been produced using a small-scale sub-model dedicated to demonstrating release through a pit hole. In one case (Figure 8-25**Error! Reference source not found.**), only the pit hole exists as release pathway and in the other case (Figure 8-26), it is assumed that at the same time as assumed for the development of a pit hole the whole canister fails.

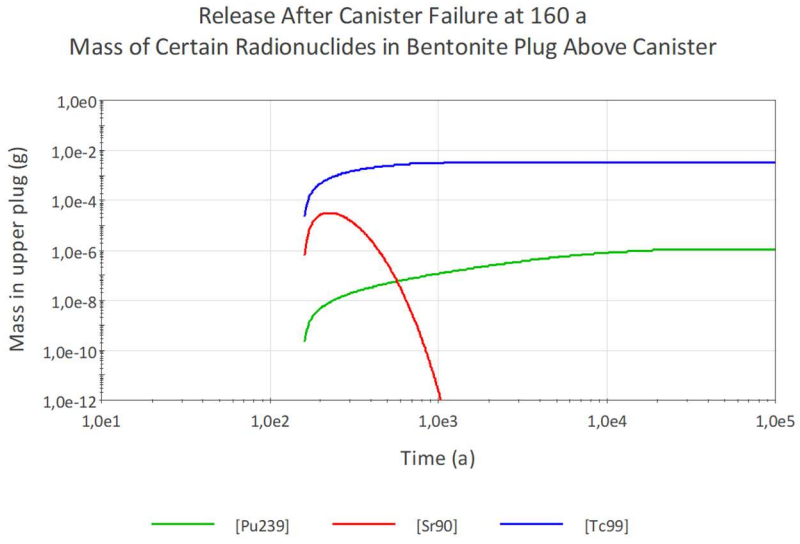

Figure 8-26. Release of Sr-90 (half-life = 2.88×10¹ years), Pu-239 (half-life = 2.41×10⁴ years) and Tc-99 (half-life = 2.11×10⁵ years) from MU, canister lifetime is set to 160 years.

Comparing the results shows that even though there is a significant retardation and decrease of diffusive transport towards the bentonite plug above the canister, a significant amount of activity is released via the pit hole.

8.4.4 Solubility limits

Once the activity has been released from the waste form and the canister has a leakage or has completely failed, further transport depends on the concentration of radionuclides in the liquid inside the canister volume and the surrounding near field.

To demonstrate how GoldSim handles solubility limits, the mass of Pu-239 inside a canister volume and its concentration in the fluid inside is visualized in Figure 8-27.

Figure 8-27 shows the curves for total mass of Pu-239 inside the canister as well as the share of that mass that could not be dissolved due to the solubility limit and, therefore, has precipitated. Due to the large amount of Pu-239 inside the canister cell and the low solubility limit, both curves are nearly identical until approximately 500,000 years. The decrease of Pu-239 mass is governed by its half-life. Similarly, the curves for solubility limit and concentration level are identical during this phase because there is always enough Pu-239 available to be dissolved until the solubility limit is reached.

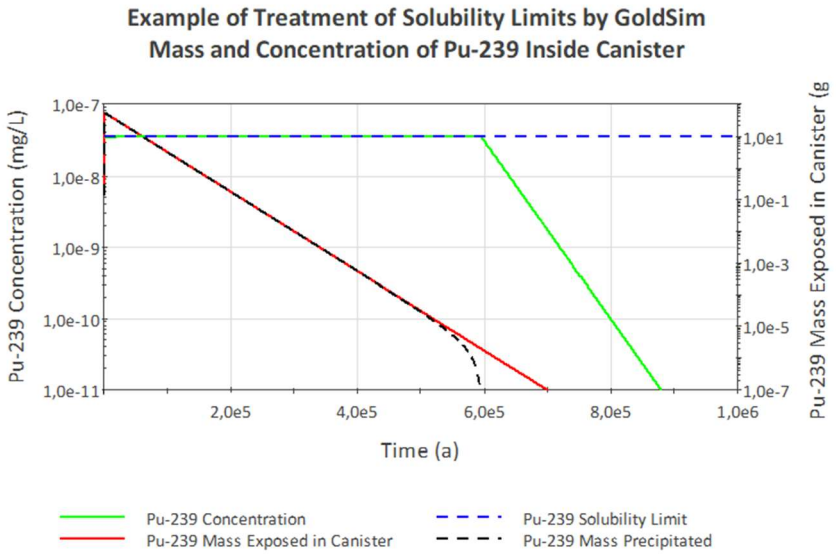

Figure 8-27. Example of application of solubility limits within the GoldSim model. For the example, instantaneous release of activity from the waste form has been assumed.

After approximately 500,000 years, the mass of Pu-239 has decreased so far that a relatively large share of the total mass is being dissolved, which is demonstrated by the strong decrease of the precipitated mass curve. At approximately 600,000 years, all mass inside the canister is in solution, indicated by the decreasing concentration curve.

8.4.5 Sorption of radionuclides on solids

Sorption of radionuclides on solids is often described by the partition coefficient K_d (mL/g), which describes the ratio between the radioelement sorbed on a material (mol/g) and the amount of radioelement remaining in solution (mol/mL).

Partition coefficients tend to lump together several equilibrium and kinetic reactions and are specific to the conditions under which they were measured (e.g., pH, ionic strength, temperature, liquid-to-rock ratio, etc.). Therefore, they offer only a rough prediction of the potential for radionuclide retardation (see, e.g., McKinley & Scholtis 1993). Nonetheless, k_d values are useful in the investigation of limits for the transport of radionuclides. Elements with a k_d value of 0 (e.g., iodine) are not sorbed. For advective transport that means that they move with the velocity of the fluids they are carried on. Elements with a k_d value of 10 or more move

with less than 1% of the fluid velocity. Delays in diffusive transport are significant for radionuclides with strong sorption.

According to Brady et al. (2009), sorption of radionuclides has rarely been measured at temperatures above 25 °C. However, they refer to sufficient experimental data suggesting that most radionuclides released from the bottom of deep boreholes are adsorbed to the bedrock, to the overlying sediments and to the bentonite used to seal the borehole. The exceptions are the isotopes of iodine, chlorine, and carbon (I-129, Cl-36, and C-14).

For this generic safety assessment of the deep borehole disposal, it is conservatively assumed that no radionuclide sorption takes place on the canister material, and neither sorption is assumed for transport through the EDZ or the crystalline bedrock surrounding the deep borehole. Sorption is only assumed for the bentonite in the disposal and in the sealing zones, and for the backfilling material of the backfilling zone.

For the present calculations, k_d values for the materials and typical conditions in deep boreholes were selected.

To demonstrate the effect that sorption has on the transport of radionuclides, a small sub-model has been built, essentially composed of a source cell at the bottom and five sealing zone segment cells on top of the sub-model. Only diffusive transport has been considered within the cells. The uppermost cell is linked via diffusive transport to a sink cell with low radionuclide concentrations.

Figure 8-28 shows the mass of Tc-99 that accumulates with time in the cells above the source due to diffusive transport if no sorption is assumed for Tc. There is obviously some retardation of Tc-99 transport with increasing distance from the source due to the time intensive process of diffusive transport.

At times larger than 100,000 years, the concentration of Tc in all segments is in the same order of magnitude. This is caused by constant transport conditions. For as long as there is precipitated Tc-99 in the source cell, concentration inside the source cell is always equal to the solubility limit leading to constant relations between concentrations inside the sealing zone cells above. Once all Tc-99 mass inside the source cell has been dissolved, concentration and mass of Tc-99 in the sealing zone cells decrease. All radionuclides show very similar curves if no sorption is considered.

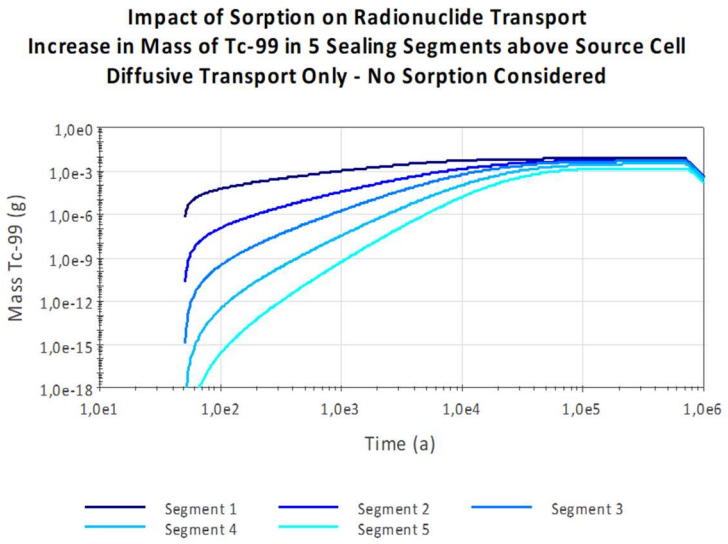

Figure 8-28. Example for the impact of sorption on radionuclide transport. Curves show the mass of Tc-99 that has been accumulated in the different cells by diffusive transport from below. The model consists of a chain of 5 sealing cells above a source cell containing a canister of metallic uranium. Segment 1 is located directly above the source. For these calculations, no sorption of Tc to the sealing cell content has been assumed.

If the assumed k_d value of 45 mL/g for Tc-99 (Freeze et al. 2013) inside the sealing zone is applied, Tc-99 is significantly retarded. Figure 8-29 shows the same curves for the five sealing zone cells.

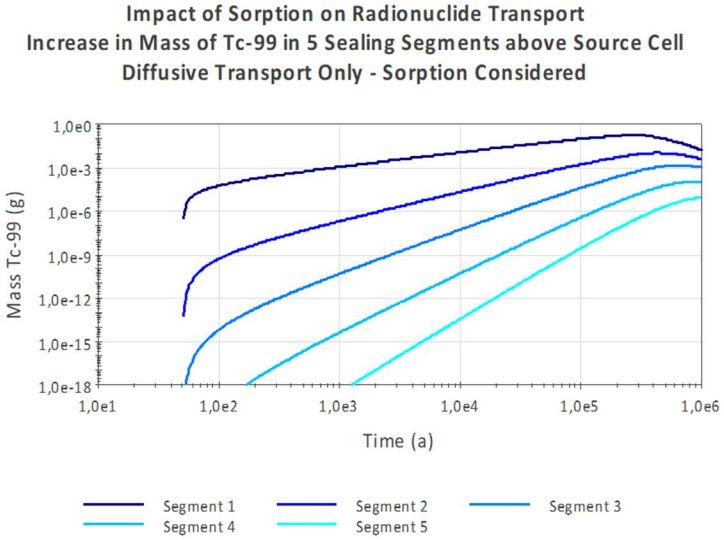

Figure 8-29. Example for the impact of sorption on radionuclide transport. Curves show the mass of Tc-99 that has been accumulated in the different cells by diffusive transport from below. The model consists of a chain of 5 sealing cells above a source cell containing a canister of metallic uranium. Segment 1 is located directly above the source.

For the cell directly above the source cell, the maximum total mass of Tc-99 inside the cell is increased because the mass of Tc-99 sorbed to the solids inside the cell add to the dissolved mass.

The assumed k_d value for technetium in the sealing zone is 45 mL/g. If the same curves are calculated for stronger sorbing radionuclides such as Pu-239, for which a k_d value of 3530 mL/g (Freeze et al. 2013) is assumed for the sealing zone, the retarding effect of sorption is significantly increased. For Pu-239 the maximum mass inside segment 5 is 15 orders of magnitude lower than for segment 1 (Figure 8-30).

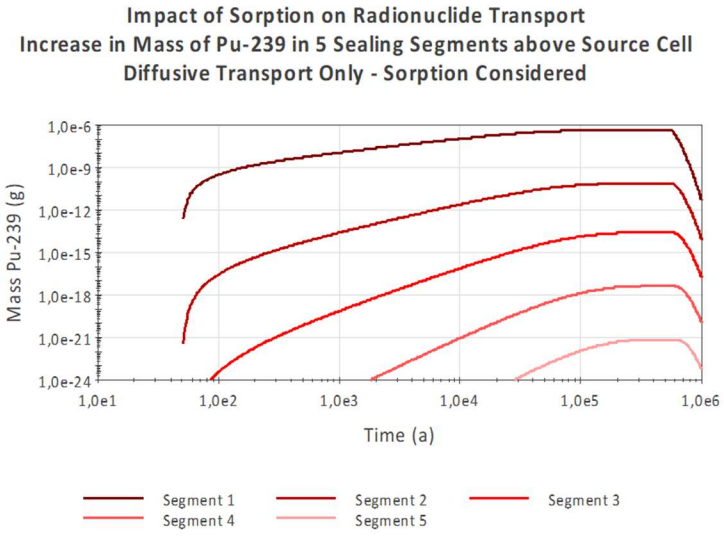

Figure 8-30. Example for the impact of sorption on radionuclide transport. Curves show the mass of Pu-239 that has been accumulated in the different cells by diffusive transport from below. The model consists of a chain of 5 sealing cells above a source cell containing a canister of metallic uranium. Segment 1 is located directly above the source.

8.4.6 Transport of radionuclides within the near field

To visualize transport of radionuclides inside the near field, the lifetime of the canister inside the lowest disposal zone segment has been set to one year, while the lifetime of the other canisters within the disposal zone has been set to values above the calculation period. This allows to assess the release and near field transport without influence from neighbouring cells. The early failure time has been chosen so that also radionuclides with relatively short half-lives can be observed. The release rate for metallic uranium has been increased to 0.1/a to show its influence on the release and transport of radionuclides.

To simulate the complete failure of the canister, the inventory of the source cell has been divided into 40 sub-waste packages that fail stepwise over a period of 200 years.

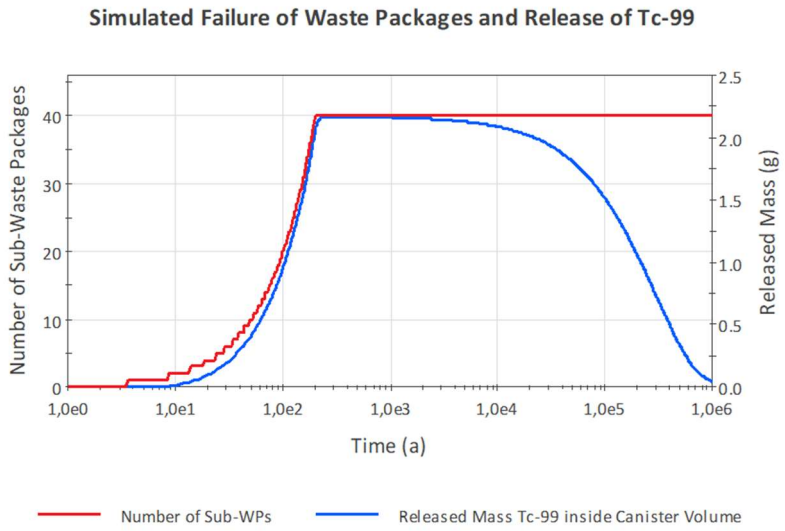

Figure 8-31. Simulated failure of canisters inside one disposal zone segment and Tc-99 mass released from waste form and outer technical barrier (canister).

Figure 8-31 shows the canister failure with time and the mass of Tc-99 that is no longer bound in the waste form of the metallic uranium. For metallic uranium the release or exposure of mass is directly linked to the failure of the canister, because the defined fractional release rate for metallic uranium is very fast. For this example. it has been set to 0.1/a. Only at early times there is a larger gap between the two curves, indicating that some of the activity assigned to the failed waste packages is still bound in the waste matrix.

For UO_2 SNF, the release of mass depends almost exclusively on the much slower fractional release rates for this waste form.

Once the radionuclides are exposed after complete failure of the canister, they are free to migrate either by advective or diffusive transport through the system. The immediate near field of the deep borehole model consists of the source cell, which is modelled as the inner volume of the canister that is filled with water, the surrounding borehole, which is filled with a bentonite/water mixture, and the annular EDZ ring.

For the model it is assumed that after failure of the canister, diffusive transport starts between the inner volume of the canister and the surrounding buffer material. Figure 8-32 shows, as an example, the concentration of Tc-99 inside the water-filled volume of the canister. It increases fast until the solubility limit is reached. Thereafter, the concentration remains constant until so much Tc-99 mass has left the source cell by diffusive transport or radioactive decay that all remaining Tc-99 is dissolved. Then, the concentration decreases further mainly due to decay.

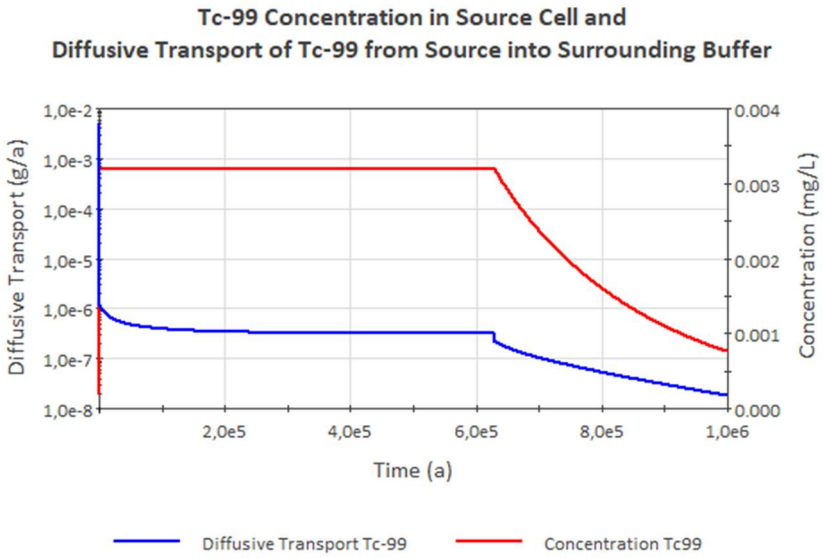

Figure 8-32. Concentration of Tc-99 inside the source cell and diffusive transport of Tc-99 from the source cell into surrounding buffer.

Diffusive transport starts with a peak because concentration differences are very large soon after the release of the source inventory. Over time, concentration along the borehole even out and diffusive transport takes on an almost constant value. When Tc-99 concentration inside the source decreases, the diffusive transport decreases as well.

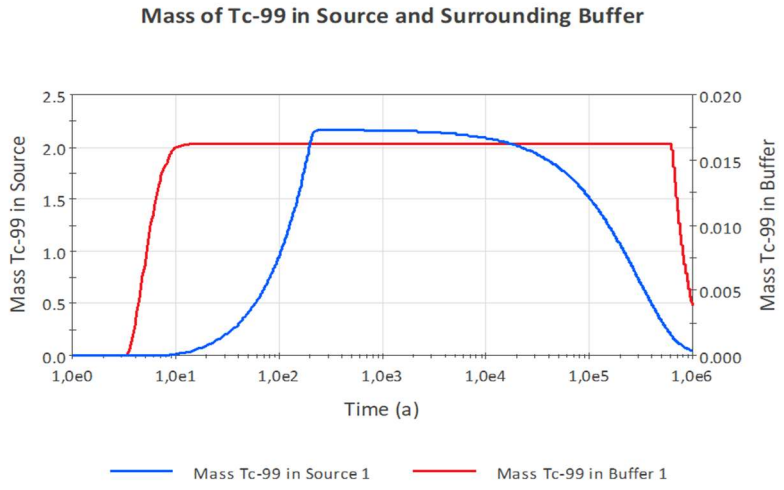

Figure 8-33. Mass of Tc-99 inside the source cell and in the surrounding buffer.

Looking at the mass of Tc-99 accumulating in the buffer surrounding the canister, it is seen that the mass of Tc-99 reaches a constant value very early (Figure 8-33). The mass of Tc-99 inside the buffer decreases long after the Tc-99 concentration inside the source starts to decrease. Concentrations of dissolved Tc-99 in the source, the surrounding buffer and the EDZ reach very rapidly an equilibrium, which until approximately 630,000 years is equal to the solubility limit. Accordingly, Tc-99 mass in the buffer is defined by the volume of water inside the buffer, the solubility limit, and the chosen k_d-value. Tc-99 mass in the EDZ ring around the buffer follows the same curve, but total values are smaller.

8.4.7 Transport of radionuclides along the borehole

Transport along the borehole is visualized by using the same example as used for the description of near-field transport above and presenting curves for the accumulation of radionuclide mass in different buffer cells with increasing distance from the source. Figure 8-34 shows the accumulation of I-129 mass in buffer cells along the disposal zone.

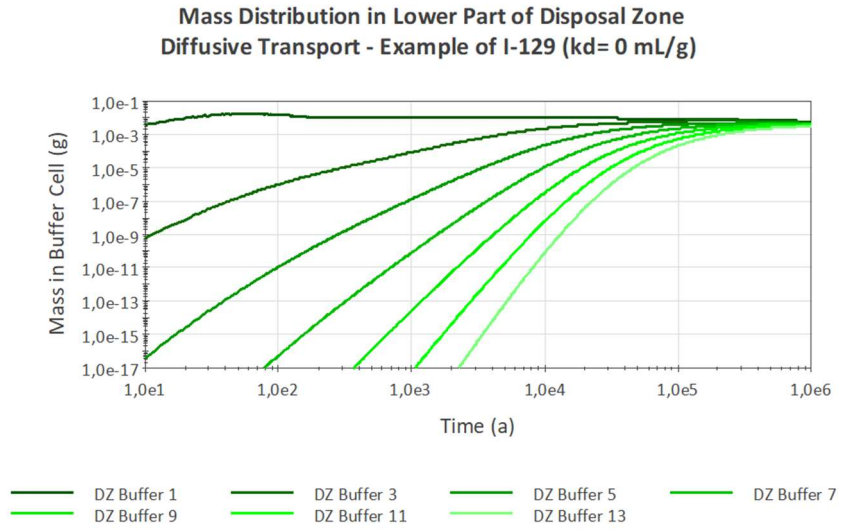

Figure 8-34. Mass of I-129 inside buffer cells along disposal zone of the borehole. The radioactive source is in the lowest Segment 1 (Buffer 1). The approximate length of a segment is 20 m.

The lowest segment is Segment 1 (Buffer 1) and increasing numbers indicate increasing distance from the bottom of the borehole and from the source. Segments 11 and 13 are located near the middle of the disposal zone. The example of I-129 has been chosen as this is a non-sorbing radionuclide with a long half-life. In this case, the observed retardation in mass built-up in the buffer cells with longer distances from the source is caused almost exclusively by the slow diffusive transport. With time, the mass distribution along this section of the disposal zone is more and more levelled out and at the end of the calculation period values for Buffer 1 and Buffer 13 differ by less than a factor 2.

Respective curves for Tc-99 with small k_d-value and relatively long half-life look like those for I-129, although differences in maximum mass values are notably larger.

Curves for the EDZ cells have the same shape but show smaller absolute values.

If a relatively strong-sorbing radionuclide is chosen even with a significantly shorter half-live like Pu-239, the resulting curves differ from this picture. As seen in Figure 8-35, the maximum value reached in the buffer cell about 200 m above the source cell is about 12 orders of magnitude smaller than the mass value in the buffer cell directly at source level.

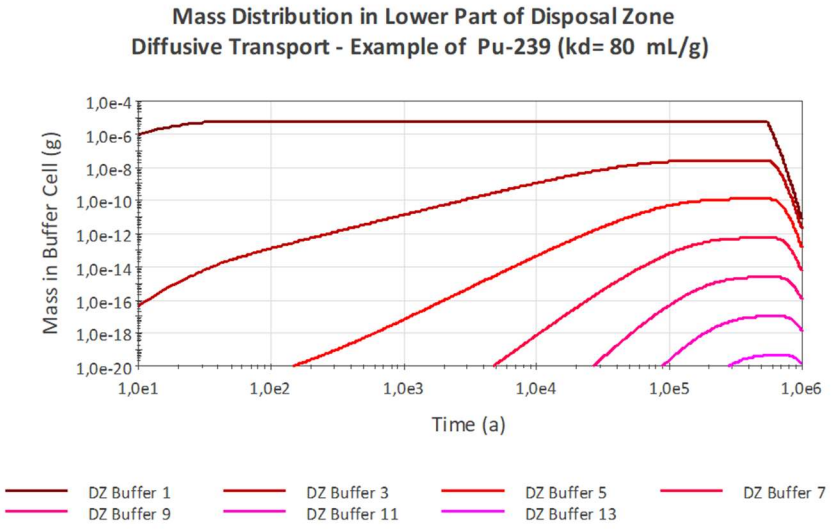

Figure 8-35. Mass of Pu-239 inside buffer cells along disposal zone of the borehole. The radioactive source is in the lowest Segment 1. The approximate length of a segment is 20 m.

The release pathway considered for the normal evolution of the repository is along the entire borehole from the disposal zone until the top of the backfilling zone via diffusive transport. To give an overview of the retardation of radionuclide migration along the borehole, the accumulation of radionuclide mass with time at different locations along the borehole has been compared in one diagram. As in the example discussed above, there is just one source of metallic uranium located at the lowest disposal zone segment and the time of canister failure is set to 1 year after disposal. The locations of the segments are presented in Table 8-2.

Figure 8-36 shows the variation in the accumulation of mass along the borehole for I-129 as an example for a non-sorbing radionuclide. Obviously only a very small share of I-129 mass reaches the uppermost parts of the disposal borehole. For radionuclides with shorter half-lives and/or sorption, this effect is significantly increased.

Table 8-2. Location and depth of the borehole segments.

Location	Borehole segment	Approximate depth of segment (m)
Bottom of disposal zone (DZ)	DZ Buffer 1	3450
Middle of disposal zone	DZ Buffer 22	3010
Middle of sealing zone (SZ)	SZ Sealing 12	2770
Top of sealing zone	SZ Sealing 22	2570
Middle of backfilling zone (BZ)	BZ Backfill 12	1350
Top of backfilling zone	BZ Backfill 22	350

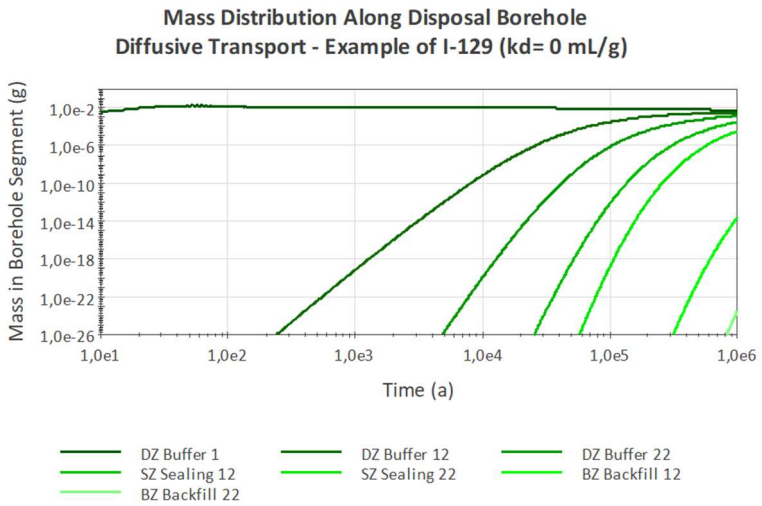

Figure 8-36. Mass of I-129 inside borehole segments along the disposal borehole. The radioactive source is in the lowest Segment DZ Buffer 1.

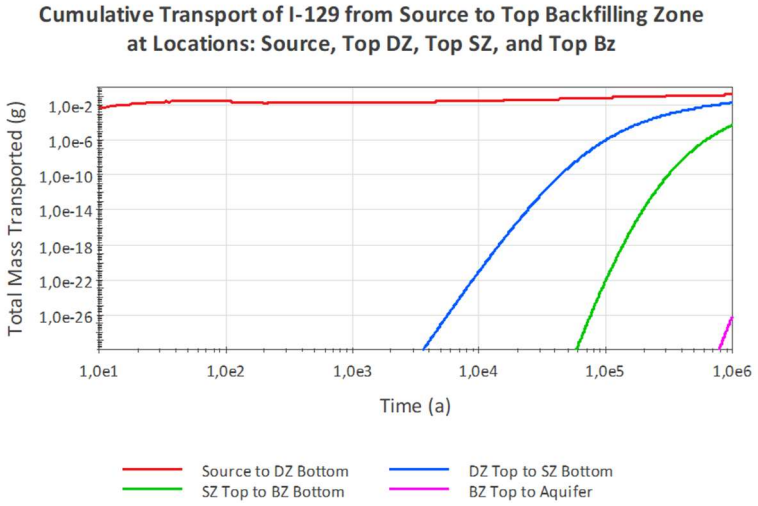

Figure 8-37. Cumulative transport of I-129 from the source at the bottom of the disposal zone towards the surface. Curves show accumulated transport for the source itself and for the top parts of the disposal zone, sealing zone and backfilling zone.

The total mass of I-129 that is transported out of the source cell into the lowest buffer cell is approximately 41% of the initial I-129 inventory of 0.365 g (see Figure 8-37). Cumulative transport from the disposal zone into the sealing zone above amounts to 5% until the end of the calculation period. And only 0.01% are transported to the upper end of the sealing zone after the period of one million years. The mass of I-129 that reaches the surface is more than 20 orders of magnitude lower than the initial inventory.

For Pu-239, the total mass transported by diffusion from the source into the surrounding buffer is already only a very small part of the total inventory in the canister. Of that amount, practically nothing (less than 26 orders of magnitude less) reaches the bottom of the sealing zone above.

Vertical advective flow

If a certain vertical flow of water from the bottom of the borehole to the surface is assumed, then in addition to the diffusive transport advective transport also takes place. Advective transport can have a significant impact on the total transport along the borehole.

To demonstrate the influence of advective transport on the results, for the given example, a vertical flow through the borehole and surrounding EDZ has been assumed that sums up to 1 L/a (Figure 8-38).

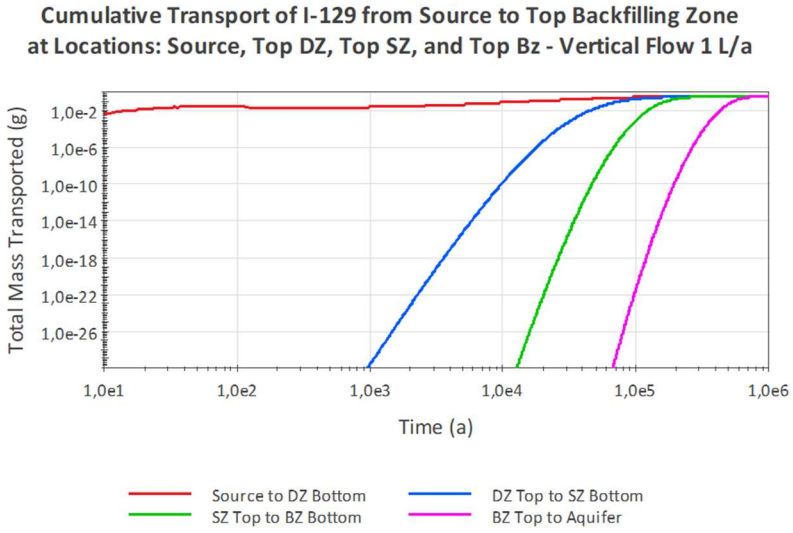

Figure 8-38. Cumulative transport of I-129 from the source at the bottom of the disposal zone towards the surface. Curves show mass transported at the bottom of the disposal zone (location of the source) and to the top parts of the disposal zone, sealing zone and backfilling zone. In addition to diffusive transport, advective transport by an upwards flow of 1 L/a through the borehole has also been assumed.

For I-129, the sum of diffusive and advective transport leads to the transport of the complete inventory from the bottom of the borehole to the surface. Obviously, this transport needs a significant amount of time, but due to the long half-life of I-129 practically the complete inventory reaches the surface.

For Pu-239, as an example of radionuclides with a solubility limit, sorption to solid material and significantly shorter half-life, advective transport also increases the total transport along the borehole. The amount of Pu-239 that is transported out of the disposal zone into the sealing zone increases by 11 orders of magnitude with respect to diffusive transport. However, the total mass entering the sealing zone is still 15 orders of magnitude lower than the mass in the disposal zone and practically no Pu-239 is transported through the sealing zone into the backfilling zone above.

8.4.8 Advective transport through fracture

If Sc-3 with the assumed intersection of the borehole by a transmissive fracture is calculated, this has a significant impact on the retardation of radionuclide transport. For radionuclide transport from the point of intersection with the borehole to the connection with the aquifer at the surface, little to no sorption and dilution has been considered at this state of the generic safety assessment model. Consequently, the concentration of radionuclides in the water entering the aquifer from the vertical fracture system is in a similar order of magnitude as the radionuclide concentration in the water leaving the borehole and the surrounding EDZ at the intersection.

To show the impact that such a shortcut around the normal release pathway along the borehole has on the transport of radionuclides towards the aquifer, the same example has been used as for assessing the impact of vertical flow through the borehole.

For the example mentioned above the following boundary conditions are assumed: direct failure of canister with metallic uranium at the bottom of the disposal zone, fractional release from the waste form is 0.1/a, failure of canister is distributed over the first 200 years, and occurrence of vertical flow through the borehole of 1 L per year.

The dose rates that would be received by a person drinking daily 3 litres of water from the aquifer for this example is shown in Figure 8-39. There are only 3 radionuclides that lead to a significant dose rate for this transport scenario: I-129, Cl-36 and Ni-59. All three do not sorb at the solids within the borehole. Accordingly, their transport velocity is equal to the water flow velocity inside the borehole. By far the most important of these radionuclides is I-129, which carries more than 98% of the maximum dose rate.

For the model calculations that are discussed here, the fracture flow rate entering the borehole cell and the EDZ cell has the same value as the upward flow through the borehole and EDZ. Accordingly, the amount of radionuclide mass transported through the uppermost part of the borehole and through the parallel fracture zone are in the same order of magnitude. Due to the faster transport through the fracture system, the first peak is higher, because radioactive decay reduces the second peak. The shorter the half-lives are, the larger the relative differences in the peaks are. I-129 has the longest half-life, followed by Cl-36 and Ni-59 (Figure 8-40). The difference in travel time accounting for the backfilled part of the disposal borehole is approximately 250,000 years.

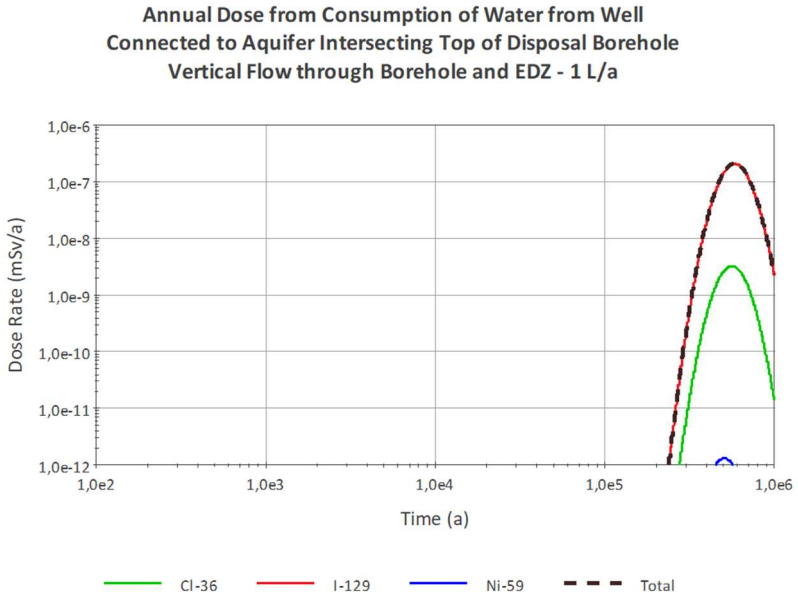

Figure 8-39. Dose rate received from daily consumption of 3 L of water from the aquifer for selected example source term and upwards flow of 1 L/a through the borehole.

If a similar fracture occurred at the middle part of the disposal zone, the results would change considerably. In this case the vertical fracture system connects the middle part of the disposal zone with the aquifer and allows to bypass nearly the complete disposal borehole. Under these conditions, also those radionuclides with strong sorption properties and shorter half-lives manage to reach the aquifer before their activities have decayed.

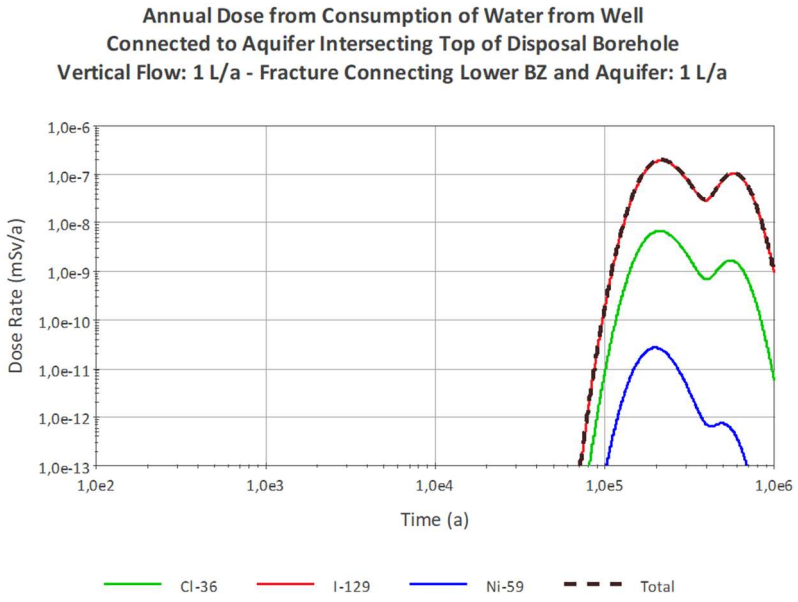

Figure 8-40. Dose rate received from daily consumption of 3 L of water from the aquifer for selected example source term and upwards flow of 1 L/a through the borehole. In addition, there is flow (1 L/a) through a transmissive fracture intersecting borehole at lower backfilling zone.

Figure 8-41 shows the results for this scenario. I-129 and Cl-36 still belong to the most important radionuclides, but the largest part of the dose rate is carried now by radionuclides Pb-210 and Ra-226.

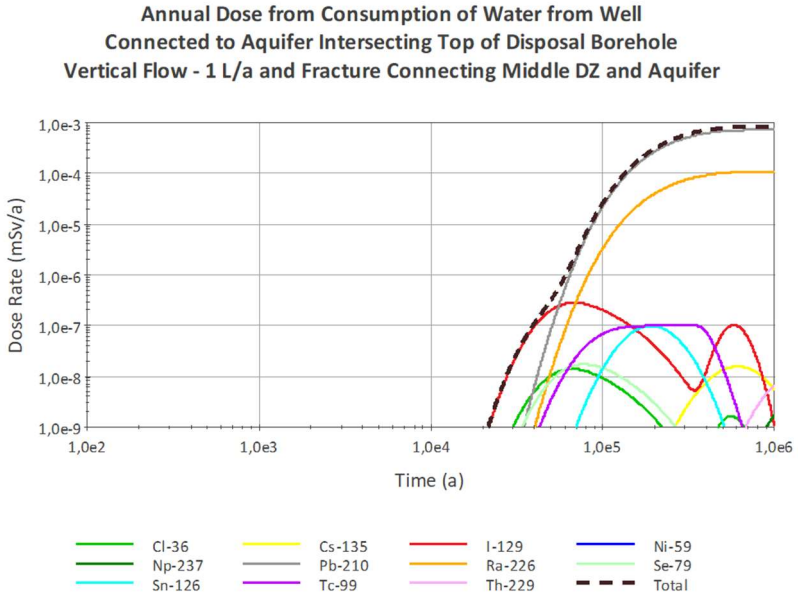

Figure 8-41. Dose rate received from daily consumption of 3 L of water from the aquifer for selected example source term and upwards flow of 1 L/a through the borehole. In addition, there is flow (1 L/a) through a transmissive fracture intersecting borehole at middle disposal zone.

Ra-226 has a long half-life (1.6×10^6 years). The reason why it did not appear in significant concentration in the aquifer for the examples described before is its sorption to solids inside the borehole. Bypassing a major part of the borehole eliminates the respective retardation to a large extent.

In case of Pb-210, which is a daughter of noble gas Rn-222, sorption did not lead to significant retardation in the other scenarios as a zero kd-value has been assigned to Pb-210 (Freeze et al. 2013). However, its half-life is very short (22.3 years), so that longer transport times lead to effective decay of the radionuclide.

8.5 Boundary conditions and assumptions for DBD scenarios

In the following, the main assumptions and parameter values used in the different scenarios and calculation cases are listed. For the normal evolution scenario Sc-1 (Section 8.5.1) this list contains all parameters and boundary conditions that are considered important for the long-term safety assessment. For the description of boundary conditions and assumptions used in the alternative scenarios and calculation cases in Sections 8.5.2. and 8.5.3, only the changes compared with Sc-1 are listed. The complete list of input data is presented in Appendix V.

8.5.1 Normal evolution scenario Sc-1

Inventory

Full Inventory	see Section 2.3 and Appendix V

Aquifer

Intersection with borehole:	yes
Groundwater (GW) velocity:	36.5 m/a
Thickness:	5 m
Flow rate upper aquifer:	production rate well
Distance to well:	100 m

Drinking water scenario

Production rate well:	600 L/h
Water consumption:	3 L/d

Vertical flow through borehole

Constant vert. flow:	no
Flow rate:	0 L/a

Fracture Intersection

Intersection foreseen at:	
Lower backfill zone:	no
Flow rate:	0 L/a
Aperture:	0.15 mm
Middle sealing zone:	no
Flow rate:	0 L/a
Aperture:	0.15 mm

Upper disposal zone:	no
Flow rate:	0 L/a
Aperture:	0.15 mm
Middle disposal zone:	no
Flow rate:	0 L/a
Aperture:	0.15 mm
Lower disposal zone:	no
Flow rate:	0 L/a
Aperture:	0.15 mm

Matrix Diffusion

Applied:	No				
Diffusion depth:	5.0 cm in both directions				
1. Fracture (in Sc-3):	No fracture in Sc-1				
Tortuosity:	1				
Aperture:	0.15 mm,	Width:	1 m,	Length:	10 m,
2. Fracture (in Sc-3):	No fracture in Sc-1				
Tortuosity:	5				
Aperture:	0.15 mm,	Width:	5 m,	Length:	Fracture depth x tortuosity

Solubilities

Solubility limits considered:	yes

Sorption

Sorption considered for:	
Sealing:	yes
Bentonite DZ:	yes
Backfill:	yes
Aquifer:	no
Fracture:	no
EDZ:	no

Canister lifetime

Number of canisters per disposal zone segment:	4
Number of assumed packages per disposal zone segment[1)]:	40
Period for failure of packages inside segment:	200 a
Failure time for first disposal zone segment (deepest of 22):	30,000 a
Time difference for failure of disposal zone segments above:	100 a
Failure time uppermost disposal zone segment (1):	32,100 a
Failure time for last package:	32,300 a

1) Increase of waste packages (10 packages per canister) for calculations to achieve smoother and more realistic values for activity release and prevent too sudden changes of activities for calculations.

Localised corrosion

For each of the 22 disposal zone source elements 0 to 4 pit-hole leaks have been defined.

Pit hole (x) = 0, for x = 1 to 22

Release of radionuclides from waste form

Assumption of fixed fractional release rates for different waste forms (Appendix I):

Metallic uranium (MU):	0.01/a
Other metal:	0.001/a
Zircalloy:	0.00004/a
UO_2:	0.00002/a

Sequence of waste canisters in disposal zone

It is assumed that all canisters containing metallic uranium will be disposed of in the lower part of the disposal zone, while the canisters containing UO2 spent fuel will be placed in the upper part of the disposal zone. The idea behind this assumption is to place the waste form with the short fractional release rates as deep as possible.

13 disposal zone segments with: MU	emplacement location	01 to 13
9 disposal zone segments with: UO_2 SNF	emplacement location	14 to 22

Characteristics of EDZ

For the model calculations, rather large values were chosen for the thickness of EDZ and its porosity as this is usually a conservative assumption. The expected thickness of seriously affected EDZ is significantly smaller (few centimetres) and the porosity probably should be similar to the expected porosity of the host rock (1% or less).

Thickness of EDZ:	35 cm
Porosity of EDZ:	4.5 %

Sc-1 Calculation cases

For these cases, the following changes are made:

Sc-1-C1 - Changed canister sequence in borehole

9 disposal zone segments with: UO_2 SNF	emplacement location	01 to 09
13 disposal zone segments with: MU	emplacement location	10 to 22

Sc-1-C2 - No solubility limits

Solubility limits considered: no

Sc-1-C3 - No sorption

Sorption considered for:	
Sealing:	no
Bentonite DZ:	no
Backfill:	no

Sc-1-C4 – Direct failure of canisters

Number of canisters per disposal zone segment:	4
Number of assumed packages per disposal zone segment:	40
Period for failure of packages inside segment:	200 a
Failure time for first disposal zone segment (deepest of 22):	0 a
Time difference for failure of disposal zone segments above:	0 a
Failure time uppermost disposal zone segment (1):	0 a
Failure time for last package:	200 a

8.5.2 Alternative scenario Sc-2 Vertical flow

For Sc-2, almost all boundary conditions and assumptions are chosen equal to the normal evolution scenario Sc-1. The only difference is the assumption that a vertical flow along the borehole will occur that causes advective transport from the bottom of the disposal zone towards the surface, where the borehole is intersected by the assumed aquifer.

Vertical flow through borehole

Constant vert. flow:	yes
Flow rate:	1 L/a

Sc-2 Calculation cases

For different calculation cases mentioned above, in addition to the vertical flow through the borehole, the boundary conditions will be changed as indicated below.

Sc-2-C1 - Reverse order of canister emplacement in borehole

13 disposal zone segments with: UO_2 SNF	emplacement location	10 to 22
9 disposal zone segments with: MU	emplacement location	01 to 09

Sc-2-C2 - No solubility limits

Solubility limits considered:	no

Sc-2-C3 - No sorption

Sorption considered for:	
Sealing:	no
Bentonite DZ:	no
Backfill:	no

Sc-2-C4 – Localised corrosion

Pit hole (22) = 1

Sc-2-C5 Direct failure of canisters

Number of canisters per disposal zone segment:	4
Number of assumed packages per disposal zone segment:	40
Period for failure of packages inside segment:	200 a
Failure time for first disposal zone segment (deepest of 22):	0 a
Time difference for failure of disposal zone segments above:	0 a
Failure time uppermost disposal zone segment (1):	0 a
Failure time for last package:	200 a

8.5.3 Alternative scenario Sc-3 Fracture

Compared with Sc-1, a reference calculation case for each of the variants of Sc-3, Sc-3.1–Sc-3.5, is defined by setting the respective intersection location to **yes** in the list of parameters (see below).

Fracture Intersection

Sc-3.1

Intersection foreseen at:	
Lower backfill zone:	**yes**
Flow rate:	1 L/a
Aperture:	0.15 mm

Sc-3.2

Middle sealing zone:	**yes**
Flow rate:	1 L/a
Aperture:	0.15 mm

Sc-3.3

Upper disposal zone:	**yes**
Flow rate:	0.1 L/a
Aperture:	0.15 mm

Sc-3.4

Middle disposal zone:	**yes**
Flow rate:	0.1 L/a
Aperture:	0.15 mm

Sc-3.5

Lower disposal zone:	**yes**
Flow rate:	0.1 L/a
Aperture:	0.15 mm

Calculation cases for Sc-3.3

For one of the variants of Sc-3 (Sc-3.3), the occurrence of a fracture in the upper disposal zone, also additional calculation cases are analysed to address the impact of several boundary conditions (see below). For these cases, values for the fracture in the upper disposal zone are set to:

Upper disposal zone:	yes
Flow rate:	0.1 L/a
Aperture:	0.15 mm

Sc-3.3-C1 - Changed canister sequence in borehole

13 disposal zone segments with: UO_2 SNF	emplacement location	10 to 22
09 disposal zone segments with: MU	emplacement location	01 to 09

Sc-3.3-C2 - No solubility limits

Solubility limits considered:	no

Sc-3.3-C3 - No sorption

Sorption considered for:	
Sealing:	no
Bentonite DZ:	no
Backfill:	no

Sc-3.3-C4 – Localised corrosion

Pit hole (22) = 1

Sc-3.3-C5 – Direct failure of canisters

Number of canisters per disposal zone segment:	4
Number of assumed packages per disposal zone segment:	40
Period for failure of packages inside segment:	200 a
Failure time for first disposal zone segment (deepest of 22):	0 a
Time difference for failure of disposal zone segments above:	0 a
Failure time uppermost disposal zone segment (1):	0 a
Failure time for last package:	200 a

8.6 Results and discussion – DBD

This section presents the dose rate results from the calculations for the deep borehole disposal. In general, the results are presented by displaying the calculated dose rates that result from the drinking water scenario. In cases where information from these graphs is limited, additional graphs on radionuclide transport along the borehole etc. are used to further explain the processes that might take place during the evolution of the disposal facility.

Analysis on the sensitivity of the model towards the assumptions made for parameters or boundary conditions is partly given based on the results of calculation cases, partly in the section(s) on sensitivity analysis.

8.6.1 Results for the normal evolution scenario – Sc-1

Reference case – Sc-1

As discussed above (Section 8.2.4) diffusive transport through the sealing zone is extremely slow. Even non-sorbing radionuclides such as I-129 hardly reach the top of the disposal borehole and thereby the biosphere in measurable amounts. Figure 8-42 shows the potential dose rates caused by drinking contaminated water from the drinking water well. I-129 is practically the only radionuclide that causes any dose. Apart from I-129 only small traces of Cl-36 appear at the surface near to the end of the calculation period.

Accordingly, the radiological impact from the deep borehole repository for the normal evolution is practically non-existent.

To demonstrate how transport of radionuclides is being retarded by diffusive upwards transport, Figure 8-43 shows the distribution of I-129 mass with time along the complete sealing zone. Retardation is already substantial after passing the sealing zone even for the non-sorbing I-129. Strongly-sorbing radionuclides or those with relatively short half-lives do not reach the top of the sealing zone at all. Release of I-129 is further retarded by diffusive transport processes through the backfilling zone on top of the sealing zone.

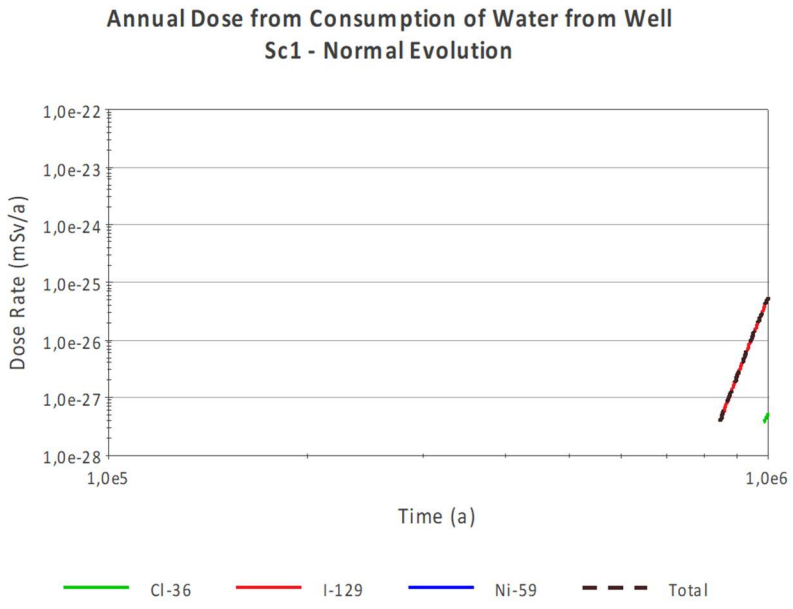

Figure 8-42. Dose rate received from daily consumption of 3 L of water from the aquifer for the Sc-1 reference case.

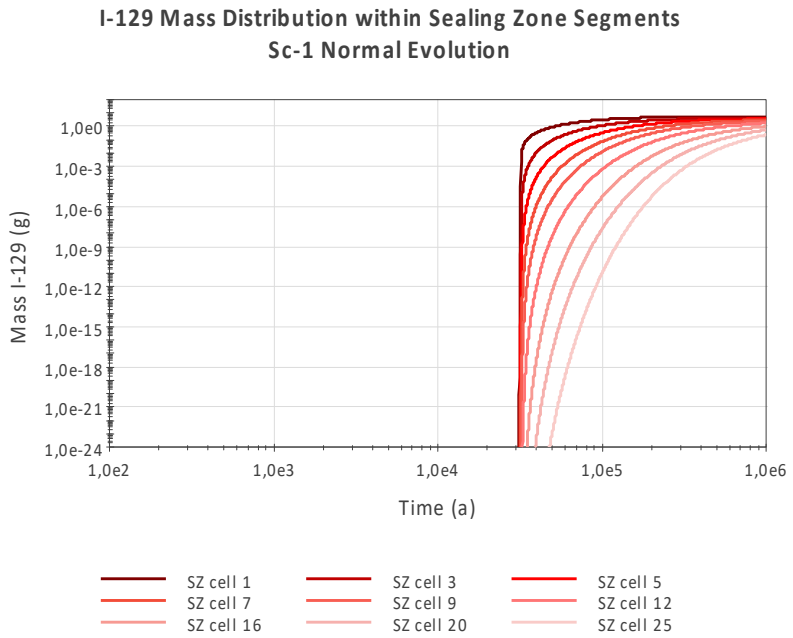

Figure 8-43. Mass of I-129 inside sealing zone cells along the sealing zone of the borehole for Sc-1 reference case. Cell 1 is the lowest sealing zone segment and cell 25 the topmost one. Each cell represents a 20-m segment of the sealing zone.

Results of the calculation cases for Sc-1

As calculation cases, the following changed boundary conditions have been considered:

- Sc-1-C1 Reversed emplacement order of canisters in borehole
- Sc-1-C2 No solubility limits
- Sc-1-C3 No sorption
- Sc-1-C4 Direct failure of all canisters

Sc-1-C1 Reversed canister sequence in borehole

If the emplacement order of canisters inside the borehole is reversed, transport towards the surface is even more retarded and within the accuracy of the calculations, no radionuclides reach the aquifer resulting in zero dose for the drinking water biosphere model.

For this calculation case, the UO_2 SNF canisters are placed approximately 260 m further below the position assumed in Sc-1 reference case. This retards even more the transport from these canisters towards the surface. As more than 99% of the total activity of the radioactive waste is carried by the UO_2 SNF, it means that the transport distance has been increased by 260 m for a major part of the disposed waste, which also represents the main source for I-129 and Cl-36. Accordingly, less activity is transported towards the surface within the calculation period and consequently a zero-dose rate is calculated for the calculation period of one million years.

Sc-1-C2 No solubility limits

In general, diffusive transport is accelerated if there are no solubility limits, because in the beginning, concentration differences inside the near field are larger than for limited solubilities, which increases the diffusively transported mass.

For I-129 no solubility limit has been defined and for Cl-36 the limit is very high. Therefore, there is no difference with respect to the results for Sc-1 reference case for these two radionuclides. For other radionuclides, for which transport has been limited by solubility limits, the changed conditions of unlimited solubility are not sufficient to accelerate diffusive transport enough to let them reach the surface before the end of the calculation period.

Sc-1-C3 No sorption

If there were no sorption inside the borehole or if the respective k_d-values were much lower than expected, this would have no effect on the transport of I-129 and Cl-36 as, for both, no sorption is considered anyway. However, under these conditions, some more radionuclides would reach the aquifer and contribute to the estimated dose rate. The radionuclides contributing most would be Pb-210 and Th-229, which each would cause about ten times the dose that is carried by I-129. The dose rate curves for this calculation case are shown in Figure 8-44.

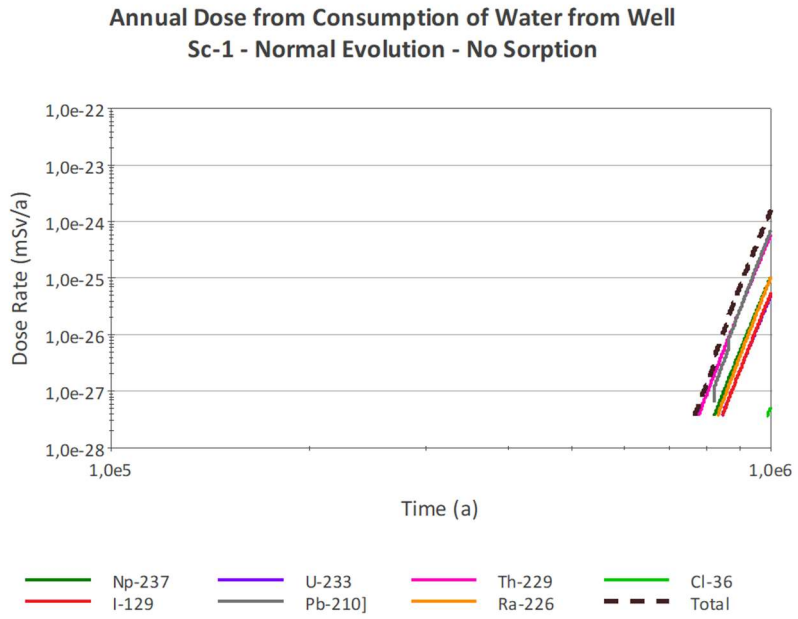

Figure 8-44. Dose rate received from daily consumption of 3 L of water from the aquifer for calculation case Sc-1-C3 no sorption.

Sc-1-C4 Direct failure of all canisters

At first glance, the assumption of direct failure of all canisters directly after closure seems to be extremely conservative. Regarding the durability of the canisters, this is certainly true but as the DBD system is a multi-barrier concept the impact on the dose results is rather limited. The main reason is that most of the inventory is bound to UO_2 SNF, which has very low fractional release rates. Consequently, the early failure of a canister certainly affects the early release of radionuclides from the near field so that transport processes start

respectively earlier. The general retardation of radionuclide transport to the surface, however, is governed by fractional release from the UO_2 SNF waste form and the restrictions regarding solubility constraints, sorption, and the diffusive transport process.

The dose rate curves resulting from the calculation case of direct failure of all canisters are essentially the same as for the normal evolution scenario. Only I-129 and Cl-36 reach the aquifer within the calculation period. Compared with normal failure of canisters around 30,000 years after closure, the curves for I-129 and Cl-36 are shifted by approximately 30,000 years to earlier times as expected (Figure 8-45).

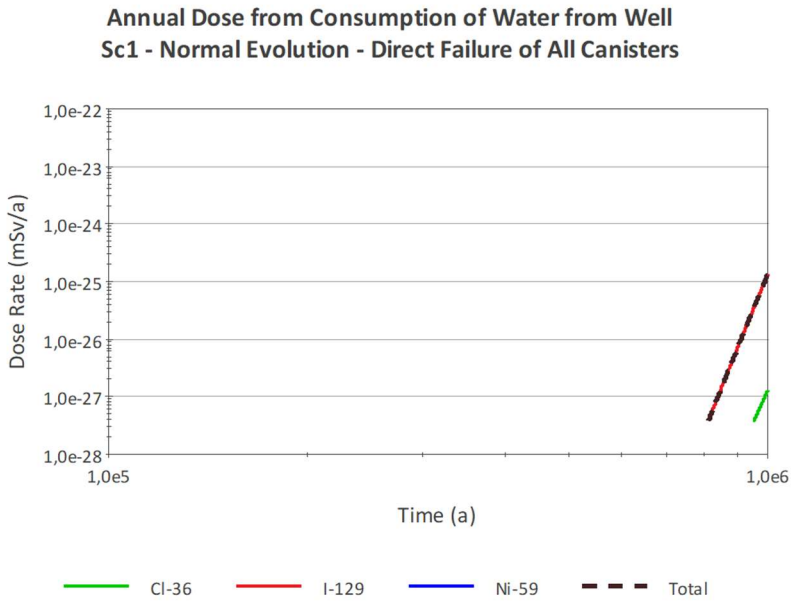

Figure 8-45. Dose rate received from daily consumption of 3 L of water from the aquifer for the normal evolution scenario Sc-1, calculation case Sc-1-C4 direct failure of all canisters.

Summary of the normal evolution scenario – Sc-1

It is summarized that for the reference case parameter set of the normal evolution scenario as well as for the evaluated calculation cases with changed boundary conditions, there is practically no radiological impact.

While the changed boundary conditions and assumptions assessed by the calculation cases have an impact on the results, the total amount of radionuclides transported to the biosphere is so small that no significant dose rate results from the release of activity.

The main reason for the very limited transport of radionuclides through the deep borehole model towards the surface is the slow diffusive transport. Once radionuclide concentrations have equalised along the pathways through the disposal zone, sealing zone and backfilling zone, concentration differences between adjacent cells along the pathways become very small.

8.6.2 Results for alternative scenario Sc-2 Vertical flow

It has been discussed above (Sections 8.1.1 and 8.3.1) that the probability of a significant vertical flow from the bottom to the top of the borehole and its surrounding EDZ is extremely low. Nonetheless, there might be some potential for such a flow even though site investigation work will be directed to avoid the selection of such a site.

In any case, it is necessary to assess the effect such flow might have on the potential radiological impact from a deep borehole repository to evaluate the importance of the hydrogeological properties of a future site and demonstrate the importance of the diffusion barrier provided by the buffer in the disposal and sealing zones and backfill in backfilling zone.

Reference case – Sc-2

Figure 8-46 shows the dose rate curves that result from calculation of the reference data set for Sc-2, which is the same as for Sc-1, but includes a constant vertical flow through the borehole and surrounding EDZ of 1 L/a allowing transport by advection in addition to diffusion.

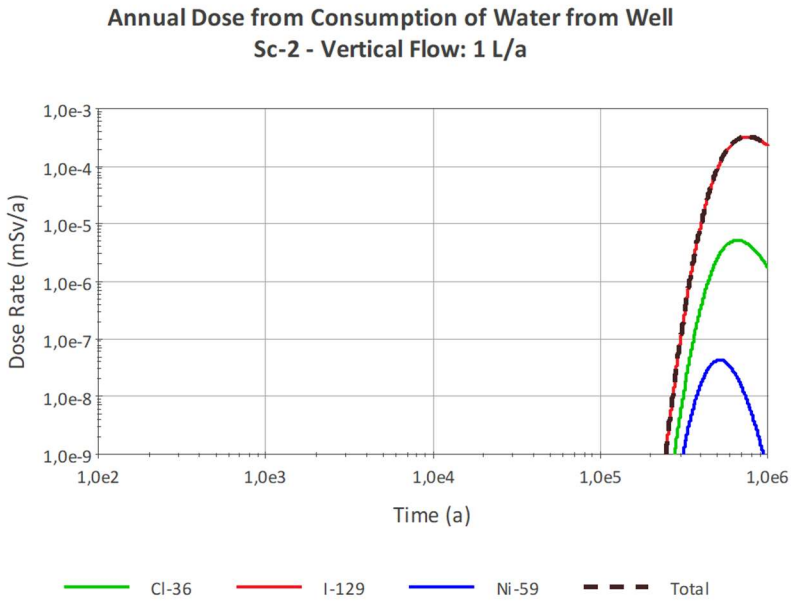

Figure 8-46. Dose rate received from daily consumption of 3 L of water from the aquifer for Sc-2, assuming constant vertical flow of 1 L/a.

Compared with the Sc-1 reference case, it is obvious that the additional advective transport through the borehole causes a dramatic increase of the dose rates related to I-129, Cl-36 and Ni-59 by more than 20 orders of magnitude. Apart from these three very mobile radionuclides (high solubility, limited sorption), which also have rather long half-lives, no other radionuclides reach the aquifer in sufficient amounts to contribute notably to the total dose rate. Compared with the Sc-1 reference case, the front of radionuclide migration advances further along the sealing zone column for all radionuclides, but retardation is still so strong that no significant transport out of the sealing zone into the backfilling zone above takes place for the other radionuclides. For instance, for Pu-239, a very small mass advances as far as 120 m into the sealing zone for Sc-1, while for Sc-2, the same amount of Pu-239 migrates approximately 180 m upwards through the sealing zone.

The dose rate maxima occur at earlier times for radionuclides with shorter half-lives. This is due to the evolution of concentration inside the aquifer reflecting the radionuclide transport that is superimposed by decrease of concentration due to decay.

Results of the calculation cases for Sc-2

In the calculation cases, the following changed boundary conditions have been defined:

- Sc-2-C1 Reverse order of canister emplacement in borehole
- Sc-2-C2 No solubility limits
- Sc-2-C3 No sorption
- Sc-2-C4 Localised corrosion
- Sc-2-C4 Direct failure of all canisters

The impact of these changed boundary conditions on the results for potential radiological impact is discussed below.

Sc-2-C1 Reverse order of canister emplacement in borehole

For this calculation case, the UO_2 SNF canisters are placed in the bottom part of the disposal zone and thereby approximately 260 m lower than in the Sc-1 reference case.

As discussed in connection with Sc-1, more than 99% of the total activity of the HLW is carried by the UO_2 SNF which now must travel additional 260 m to reach the aquifer. Figure 8-47 shows that a dose rate of $1 \cdot 10^{-9}$ mSv/a is reached later than for the reference parameter set of Sc-2, because the amounts of radionuclides released from the canisters in the upper part of the disposal zone is smaller.

At later times, approximately 600,000 to 700,000 years after closure the curves for I-129 and Cl-36 show a point of inflection indicating the arrival of radionuclides from the lower disposal zone, where UO_2 SNF canisters are emplaced.

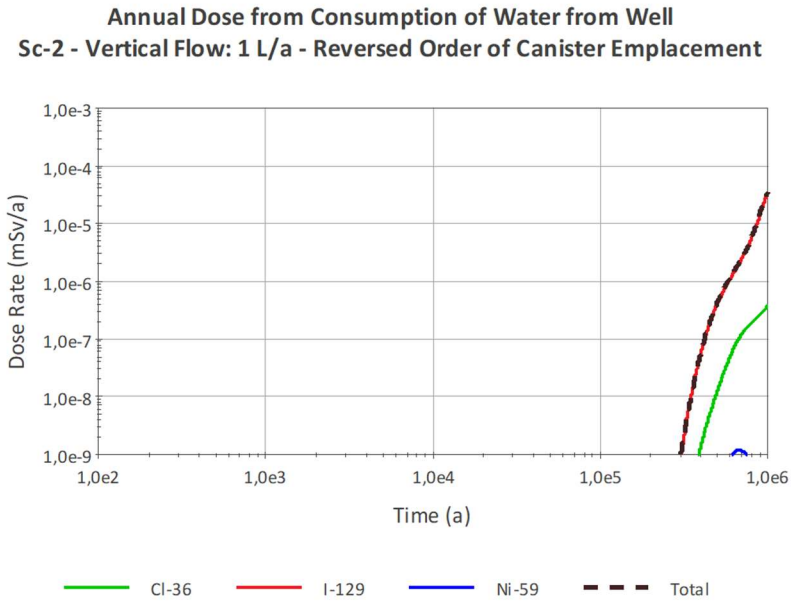

Figure 8-47. Dose rate received from daily consumption of 3 L of water from the aquifer for Sc-2, constant vertical flow of 1 L/a – Sc-2-C1 reverse order of canister emplacement. All UO_2 SNF canisters at the bottom of the disposal zone.

Sc-2-C2 No solubility limits

As discussed in relation to the corresponding calculation case for the Sc-1, in general, ignoring solubility limits leads to an increase in diffusive transport, but even more so for advective transport because radionuclide concentrations are significantly increased.

For I-129 and Ni-59 no solubility limit has been defined and for Cl-36 the limit is very high. Therefore, there is no difference for these three radionuclides. For other radionuclides, for which transport had been limited by solubility limits, transport along the sealing zone is increased, but the changed conditions of unlimited solubility are not sufficient to allow them to reach the surface in calculable amounts before the end of the calculation period.

Sc-2-C3 No sorption

If there were no sorption inside the borehole or if the respective kd-values would be much lower than expected, this would have no effect on the transport of I-129, Cl-36, and Ni-59 as for these radionuclides no sorption is considered in the model calculations. However, as discussed above for the corresponding calculation case of Sc-1, if zero k_d-values are assigned to all radionuclides, several of them would reach the aquifer in significant amounts and contribute to the estimated dose rate.

The radionuclides with the largest contribution to the dose rate in this case would be Pb-210, Ra-226 and Th-229, while I-129 would carry less than 1% of the total dose rate. Consequently, the maximum dose rate estimated for this calculation case increases to approximately 0.05 mSv/a, and is, therefore, near to the assumed regulatory limit of 0.1 mSv/a. The dose rate curves for this calculation case are shown in Figure 8-48.

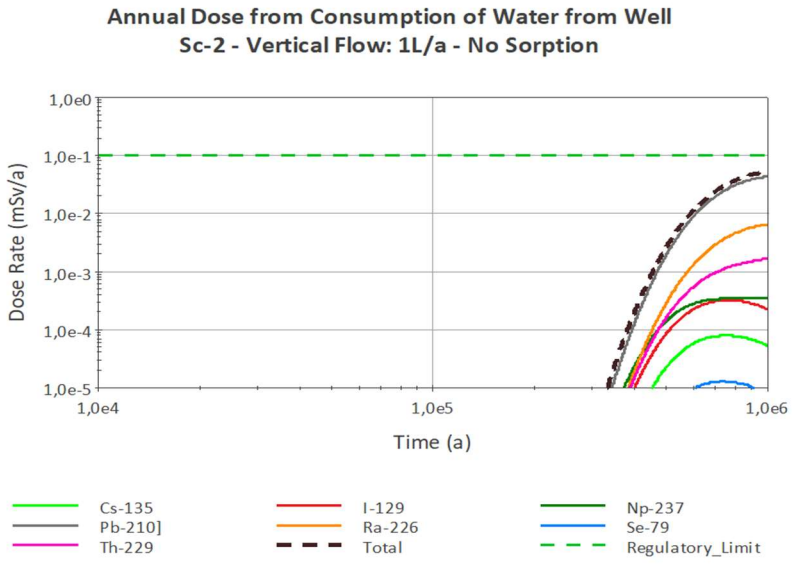

Figure 8-48. Dose rate received from daily consumption of 3 L of water from the aquifer for Sc-2 – Vertical Flow, calculation case Sc-2-C3 No sorption.

Sc-2-C4 Localised corrosion

The case of localised corrosion with a pit hole assumes corrosion rates significantly higher than in case of general corrosion. Even though it will lead to a limited leak from the canister compared to complete failure of the canister, the much earlier release of radionuclides might still have a significant effect on the dose rate results.

To assess the impact of early localised corrosion, it has been assumed that corrosion with a rate of 0.5 mm/a will take place for the uppermost canister (UO_2 SNF). The final diameter of the pit hole is assumed to be 1 cm² and it is assumed to take 20 years for such a hole to develop.

The effect of the early release of radionuclides via diffusive transport through the pit hole is seen in Figure 8-49 using the examples of the very mobile I-129 radionuclide and the significantly less mobile Pu-239. The figure shows the steady increase of radionuclide mass inside the sealing segment located directly above the canister, for which localised corrosion has been assumed. The increase starts directly after completion of the pit hole at 160 years after closure and continues until complete failure of the canister at around 32,000 years later, when transport of radionuclides is strongly increased.

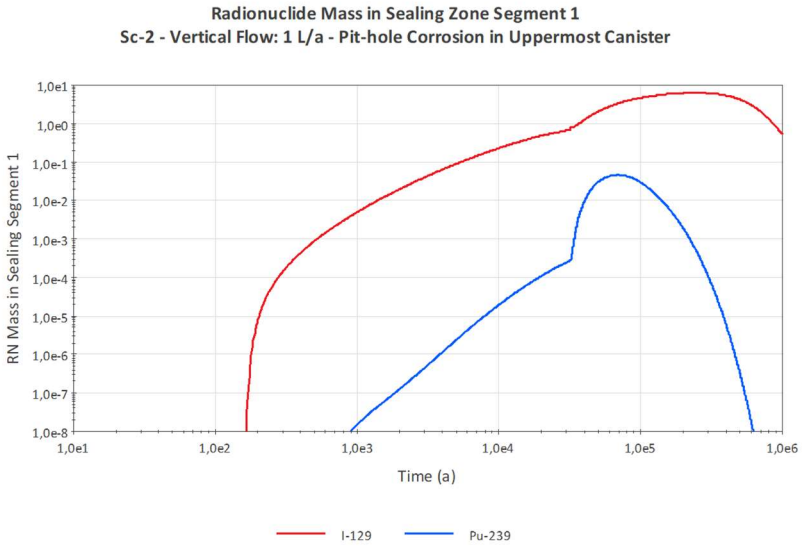

Figure 8-49. Radionuclide content inside the first sealing zone segment above the disposal zone. Localised corrosion takes place in the uppermost canister directly below the sealing zone.

If the resulting dose rate curves are compared with those calculated for the reference parameter set for Sc-2 (see Figure 8-46), no difference can be found. Due to the long transport pathway towards the aquifer, the small amount of activity being released in advance to the major part makes no significant difference.

Even if localised corrosion is assumed to occur for each of the 88 SNF canisters that are represented by the 22 disposal zone segments in the model, there is little difference compared to the Sc-2 reference case. The dose rate curves are shifted about 30,000 years towards earlier times and there is a minor increase in the maximum dose rate, but the logarithmic presentation is essentially the same as in Figure 8-46 for the Sc-2 reference case.

Sc-2-C5 Direct failure of all canisters

Similar as for the corresponding case in Sc-1, also for Sc-2, the initial failure of all canisters does not have a strong influence on the calculated total dose rates. The major properties that govern the release of radio--nuclides and the transport towards the aquifer is the fractional release rate from UO_2 SNF and the diffusive and advective transport parameters that are not changed by the assumed failure of all canisters.

Similar to the localised corrosion case, which also leads to an early release of activity from the canisters, the dose rate curves for I-129, Cl-36 and Ni-59 are shifted towards earlier times by approximately 32,000 years and there is a minor increase in the maximum dose rate. The maximum total dose rate is increased by less than 0.2% but for Cl-36 and for Ni-59 the maxima are increased by 8 % and 61 %, respectively, because for the radionuclides with shorter half-lives a shift towards earlier times also means that less activity has already decayed. The effect is a bit stronger than when assuming that all canisters are subject to localised corrosion, but differences are very minor and difficult to recognize in the logarithmic dose rate graphs as in Figure 8-46 for the Sc-2 reference case.

Summary of the alternative scenario Sc-2 Vertical flow

For the Sc-2 reference case (where the parameter set is as in Sc-1 apart from the assumed upward flow of 1 L/a) as well as for most calculation cases with changed boundary conditions, the maximum total dose rate is in the order of 1 µSv/a. It is largely due to I-129, and it occurs approximately 750,000 years after closure of the facility. For one calculation case, Sc-2-C3 No sorption, the total dose rate is significantly increased and with a value of 0.05 mSv/a it is in the same order of magnitude as the assumed regulatory limit of 0.1 mSv/a.

Compared with Sc-1, the increase in dose rate is extremely large because the advective transport is much more efficient than the diffusive transport. However, under otherwise realistic boundary conditions, the dose rates are more than two orders of magnitude below the assumed regulatory limit. It is only the assumption that no sorption would occur for any of the radionuclides, which causes a dose rate near to this limit. It needs to be kept in mind, however, that the assumption of vertical flow is pessimistic as such, and the no-sorption case is unrealistic and thus a what-if case to demonstrate the general importance of sorption properties for radionuclide migration.

8.6.3 Results and analysis of alternative scenario Sc-3 Fracture

Discussion in Sections 8.1.1 and 8.3.2 has emphasized that the existence of a highly transmissive fracture, which intersects the disposal borehole and is also connected to the near-surface aquifer via a well-connected fracture network is considered unlikely. In particular, for the deeper parts of the borehole, the disposal zone and the sealing zone, the site characterization should largely exclude such a possibility.

In the framework of this generic safety assessment, Sc-3 Fracture is considered a worst-case scenario, which is assessed to evaluate the importance of site characterisation and to define an upper bound of the potential radiological impact from the deep borehole disposal.

The results of this calculation case can also be used to define, e.g., maximum acceptable fracture transmissivities or hydraulic gradients in the deep underground.

Five different intersection locations have been considered as alternative calculation cases for Sc-3 representing the variants of this alternative scenario. In addition to these calculation cases, for the variant Sc-3.3 with a fracture intersection at the top of the disposal zone, the same calculation cases as for the normal evolution scenario and Sc-2 have been carried out to demonstrate the impact of the respective boundary conditions for this alternative scenario:

- Sc-3.1 Fracture at the bottom of the backfilling zone
- Sc-3.2 Fracture in the middle of the sealing zone
- Sc-3.3 Fracture at the top of the disposal zone
  - C1 Reversed emplacement order of canisters in borehole
  - C2 No solubility limits
  - C3 No sorption
  - C4 Localised corrosion
  - C5 Direct failure of all canisters
- Sc-3.4 Fracture in the middle of the disposal zone
- Sc-3.5 Fracture at the bottom of the disposal zone

A fracture in the disposal zone has been chosen to assess the impact of other boundary conditions, because for fractures occurring in the sealing zone within some distance to the disposal zone or even in the backfilling zone, only a few radionuclides appear in the results, as most have decay before reaching the respective locations. It needs to be kept in mind that the existence of a highly transmissive fracture is considered more probable in the backfilling zone than in the disposal or sealing zone.

Sc-3.1 - Fracture at the bottom of the backfilling zone

The alternative calculation case of assuming a transmissive fracture intersecting the lower part of the backfilling zone is the most probable of the different fracture cases. While the planned borehole section for the disposal and the sealing zone will be selected with particular care, existence of minor fractures in the backfilling zone will be considered as less problematic as the actual sealing function is assigned to the zones below. Moreover, the creation of new fractures or their reactivation becomes more probable with decreasing depth.

In this case, a fracture is assumed to intersect the bottom part of the backfilling zone. This assumption represents the most conservative option of a fracture intersecting the backfilling zone. It minimises sorption inside the backfilled part of the borehole and travel times towards the biosphere. Conservatively, no sorption is considered for the fracture pathway. Based on the simplified assumptions for the fracture system, advective transport through this pathway is much faster than advective transport through the backfilling zone of the borehole and, of course, even faster than diffusive transport.

Figure 8-50 shows the dose rate curves that result from the calculation with the reference data set for Sc-3.1 Fracture at the bottom of the backfilling zone. The parameter values are the same as in the normal evolution scenario, but an intersection of a transmissive sub-horizontal fracture with the borehole is assumed to occur in the lower part of the backfilling zone (backfilling zone segment 2). In the fracture, a flow rate of 1 L/a is assumed, which is equally distributed between the EDZ cell and the borehole cell of the intersected backfilling zone segment.

The results show that this alternative scenario does not lead to significant releases of radionuclides to the biosphere. These results were expected, as retardation in the sealing zone prevents all but the most mobile radionuclides from reaching the lower backfilling zone.

Those radionuclides that reach the fracture experience much less retardation on the remaining path towards the aquifer. Consequently, they reach the aquifer at notably higher concentrations than for the normal evolution scenario Sc-1 within the calculation period. This also leads to significantly increased dose rates, but the calculated total dose rates are still far below regulatory limit. This supports the robustness of the disposal concept that focusses on the depth and tightness of the disposal zone and the sealing zone.

Compared with the normal evolution scenario, the dose rates related to I-129, Cl-36 and Ni-59 increase by more than 18 orders of magnitude. Apart from these three very mobile radionuclides (high solubility, little sorption), which also have rather long half-lives, no other radionuclides reach the backfilling zone in sufficient amounts to be released through the fast pathway via the fracture system.

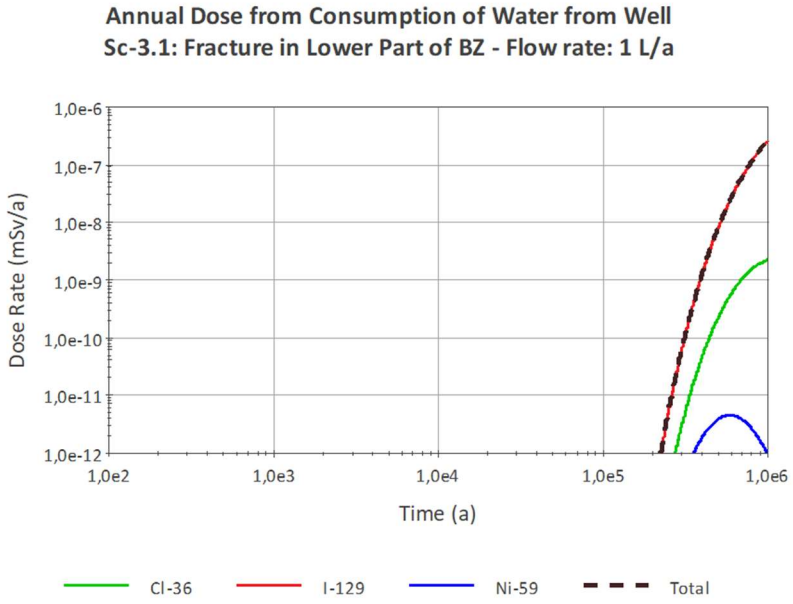

Figure 8-50. Dose rate received from daily consumption of 3 L of water from the aquifer for Sc-3.1, fracture at the bottom of the backfilling zone, constant horizontal flow of 1 L/a.

Sc-3.2 - Fracture in the middle of the sealing zone

Sc-3.2 assumes a water-conducting fracture intersecting the borehole in the middle of the sealing zone. This scenario is unlikely as such a fracture will be detected, and then the sealing would be planned to limit inflows from any fracture and along the borehole. Also, it could be argued that depending on the kind of sealing material, a newly created fracture could be sealed. Nevertheless, assuming that a relatively highly transmissive fracture was created, flow through this fracture might enter the sealing zone of the borehole and the EDZ around it and, thereby, enable advective transport of radionuclides through a fracture network towards the biosphere.

As expected, bypassing of half of the sealing zone increases the activity of the non-sorbing radionuclides (Figure 8-51) compared to Sc3.1 with a fracture intersecting the lower backfilling zone. As discussed before, e.g., for Pu-239 (see Figure 8-35), diffusive transport through the sealing zone retards the radionuclide transport of sorbing nuclides drastically. Even reducing the travel distance through the sealing zone to half of the original does not change that. The less mobile radionuclides still do not reach the middle of the sealing zone in sufficient quantities to contribute significantly to the total dose rate.

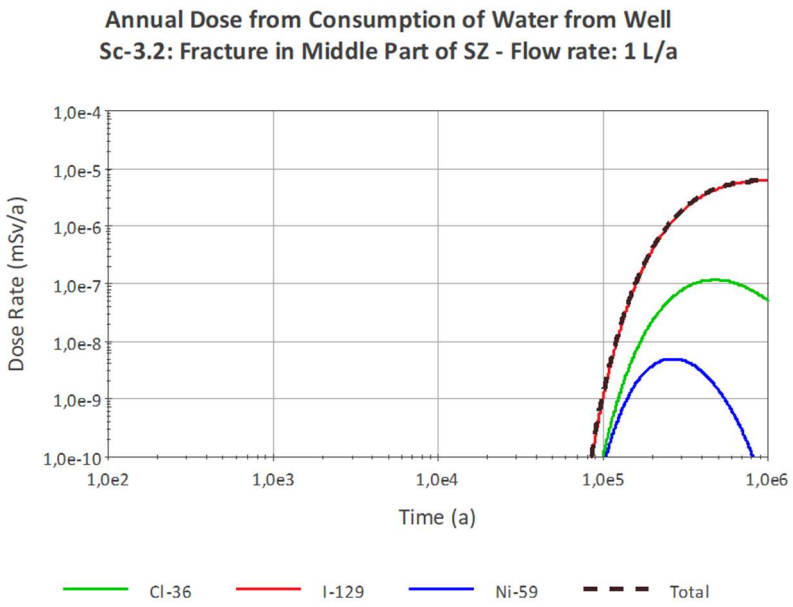

Figure 8-51. Dose rate received from daily consumption of 3 L of water from the aquifer for Sc-3.2, fracture in the middle part of the sealing zone, constant horizontal flow of 1 L/a.

Sc-3.3 - Fracture at the top of the disposal zone

As mentioned before, it is expected that no site will be selected with water-conducting fractures in the foreseen disposal zone or, where potential of future creation or reactivation of highly transmissive fractures is likely. Accordingly, the probability of the alternative fracture scenarios becomes the more unlikely the deeper the assumed intersection is located. Consequently, the assumed flowrate has been reduced to 0.1 L per year compared to the flowrate of 1 L per year for fractures in the backfilling zone or sealing zone (for detailed information see Chapter 8.2.2).

Locating the assumed intersection of a highly transmissive water-conducting fracture in the disposal zone makes a significant difference to the results. Despite the depth of more than 3000 m, the model assumes that transport to the biosphere will be rather fast. There are two main reasons for that. First, assuming a fracture network of individual fractures with very small apertures leads to rather high particle velocities. Second, because conservatively no sorption has been assumed for the fracture pathway there is no retardation for those radionuclides released from the canisters near to the fracture.

Figure 8-52 shows the total dose rate calculated for Sc-3.3 as well as the dose rates curves for the most important radionuclides. The five most contributing ones are Pb-210, Ra-226, Th-229, Np-239, and I-129. I-129 is no longer the main contributing nuclide to the dose and contributes two orders of magnitude less to the total dose rate than Pb-210.

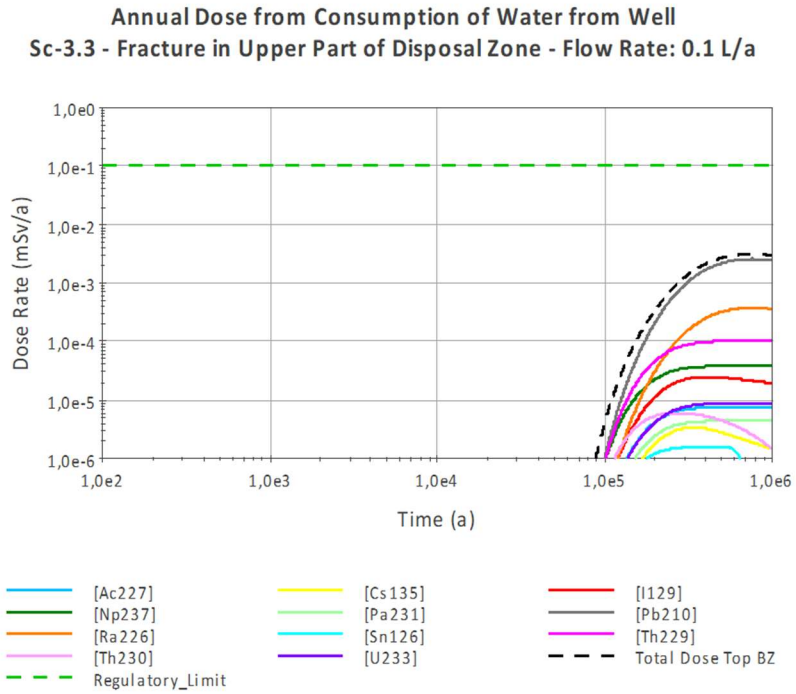

Figure 8-52. Dose rate received from daily consumption of 3 L of water from the aquifer for Sc-3.3, fracture at the top of the disposal zone, constant horizontal flow of 0.1 L/a.

Sc-3.4 – Fracture in the middle of the disposal zone

Scenario Sc-3.4, fracture in the middle of the disposal zone, yields essentially the same results as Sc-3.3. The main reason for this is that the disposal zone segment intersected in the middle part of the disposal zone contains UO_2 SNF canisters, as does the segment in the upper part of the zone. Because the release of activity inside the intersected disposal zone segment is decisive for the activity transported to the aquifer, which are equal for the two segments, there are only some minor differences. These are due on the one hand to the slightly increased transport through the fracture system for the segment from the middle disposal zone and, on the other hand, to the influence of diffusive transport between the segment intersected by the fracture and the disposal segment located directly below, which contains metallic uranium with a significantly different inventory.

Sc-3.5 – Fracture at the bottom of the disposal zone

Scenario Sc-3.5, fracture at the bottom of the disposal zone, differs from the two calculation cases discussed above in the assumption that canisters inside this disposal zone segment contain metallic uranium.

Figure 8-53 shows the dose rate curves for the five most contributing radionuclides and the total dose rate. The different inventory of the lower disposal zone segment compared to the middle and upper disposal zone segments is clearly reflected in the dose rate curves that result from simulating transport from the bottom of the disposal zone towards the aquifer via the fracture system in the neighbouring host rock.

The main radionuclides in this case are Pb-210, followed by Ra-226, as for the case with intersected disposal segments containing UO_2 SNF, but the following most important radionuclides are Th-230, Ac-227 and Pa-231.

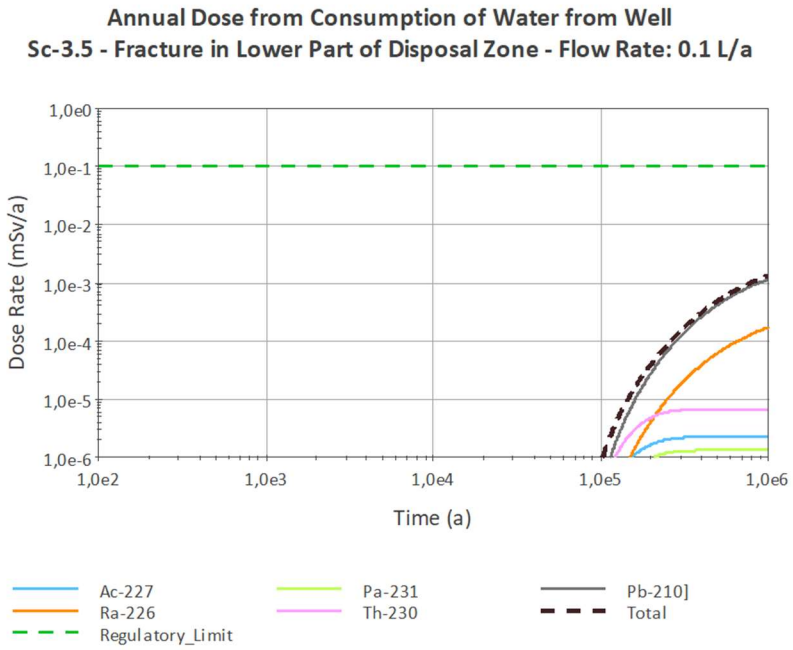

Figure 8-53. Dose rate received from daily consumption of 3 L of water from the aquifer for Sc-3.5 fracture at the bottom of the disposal zone, constant horizontal flow of 0.1 L/a.

Although the inventory of the UO_2 SNF canisters is about two orders of magnitude larger than that of the metallic uranium, for alpha-emitting radionuclides even three orders of magnitude, the total dose rates calculated for the respective fracture calculation cases are in the same order of magnitude. This is because the large activities of UO_2 SNF are largely bound to strongly sorbing radionuclides (e.g., Pu) and short-lived radionuclides such as strontium that do not contribute to the dose rate.

Results of the calculations cases for Sc-3.3

As calculation cases, the following changed boundary conditions have been defined:

- Sc-3.3-C1 Reversed emplacement order of canisters
- Sc-3.3-C2 No solubility limits
- Sc-3.3-C3 No sorption
- Sc-3.3-C4 Localised corrosion
- Sc-3.3-C5 Direct failure of all canisters

All other parameters for Sc-3.3 like the assumed flowrate have been kept constant. The impact of the changed boundary conditions on the results for potential radiological impact are discussed below.

Sc-3.3-C1 Reversed emplacement order of canisters

For this calculation case, the UO_2 SNF canisters are placed in the bottom part of the disposal zone and thereby, approximately 260 m lower than in the other case.

As discussed above, the results from the fracture calculation cases for the disposal zone reflect mainly the content of the canisters inside the intersected disposal zone segment. Changing the emplacement order

changes the content of the disposal zone segment in the upper part of the disposal zone from UO_2 SNF to metallic uranium.

Consequently, the dose rate curves calculated for the case Sc-3.3-C1 reversed emplacement order of canisters are the same as for Sc-3.5 assuming fracture at the bottom of the disposal zone.. The peak dose rates are slightly larger by approximately 10% for Sc-3.5 due to the larger diffusive transport towards the sealing zone at the top of disposal zone.

Sc-3.3-C2 No solubility limits

As discussed in relation to the corresponding calculation case for the normal evolution scenario Sc-1, in general, omitting solubility limits leads to an increase in diffusive transport, but even more so for advective transport because radionuclide concentrations can be significantly increased.

Out of the five most dose contributing radionuclides for Sc-3.3, Pb-210, Ra-226 and I-129 have been assigned no solubility limits in any case. Therefore, this special calculation case will have no effect on their transport towards the aquifer.

For other radionuclides, for which no solubility limits are applied in this case, transport out of the near field is strongly increased. Figure 8-54 shows the dose rate curves for the most contributing radionuclides. The contribution of elements such as plutonium, uranium or zirconium become significantly more important to the total dose rate

Despite the large number of radionuclides that carry a significant dose for this special calculation case, the maximum total dose rate increases by less than a factor 2, compared with the corresponding calculation case with solubility limits. Its time of occurrence is shifted by approximately 200,000 years to earlier times.

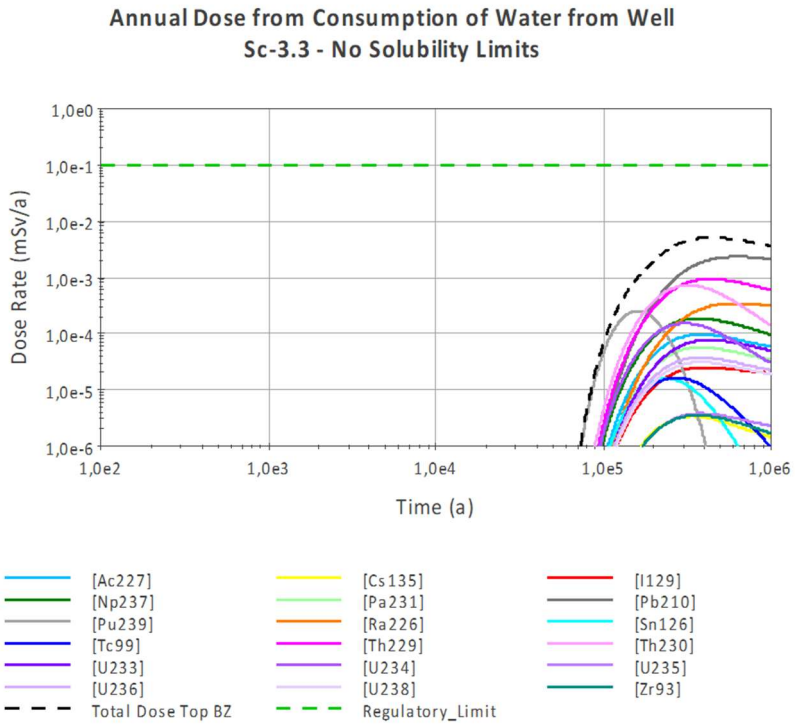

Figure 8-54. Dose rate received from daily consumption of 3 L of water from the aquifer per year for Sc-3.3 fracture at the top of the disposal zone, constant horizontal flow of 0.1 L/a and calculation case Sc-3.3-C2 no solubility limits.

Sc-3.3-C3 No sorption

The dose rate results for the most important radionuclides for Sc-3.3 and the calculation case Sc-3.3-C3 no sorption are shown in Figure 8-55.

The dose rate curves for the main contributing radionuclides differ only little from the curves for Sc-3.3 with sorption (Figure 8-49). A notable change only occurs for radionuclides Ra-226, Ac-227, Pa-231 and Cs-135, which all show increased dose rates. Their contribution to the total dose rate leads to an increase of the maximum total dose rate of approximately 7% and a shift of its time of occurrence towards the end of the calculation period.

The difference between the calculation cases with and without sorption would be significantly larger, if the transport pathway, in which sorption takes place, would be longer. In this case, the difference is due to the inventory. That means that for Sc.3.3, sorption for most radionuclides that are significantly contributing to the total dose takes place only in the buffer material around the canister. Once leaving the buffer, transport takes place via the fracture system, for which sorption has been conservatively omitted for all the scenarios and calculation cases.

Any activity from canisters emplaced below the intersected disposal zone segment, which would have to travel further through sorbing porous material, plays a minor role for the total dose rate.

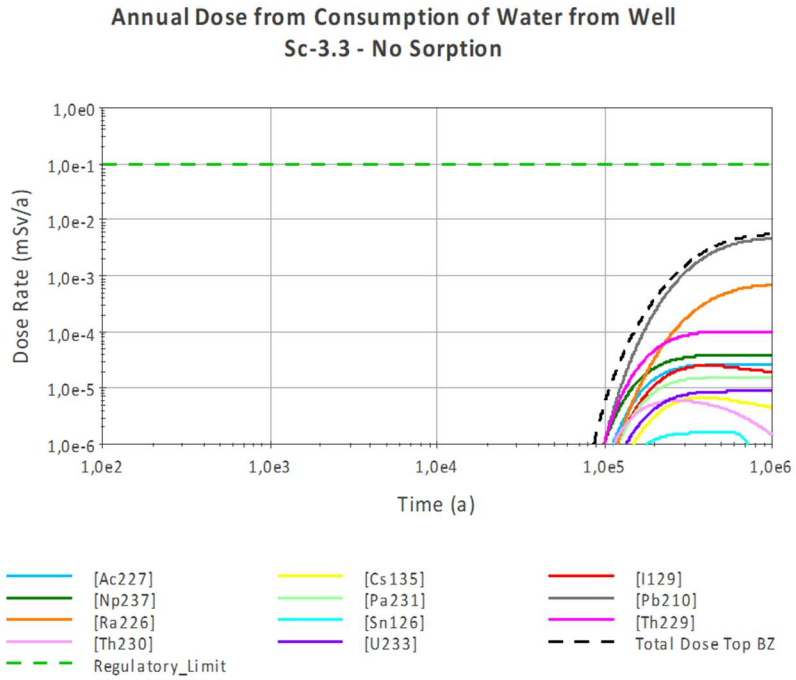

Figure 8-55. Dose rate received from daily consumption of 3 L of water from the aquifer for calculation case Sc-3.3-C3 No sorption.

Sc-3.3-C4 Localised corrosion

To assess the impact that a pit hole developed by localised corrosion may have on the results, it has been assumed that all four canisters that are representing the source term of the fractured disposal zone segment, develop a pit-hole leak shortly after closure of the facility.

The effect of the early release of radionuclides via diffusive transport through the pit holes can be seen in the respective dose rate curves by a slight shift of the lower part of the dose rate curves to earlier times. However, this early release of radionuclides does not significantly change the curves, which are mainly reflecting the influence of the main part of radionuclides that are released after complete failure of the canister.

The total dose rate maximum and its time of occurrence do not change by the assumed pit-hole leaks.

Sc-3.3-C5 Direct failure of all canisters

The calculation case Sc-3.3-C5 direct failure of all canisters yields results similar to the corresponding calculation cases for Sc-1-C5 and Sc-2-C5.

The dose rate curves are shifted by approximately 30,000 years to earlier times, but apart from that the form of the curves as well as their maximum values show no significant difference.

The main reason for that is the fact that the main dose rates occur for times later than 200,000 years and the release of radionuclides from the source term is largely governed by the fractional release of radionuclides from the waste form, sorption to the buffer material, and solubility limits. If release from the canister starts approximately 30,000 years earlier this has no significant effect on the dose rate curves.

Summary of the alternative scenario Sc-3 Fracture

It is summarized that for the fracture scenario, using the reference case parameter set of the Sc-1 apart from the assumed intersection by a highly transmissive water-conducting fracture, the results mostly depend on the assumed location of the fracture.

If the fracture, connecting the borehole with the aquifer, is in the backfilling zone (Sc-3.1), only the mobile radionuclides contribute to a dose rate from consumption of contaminated water. All other radionuclides are effectively retarded within the borehole and do not reach the backfilling zone in significant amounts. In this case, the maximum dose rate of approximately 1 nSv/a is mainly due to I-129 and occurs at the end of the calculation period.

For a fracture location inside the sealing zone (Sc-3.2), the situation is similar. For most radionuclides, migration into the sealing zone is limited to a short distance of less than half of the sealing zone length. Accordingly, for the assumed fracture location at the middle of the sealing zone, significant contributions to the total dose rate are due to the three mobile radionuclides: I-129, Cl-36 and Ni-59. The maximum dose rate is increased compared to Sc-3.1 by one order of magnitude and its time of occurrence is shifted to earlier times because of slow diffusive migration through the second half of the sealing zone.

If the fracture is located inside the disposal zone, the situation changes notably. In this case, the radionuclides representing the inventory of the disposal zone segment that is intersected by the fracture do not have to pass any diffusive transport pathway to enter the fracture system pathway towards the aquifer. Accordingly, there is no strong separation between the mobile and less mobile radionuclides and the total dose rate is no longer mainly due to the most mobile radionuclides.

The dose rate and the composition of the most contributing radionuclides depend on the type of waste representing the inventory of the respective disposal zone segment. Although there is some diffusive transport between adjacent disposal zone segments, transport of radionuclides through the fracture system primarily depends on the inventory of the intersected disposal zone segment.

If the inventory consists of the metallic uranium contained in four canisters, the maximum dose rate is approximately 1 µSv/a, occurring at the end of the calculation period. If the waste contained in the disposal zone segment is UO_2 SNF, then the maximum dose rate is about three times as large, and its time of occurrence is approximately 750,000 years after closure.

The depth the fracture exactly intersects the disposal zone, has little effect on the dose rates. Advective transport through the fracture system does not lead to significant retardation, because no sorption has been considered for this pathway. There is a certain influence, however, by the neighbouring borehole segments. Depending on their respective inventory a certain amount of diffusive transport out of or into the intersected borehole segment may take place. For instance, the maximum total dose rate resulting from a fracture in the lowermost part of the disposal zone is significantly larger than for the same scenario in the uppermost disposal zone cell directly below the sealing zone. The total dose rate in case the fracture intersects the bottom of the disposal cell is twice as large for UO_2 SNF and 50% larger for metallic uranium SNF.

To assess the influence of other boundary conditions than the location of the fracture, the same calculation cases have been assessed as for Sc-2. Variant Sc-3.3 was selected as reference fracture case. The calculation cases assuming no solubility limits and no sorption respectively show both the effect of reduced retardation for individual radionuclides in form of increased dose rate contributions, especially the case of no solubility limits. Here several additional radionuclides contribute to the total dose rate. In both cases, the maximum total dose rate is approximately doubled. The early failure of the canisters either by localised corrosion or direct failure leads to an earlier occurrence of small dose rates, but apart from that, the dose rate behaviour with time shows little change.

8.6.4 Sensitivity analyses for Sc-3.3 Fracture at the top of the disposal zone and Sc-2 Vertical flow

A comprehensive sensitivity analysis has been carried out to assess the influence of uncertainties of various parameters (values) or assumptions on the results. The objectives of these sensitivity analyses are to identify parameters that, on one hand, exhibit a substantial level of uncertainty and, on the other hand, have a significant impact on the release and transport of radionuclides. These parameters define areas for which additional research may be required to increase the accuracy of the long-term assessment.

Another purpose of the sensitivity analysis is to determine the general robustness of the model against parameter changes.

If release of radionuclides to the biosphere is limited to diffusive transport along the borehole as in Sc-1 (normal evolution scenario), most radionuclides do not reach the surface within the calculation period and consequently no significant dose rate results. Accordingly, Sc-1 does not allow to assess the impact that changed parameter values or assumptions have on the performance of the deep borehole repository. At least, it is not possible if the dose rate is used as criterion. Changing parameter values would not make much difference as there is either no major uncertainty in the parameters and their values or conservative assumptions have constrained the impact on the results as demonstrated by the calculation cases for Sc-1 (sorption k_{ds}, solubilities). Therefore, Sc-3.3 has been used as a reference case for sensitivity analysis because it leads to significant release of radionuclides to the biosphere and dose rates, even if this is a what-if case considering the large number of pessimistic assumptions (see Section 8.5.3). The main disturbance assumed for this case is the occurrence of a horizontal fracture system intersecting the disposal zone (DZ) of the borehole directly below the sealing zone. This horizontal fracture system is assumed to be connected to a vertical fracture system very near to the borehole, which again will be connected via a fast fracture pathway to an aquifer at an approximate depth of 100 m.

For some parameters, e.g., those related to characteristics of the sealing zone or the backfilling zone, Sc-3.3 is obviously not suited as a reference case, because the main transport of activity bypasses these zones. Sc-2 has, thereby, been used as another reference case for the sensitivity analysis.

The sensitivity analysis focuses on parameters that are known to have a significant impact on the results or which might be considered likely to do so, and selected from the following parameter groups:

- Source term performance:
  - Inventory (activity content)
  - Fractional release rates from the waste form
  - Canister failure (changed general corrosion rates or stability requirements)
  - Occurrence of a pit hole due to localised corrosion
  - Waste package (WP) emplacement sequence
- Material and radionuclide properties:
  - Properties of borehole materials (porosity, permeability, and k_d-values)
  - Radionuclide solubility limits
- Geosphere:
  - Number, width, and aperture of sub-horizontal and vertical fractures
  - Tortuosity of vertical fracture system
  - Distance to well
  - Matrix diffusion
  - Vertical flow rate
  - Fracture flow rate

In addition, also a case assuming no EDZ was studied for scenarios Sc-1, Sc-2 and Sc-3.3. According to the results, slight increase of radionuclide concentration in the borehole, and faster transport to the biosphere and consequently slightly higher doses (about 10%) could occur for Sc-2 and Sc-3.3. For the other scenarios, dose rates will be the same or lower. However, the results do not affect the general statement about compliance of the radiological impact with regulatory limits.

For the chosen biosphere model no sensitivity calculations have been carried out. If the amount of drinking water per day is changed compared with the assumed 3 litres, this leads to a simple linear increase or decrease of the calculated dose rates.

The same is valid for the assumption that the dilution in the aquifer will be limited by the expected production rate for a drinking water well and for the assumption that 100% of the released activity in the water will enter the well.

To analyse the sensitivity of the model towards variation of the values of individual parameters, all parameters of the reference cases Sc-2 and Sc-3.3 have been kept constant, while for the parameters of interest, extreme values have been selected. The results and changes of the long-term calculations resulting from the parameter variation are listed in the table below: the maximum annual total dose rate, its time of appearance, the relation to the maximum value for the reference data set and shift in time for the peak dose.

The choice of minimum and maximum values for the parameters is not based on assumptions about the extreme values that are realistically to be expected. Instead, the values have been mainly selected, to demonstrate the influence individual parameters have on the total annual dose.

Sensitivity analysis for Sc-3.3

For those assumptions or boundary conditions mentioned above that have already been addressed as calculation cases, references are given in the table below. In Table 8-3, the results from sensitivity calculations for Sc-3.3 are listed.

In the table, the parameters that lead to changes of the maximum total dose rate by more than 10% have been colour coded in light yellow. Because the extreme values used for this sensitivity analysis have been somewhat arbitrarily chosen, this limit of 10% also defines somewhat arbitrarily, to which parameters the

system is particularly sensitive, because the extreme values are not reflecting a uniform level of uncertainty. Nevertheless, the approach aims to give a good overview of the most influencing parameters in the assessment of the disposal system. The paragraphs below summarize comments on the sensitivity of the model towards certain groups of parameters or individual ones.

Table 8-3. Results of sensitivity analysis based on the reference case Sc-3.3. Given are the values of the changed parameters, resulting peak dose and time of occurrence. In addition, the differences between these results and those for the Sc.3.3 are listed as relation of peak values and time shift between respective times of occurrence. Positive numbers indicate a shift into the future.

Results of Sensitivity Analysis – Reference case Sc-3.3							
Parameter Name as listed in Appendix V	**Min**	**Default** Ref. Sc.	**Max**	**Min** Dose rate (mSv/a) Time	**Max** Dose rate (mSv/a) Time	**Min** Diff-Factor Time shift	**Max** Diff-Factor Time shift
Reference scenario							
All parameters set to default values for **Sc-3.3** as listed in Appendix V		**yes**		**3.13E-03** **760,500 a**		**1.00** **+0 a**	
Source Term Performance							
Factor_Inventory	0.1	1	10	3.50E-04 682,000 a	3.00E-02 762,000 a	0.11 -78.500 a	9.57 +1,500 a
Reversed order of SNF canister emplacement	MU top	UO_2 top		6.95E-04 1,000,000 a		0.22 +239,500 a	
Fractional release rate UO_2 SNF	2 E-06 1/a	2 E-05 1/a	2 E-04 1/a	2.72E-03 1,000,000 a	3.12E-03 765,500 a	0.87 +239,500 a	1.00 +5,500 a
Fractional release rate Zircalloy	4 E-06 1/a	4 E-05 1/a	4 E-04 1/a	3.13E-03 760,500 a	3.13E-03 760,500 a	1.00 +0 a	1.00 +0 a
Fractional release rate other metal	1 E-04 1/a	1 E-03 1/a	1 E-02 1/a	3.13E-03 760,500 a	3.13E-03 760,500 a	1.00 +0 a	1.00 +0 a
Fractional release rate metallic uranium SNF	1 E-03 1/a	1 E-02 1/a	1 E-01 1/a	3.13E-03 760,500 a	3.13E-03 760,500 a	1.00 +0 a	1.00 +0 a
Minimum failure time of canisters	0	30,000 yr	60,000 yr	3.13E-03 763,000 a	3.14E-03 757,000 a	1.00 +2,500 a	1.00 -3,500 a
Occurrence of pit-hole corrosion (each canister)	yes	no		3.13E-03 763,000 a		1.00 +2,500 a	
Material and Radionuclide Properties							
Porosity bentonite buffer	30%	50%	70%	3.18 E-03 741,000 a	3.13 E-03 776,000 a	1.01 -19,500 a	1.01 +15,500 a
Porosity EDZ buffer	2.25%	4.5%	9%	3.25 E-03 765,000 a	2.92 E-03 755,500 a	1.04 +4,500 a	0.93 -5,000 a
kd-values buffer bentonite	x 0.1	See App. V	x 10	3.24 E-03 757,500 a	2.45 E-03 778,000 a	1.03 -3,000 a	0.78 +17,500 a
Solubility limits	x 0.1	See App. V	No limits	3.00 E-03 762,000 a	5.13 E-03 439,000 a	0.96 +1,500 a	1.65 -321,500 a

Results of Sensitivity Analysis – Reference case Sc-3.3							
Parameter Name as listed in Appendix V	**Min**	**Default** Ref. Sc.	**Max**	**Min** Dose rate (mSv/a) Time	**Max** Dose rate (mSv/a) Time	**Min** Diff-Factor Time shift	**Max** Diff-Factor Time shift
Sc-3.3 Geosphere Parameters							
Number vertical fractures	2	10	20	3.07 E-03 814,500 a	3.14 E-03 754,000 a	0.98 +54,000 a	1.00 -6,500 a
Width vertical fractures	1 m	5 m	10 m	3.34 E-03 613,000 a	2.05 E-03 1,000,000 a	1.06 -147,500 a	0.65 +239,500 a
Aperture vertical fractures	0.05 mm	0.15 mm	0.45 mm	3.14 E-03 751,500 a	3.10 E-03 787,500 a	1.00 -9,000 a	0.99 +27,000 a
Tortuosity vertical fractures	1	5	10	3.34 E-03 613,000 a	2.89 E-03 963,000 a	1.06 -147,500 a	0.92 +202,500 a
Matrix diffusion (depth)	no	50 mm	100 mm	3.41 E-03 590,000 a	2.91 E-03 949,500 a	1.09 -170,500 a	0.93 +189,000 a
Fracture flow rate through intersecting fracture	0.01 L/a	0.1 L/a	1 L/a	2.28 E-05 1,000,000 a	1.54 E-02 440,800 a	0.01 +239,500 a	4.91 -319,700 a

Source term performance

Inventory

The results in Table 8-3 are to be expected. The differences in dose rate do not exactly match the differences in inventory activity. The reason is that release of some of the radionuclides from the source term is limited by solubility limits. In these cases, a changed total activity or mass of these radionuclides has no or only little influence on their transport through the system.

Sc-3.3-C1 Reverse order of canister emplacement

For Sc-3.3-C1 this leads to a significant change in the calculated dose rate. The reason is that the inventories for metallic uranium (MU) and UO_2 SNF are significantly different. For the calculated dose rate from a scenario of a fracture inside the disposal zone, the type of spent fuel inside the disposal zone segment, which is intersected by the fracture, is decisive for the measured dose rate.

For Sc-3.3, in the initially assumed emplacement order, the fractured disposal zone segment contains UO_2 SNF, while for the reverse emplacement order it would be metallic uranium. As the location of a potential fracture is completely unknown, the different calculation results have little relevance for the question whether the emplacement order has advantages or not. For this question, the sensitivity calculations for Sc-2 are more relevant.

Fractional release rates

At first glance, accelerated fractional release rate for UO_2 would be suspected to have a rather large effect, because UO_2 SNF carries most of the inventory and has the slowest release rate. Despite that, an increase by one order of magnitude has hardly any effect on the peak dose rate results. The reason is that the main dose rate contributing radionuclides, Pb-210 and Ra-226 are daughter products of U-234 and Th-230. The release of uranium and thorium is, however, mainly governed by the solubility limits and not so much by the

release rates for the conditions in Sc-3.3. In the long term, activity concentrations of the shorter-lived daughter nuclides Ra-226 and Pb-210 equal out with the activity concentrations of U-234 and Th-230. As an increased fractional release from the waste form does not lead to an accelerated transport of these radionuclides, it does not significantly change the general dose rate results.

The impact of a changed fractional release rate on the total dose rate is stronger if the change leads to slower release rates. If the fractional release rate is decreased by one order of magnitude, the total dose rate is approximately 13% lower and the maximum is shifted towards the end of the calculation period, which is the result of a general delay of radionuclide transport caused by the delayed fractional release rate.

Fractional release rates for zircalloy, other metals and metallic uranium SNF do not play a significant role for the calculation of the total dose rate, neither if they are increased by a factor 10 nor if they are decreased by the same factor. For Sc-3.3, there is no change in the calculated maximum total dose rate or in the time of its occurrence, nor does the shape of the curve show any significant changes.

Canister failure

The length of the period that passes by before the canisters are assumed to fail has far less influence on the general potential radiological impact than would be expected. The reason is the same as mentioned before when discussing the results from the “initial canister failure” calculation cases for the different scenarios. The main factors that govern the release of activity from the source term are the fractional release rates from the different waste forms and the solubility limits. If the canister lifetime is extended by a factor of 2 to approximately 60,000 years, the dose rate curves are shifted towards later times in the beginning, but the maximum total dose rate shows only a very small increase. Its time of occurrence is slightly shifted by 3,500 years to earlier times, due to the larger pulse of activity released from the waste form at the time of canister failure.

If instantaneous failure of all canisters is assumed, there is also little change regarding the total dose rate and its time of occurrence. The dose rate curves are shifted in the beginning towards an earlier time by about 30,000 years, but the maximum total dose rate and its time of occurrence are hardly altered.

If localised corrosion and development of pit holes are assumed to take place, there is also little difference regarding the main results of the dose rate curves, even though, a pit-hole leak has been assumed for each canister. In the beginning the curves are shifted to earlier times because the first release from the canisters takes place as soon as 160 years after closure of the facility instead of 30,000 years, but there is little change in the general shape of the curves or the maximum total dose rate. The result is not surprising as the initial total failure of all canisters also has only minor consequences for the release of radionuclides to the biosphere.

Material and radionuclide properties

k_d-values

The main material properties with influence on the transport of radionuclides inside the disposal system are porosity, permeability/hydraulic conductivity, and sorption properties (k_d-values) of those materials through which radionuclides migrate during transport towards the biosphere.

For Sc-3.3, the respective properties of the bentonite buffer and the EDZ do not strongly affect the main total dose rate results apart from the sorption capacity of the bentonite buffer. Reducing the k_d-values by a factor of 10 does not change the results very much but increasing k_d-values by a factor 10 results in a total dose rate that is 22% lower than for the reference value.

Porosities

For Sc-3.3, the decrease of EDZ porosities has the strongest influence on the dose rate results. Decreasing the porosities in the EDZ reduces the total volume of water inside the borehole/EDZ system, which increases the radionuclide concentration in the water. Accordingly, decreasing the porosity increases the total maximum dose rate and vice versa. The chosen model assumption of 4.5% porosity for the EDZ is probably too large. If the EDZ porosity was set to zero, the maximum total dose would be increased by 9%.

Solubility limits

If the solubility limits for the individual radionuclides are reduced by a factor of 10, the maximum total dose rate and its time of occurrence do not change very much, because the largest part of the total dose rate is carried by radionuclides for which there are no solubility limits. Consequently, there is little change in the total dose rate curve. For those radionuclides that have solubility limits and occur in such quantities that these limits are reached over longer phases of the calculation period, the individual dose rates decrease by approximately the same factor of 10. This is the case, e.g., for Th, U, Np and Sn.

If no solubility limits are considered at all, there is a significant increase in the total dose rate (+65%), and the dose rates of individual radionuclides, the release of which is normally governed by solubility limits, experience much larger increases (see “No solubilities” calculation case in Section 8.5.3).

Sc-3.3 Geosphere parameters

The number of vertical fractures contribute to matrix diffusion-. Aperture, fracture width and tortuosity contribute to the calculation of the amount of water inside the individual vertical fractures and thereby define the transport velocity for the contaminated water from the depths of the disposal borehole to the aquifer. Matrix diffusion is strongly increased by doubling the expected diffusion depth

The assumed flow rate of the fracture intersecting the disposal zone has the largest impact on the dose rate results. Reducing the reference flow rate of 0.1 L/a by a factor of 10 reduces the maximum dose rate to about 1% of its reference value at the end of the calculation period. The dose rate maximum is shifted towards times significantly beyond the end of the calculation period.

Increasing the flow rate of the fracture by a factor 10 to 1 L/a, shifts the dose rate curves to earlier times than for the reference case and increases the maximum total dose rate approximately five times. Further ten-fold increase of the flowrate to 10 L/a increases twice the maximum dose compared with using the value of 1 L/a. This shows that the relation between increase in flow rate and increase in maximum dose rate is not constant but strongly decreasing with the flow rate value. The strongest effects are related to the very small flow rates. However, the fracture flow rate is obviously one of the most influencing parameters in the Sc-3.3 model for the deep borehole.

Sensitivity analysis for Sc-2

For the assumptions or boundary conditions mentioned above that have been addressed as calculation cases, references are given in the table below. In Table 8-4, the results of sensitivity calculations for Sc-2 as a reference case are listed.

In the same way as for the sensitivity analysis for reference case Sc-3.3, the table below indicates the parameters that lead to changes in the maximum total dose rate of more than 10% for reference scenario Sc-2 by yellow colour-coding. As well as for Sc-3.3, this approach does not lead to a properly quantified selection of the most important parameters but aims to allow a quick view of the most influential parameters. The results are discussed in more detail in the paragraphs below.

Table 8-4. Results of the sensitivity analysis based on reference case Sc-2. The values of the changed parameters, resulting peak dose and time of occurrence are given. In addition, the differences between these results and those for the Sc-2 reference case are listed as relation of peak values and time shift between respective times of occurrence. Positive numbers indicate a shift into the future.

Results of sensitivity analysis – reference scenario Sc-2							
Parameter Name as listed in Appendix V	**Min**	**Default** Ref. Sc.	**Max**	**Min** Dose rate (mSv/a) Time	**Max** Dose rate (mSv/a) Time	**Min** Diff-Factor Time shift	**Max** Diff-Factor Time shift
Reference scenario							
All parameters set to default values for Sc-2 as listed in Appendix V		**yes**		**3.24 E-04** **760,000 a**		**1.00** **+0 a**	
Source Term Performance							
Factor_Inventory	0.1	1	10	3.24 E-05 760,000 a	3.24 E-03 760,000 a	0.1 0 a	10 0 a
Reversed order of SNF canister emplacement	MU top	UO2 top		3.53 E-05 1,000,000 a		0.11 +240,000 a	
Fractional release rate UO_2 SNF	2 E-06 1/a	2 E-05 1/a	2 E-04 1/a	1.77 E-04 1,000,000 a	3.34 E-04 709,500 a	0.55 +240,000 a	1.03 -50,500 a
Fractional release rate Zircalloy	4 E-06 1/a	4 E-05 1/a	4 E-04 1/a	3.24 E-04 760,500 a	3.24 E-04 760,000 a	1.00 +500 a	1.00 +0 a
Fractional release rate other metal	1 E-04 1/a	1 E-03 1/a	1 E-02 1/a	3.24 E-04 760,000 a	3.24 E-04 760,000 a	1.00 +0 a	1.00 +0 a
Fractional release rate metallic uranium SNF	1 E-03 1/a	1 E-02 1/a	1 E-01 1/a	3.24 E-04 760,000 a	3.24 E-04 760,000 a	1.00 +0 a	1.00 +0 a
Minimum failure time of canisters	0	30,000 yr	60,000 yr	3.24 E-03 728,000 a	3.23 E-04 790,000 a	1.00 -32,000 a	1.00 +30,000 a
Occurrence of pit-hole corrosion (each canister)	yes	no		3.24 E-04 729,000 a		1.00 -31,000 a	
Material and Radionuclide Properties							
Hydraulic conductivity buffer	1 E-09 m/s	1 E-08 m/s	1 E-07 m/s	3.24 E-04 760,000 a	3.24 E-04 760,000 a	1.00 +0 a	1.00 +0 a
Hydraulic conductivity bentonite sealing	1 E-10 m/s	1 E-09 m/s	1 E-08 m/s	3.24 E-04 760,000 a	3.24 E-04 760,000 a	1.00 +0 a	1.00 +0 a
Hydraulic conductivity backfill	1 E-08 m/s	1 E-07 m/s	1 E-06 m/s	3.24 E-04 760,000 a	3.24 E-04 760,000 a	1.00 +0 a	1.00 +0 a
Hydraulic conductivity EDZ	1 E-10 m/s	1 E-09 m/s	1 E-08 m/s	3.24 E-04 760,000 a	3.24 E-04 760,000 a	1.00 +0 a	1.00 +0 a
Porosity bentonite buffer	30%	50%	70%	3.29 E-04 763,000 a	3.18 E-04 757,500 a	1.02 +3,000 a	0.98 -2,500 a
Porosity bentonite sealing	20%	35%	50%	3.26 E-04 730,000 a	3.21 E-04 790,500 a	1.01 -30,000 a	0.99 +30,500 a

Results of sensitivity analysis – reference scenario Sc-2							
Parameter Name as listed in Appendix V	**Min**	**Default** Ref. Sc.	**Max**	**Min** Dose rate (mSv/a) Time	**Max** Dose rate (mSv/a) Time	**Min** Diff-Factor Time shift	**Max** Diff-Factor Time shift
Porosity backfill	20%	30%	40%	3.44 E-04 600,000 a	3.00 E-04 916,500 a	1.06 -160,000	0.93 +165,500 a
Porosity EDZ	2.25 %	4.5 %	9.0 %	3.37 E-04 677,500 a	2.97 E-04 924,500 a	1.04 -82,500 a	0.92 +164,500 a
kd-values buffer bentonite	x 0.1	See table in App. V	1)	3.24 E-04 760,000 a		1.00 0 a	
kd-values sealing bentonite	x 0.1	See table in App. V	1)	3.24 E-04 760,000 a		1.00 0 a	
kd-values backfill	x 0.1	See table in App. V	1)	3.24 E-04 760,000 a		1.00 0 a	
kd-values sealing bentonite buffer bentonite and backfill	x 0.01	See table in App. V	1)	3.36 E-04 763,000 a		1.04 3,000 a	
kd-values sealing bentonite buffer bentonite and backfill	zero kds		1)	5,25 E-02 1,000,000 a		162.00 +240,000 a	
Solubility limits	1)	See table in App. V	x 10		3.24 E-04 760,000 a		1.00 0 a
Solubility limits	1)	See table in App. V	No limits		3.24 E-04 760,000 a		1.00 0 a
Geosphere and Sc-3.3 Parameters							
Flowrate aquifer	0.365 m/a	36.5 m/a	150 m/a	3.24 E-04 760,000 a	3.24 E-04 760,000 a	1.00 0 a	1.00 0 a
Constant vertical flow upwards the borehole	0.1 L/a	1 L/a	10 L/a	2.07 E-14 1,000,000 a	2.05 E-03 129,400 a	6.41 E-11 +240,000 a	6.33 -630.600 a
Constant vertical flow upwards the borehole		1 L/a	100 L/a		4.47 E-03 41,100 a		13.8 -718,900 a

1) *Not meaningful to calculate, because chosen reference parameters prevent as such all less mobile radionuclides from reaching the biosphere. Changing parameters to more restrictive conditions by multiplication do not cause any changes as dose carrying radionuclides have zero kd-values and unlimited solubilities assigned.*

Source term performance

Inventory

The differences in dose rates match exactly the differences in inventory activity, and the time of occurrence of the maximum total dose rate does not change. This result is slightly different from the results for Sc-3.3, where the total dose rate was also carried by radionuclides with limited solubility. For Sc-2, the total dose rate is, in practice, exclusively carried by radionuclides, for which no solubility limits have been defined. Consequently, a change of the total inventory leads to the same relative change in the total dose rate.

Reverse order of canister emplacement

The order of canister emplacement obviously plays a significant role for the dose rate results of Sc-2. For the reference data set, it has been assumed that the metallic uranium SNF would be emplaced in the lower part of the borehole and the UO_2 SNF on top of that. Reversing this order of emplacement leads to a reduction of the maximum total dose rate within the calculation period to approximately 11%. This is caused by the longer average transport pathway between the main inventory, which is associated with the UO2 SNF, and the surface that results from the reversed emplacement order. Consequently, the radionuclides arrive later at the surface and the maximum total dose rate value is not reached within the calculation period.

Fractional release rates

In a similar way as for the corresponding sensitivity calculation for Sc-3.3, it is not expected that the increase in the fractional release rate of UO_2 SNF would affect the total dose rate for Sc-2. The main reason for the limited sensitivity in case of Sc-2 is the fact that the total dose rate is practically carried by I-129 alone. For this radionuclide a rather large share of 5% of the total UO2 SNF inventory is assumed to be instantaneously released. That means that a high I-129 activity is released spontaneously at the time of canister failure and is then transported upwards. The dose rate maximum is largely carried by this I-129 pulse.

Compared to that, the impact of a slower fractional release rate on the total dose rate is much stronger. If the fractional release rate is decreased by one order of magnitude, the total dose rate is approximately 45% lower and the maximum is shifted towards the end of the calculation period, which is the result of a general delay of radionuclide transport associated with the delayed fractional release rate.

Fractional release rates for zircalloy, other metals and metallic uranium SNF do not play a role for the calculation of the total dose rate, neither if they are increased by a factor of 10 nor if they are decreased by the same factor. For Sc-2, there is no change in the calculated maximum total dose rate or in the time of occurrence, nor does the shape of the curve show any significant changes.

Canister failure

Similar to the results for the reference case Sc-3.3, the length of the period that passes by before the canister are assumed to fail has only a minor influence on the general potential radiological impact. The total dose remains the same and the time of its occurrence reflects the changes in the failure time. As mentioned before, the reason for this behaviour is that with failure of the canisters a certain amount of activity is – at least in relation to the total calculation period and the transport times - instantaneously released. This leads to a pulse of mass transport rates, especially for the radionuclide which carries the major dose rate for Sc-2, I-129. Consequently, the time of occurrence of the calculated maximum dose rate reflects the canister failure time, but the value remains practically constant as the total amount of released I-129 depends largely on the instantaneously released fraction of that radionuclide.

For the same reasons, there is little difference between the dose rate results for initial failure of the canisters and assumed occurrence of pit-hole leaks for each canister. The maximum dose rate remains unchanged, and its time of occurrence is shifted by 31,000 years. For the very mobile I-129 radionuclide, the effect of total failure and massive occurrence of pit-hole corrosion is obviously very similar.

Material and radionuclide properties

Hydraulic conductivity

Changes of the assumed hydraulic conductivities do not have any impact on the dose rate results. That is because in the GoldSim model, the hydraulic conductivity is not used to calculate flow through the borehole, but only to distribute the defined total vertical flow into one part that uses the EDZ flow path around the borehole and another part that flows through the borehole itself. This could lead to differences in the calculated flow rates if flow rates are high and differences regarding sorption are very different for the different pathways. For the reference conditions these differences are of no importance. Probably, diffusive exchange

of activity between EDZ volume and borehole volume balances out any difference in radionuclide concentration.

Porosities of EDZ and materials inside borehole

The influence of changes in the assumed porosities of the media through which advective radionuclide transport takes place is mainly due to the changed amount of water inside the borehole or the EDZ. If porosity is increased, the water volume is increased, and the assumed vertical flow of 1L/a needs longer to reach the surface. In addition, the radionuclide concentration in the water is slightly increased. This is especially pronounced for changes of the backfill porosity and that of the EDZ. The volume of the water-filled porosity of the EDZ along the total borehole length and the backfilling zone of the borehole are significantly larger than the volumes of the buffer in the disposal zone or the sealing zone. Changes in the porosity of these materials, therefore, result in relatively large changes in the total volume of water inside the borehole and EDZ. According to the faster transport towards the surface, smaller porosities lead to higher maximum dose rates and an earlier time of occurrence of the maximum. In the same way, larger porosities lead to delay of radionuclides and smaller dose rates. Due to the specific relation between total porosity of backfill and EDZ, the assumed changes in porosity lead to nearly identical increase of total water volume for the chosen maximum values of porosity, which leads to nearly the same changes in total dose rate and its time of occurrence. In general, the dose rate values change approximately linear with the changed volume of water in the borehole / EDZ system.

For sorbing radionuclides, a decreasing porosity would lead to a stronger retardation and thereby potentially to a reduction in transport, because the sorbing mass is increased. Consequently, lower porosities would potentially lead to a decrease in total dose rate. This effect is not to be seen for Sc-2 because the radionuclides I-129, Cl-36 and Ni-59 contributing to the dose rate are not sorbed.

k_d-values

As mentioned above, sorption to solids of the porous media through which advective transport takes place is one of the main material properties with influence on the transport of radionuclides.

For Sc-2, no sorbing radionuclides manage to reach the biosphere in calculable quantities, and it is, thereby, obvious that increased k_d-values can have no effect on the dose rate results. Therefore, for Sc-2, the only cases of interest are those where the k_d-value has been reduced.

For Sc-2, changing the k_d-values of the bentonite buffer by a factor of 10 towards higher or lower values has no influence on the main total dose rate results at all. The same result is obtained if the k_d-values for the bentonite inside the sealing zone or that of the backfilling zone is varied by multiplying or dividing it with a factor of 10.

The reason why – despite the relevance of sorption for the transport of radionuclides – significant changes in the kd-values do not lead to calculable differences is the fact that sorption in either the backfilling zone or the sealing zone alone is sufficient to retard the radionuclides so strongly that only the known very mobile radionuclides with zero k_d-values reach the biosphere in significant amounts. As their transport properties are not affected by relative changes of the k_d-values, the dose rate results remain the same.

If k_d-values for all Sc-3.3 cases are reduced by a factor of 10, there is still no difference because only non-sorbing radionuclides reach the biosphere in notable amounts. Only if k_d-values are reduced by a factor of 100, Se-79, which has low reference k_d-values in the first place, contributes by a few percent to the total dose rate.

A significant difference in the dose rate results is only achieved if all k_d-values are set to zero (see Section 8.5.2, calculation case Sc-2-C3 no sorption).

Solubility limits

As discussed above in Section 8.5.2, solubility limits have no significant impact on the results for Sc-2.

Sc-2 Geosphere parameters

Aquifer flow rate

Changes in aquifer flow rate have no impact on the radionuclide transport. The velocity of the groundwater flow in the aquifer is decisive for the groundwater flow rate through the upper part of the disposal borehole, by which radionuclides that have migrated to the top of the borehole are transported towards the drinking water well. For as long as the volume of water flowing at the intersection of the borehole and the aquifer is significantly larger than the amount of vertical flow through the borehole, all activity reaching the uppermost borehole segment is more or less directly flushed out into the aquifer. Under the chosen boundary conditions, reducing the groundwater flow velocity to 0.365 m/a, which is one percent of the chosen reference value, still corresponds to a horizontal flow of water through the borehole, which is more than three orders of magnitude larger than the upward flow through the borehole.

Vertical flow rate

As is to be expected, considering the difference between the normal evolution scenario and Sc-2, which only differs regarding the assumed vertical flow, the vertical flow rate plays an important role for the transport calculation and the resulting dose rates.

Reducing the vertical flow rate by one order of magnitude to 10% of its reference value decreases the maximum dose rate by ten orders of magnitude, whereas an increase by a factor of 10 increases the total dose rate by a factor of 6.3. The time of occurrence is significantly shifted to earlier times around 130,000 years. In addition, a second maximum occurs at later times (870,000 years), where the maximum dose rate is approximately 1% of the main maximum and is mostly carried by Se-79. If the vertical dose rate is increased by another order of magnitude, the main dose rate carried by I-129 is further shifted towards earlier times and approximately doubled compared with the 10 L/a flow rate. In this case, the calculation shows also a second maximum, but this is carried by Sn-126, occurs around 212,000 years and is about 50% of the main maximum. Sn-79 still appears as a contributing radionuclide but only as a minor one.

Summary of sensitivity analysis

As seen in the tables above, almost none of the parameters affect the outcome of the long-term calculations significantly. That is, these parameters do not influence the results either regarding the time when maximum dose rates are observed or regarding their absolute value. Other results such as the distribution of radionuclides along the borehole or the release of radionuclides from the source term might show significant differences, but regarding potential contamination of the biosphere they do not play an important role.

For these parameters or boundary conditions, the uncertainty of their actual value is of reduced interest to the overall results. They also are not in the focus of interest for possible future research to reduce such uncertainty. As a first threshold to identify the parameters of significant influence, a change of 10 % of the total annual dose has been selected. The parameters and boundary conditions and the corresponding influence on the release of radionuclides towards the biosphere are listed in Table 8-5.

Of course, it needs to be kept in mind that the sensitivity of calculation results to changes of a specific parameter could vary significantly if a different set of reference case parameters were selected. However, at this stage, the results intend to give a good first assessment about the most important parameters and boundary conditions.

Table 8-5. Results of sensitivity analysis. Only the values with a significant impact on the maximum dose rates are listed. The values of the changed parameters and the differences between the reference data set and the modified one are given. Green coloured rows indicate results for Sc-3.3 and purple-coloured rows results for Sc-2.

Results of sensitivity analysis – reference cases for Sc-2 and Sc-3.3 Parameters with significant impact on calculated maximum dose rates							
Parameter Name as listed in Appendix V	**Min**	**Default** Ref. Case	**Max**	**Min** Dose Rate (µSv/a) Time	**Max** Dose Rate (µSv/a) Time	**Min** Diff-Factor Time shift	**Max** Diff-Factor Time shift
Source Term Performance							
Sc-3.3 All parameters set to default values as listed in Appendix V		yes		3.13 E-03 760,500 a		1.00 +0 a	
Factor_Inventory	0.1	1	10	3.50 E-04 682,000 a	3.00 E-02 762,000 a	0.11 -78.500 a	9.57 +1,500 a
Reversed order of SNF canister emplacement	MU top	UO2 top		6.95 E-04 1,000,000 a		0.22 +239,500 a	
Fractional release rate UO2 SNF	2 E-06 1/a	2 E-05 1/a	2 E-04 1/a	2.72 E-03 1,000,000 a	3.12 E-03 765,500 a	0.87 +239,500 a	1.00 +5,500 a
Sc-2 All parameters set to default values as listed in Appendix V		yes		3.24 E-04 760,000 a		1.00 +0 a	
Factor_Inventory	0.1	1	10	3.24 E-05 760,000 a	3.24 E-03 760,000 a	0.1 0 a	10 0 a
Reversed order of SNF canister emplacement	MU top	UO2 top		3.53 E-05 1,000,000 a		0.11 +240,000 a	
Fractional release rate UO2 SNF	2 E-06 1/a	2 E-05 1/a	2 E-04 1/a	1.77 E-04 1,000,000 a	3.34 E-04 709,500 a	0.55 +240,000 a	1.03 -50,500 a
Material and Radionuclide Properties							
Sc-3.3 All parameters set to default values as listed in Appendix V		yes		3.13 E-03 760,500 a		1.00 +0 a	
Kd-values buffer bentonite	x 0.1	See App. V	x 10	3.24 E-03 757,500 a	2.45 E-03 778,000 a	1.03 -3,000 a	0.78 +17,500 a
Solubility limits	x 0.1	See App. V	No limits	3.00 E-03 762,000 a	5.13 E-03 439,000 a	0.96 +1,500 a	1.65 -321,500 a
Sc-2 All parameters set to default values as listed in Appendix V		yes		3.24 E-04 760,000 a		1.00 +0 a	
Kd-values sealing bentonite buffer bentonite and backfill	zero kds		1)	5,25 E-02 1,000,000 a		162.00 +240,000 a	
Geosphere Parameters							
Sc-3.3 All parameters set to default values as listed in Appendix V		yes		3.13 E-03 760,500 a		1.00 +0 a	
Width vertical fractures	1 m	5 m	10 m	3.34 E-03 613,000 a	2.05 E-03 1,000,000 a	1.06 -147,500 a	0.65 +239,500 a

Results of sensitivity analysis – reference cases for Sc-2 and Sc-3.3 Parameters with significant impact on calculated maximum dose rates							
Parameter Name as listed in Appendix V	**Min**	**Default** Ref. Case	**Max**	**Min** Dose Rate (µSv/a) Time	**Max** Dose Rate (µSv/a) Time	**Min** Diff-Factor Time shift	**Max** Diff-Factor Time shift
Fracture flow rate through intersecting fracture	0.01 L/a	0.1 L/a	1 L/a	2.28 E-05 1,000,000 a	1.54 E-02 440,800 a	0.01 +239,500 a	4.91 -319,700 a
Sc-2 All parameters set to default values as listed in Appendix V		yes		3.24 E-04 760,000 a		1.00 +0 a	
Constant vertical upward flow through borehole	0.1 L/a	1 L/a	10 L/a	2.07 E-14 1,000,000 a	2.05 E-03 129,400 a	6.41 E-11 +240,000 a	6.33 -630.600 a

The parameters with a strong influence on the total annual dose are assigned to three main groups:

- source term performance,
- material and radionuclide parameters, and
- geosphere parameters.

In addition to these parameters, the assumptions directly related to the biosphere model, which are:

- dilution of contaminated water from the borehole in the aquifer, and
- daily consumption of contaminated water,

cause a linear change of the dose rates. Consequently. they can have a strong influence on the results as well.

Source term performance

Among the parameters and boundary conditions defining the source term performance that have strong influence of the dose rate results are the total inventory of the facility, the order of canister emplacement in the disposal zone and the fractional release rate for UO_2 SNF. Changes in the inventory lead to linear changes in the calculated dose rate results, which was to be expected.

The emplacement order of the canisters has been analysed for two variants: all metallic uranium SNF canisters at the bottom and the UO_2 SNF canisters on top (reference assumption) and the reversed order. For both reference scenarios the reversed emplacement order leads to significantly lower values. For the fracture scenario the results are not generally lower if the emplacement order is changed, but the results depend on the type of HLW inside the disposal segment, which is intersected. As in a real facility, such a fracture might occur – if at all – at any depth, there is little chance to influence the result by the preselected sequence of canisters. It could be argued, however, that the occurrence of fractures, especially with fast connection to the surface would be reduced with increasing depth. From this point of view, location of the high activity UO_2 SNF at the bottom of the disposal zone should be preferred. For Sc-2, there is also a significant decrease of the dose rate results if the UO_2 SNF canisters are emplaced at the bottom the disposal zone. Accordingly, this result would be worth to consider for the future concept.

Changes in the fractional release rates that have been assumed for the different waste streams have little or no influence on the calculated results. Only if the release rate for UO_2 SNF is reduced by a factor of 10, the dose rates decrease significantly. The reason is that UO_2 SNF is associated with a major part of the inventory, accordingly, release rate changes for the other waste streams have no large effect on the total dose rates. A significantly slower fractional release rate for UO_2 SNF shifts the total release of radionuclides towards later times so that the maximum dose rate does not occur anymore within the calculation period. However, it seems unlikely that much slower release rates fall into the range of uncertainty for the assumed fractional release rate for UO_2 SNF.

Material and radionuclide properties

For both scenarios, the selected k_d-values have a significant impact on the dose rate results. For Sc-3.3, there is only the sensitivity towards the k_d-values of the bentonite in the buffer around and between the canisters, because the main pathway for radionuclide release is bypassing the sealing and backfilling zone. Also, it is mainly the activity from the intersected disposal zone segment which is responsible for the main dose rate. Accordingly, sorption is limited to a very small amount of buffer material. However, if the fracture is assumed to intersect the sealing zone or the backfilling zone, then their respective k_d-values would be important for the transport calculations, because all activity would have to travel along the borehole before reaching the fracture location.

For Sc-2, the radionuclides that are retarded due to the sorption capacities of bentonite and backfill do not reach the biosphere. Retardation is so large that also strongly reduced sorption in parts of the total borehole pathway towards the surface has no significant influence. Only if sorption is considerably lower for the compete pathway, a significant increase of the calculated dose is observed.

Solubility limits play a significant role for the release of radionuclides from the source term. For the reference scenarios, they are of limited importance, because for Sc-2, the total dose rate is carried only by radionuclides that have no solubility limits assigned. Relative changes of the respective limits are therefore without consequence for the calculation of release and transport of these radionuclides.

For Sc-3.3, the situation is similar, i.e., most of the dose rate is carried by radionuclides with unlimited solubility. Consequently, no large change occurs if solubility limits for the radionuclides with limited solubility are reduced. However, if solubility limits are significantly increased or unlimited solubility is assumed for this scenario, the relative importance of other radionuclides increases. For the “no solubility limits” case, their contribution to the total dose rate is approximately 40%.

Geosphere parameters

As to be expected, assumptions about the pathway through the geosphere towards the surface are of special importance. This is clearly demonstrated by the differences between the reference case results for the different scenarios Sc-1, Sc-2, and Sc-3, which essentially differ only in the assumptions regarding the associated release pathway towards the biosphere. For the alternative scenarios Sc-2 and Sc-3, which both consider advective transport in addition to diffusive transport, the respective flow rates have a strong influence on the transport of radionuclides. Interestingly, starting from the flow rate values assumed for the reference cases, the relative decrease of dose rates for reduced flow rates is larger than the relative increase caused by enhanced flow rates. For the chosen boundary conditions, the sensitivity to flow rates is obviously decreasing with increasing flow rates.

For Sc-3.3, the assumptions regarding the fracture pathway from the borehole to the aquifer are important as well. As to the parameter variations used in this sensitivity assessment, only the width of the vertical fractures causes changes of more than 10%, but the sum of the assumptions has a much stronger influence.

8.6.5 Uncertainty aspects of post-closure safety assessment – Deep borehole model

Quantitative results of safety assessments for geological disposal facilities are always associated with a considerable level of uncertainty. This is caused on the one hand by the extremely long calculation periods, here one million years, and on the other hand by the fact that such facilities include natural components such as host rock, etc., with their intrinsic variations in time and space.

At an early stage of a disposal project, uncertainties must be addressed by a comprehensive scenario development using adequate FEPs and a variety of calculation cases including sensitivity analyses.

For this generic safety assessment, not all FEPs have been considered explicitly for scenario development. The main examples are climate changes or earthquakes and their associated consequences, e.g., for the hydrogeological conditions in the host rock. Instead, at this stage of the disposal project, the attempt has been made to cover potential impacts from such natural events by conservative assumptions regarding the postulated hydrogeological conditions.

Another example of FEPs that have not been considered for this generic safety assessment is the potential production of gas, due e.g., to corrosion of metal. Thermo-chemical reactions, e.g., corrosion of waste canisters that release water or gas within the disposal zone, have been identified as a potential source for upward flow through the borehole and surrounding EDZ (e.g., Brady et al. 2009). However, in most generic safety assessments for DBD facilities, this process (i.e., gas generation) has not been considered in the modelling, with reference to the early stage of the generic safety assessment models.

Proper consideration of this process would have to address several aspects, such as possible initiation of vertical flow up the borehole, potential diffusion of dissolved gases or dissipation of possible free gas phases away from the repository into the host rock, or possible delay of water access to the borehole due to over pressure inside the borehole.

In this work, the production of gases from corrosion as a potential source for upward flow has been covered for the deep borehole by assessing an alternative scenario, for which vertical advective flow through the borehole has been assumed, which could be caused by different processes and conditions. The present stage of the DBD concept and the uncertainties about the future site do not justify a more detailed assessment of FEPs related to gas generation and transport.

Uncertainty in parameter values or conditions are usually addressed using pessimistic or conservative assumptions so that the calculated potential radiological impact covers a broad bandwidth of parameter variations.

Especially, the results of a sensitivity analysis allow to identify those parameters and boundary conditions that have the largest impact on the safety assessment results. Future research work on the measurement and identification of parameter values as well as on further development of mathematical models can then concentrate on the areas that are important for the assessment results and at the same time have a large level of uncertainty.

A typical approach to address uncertainties in safety assessment calculations is the use of probabilistic calculations. This allows the mathematical consideration of uncertainties, but also leaves significant room for shifting mean results depending on the choice of probability distributions and parameters. Moreover, probabilistic models often lead to results that are difficult to comprehend and reproduce. Compared to probabilistic treatment of uncertainties the deterministic one is easier to communicate and understand. Therefore, respective regulations normally require deterministic calculations. Probabilistic calculations are either allowed or required only in addition to the deterministic ones.

Therefore, for this safety assessment, the approach has been to focus the assessment on deterministic calculations and assessing the effect of uncertain parameters carrying out a comprehensive sensitivity analysis.

This approach has also been considered appropriate because the purpose of this generic safety assessment was to develop a high-level simulation model as a first step in the development of a safety case for a future DBD facility. This study aimed at providing the possibility to evaluate and improve the understanding of the repository system performance and the most relevant processes that govern the evolution of the repository at this early stage of the project. Considering the generic character of this assessment, an additional probabilistic assessment did not seem to be justified. However, the computer model has been prepared to allow the input of probability distributions for a number of parameters to facilitate the execution of probabilistic calculations should that be required in the future.

The preliminary quantitative results from this generic safety assessment for high-level radioactive waste indicate that radionuclide releases from a hypothetical deep borehole repository, and the annual radiation doses to hypothetical future humans associated with those releases, may be extremely small.

For the normal evolution scenario, radionuclide releases and calculated dose rates are nearly zero. Also, two alternative scenarios have been considered, which are both considered to be less likely, especially, the geosphere pathway assumed for Sc-3 is considered very pessimistic/overconservative.

Scenario Sc-2, assuming a hydraulic gradient leading to vertical flow through the borehole, leads to dose rates in the order of $3 \cdot 10^{-4}$ mSv/a. The other alternative scenario, Sc-3, assumes that a transmissive fracture intersects the borehole. That fracture is connected via a vertical fracture system and a hydraulic gradient drives water through this fracture system towards the surface. Dose rates for this scenario reach maximum values in the order of $3 \cdot 10^{-3}$ mSv/a.

Obviously at the present stage of the project there is still much work to be done to improve the model assumptions, but these first results suggest that a deep borehole may be a viable alternative to a mined repository for disposal of the Norwegian high level radioactive waste.

The current generic safety assessment has also identified the following technical issues and/or knowledge gaps that have the largest potential to improve and enhance the confidence of future models and analysis.

- The assumed radionuclide release pathways and scenarios are decisive for the release and transport of radionuclides from the disposal zone towards the biosphere and the quantitative potential radiological impact.
  - Additional studies are needed to improve the selection of normal and alternative scenarios that are plausible for deep borehole disposal in crystalline rock and the associated conceptual and mathematical models for the radionuclide release pathways.
- Solubility and k_d-values are important parameters for the calculation of radionuclide release and transport. There are not many sources for these data where specific conditions in the deep geological underground have been taken into consideration.
  - Additional studies and experimental work to better characterise and quantify important geochemical processes in deep borehole environments, including chemically reducing, high ionic strength brines at elevated temperatures would significantly lower the present uncertainties.
- The radionuclide inventory is another decisive input for the safety assessment. Currently, it is based on available information on the Norwegian wastes and amended using data on similar waste types.
  - For future safety assessments an improved waste characterisation is needed.

8.6.6 Summary of calculations for deep borehole

The preliminary results from this generic safety assessment for the simplified deep borehole indicate that highly mobile radionuclides such as I-129, Cl-36, Ni-59, and Se-79, are the major dose contributors, and that the expected potential radiological impact to future humans associated with those releases is extremely small.

The results of the normal evolution scenario Sc-1, based on purely diffusive transport along the borehole leads to maximum total dose rates that are more than 20 orders of magnitude below the expected regulatory limit of 0.1 mSv/a even for calculation cases assuming pessimistically changed boundary conditions. This is in accordance with the results in Brady et al. (2011), where diffusion is not considered as a relevant transport mechanism for DBD.

The two alternative scenarios lead to significantly increased maximum dose rates, but these are still 1.5–2.5 orders of magnitude below the regulatory limit. It needs to be kept in mind that the alternative scenarios Sc-2 and Sc-3 are considered unlikely. Both scenarios require sustained hydraulic gradients in the deep underground as drivers for the assumed advective flow, which is unlikely, if the site is properly selected.

In addition, to the pessimistic assumption concerning the presence of a sufficient hydraulic gradient, the assumptions for advective transport via a fracture system through the crystalline host rock, chosen as boundary condition for Sc-3 is also considered as a very pessimistic boundary condition.

Nevertheless, scenarios Sc-2 and Sc-3 have been considered, but as mentioned before, not as equally likely scenarios as the Sc-1, but more as a kind of what-if scenarios. The results from assessing these scenarios indicate that even under very improbable and pessimistic conditions the potential radiological impact from the deep borehole disposal would still be acceptable for the public.

9 Safety assessment modelling for LILW disposal

The work presented in this chapter is based on a generic LILW repository design and site and the LILW inventory in Chapter 2, which needs to be further updated. Thus, the emphasis is on the modelling methodology and calculations to assess long-term safety. The selected parameter values and results are therefore of exemplary nature and only a first indication for the appropriate level of long-term safety of the LILW disposal. A pessimistic approach is used, so that the resulting doses are mostly overestimated.

9.1 Scenario development

The selection and justification of scenarios is performed by identifying and considering features, events, and processes (FEPs) associated with the LILW repository, especially those that may influence the potential release and migration of radionuclides from the repository or the subsequent radiation exposures to humans. The list of selected FEPs (see Table 6-2*)* is strongly related to the design of the facility, to the site characteristics and the related potential natural hazards, and to the activities planned during the life cycle of the repository. Potential release pathways have been selected taking into consideration the site characteristics and land use.

The long-term safety analysis is based on the evaluation of the radiological impact of radionuclide releases from the LLW and ILW chambers for a set of selected scenarios. The derivation of the activity limits is performed by calculating the peak doses for each of the selected scenarios resulting from a unit activity (concentration (Bq/g) or total amount (Bq) of radionuclides). Then, the maximum dose rates for the different scenarios are compared to identify the limiting scenario for each radionuclide, i.e., the most restrictive scenario regarding acceptable activity. Finally, after calculating the activities for each radionuclide, it is shown that the sum of the doses of all radionuclides remain under the dose limits defined in Chapter 4.

9.1.1 Identification of safety relevant post-closure scenarios

The selection of appropriate scenarios is a key element of the long-term safety assessment, as it will strongly influence its results.

To assess the long-term safety of a waste disposal facility, potential evolution lines are considered (see Chapter 7). This is achieved by developing a set of scenarios that describe the so-called normal and alternative evolutions of the repository.

A common element in scenario generation methodologies is the utilisation of FEP lists that comprise all FEPs that may influence the evolution of the disposal system and the potential release of radionuclides. For this reason, the identification of the potential scenarios that may be considered for the safety assessment of the facility is based on the results of the analysis of the FEPs applicable to the disposal system. Finally, judgements as to which of the identified scenarios shall be selected for further analysis are made.

Based on the analysis of the FEPs applicable to the LILW repository (see Table 6-2), some illustrative scenarios have been identified. The scenarios have been generated by using the following (conservative) assumptions concerning geology (geosphere), engineered barrier system, waste conditions and human activities. Inclusion of further assumptions and extension of the number of investigated scenarios is certainly advisable for future, site-specific safety assessments. The current assumptions are based on relatively credible evolutions that encompass simplifications to allow reasonable modelling accounting for the existing uncertainties regarding the site and evolution of the disposal system.

Assumptions for the geosphere:

- The geosphere and the hydraulic environment are not expected to change during the safety assessment period of one million years, although different hydraulic conductivity values for the host rock are assumed for different scenarios.
- Groundwater flow through the ILW chamber and the LLW chambers is independent.

Assumptions for the engineered barrier system, including the waste packages (WPs):

- In the case of concrete barriers: Partial degradation – the barriers retain their integrity but with decreasing isolating capacity or local loss of integrity.
- In the case of WPs: the WPs lose any barrier function after a certain amount of time.

Assumptions for the waste matrix:

- Full degradation – after container failure, the matrix is in direct contact with the environment.
- Inclusion of additional amounts of waste (i.e., sealed sources).

Regarding human activities, the following is assumed:

- No access to site –institutional control of around 300 years.
- Human intrusion as a drilling operation into a WP after the institutional control period.
- Access by drinking water well close to the shaft.

9.1.2 Selection of scenarios

A few scenarios were chosen to be modelled for this generic safety assessment to show the methodology and illustrative results. The scenarios are listed in Table 9-1. While the scenarios for human activity and Human intrusion appear to be very similar at first glance (drilling in the proximity or into the disposal facility), they significantly differ in release pathways and dose calculations. Therefore, it is reasonable to investigate them individually.

*Table 9-1. Selection of scenarios chosen to be modelled (*underground openings are called infrastructural area (e.g., access drifts, shafts etc.). These exclude the LLW and ILW disposal chambers.*

Scenario designation	Geologic/Hydraulic assumptions	EBS assumptions	Waste assumptions	Human activity
Reference	Independent groundwater flow through ILW and LLW chambers	Concrete barriers degrade/are in degraded state WPs loose gradually their barrier function	Matrix is in direct contact with the surrounding environment after WP failure	No human activity
Human Activity (HA)	Groundwater flow partially from ILW and LLW through plugs into the infrastructural area*			Operating drinking water well close to the shaft
Human Intrusion (HI)	Independent groundwater flow through ILW and LLW chambers		Matrix is in direct contact with environment after WP failure Drilling is assumed to hit WPs with special waste (Appendix IV)	Drilling operation into WPs containing special waste

The evolution leading to the reference scenario, and the corresponding assumptions have been discussed in Section 7.2. Further assumptions/data are presented in Section 9.2.

Alternative scenarios are variations from the reference scenario. In general, the same model is used to calculate the potential radiological impact, but certain parameter values are changed to account for alternative evolution(s) of the repository.

In the human activity (HA) scenario, a drinking water well next to the shaft is assumed to create a hydraulic gradient towards the surface. In this case, the radionuclide concentration in the infrastructural area below the shaft is decisive for the resulting dose. In this scenario, part of the flow passes from the ILW and LLW chambers through the plugs at the entrances of the chambers.

The human intrusion (HI) scenario accounts for the disposal of additional special waste (Appendix IV). Due to the high activity of this type of waste, one of the related WPs is used as the target for intrusion. Human intrusion assumes drilling directly into the WP. The critical individual in this scenario is a drilling worker. Drilling is assumed to take place directly after the end of the institutional control period. According to present planning, this would be 300 years after the closure phase. Despite this assumption, the calculations are carried out for the complete post-closure period to demonstrate the change in the potential radiological impact should such an event take place at an earlier or later point of time.

9.2 Model development and simulations

9.2.1 Assumptions for the reference scenario

The main assumptions that form the basis for the reference scenario are:

- It is assumed that there is an active institutional control for 300 years after closure of the facility.
- Geosphere conditions at the site will remain essentially the same as today (although groundwater flow is varied in the analysis of other scenarios).
- Geosphere conditions/properties are defined in Hagros et al. (2021).
- It is assumed that there is no sorption within the geosphere, which is a conservative assumption.
- It is assumed that the total amount of groundwater passing through the repository will end up in a drinking water well.
- The groundwater flow through the repository is not diluted in the geosphere until it reaches the groundwater well; dilution in the well is assumed to happen in a reasonably sized well for drinking water production.
- No radioactive decay is assumed between time of activity estimation and closure of the disposal facility.
- The solubility of radionuclides is assumed to be unlimited, which is also a conservative assumption.
- It is assumed that the complete volume of the waste chambers, including backfill and concrete, is saturated by water at the time of closure.
- It is assumed that the total inventory of a WP is saturated by water at the time of failure of a WP, that is:
  - no radionuclides are bound to any kind of waste matrix,
  - all infiltration will be equally distributed over the waste volume of all failed WPs, and
  - after failure of all WPs, the total inventory is evenly saturated with water.
- Type and position of the engineered barriers is according to the design presented in Ikonen et al. (2020).
- Operation and closure of the disposal facility is according to the design presented in Ikonen et al. (2020).
- The most exposed individual consumes all their drinking water from the assumed groundwater well.
- The well is assumed to be a short distance from the disposal facility.

Deviations from these assumptions are partly considered by sensitivity analyses or in alternative scenarios. These deviations are explained in the respective sections.

9.2.2 Conceptual model for the reference scenario – release pathways

The only release pathway for radionuclides from the LILW repository is the groundwater pathway which transports the radionuclides from the facility to a drinking water well.

The main water fluxes considered in the repository model for the reference scenario are presented in Figure 9-1. Water flows from the host rock into the waste chambers. In the case of ILW, the concrete vault serves as a hydraulic barrier, although within the saturated ILW vault, water is contaminated, and radionuclides leave the vault by diffusion through the concrete. In the LLW chambers, groundwater flow comes in direct contact with the WPs. The LLW chambers are presented as one singular volume that contains all materials and the volume of all 8 LLW chambers. From both, the ILW and LLW chambers, water flows towards the host rock. Through fracture(s) in the rock, the contaminated water is transported into an aquifer/large fracture that is used for drinking water production in a well.

The waste chambers are connected to the infrastructural area of the repository. The accesses to the chambers are closed by concrete plugs. In the reference scenario, there is no hydraulic gradient and, thus, no flow of groundwater in the direction of these plugs. However, part of the radionuclides will pass through the plugs and enter the infrastructural area by diffusion. From the infrastructural area, groundwater flow will transport the contaminated water into the host rock. All contaminated water ends up in the same set of fractures and the aquifer that supplies the drinking water well.

The ILW and LLW waste packages will, for a certain time after closure, contain most part of the waste. Due to potential mechanical and chemical impacts, their lifetime under repository conditions is limited. For the LLW steel drums, it is assumed that 30% of drums have already failed at closure, while the remaining 70 % will uniformly fail over a period of 50 years. For the ILW concrete packages, it is assumed that 10 % of packages already failed at closure and the rest fails uniformly over a period of 100 years. The ILW steel drums within the concrete packages are not assumed to retard the exposure of ILW to groundwater. There is uncertainty in these estimations, however, they are on the conservative side.

The degradation of the concrete of the vault is not modelled. Instead, its initial permeability is set to the value of already degraded concrete from the beginning of the simulation on. The concrete plugs are assumed to be important parts of the closure system to separate the repository from the surface environment. Therefore, a very low initial permeability is assumed for the concrete plugs that will degrade over a period of several thousand years.

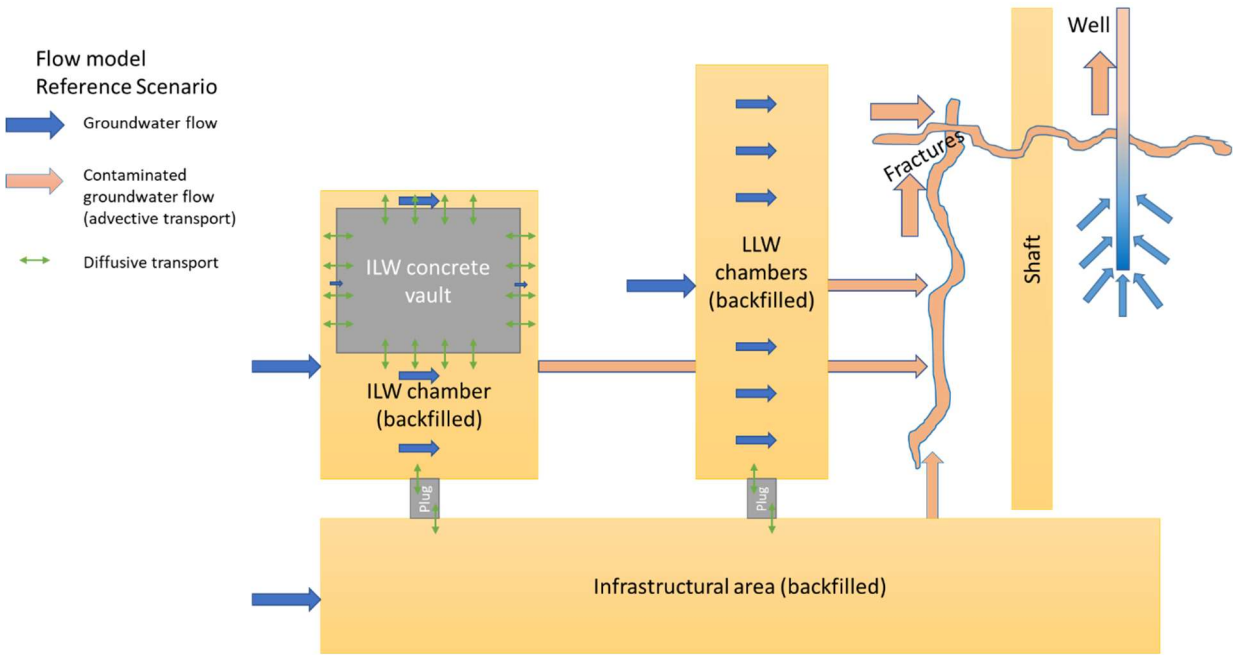

Figure 9-1. Flow model of the reference scenario.

9.2.3 Mathematical model for the reference scenario

The computer code used for carrying out the long-term calculations is GoldSim Simulation Environment extended by the Radionuclide Transport Module.

Despite GoldSim's ability to run probabilistic calculations, for the purpose of the safety assessment, the calculations are focused on deterministic calculations and sensitivity analyses to investigate the influence of changing parameters values. Compared to probabilistic calculations, deterministic calculations are easier to understand and interpret and to reproduce in the case of an independent review using a different software code.

GoldSim near-field and geosphere model for LILW disposal

The implementation of the conceptual model for the reference scenario into a GoldSim model is sketched in Figure 9-2. This figure displays the user interface that contains the pathways considered for the LILW disposal model.

As shown in Figure 9-2, the conceptual model described above is implemented in GoldSim as source elements for ILW and LLW inventories and a series of mixing cells and pipes simulating the different pathways between the waste and the aquifer.

For each time step and pathway cell or pipe, the computer model calculates the distribution of radionuclides between the solid and liquid media inside the cell to determine the radionuclide concentration in the water flowing out of it. The whole system is completely saturated with water from the start of the simulation period onwards. Consequently, the waste of all WPs with ILW and LLW that are assumed to have failed is also saturated.

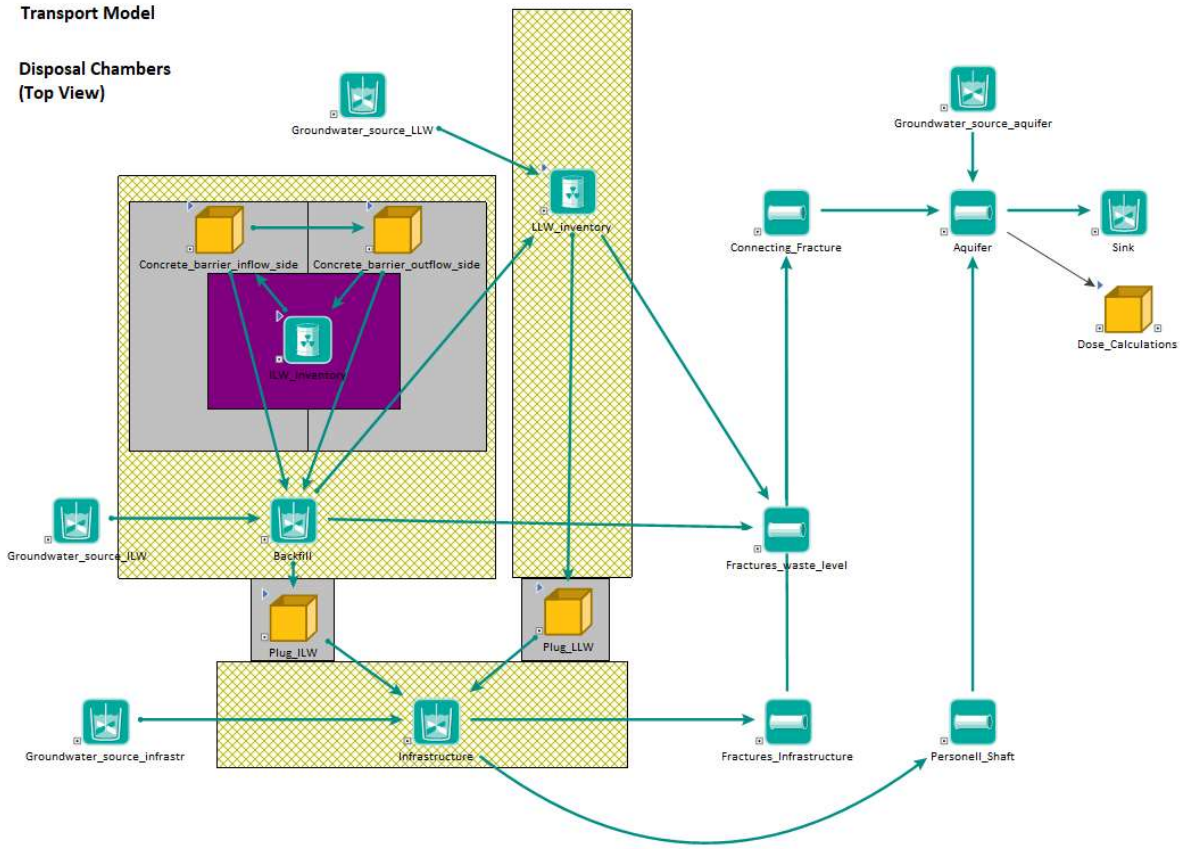

Figure 9-2. GoldSim transport model for the LILW disposal depicted as the user interface of GoldSim.

The mixing cells called “Groundwater_source…” represent infinite reservoirs of groundwater that flows into the mixing cells in the waste chambers with a defined flow rate. From these reservoirs, groundwater enters the repository model via several mixing cells:

- the mixing cell “Backfill” in the ILW chamber,
- the cell behind the source element “LLW_inventory” and
- the cell “Infrastructure”

Contamination of water occurs directly in the LLW chambers since part of the inventory is exposed to the groundwater. This is defined in the source element “LLW_inventory”. Corresponding radionuclides go into solution within the cell and are advectively transported by the flow, which goes into the pipe element “Fractures_waste_level”, thus entering the geosphere.

The groundwater flow passes through the cell “Backfill” in the ILW chamber in a similar way. Due to the low hydraulic conductivity of the concrete vault of 10^{-7} m/s, represented by the mixing cells in “Concrete_barrier_inflow_side” and “Concrete_barrier_outflow_side”, there is only very little groundwater flowing through ILW. Flow through the vault is assumed only in the reference scenario. However, both, the mixing cell behind the source element “ILW_inventory” and the cells of the concrete barrier are saturated with water. Depending on how many WPs have failed at the time, as defined in the source element, the corresponding nuclides go into solution. Since all cells (source element mixing cell, concrete barrier mixing cells, backfill mixing cell) have diffusive links, the radionuclides are diffusively transported through the concrete vault into the chamber and into the cell “Backfill”. Here, they enter the groundwater flow and progress also to the cell “Fractures_waste_level”, entering the geosphere.

Further diffusive links are integrated into the connection between “Backfill” and “Plug_ILW”, between “LLW_inventory” and “Plug_LLW” as well as between these plugs and the cell “Infrastructure”. By diffusive transport, radionuclides from ILW or LLW will therefore also occur in “Infrastructure”. From here, groundwater flows into the cell “Fractures_Infrastructure” and thus, into the geosphere.

The geosphere model is a simplified representation of a fracture system within the crystalline host rock that uses the pipe elements of GoldSim to represent a variety of hydraulically relevant fractures. The flow goes through the “Fractures_Infrastructure” and “Fractures_waste_level” into the “Connecting_Fracture” and then the “Aquifer” (see Figure 9-2). Along the way, the parameters of the pipe elements define the velocity of flow and retardation of radionuclides by matrix diffusion. The concentration of radionuclides in the aquifer is the major parameter for dose calculations (see Section 9.2.2) since it feeds the drinking water well. Except for the contaminated water coming from the facility, the aquifer is also supplied with fresh water from another practically infinite groundwater source (“Groundwater_source_aquifer”) to model enough water to qualify as a well aquifer. The mixing cell “Sink” is used as an exit to the model and accumulates all flows and radionuclides for mathematical balance.

The flow connection between “Infrastructure” and “personnel shaft” is conditional and not activated in the model for the reference scenario.

Mass transport through GoldSim model

Inflow

The inflow of water into the chambers is constant across the simulation time of 1 million years. Inflow into the ILW vault itself is negligible (4.4×10^{-6} m³/a) since the vault is surrounded by highly permeable backfill. Inflow into the ILW chamber is assumed to be 3.5 m³/a. The inflow into the LLW chambers amounts to 1.8 m³/a.

Transport through and from the chambers

The mass transport in the GoldSim model starts in the cells from the respective source elements. In the ILW chamber, the waste is enclosed by a concrete vault. Transport through the concrete vault wall is assumed to occur mostly by diffusion in the reference scenario. Over time, radionuclides will enter the crushed rock backfill of the chamber. Once radionuclides are present in the backfill of the chamber, the groundwater flow

through the chamber advectively transports the radionuclides into the host rock. In the LLW chamber(s), the situation is similar although without the concrete vault. Radionuclides in solution are directly transferred to groundwater. All volumes in the model are assumed to be saturated with water from that start of the simulation on. The only exception are the volumes of those WPs that have not yet failed.

The different WPs in the planned repository are modelled as one source element per waste category containing the total number of containers. Each source element contains a cell that represents the volume and inventory with all WPs of that waste category. The source element and its cell include information on the total number of containers as well as the container failure rate and represents the material contents of waste, conditioned concrete, and water. In the ILW source element, the cell also contains concrete of the WPs themselves and concrete backfill of the spaces between WPs. In the LLW chamber(s), the respective cell also contains the crushed rock backfill around the WPs (steel drums).

Figure 9-3 shows the retardation of radionuclide transport through the concrete vault wall for U-238. The concentration decreases as the distance from the source increases. The volumes of all concrete wall parts are identical. The total amount of U-238 in the vault is around 18 kg. Due to the very long half-life of U-238, its decay does not cause reduction of U-238 mass along the pathway.

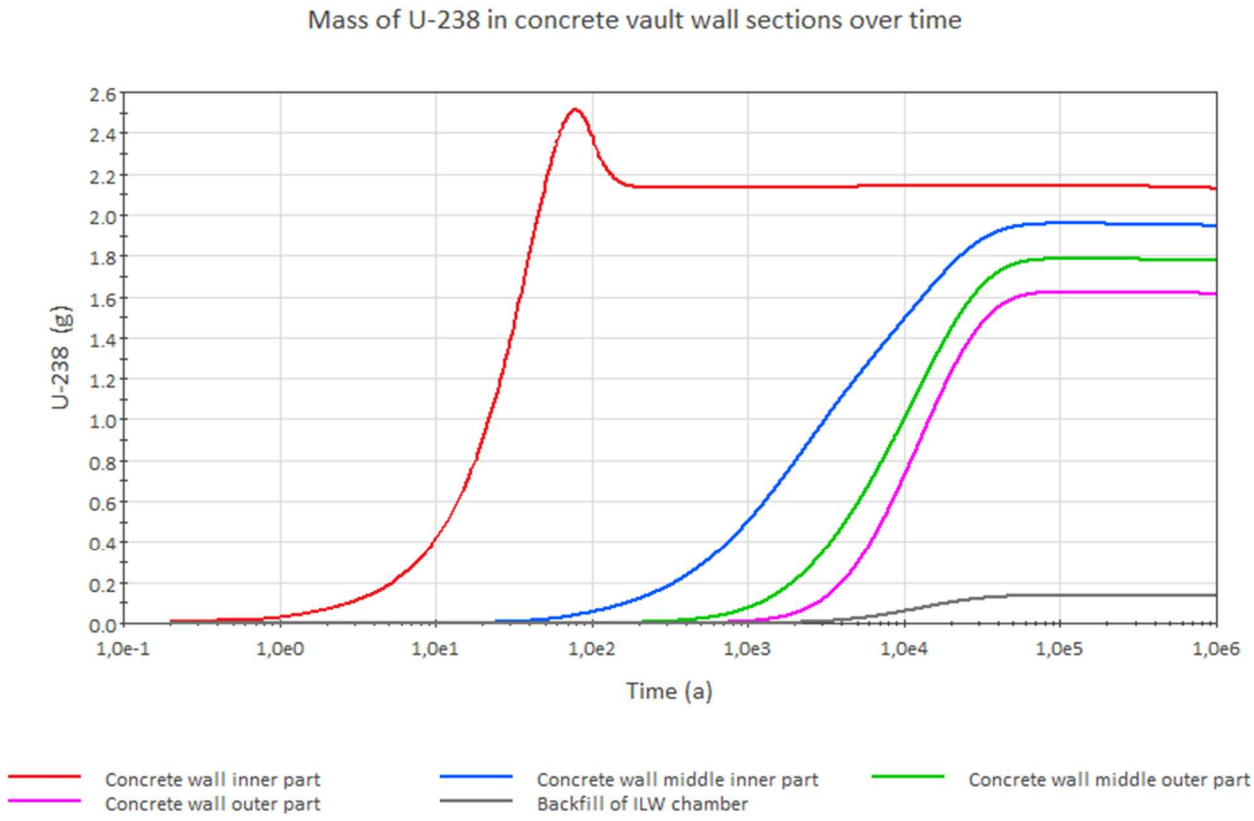

Figure 9-3. Example of effect of retardation of U-238 while passing through the concrete vault wall surrounding the ILW WPs. The graph shows the mass of U-238 inside the four layers into which the wall is divided for the model calculations (inner, middle inner, middle outer, outer part) with time. In addition, the figure presents the mass of U-238 with time inside the backfill material surrounding the vault.

Transport along groundwater pathway

The groundwater pathway is modelled as a series of pipe elements representing fractures through the host rock. Transport within these pipe elements is purely advective. A retarding element is introduced by matrix diffusion. In addition, in the aquifer dilution further reduces the concentration since the aquifer is serviced by further groundwater to qualify as an aquifer for well operation. Figure 9-4 shows the retardation and dilution of Ag-108 through the groundwater pathway. In this example, the chosen nuclide has a half-life of only 418 years. For this reason, it can be observed that the concentration of Ag-108 drops rapidly during the simulation period.

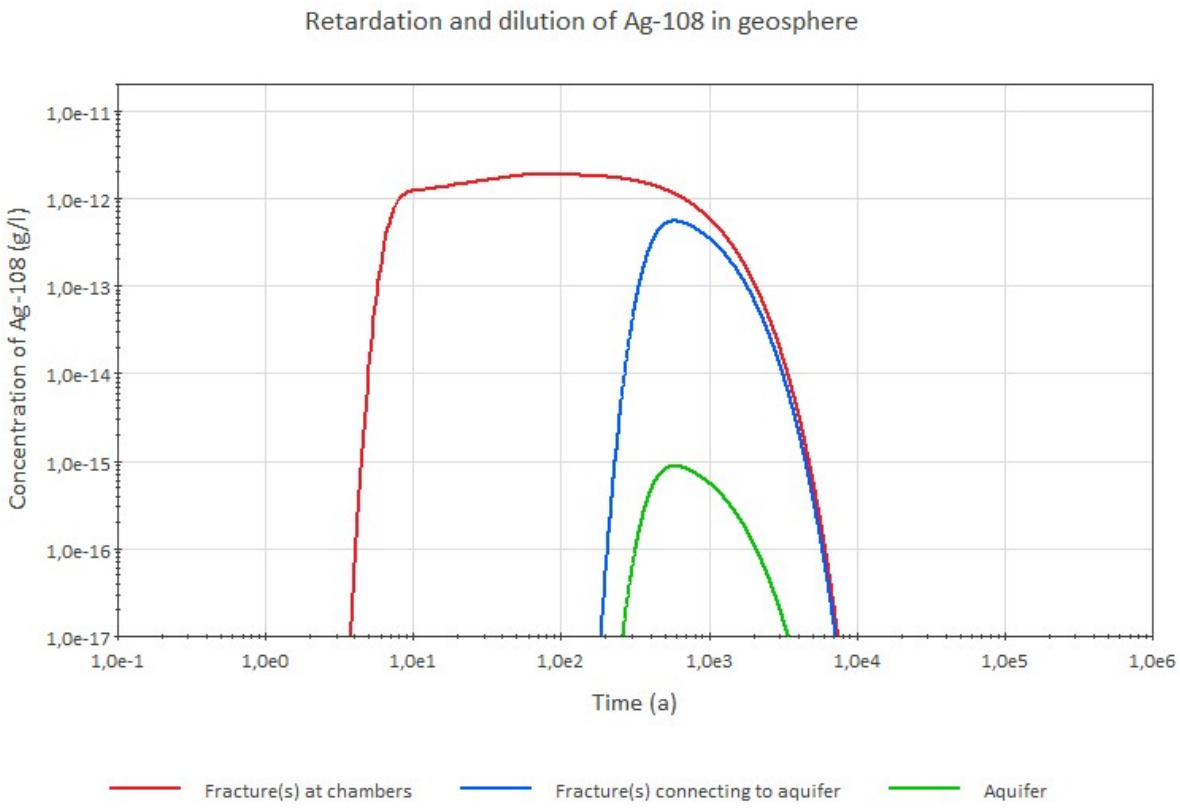

Figure 9-4. Effect of retardation, dilution, and decay of Ag-108 during transport through the geosphere.

Total release

The total release of activity from the ILW vault with time is presented in Figure 9-5. It becomes apparent that the release from the vault has its maximum at 1.1×10^{10} Bq, which is only around 0.01% of the total activity emplaced in the vault. Calculating the release from the WPs into the concrete vault wall, around 5×10^{10} Bq are released which corresponds to 0.05% of the total ILW activity, which is only slightly higher than the release from the vault. Therefore, a major contributor to the enclosure of the waste is sorption of radionuclides in the concrete backfill within the vault.

The total release of activity from the LLW chamber is shown in Figure 9-6. The total release is 8.8×10^{8} Bq, which is 1.6% of the emplaced waste.

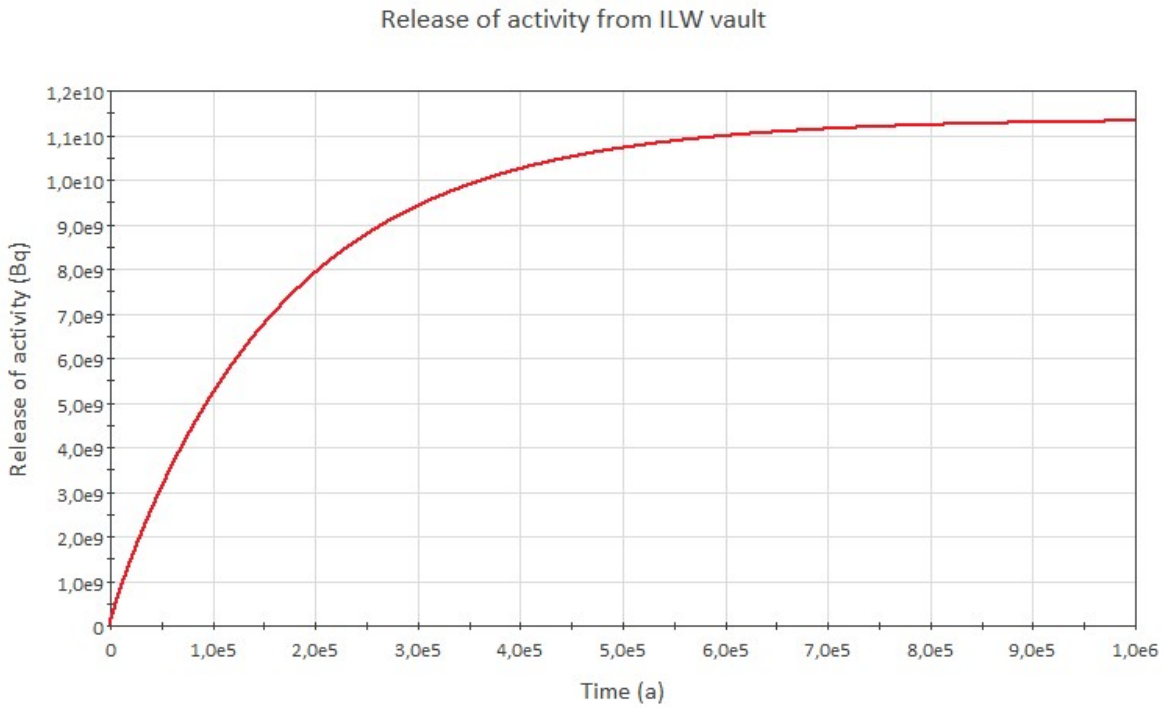

Figure 9-5. Cumulative release of total activity from the ILW concrete vault

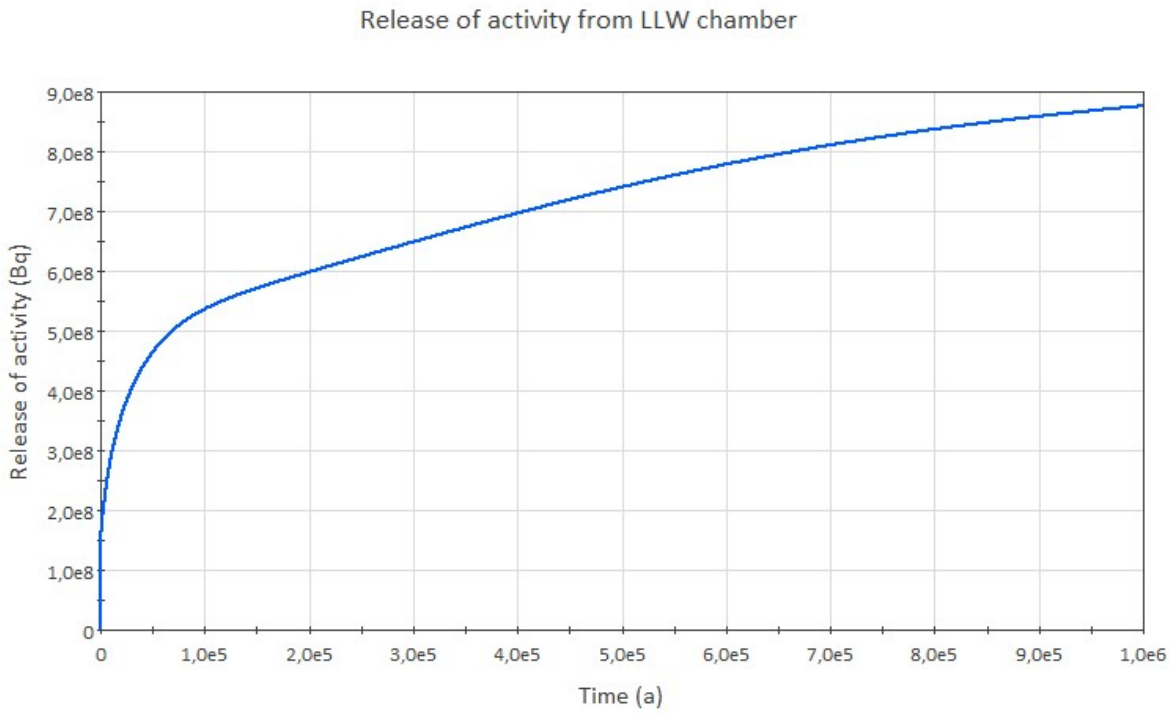

Figure 9-6. Cumulative release of total activity from the LLW chamber

To investigate, what portion of release (or lack thereof) is based on radioactive decay, GoldSim allows to switch off the decay of species. Running the simulation and the analyses as before but without decay leads to a release from ILW vault of 5.4% and from LLW chamber of 99.8% from the emplaced total activity. In conclusion, the decay of species before leaving the vault/chamber is an important aspect when analysing the total release. Especially for LLW, the decay of short-lived radionuclides is an essential factor. The reason for the significant difference between ILW vault and LLW chamber is the high amount of concrete within the ILW vault which leads to sorption of radionuclides. Sensitivity analysis regarding the role of sorption for the resulting annual dose are presented in Section 9.3.2. This effect might also be sensitive to the radionuclides present in the inventory and their corresponding sorption coefficients in concrete. Updating the inventory vector in future iterations of the safety assessment might therefore result in lower or higher sensitivity of sorption to the resulting annual dose.

The biosphere model for the LILW disposal

To assess the radiological impact of the LILW disposal a very simple biosphere model has been used to calculate doses for members of the public, as in the biosphere model for the DBD disposal (see Section 8.2) It is assumed that a member of the public will drink 3 litres of water per day from a contaminated well.

This simple biosphere model has been chosen because it is considered to give a good estimate of what could be the radiological impact under unfavourable conditions and because this is a generic safety assessment (further details in Section 8.2).

Calculation of Potential Dose Rates:

The dose due to ingestion of water is calculated using Equation 8-1. Concentration of radionuclides in water (C_{water}) is given by the geosphere calculations and the interface features (well extraction). In the GoldSim model radionuclide concentration of the water inside the aquifer is calculated based on the model for simulating radionuclide migration through the near field and the geosphere as described above.

9.2.4 Conceptual and mathematical model for alternative scenarios

The following alternative scenarios are considered:

- HA Human activity
- HI Human intrusion

The conceptual and mathematical model for the reference scenario has been explained in the sections above. The alternative scenarios are calculated using essentially the same conceptual and mathematical model as in the reference scenario, although taking into consideration the impact the alternative evolution has on the performance of the repository and the environment, and thus on the selected parameter values.

Human activity

The HA scenario assumes that a drinking water well is constructed close to one of the former shafts of the facility. This is modelled by introducing a shortcut from the facility to a drinking water well via the shaft (Figure 9-7). It is activated by changing the direction of the outflow from the infrastructural area. Instead of going into the host rock and fracture system, it goes directly into the shaft, which intersects the aquifer close to the surface. As can be seen in Figure 9-2, the shaft is introduced in GoldSim as a pipe element that connects the mixing cell representing the infrastructural area and the pipe element representing the aquifer.

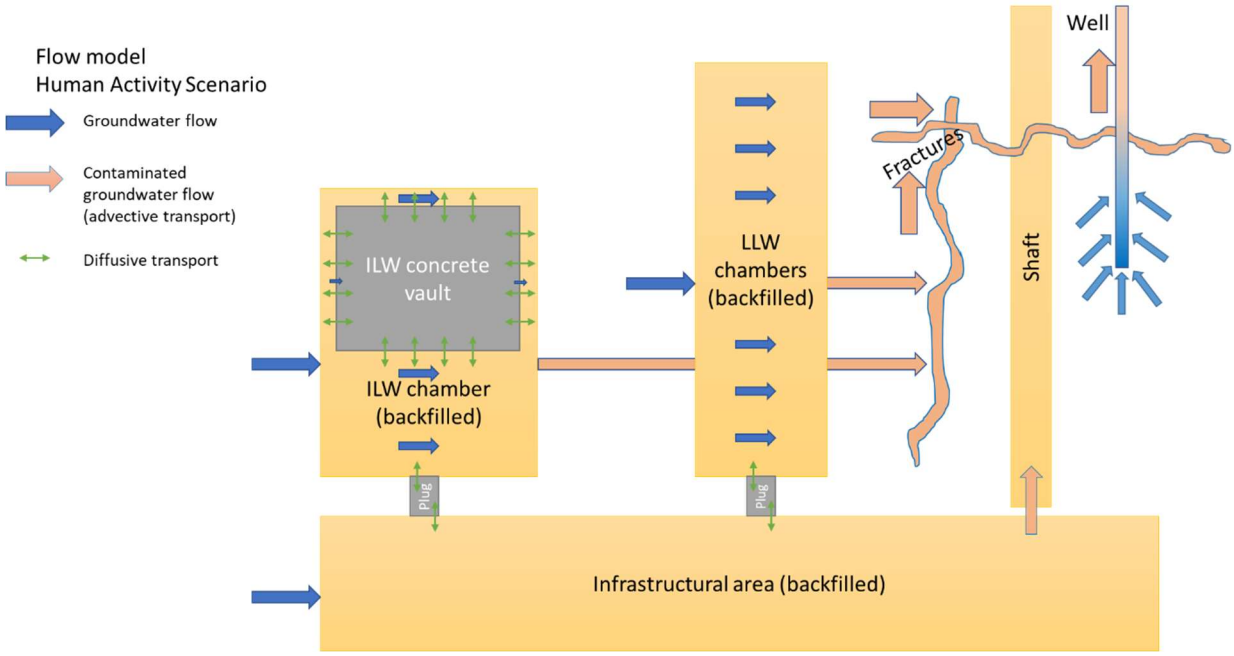

Figure 9-7. Flow model of the alternative human activity scenario.

Human intrusion

This scenario differs significantly from the reference one in two aspects: the waste and the release and exposure pathways.

The additional special waste (see Section 2.5 and Table 2-4) considered is described in Appendix IV. Since it is expected that these WPs contain waste with a higher specific activity, they are each chosen individually to be analysed in this scenario. The scenario assumes a drilling operation that penetrates a WP and transports the waste material to the ground surface. The drilling workers are thus exposed to a mixture of drilling bits and fluid. This mixture of materials is modelled as diluted waste material by multiplying the specific activity with a dilution factor. Consequently, the material at the ground surface has a smaller specific activity than the waste material underground.

The drilling workers receive a radiological dose by breathing and ingesting dust as well as direct radiation due to the time spent in the proximity to radioactive materials. The respective doses are calculated individually and then summed up. In general, the calculations follow the principles laid out in Section 9.2.3, where the calculation of dose based on ingestion is already presented. In this human intrusion scenario, calculations for the doses by breathing and direct radiation must be included and are calculated as follows (IAEA 2003).

Calculation of Potential Dose Rates

The dose due to breathing of dust is expressed as:

$$D_{br} = A_{dil} \cdot T_{dril} \cdot B \cdot C_D \cdot DF_{br} \qquad \textit{(Equation 9-1)}$$

where

D_{br}	is the dose due to breathing dust (Sv/a),
A_{dil}	is the specific activity of the drilling material containing waste (Bq/kg),
T_{dril}	is the yearly drilling time during which workers are exposed (hr/a),
B	is the breathing rate of a worker (m³/hr),
C_D	is the concentration of dust in the air (kg/m³), and
DF_{br}	is the dose conversion factor for breathing (Sv/Bq).

The dose due to direct radiation is expressed as:

$$D_{ra} = A_{dil} \cdot T_{pres} \cdot DF_{ra} \quad \text{(Equation 9-2)}$$

where

D_{ra}	is the dose due to direct radiation (Sv/a),
A_{dil}	is the specific activity of the drilling material containing waste (Bq/kg),
T_{pres}	is the time during which workers are present on the drilling site (hr/a), and
DF_{ra}	is the dose conversion factor for direct radiation [(Sv/s)/(Bq/kg)].

9.3 Results and analysis of the LILW disposal scenarios

For the assumed inventory and different scenarios, calculations have been carried out to evaluate the potential radiological impact. In addition, a comprehensive sensitivity analysis has been carried out to point out areas for future investigations or research as well as existing safety margins.

To assess the potential radiological impact for the reference scenario of the LILW disposal facility, the models for the source term, the near field and the geosphere were selected as described above. For the biosphere, a simple drinking water scenario was selected.

A two-step approach has been used to assess the consequences, which could be followed by another iteration if required. In the first step, a set of conservative initial parameter values and conditions are selected, and deterministic calculations are carried out to get a first estimate of the expected dose rate for an individual of the exposure group. In the second step, the chosen set of parameter values and assumptions is investigated regarding the sensitivity of the model towards the selected parameters values. To this purpose, deterministic sensitivity calculations are carried out and the results for individual radionuclides and release pathways are examined in detail. This second step also serves to evaluate the degree of conservatism inherent to the model.

Lessons learnt from the second step could then lead to adjustments of the design of the repository and, correspondingly, to new scenarios for future safety assessment updates.

9.3.1 Results for the reference scenario – reference data set

This section describes the results for the reference scenario and the assumed inventory. It must be kept in mind that there are large uncertainties regarding the inventory and geosphere. Nonetheless, the results can be used to define the expected order of magnitude of future radiological impact and the upper limits of that impact, but they cannot be used as an accurate quantitative forecast of the future impact.

The results for the total annual dose resulting from the application of the data set as listed in Appendix VI are shown in Figure 9-8. In addition to the curve for the total annual dose, the contribution of the most relevant individual radionuclides is also shown. The dose rates curves caused by other individual radionuclides contributing to the total dose are not shown due to their very small quantities.

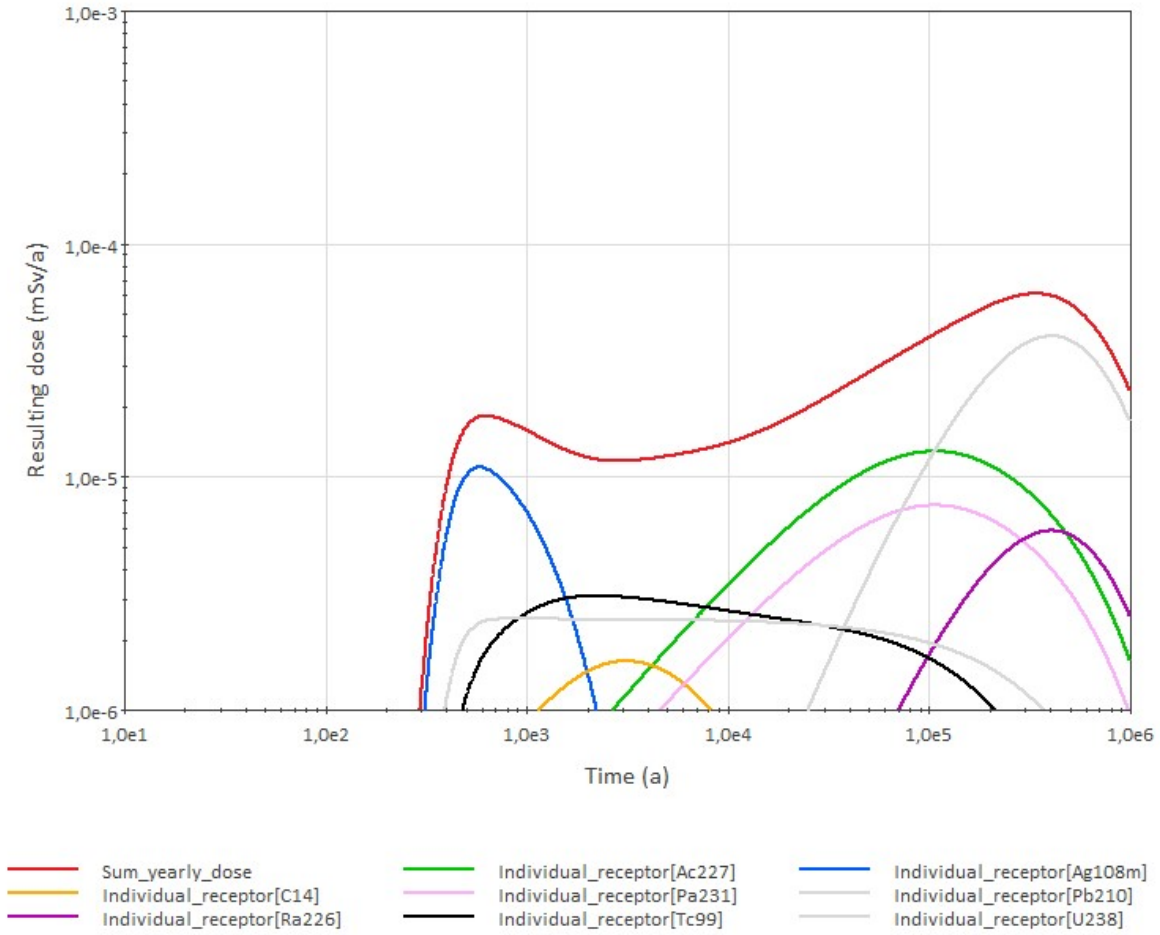

Figure 9-8. Resulting annual dose rate for individual and most important contributing radionuclides in the reference scenario

The curve of total dose rate shows two clearly defined maxima: 1.83×10^{-5} mSv/a at 620 years and 6.12×10^{-5} mSv/a at 339,000 years. These values are significantly below the usual regulatory dose rate limit of 0.1 mSv/a. The individual contributions of radionuclides not plotted in the figure above contribute less than 1 nSv/a to the total dose.

If the period for the calculations is increased to 10 million years, the resulting dose keeps diminishing to very low values, mostly caused by lingering concentrations of Pb-210 and (to a lesser extent) Ra-226. This simulation has been done mainly to confirm that the calculations render theoretically reasonable results. The assessment time of 1 million years is considered reasonable, although uncertainties in the evolution of the repository increases with time.

Short-lived radionuclides, which form the largest part of the expected initial activity of the waste in the repository, such as Cs-137, Co-60 and Sr-90, do not appear in Figure 9-8, as they are retarded in the technical barriers and the geosphere, so that no significant amount reaches the aquifer. Otherwise, these radionuclides would also contribute a significant part to the total dose curve. To demonstrate this, a variant calculation case is analysed, where the radioactive decay for the inventory has been switched off in the GoldSim model.

Figure 9-9 shows the results for that calculation. As decay is switched off, the figure does not show any daughter nuclides. Particularly Sr-90, Co-60 and Cs-137 would indeed contribute significantly to the dose rate if there were no decay.

Consequently, the technical and natural barriers of the repository effectively prevent the release of short-lived radionuclides like Cs-137, Sr-90 or Co-60 to the biosphere. The results of the reference scenario are further discussed in context with the results from the sensitivity analysis in the next section.

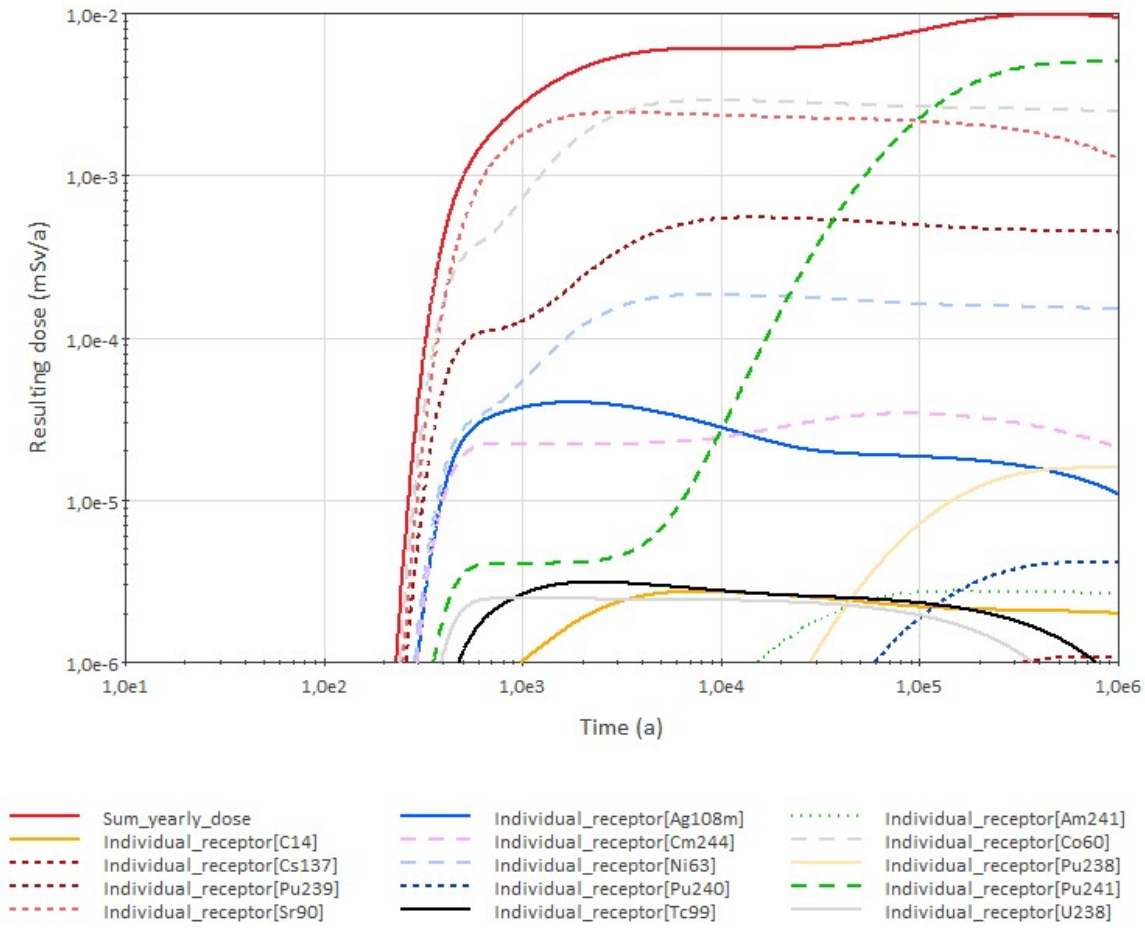

Figure 9-9. Resulting annual dose rate for individual and most important contributing radionuclides in a variant of the reference scenario that assumes no radioactive decay.

9.3.2 Sensitivity analysis related to the reference scenario

A sensitivity analysis has been carried out to investigate the influence the uncertainties of various parameters have on the results of the long-term assessment. The main objectives of these calculations were to identify parameters, for which additional research may be required to increase the accuracy of the long-term assessment and to determine whether overly optimistic or overly pessimistic (conservative) assumptions and parameters have been used for the initial deterministic calculations. Another purpose of the sensitivity analysis is to determine the general robustness of the model against parameter changes. The sensitivity analysis concentrated on parameters from the following parameter groups:

Inventory

- ILW and LLW inventory activity

Barrier Performance

- Degradation of concrete vault
- Degradation of WPs (initial failure rate, time until complete failure)

Material Properties

- Properties of near field materials (Kd-values)
- Fraction of contaminated concrete in WPs
- Fraction of concrete in WPs (concrete used as WP material, e.g., as backfill or lining on the inside)

Geosphere

- Groundwater flow rate
- Distance to well

Biosphere

- Amount of drinking water
- Size of drinking water well

For the selected biosphere model, the amount of drinking water per day and the size of the well are changed. It is expected that these values have a linear relation to the resulting annual dose. The same relation is expected from multiplying the inventory activities with a constant factor. This relation might be more interesting, however, since the facility contains two different types of waste and their corresponding activity, which might have different influence on the combined result.

To analyse the sensitivity of the model towards variation of individual parameter values, all other reference case parameter values of the reference scenario have been kept constant, while for the parameters of interest, extreme values have been selected. The changes in the calculations resulting from the variation in the parameter values are listed in Table 9-2 for the maximum annual total dose rate and the time of its appearance plus the relation to the maximum value for the reference data set and shift in time for the peak dose. The minimum and maximum values are shown to demonstrate the influence of individual parameter values on the total annual dose.

Table 9-2. Results of the sensitivity analysis. The changed parameters and values are given, the resulting peak dose and time of occurrence. In addition, the differences between these results and those for the reference case are listed as relation of peak values and time shift between respective time of occurrence. Positive numbers indicate a shift into the future.

Results of sensitivity analysis – Reference scenario – Drinking water scenario							
Parameter Name as listed in Appendix VI	**Min**	**Default** Ref.Case	**Max**	**Min** Dose Rate (mSv/a) Time (a)	**Max** Dose Rate (mSv/a) Time (a)	**Min** Dose factor Time shift (a)	**Max** Dose factor Time shift (a)
Reference Case (Reference Data Set)							
All parameters set to default values as listed in Appendix VI		Yes		6.12e-5 339,000 a		1 +0	
Inventory							
ILW_Inventory_factor	0.5	1	2	6.02e-5 341,500	6.33e-5 334,000	0.98 +2,500	1.03 -5,000
LLW_inventory_factor	0.5	1	2	3.16e-5 334,000	1.2e-4 341,500	0.52 -5,000	1.97 +2,500
Barrier Performance							
Vault_Wall_thickness	0.1 m	1 m	2 m	6.17e-5 337,833	6.09e-5 339,833	1,008 -1,167	0.995 +833
Concrete_vault_conductivity	1e-2 m/s	1e-7 m/s	1e-9 m/s	6.12e-5 339,000	6.12e-5 339,000	1.001 0	1 0
ILW_WP_failed_at_closure	0%	10%	100%	6.12e-5 339,000	6.12e-5 339,000	1 0	1 0
ILW_WP_failure_period	10 a	100 a	1,000 a	6.12e-5 339,000	6.12e-5 339,000	1 0	1 0
LLW_WP_failed_at_closure	0%	30%	100 %	6.12e-5 339,000	6.12e-5 339,000	1 0	1 0
LLW_WP_failure_period	5 a	50 a	500 a	6.12e-5 339,000	6.12e-5 339,000	1 0	1 0
Material Properties							
Concrete_Kd_factor	0.1	1	2	1.1e-4 27,950	4.69e-5 499,000	1.80 -311,050	0.77 +160,000
Concrete_contam_ILW	0	0	0.5	-	5.95e-5 342,667	-	0.97 +3,667
ILW_Drum_Concr_Frac	0	0.3	0.5	6.14e-5 339,000	6.11e-5 339,333	1.003 0	0.998 +333
Concrete_contam_LLW	0	0	0.5	-	6.29e-6 1,110	-	0.10 -337,890
LLW_Drum_Concr_Frac	0	0.3	0.5	3.17e-4 660a	5.15e-5 452,333	5.18 -338,340	0.84 +113,333

Results of sensitivity analysis – Reference scenario – Drinking water scenario							
Parameter Name as listed in Appendix VI	**Min**	**Default** Ref.Case	**Max**	**Min** Dose Rate (mSv/a) Time (a)	**Max** Dose Rate (mSv/a) Time (a)	**Min** Dose factor Time shift (a)	**Max** Dose factor Time shift (a)
Geosphere							
Distance_to_Well	10 m	100 m	1,000 m	6.13e-5 339,167	6.01e-5 337,500	1.002 +167	0.98 -1,500
Hydraulic_gradient	0.001	0.01	0.1	6.70e-6 834,000	1.20e-3 56	0.11 +495,000	19.21 -338,944
Biosphere							
Water_daily_consumption	1 l	3 l	5 l	2.04e-5 339,000	1.00e-4 339,000	0.33 0	1.67 0
median_well_yield	200 l/hr	600 l/hr	5,000 l/hr	1.80e-4 339,000	7.34e-6 339,000	3 0	0.12 0

As seen in the table above, most of the changes in parameter values affect the outcome of the results only marginally. These parameters do not affect the results significantly. For these parameters, the uncertainty of their actual value is of minimum significance to the overall results, thus they are also not in the focus of interest for possible future studies. As a first threshold to identify the parameters of significant influence, a change of 5% in the total annual dose has been selected. The following factors have a higher influence on the total annual dose:

LLW inventory: While the resulting total dose rate is less sensitive to the activity changes in the ILW inventory, the overall activity of the LLW inventory has an almost linear effect on that dose. This is due to the lack of any technical barriers (except WPs) in the LLW chamber. As soon as a WP fails, its waste content is exposed to groundwater flow.

The k_d factor used for the concrete in the repository is extremely important for the resulting total dose. Concrete is present in WPs (as backfill), as WP material (in case of ILW) and as vault material (also ILW). Sorption of radionuclides in concrete is obviously a major factor for the long-term safety of the disposal facility.

For the same reason, the resulting dose rate is very sensitive to the amount of concrete in WPs and contaminated concrete in the LLW WPs. Increase of concrete amount leads to more sorption and a smaller dose while decreasing the amount of concrete backfill leads to less sorption and a significantly higher dose. This is especially relevant for LLW due to the relatively small amount of concrete in the chamber(s) in the reference case (only some concrete in WPs). Reducing the amount of concrete within the WPs to zero results in 5.2 times the dose of the reference scenario occurring as soon as 660 years after closure. Although the resulting dose rate of 3.17×10^{-4} mSv/a is still acceptable low, it is concluded that the results are sensitive to the sorption in concrete in the LLW chamber.

An interesting observation is that the resulting total dose is not very sensitive regarding hydraulic properties of the concrete vault. In the reference case, this is due to the pathway for radionuclide transport through the geosphere. For as long as the hydraulic properties of the host rock remain unchanged, the hydraulic conductivity in the EBS is of less importance.

The flow rate through the repository because of hydraulic gradient (as varied) and rock permeability are of major importance for the resulting dose. The relationship is almost linear. For future updates, when a site is selected, it is of utmost importance that the properties of the host rock are well known and meet the target properties set for site selection.

For water consumption and dilution within the aquifer, there is also a linear relationship regarding the resulting dose, as expected.

9.3.3 Results and analysis for alternative scenarios

The human activity scenario (HA scenario)

The results of the HA scenario are shown in Figure 9-10. The resulting dose is at its peak 2.16×10^{-5} mSv/a, at 798,000 years after closure. The first peak of the HA scenario, at 595 years, is not much smaller, however. At first glance, it is curious that the maximum peak of the HA scenario would lead to a dose only 0.35 times the maximum dose in the reference scenario (2.16×10^{-5} mSv/a vs. 6.12×10^{-5} mSv/a). From the sensitivity analyses, it is however, known that sorption is a major factor for retention of the radionuclides released from the LLW chamber that encounter concrete plugs in the direction of the shaft. As a result, there is better retention of radionuclides from the LLW than in the reference scenario, which lowers the amounts of radionuclides reaching the aquifer. In addition, a pathway through the infrastructural area and the shaft exposes the radionuclides to large volumes of water, in which they are diluted.

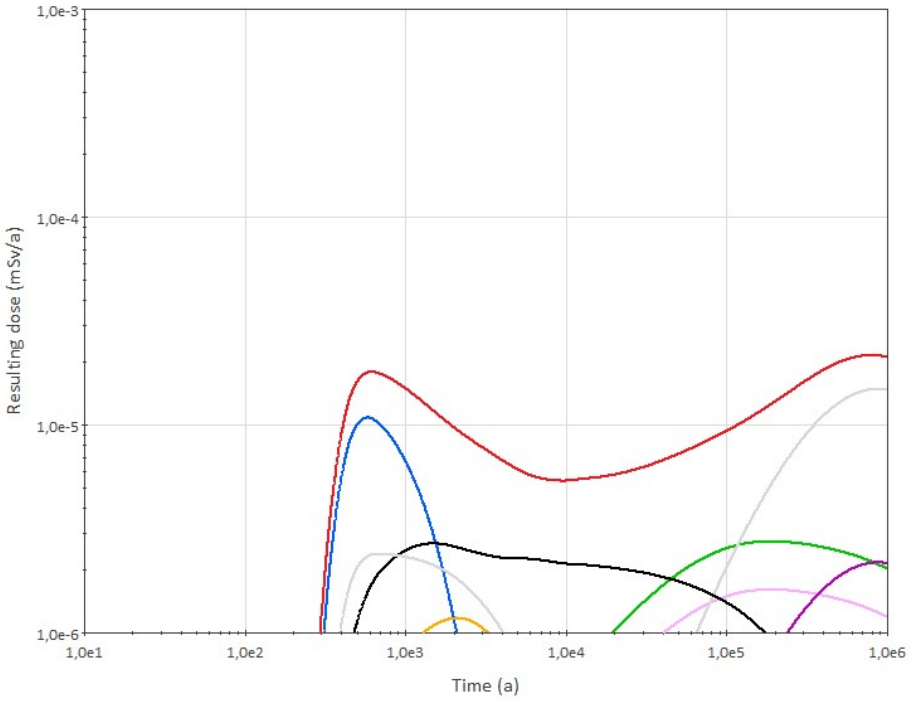

Figure 9-10. Resulting annual dose for individual and most important contributing radionuclides in the HA scenario.

The human intrusion scenario

The results of the HI scenario are shown in Figure 9-11. Depending on the WP drilled into and the time of occurrence, the resulting dose rates can exceed 1,300 mSv/a. However, for most WPs, the resulting dose rate of such an inadvertent intrusion decreases rather rapidly in the post-closure period. Assuming a period of institutional control of 300 years after closure, resulting dose rates drop to less than 10 mSv/a. According to the ICRP (2013), values between 20 and 100 mSv in such a scenario are an indicator of the robustness of the repository.

An outlier is WP3 with a very high activity of 143 GBq in Ra-226. The resulting dose only drops under 100 mSv at 5,700 years after closure. The description of the WPs and their contents as well as an analysis of the results are found in Appendix IV.

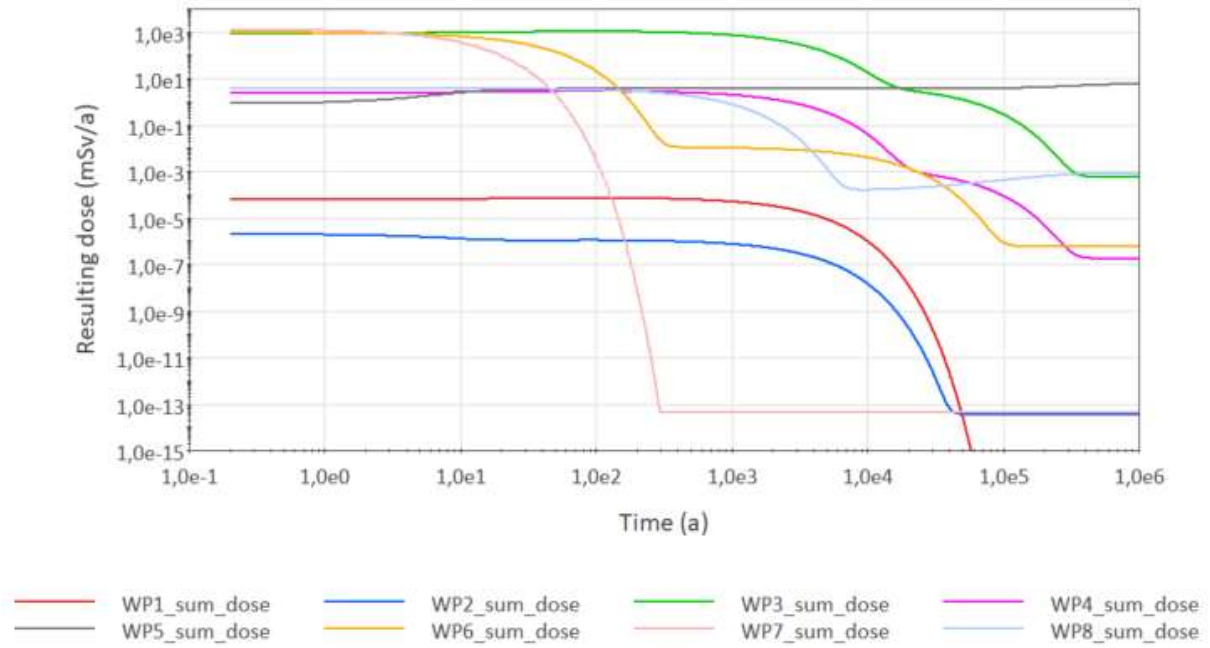

Figure 9-11. Resulting annual dose rates for a drilling worker depending on which WP of the special waste is drilled into.

9.3.4 Uncertainty in post-closure assessment

It needs to be acknowledged that a significant level of uncertainty is associated with the results of such a quantitative safety assessment. This is a general fact simply due to the long times that are considered in the calculations.

Unlike the operational safety cases, which can benefit from operational experience, such experience is not available for the post-closure safety cases. Hence, the reduction of uncertainties for long-term analyses must be sought by approaches such as a comprehensive scenario development, the comparison of different scenarios or what-if cases and sensitivity analysis.

In discussing uncertainties, it needs to be kept in mind that there are two different kinds of uncertainty: Variability or aleatory uncertainty and epistemic uncertainty. Typical examples for these two types are listed below.

Variability (aleatory uncertainty, stochastic uncertainty)

- Spatial variability
- Temporal variability

Epistemic uncertainty (informational uncertainty)

- Variability in parameter values variability (e.g., degradation rates)
- Inability to measure individual parameters

For post-closure safety assessments epistemic uncertainties usually dominate because, as the assessment looks farther into the future, more uncertainties arise, especially regarding changes in climate evolution, etc. Normally, little can be done to reduce variability. Consequently, it must be addressed in safety assessments by probabilistic calculations or sensitivity analysis or by covering uncertainties by using conservative approaches. Epistemic uncertainty can in certain cases be reduced by additional scientific investigations to

increase the accuracy of certain parameters. In other cases, uncertainties must be addressed by investigating alternative scenarios, sensitivity cases or in the same way as variability.

Probabilistic treatment of uncertainties has the advantage that it is easier to develop decision rules, such as a maximum dose rate for a certain probability. However, using a large number of probabilistically distributed parameters often lead to results that are difficult to communicate and also difficult to comprehend and reproduce. However, the computer model has been developed to allow for probabilistic calculations as well should that be required by the operator or the regulator in the future.

This safety assessment has shown that for the current disposal facility design, sorption properties of the EBS and the hydraulic properties of the geosphere are of utmost importance for any safety assessment. This includes knowledge of concrete degradation and k_d values, as well as the evolution of groundwater flow over one million years. Tackling the uncertainties in these areas is of primary importance to gain better insight in the safety of the disposal facility.

9.4 Determination of preliminary activity limits for LLW/ILW

The results of a long-term safety assessment for a radioactive waste disposal facility usually describe its expected radiological impact based on the estimated inventory and the identified scenarios as well as the boundary conditions given by the repository itself and its environment. In addition, as part of the safety assessment, the Admissible Maximum Activity (AMA) per radionuclide in the repository can be derived from the results of the assessment.

To determine the AMA for each radionuclide in a repository, it is necessary to assess the activity (Bq) of each radionuclide, which just matches the dose constraint. This assessment must be done for the normal evolution scenario as well as for alternative evolutions or accident scenarios.

For this purpose, the activity A_i from the activity vector for each radionuclide I is used in context with the resulting dose that this nuclide causes D_{iY} in scenario Y.

Dividing the resulting dose rate by the limiting value LV_Y for scenario Y gives the factor, by which the activity has to be multiplied to render the Admissible Maximum Activity of radionuclide i in the repository for scenario Y (AMA_{iY}).

$$AMA_{iY} = A_i \cdot (LV_Y / MD_{iY}) \qquad \textit{(Equation 9-3)}$$

The AMA's corresponding to radionuclides with daughter products are calculated by summing up the doses of the initial radionuclide and all daughter products according to the time of their occurrences. That means that in each time step the total dose for the initial radionuclide is the sum of all doses from the initial radionuclide itself and all daughter products. The maximum total dose defines the AMA for the initial radionuclide.

The current repository design foresees disposal of ILW and LLW in different chambers, enclosed by different EBS components. AMAs for radionuclides (RN) of ILW and LLW will therefore differ as sensitivity of the activity for the overall resulting dose rate is also different. AMAs have been developed independently for ILW and LLW.

The following calculation is an example to define the AMA for C-14 from the reference scenario, but only LLW is simulated. Consequently, this AMA refers to C-14 in LLW.

$A_{C\text{-}14}$ = 2.7×10^{8} Bq
LV_{Norm} = 0.1 mSv/a (assumed reg. limit for the reference scenario)
$MD_{C\text{-}14\ Ref}$ = 6.62×10^{-7} mSv/a
$AMA_{C\text{-}14\ Ref}$ = 4.1×10^{13} Bq

In the same way, AMA values are calculated for all radionuclides and scenarios, where the dose rate received by the members of the public are dependent on the total activity in the repository. Usually these are related to variations in groundwater flow, where water enters the repository, radionuclides are dissolved and transported through the geosphere and enter the biosphere. The minimum of all AMA_Y-values determined for a specific radionuclide defines then the total maximum activity limit for that radionuclide.

The total resulting dose is usually made up by more than the effect of one specific radionuclide. Assigning the maximum activity of each radionuclide as the only waste acceptance criterion would leave the option to dispose of waste that, in total, leads to a violation of the regulatory dose limit. Therefore, regarding the maximum capacity of the repository, the total inventory of LLW or ILW must also meet the sum rule for the AMA values.

$$\sum_i A_i \,/\, AMA_i \leq 1 \qquad \textit{(Equation 9-4)}$$

where

A_i = Total activity of radionuclide i in the repository, and
AMA_i = Admissible Maximum Activity of radionuclide i in the repository.

It should be noted that a certain amount of conservatism is inherent to the application of the sum rule because the maximum dose rates associated with the individual radionuclides normally do not occur at the same time. In the same way, the maximum specific activities per radionuclide can be determined by using scenarios, where the specific activity of waste defines the dose rate of potential radiological impact. Typical examples of such scenarios are accident scenarios concerning individual WPs or human intrusion scenarios, especially for surface disposal facilities.

This calculation was carried out for all individual radionuclides in the reference scenario as an example. This is a conservative choice, as the comparison of the reference scenario with the HA scenario has shown. For the analysis, the activity of only one radionuclide in one waste category was simulated at a time. The resulting annual dose is then constituted by the sum of resulting annual doses caused by the simulated radionuclide and by the radionuclides in its decay chain. The AMA per radionuclide is then calculated according to Equation 9-3. The results of the analyses are shown in Table 9-4. At the bottom of the table, the individual AMAs for the radionuclides are summed up according to Equation 9-4 to inform about the total AMA of the waste category. The current LLW inventory makes up about 8% of the total AMA whereas only 1 % of total AMA is reached by the ILW inventory. For LLW, the most important radionuclides are U-235 and U-238. For ILW, the spread of important radionuclides is wider, the most dominant ones being Ag-108m, C-14 and Tc-99. Some of the AMA values reach very high magnitudes which would correspond to extremely high amounts of acceptable radionuclides in the repository. These are just theoretical values and do not relate to any expected potential activity of these radionuclides in the respective waste streams.

When disposing of different types of waste in the same facility, using different disposal concepts, as is the case for the LILW repository in question, the application of AMAs separately for ILW and LLW could lead to unacceptable annual doses as the radiological impact of both parts of the ILW and LLW chambers is combined due to their proximity. A safe approach would be to use the more restrictive AMA of the two types of waste per radionuclide and apply it to the whole facility. As an alternative, it would be possible to use the same EBS for LLW as for ILW to ensure that radionuclide activities in both waste streams are equally sensitive for the overall radiological result of the facility. It would no longer be necessary to differentiate between LLW and ILW to deduce AMAs. On the other hand, the technical effort for disposal of LLW would be exaggerated just for that purpose.

Table 9-4: Results of AMA calculations; activity in Bq, doses in mSv/a

Species ID	Reg. Limit	LLW activity	LLW peak dose	LLW AMA	% of AMA	ILW activity	ILW peak dose	ILW AMA	% AMA	Peak doses include RN in decay chain
Ag-108m	0.1	2.90E+07	9.32E-06	3.11E+11	9.32E-03	4.35E+09	2.74E-06	1.59E+14	2.74E-03	
Am-241	0.1	3.50E+06	7.04E-08	4.98E+12	7.04E-05	1.90E+10	1.09E-09	1.74E+18	1.09E-06	Np-237, Th-229, U-233
Am-243	0.1	6.20E+04	3.23E-09	1.92E+12	3.23E-06	4.12E+07	4.89E-10	8.41E+15	4.89E-07	Ac-227, Pa-231, Pu-239, U-235
C-14	0.1	2.70E+08	6.62E-07	4.08E+13	6.62E-04	2.71E+11	1.17E-06	2.32E+16	1.17E-03	
Ca-41	0.1					7.02E+07	decayed			
Cl-36	0.1	7.20E+04	2.15E-08	3.35E+11	2.15E-05	6.80E+07	5.14E-07	1.32E+13	5.14E-04	
Cm-243	0.1	1.60E+04	4.16E-13	3.84E+15	4.16E-10	1.08E+07	1.99E-14	5.44E+19	1.99E-11	Ac-227, Am-243, Pa-231, Pu-239, U-235
Cm-244	0.1	1.50E+06	6.09E-11	2.46E+15	6.09E-08	3.79E+08	1.36E-13	2.79E+20	1.36E-10	Pu-240, Ra-228, Th-228, Th-232, U-236
Co-60	0.1	2.50E+09	1.29E-19	1.93E+27	1.29E-16	6.26E+12	6.10E-25	1.03E+36	6.10E-22	
Cs-137	0.1	3.40E+09	7.68E-09	4.43E+16	7.68E-06	5.23E+12	1.86E-12	2.81E+23	1.86E-09	
Eu-152	0.1	7.50E+07	1.83E-16	4.10E+22	1.83E-13	1.81E+09	decayed			
Eu-154	0.1	5.20E+07	1.37E-19	3.79E+25	1.37E-16	1.03E+11	decayed			
Eu-155	0.1	5.60E+06	5.49E-27	1.02E+32	5.49E-24	2.28E+10	decayed			
H-3	0.1	1.50E+06	3.28E-18	4.57E+22	3.28E-15	1.99E+10	5.29E-17	3.77E+25	5.29E-14	
Ho-166m	0.1	1.20E+06	4.81E-08	2.49E+12	4.81E-05	3.37E+08	2.24E-07	1.51E+14	2.24E-04	
I-129	0.1	2.20E+04	5.52E-08	3.98E+10	5.52E-05	3.79E+07	5.03E-07	7.54E+12	5.03E-04	
Mo-93	0.1	1.40E+06	5.41E-15	2.59E+19	5.41E-12	6.16E+08	2.21E-24	2.79E+31	2.21E-21	Nb-93m
Nb-93m	0.1	2.20E+07	5.56E-10	3.96E+15	5.56E-07	6.86E+10	6.48E-10	1.06E+19	6.48E-07	
Nb-94	0.1	9.20E+05	7.81E-10	1.18E+14	7.81E-07	1.19E+09	1.04E-09	1.14E+17	1.04E-06	
Ni-59	0.1	3.70E+08	1.07E-07	3.47E+14	1.07E-04	7.22E+11	5.76E-07	1.25E+17	5.76E-04	
Ni-63	0.1	4.60E+10	9.82E-07	4.69E+15	9.82E-04	7.83E+13	4.06E-08	1.93E+20	4.06E-05	

Species ID	Reg. Limit	LLW activity	LLW peak dose	LLW AMA	% of AMA	ILW activity	ILW peak dose	ILW AMA	% AMA	Peak doses include RN in decay chain
Np-237	0.1	1.90E+03	1.17E-10	1.63E+12	1.17E-07	5.96E+06	1.70E-09	3.51E+14	1.70E-06	Th-229, U-233
Pu-238	0.1	3.30E+06	1.04E-09	3.17E+14	1.04E-06	5.02E+11	4.92E-07	1.02E+17	4.92E-04	Pb-210, Ra-226, Th-230, U-234
Pu-239	0.1	9.10E+05	1.15E-08	7.89E+12	1.15E-05	3.14E+10	4.73E-08	6.65E+16	4.73E-05	Ac-227, Pa-231, Pu-239, U-235
Pu-240	0.1	1.80E+06	2.16E-08	8.33E+12	2.16E-05	1.21E+11	1.56E-08	7.77E+17	1.56E-05	Ra-228, Th-228, Th-232, U-236
Pu-241	0.1	3.40E+07	2.27E-08	1.50E+14	2.27E-05	1.60E+13	3.05E-08	5.25E+19	3.05E-05	Am-241, Np-237, Th-229, U-233
Pu-242	0.1	6.20E+03	7.70E-11	8.05E+12	7.70E-08	3.34E+08	5.83E-09	5.73E+15	5.83E-06	Pb-210, Ra-226, Th-230, U-234, U-238
Sm-151	0.1	1.90E+07	9.16E-10	2.07E+15	9.16E-07	2.67E+10	9.48E-10	2.81E+18	9.48E-07	
Sr-90	0.1	3.30E+08	1.03E-08	3.22E+15	1.03E-05	6.12E+11	3.63E-09	1.69E+19	3.63E-06	
Tc-99	0.1	3.50E+07	6.94E-07	5.04E+12	6.94E-04	1.58E+10	2.57E-06	6.15E+14	2.57E-03	
U-234	0.1	2.10E+03	1.85E-09	1.13E+11	1.85E-06	1.30E+06	3.57E-09	3.64E+13	3.57E-06	Pb-210, Ra-226, Th-230
U-235	0.1	3.00E+07	2.09E-05	1.43E+11	2.09E-02	1.73E+07	4.63E-08	3.75E+13	4.63E-05	Ac-227, Pa-231
U-236	0.1	6.20E+02	1.49E-11	4.15E+12	1.49E-08	5.26E+05	3.36E-11	1.57E+15	3.36E-08	Ra-228, Th-228, Th-232
U-238	0.1	9.90E+07	4.70E-05	2.11E+11	4.70E-02	2.24E+08	9.66E-07	2.32E+13	9.66E-04	Pb-210, Ra-226, Th-230, U-234
Zr-93	0.1	3.00E+05	5.78E-09	5.19E+12	5.78E-06	8.67E+07	6.74E-09	1.29E+15	6.74E-06	Nb-93m
				Total % AMA	7.99%			Total % AMA	1.00%	

9.5 Summary of LILW calculations

The preliminary results from the generic safety assessment for the simplified LILW repository indicate that there will be two peaks in the development of resulting annual dose for an individual at the surface in the reference case. The first peak at around 620 years at 1.83×10^{-5} mSv/a is mainly dominated by the radionuclides Ag-108m, U-238 and Tc-99. The second peak occurs at around 339,000 years and reaches 6.12×10^{-5} mSv/a. This peak is dominated by Ac-227, Pb-210, Pa-231 and Ra-226. Radionuclides with a rather short half-life such as Sr-90 or Cs-137 are no major contributors due to the retardation in the EBS and the duration of travel in the geosphere. The results of the rather pessimistic reference scenario thus led to maximum total dose rates that are about 4 orders of magnitude below the expected regulatory limit of 0.1 mSv/a.

The alternative HA scenario differs from the reference scenario in the assumed existence of a fast transport pathway towards the surface. Due to the already very pessimistic nature of the reference assumptions, calculated dose rates remain in the same order of magnitude as the reference scenario and are even smaller.

The third scenario that has been assessed, the HI scenario, is a what-if scenario, assuming that a hole is drilled through a waste package with high specific activity and some of its content is brought to the surface. It has been specifically implemented to evaluate the potential consequences from disposing certain waste packages with high activity content in the ILW disposal chamber. This scenario leads partly to significantly increased total dose rates. Due to the small likelihood of this scenario, resulting doses can mostly be accepted or even used as an argument for the robustness of the facility. Only one waste package leads to unacceptable doses of more than 1,000 mSv/a even after a period of institutional control, during which no Human Intrusion is assumed to occur. Actions related to emplacement of the waste are proposed to mitigate this issue (see Appendix IV).

The sensitivity analyses based on the Reference Scenario showed that the annual resulting dose is highly sensitive to the amount of concrete in and around the waste and the sorption properties of that concrete. In the ILW chamber, the results are more sensitive to these parameters than to the hydraulic properties of the concrete in vault. The results indicate the importance of the sorption capacity of the concrete surrounding the waste. Nonetheless, this only remains true for as long as the host rock provides hydraulic properties close or equal to the target properties (defined in Hagros et al. 2021). The host rock quality and the resulting groundwater flow through the repository are, therefore, also of very high importance for long-term containment of LILW.

10 Summary and conclusions

A key element in the development of a disposal programme is a safety case, which demonstrates the safety of the disposal concept, identifies the remaining uncertainties, and provides feedback on the further research and development needed in the following programme steps. A safety assessment represents an important part of such a safety case (Section 1.3).

NND is studying several concepts for how to update the Norwegian infrastructure for the management of radioactive waste. One concept consists of combining individual repositories for different kinds of waste into a National Facility for management of radioactive waste at a single disposal location. One possibility is a combination of a deep borehole repository for HLW and an intermediate depth repository for LLW and ILW. This work focuses on the development of a generic post-closure safety assessment for the two repository types mentioned above. Long-term safety calculations have been carried out to assess the suitability of the considered disposal concepts. An important aspect has been to describe the processes and methodology and to provide NND an example of a tool that can be applied to future safety assessments.

Due to the early stage of the disposal project and the fact that no site has yet been selected, several assumptions were made to account for uncertainties in the available data or lack of data. The most important ones are summarised below:

- The intermediate depth repository is assumed to be located at 100 m depth and the disposal zone of the DBD borehole at a depth between 3000 and 3500 m.
- The intermediate depth repository for LLW and ILW and the HLW repository are assumed to be located at a single site in crystalline rock.
- As no site has yet been selected for the facility, generic properties for a crystalline site are assumed.
- The design of the repositories is according to Fischer et al. (2020) and Ikonen et al. (2020).
- Inventory data have been estimated based on available information from NND complemented with additional data on similar type of wastes.

Due to lack of detailed information on the site and technical details of the repository designs and implementation, at this stage a set of simple scenarios that cover a pessimistic evolution of the repository system has been developed. In addition, what-if-cases have been considered to estimate theoretical upper limits of potential radiological impact.

The scenarios considered in this generic safety assessment do not cover all the FEPs that might influence the evolution of the repository and its related radiological impact. For example, natural events and processes such as earthquakes and glaciation have not been considered explicitly. Another example of FEPs that have not been considered in detail is processes related to gas production and transport. Instead, an attempt has been made to cover potential consequences of these events and processes, e.g., advective upward flow through the DBD borehole or creation of new fractures in the host rock, by implementing pessimistic assumptions for the selected scenarios and calculation cases. However, it is quite clear that at this stage of the disposal project and for the generic nature of this study, there are aspects that have not been included in detail in the models used for calculations.

The scenarios have been developed and consequently, the modelling has been carried out separately for the LILW- and DBD-repositories using generic site properties. To assess the combined radiological impact of the LILW- and DBD-repositories, if located at the same site, the respective main results like radionuclide concentration in water or dose rate can easily be added up accounting for the timing of the releases.

The following sections summarise the objectives of this generic safety assessment, the key findings from the long-term calculations as well as an evaluation of these results concerning their compliance with the assumed regulatory limits. In addition, main areas of future R&D work are presented. The need for further work is identified based on the uncertainties in assumptions and parameters and results of the sensitivity analysis and calculation cases for the DBD scenarios. Finally, an evaluation of the potential of the disposal concepts that were analysed is given concerning their suitability as a solution for Norwegian radioactive waste management.

10.1 Objectives

The objective of this generic safety assessment at this stage of the project is to give a first – generally conservative – estimate of the performance of the system to allow a first evaluation of the safety and the general suitability of the considered concepts. In addition, the boundary conditions and parameters used in the models aim at identifying, which of them have the largest impact on the performance of the system and should, therefore, be the focus of future R&D work for the disposal project.

The GoldSim simulation model aims at providing NND with a tool to assess the impact of alternative conditions like changed inventory or different material parameters would have on the potential radiological consequences of the facility.

The model of the repositories used to simulate the release of radionuclides assuming different evolutions of the system as well as the associated potential radiological impact have been prepared to achieve these objectives. It is important to keep in mind that, at the present stage, there is uncertainty in the assumptions and data used and many features and processes have been implemented in a simplified way. However, the model allows updating with advancing technical planning of disposal concepts and site-specific information once they become available.

10.2 Key findings

Summary of DBD calculations

The preliminary results from the generic safety assessment for the normal evolution of the deep borehole repository indicate that highly mobile radionuclides such as I-129, Cl-36, Ni-59, and Se-79, are the major dose contributors, and that the expected potential radiological impact to future humans associated with those releases is extremely small.

The results of the normal evolution scenario Sc-1, based on purely diffusive transport along the borehole, lead to maximum total dose rates that are more than 20 orders of magnitude below the expected regulatory limit of 0.1 mSv/a even for calculation cases assuming pessimistically changed boundary conditions. This is in accordance with the results presented in Brady et al. (2011), where diffusion is considered as non-significant transport mechanism for deep borehole disposal.

Two alternative scenarios have been assessed that both assume that there will be a hydraulic gradient leading to advective flow either upward through the borehole and surrounding EDZ (Sc-2) or between certain parts of the borehole and the surface via a transmissive fracture system (Sc-3). If the site is properly selected both scenarios should be possible to exclude. Therefore, scenarios Sc-2 and Sc-3 are both considered as unlikely scenarios or even as what-if scenarios.

Despite the pessimistic assumptions chosen for Sc-2 and the five variants of Sc-3, the maximum dose rates are significantly lower than the expected regulatory limit. Figure 10-1 shows the total dose rate curves for the reference cases of Sc-2 and the variants of Sc-3. For Sc-2, the maximum dose rate is 2.5 orders of magnitude lower than the expected limit and for Sc-3 only those cases that assume a direct connection between the disposal zone and the surface (Sc-3.3–Sc-3.5) lead to dose rates of several µSv/a.

From the results of the sensitivity analysis and several calculation cases, it is apparent that the hydrogeological conditions in the deep host rock formation play the most important role for the potential radiological impact as they govern possible advective transport from the disposal zone towards the surface. Other important factors are the physical and chemical conditions in the deep underground and their impact on the sorption and solubility limits of the radionuclides. The estimated inventory has a substantial impact on the results, and it is also a significant source of uncertainty.

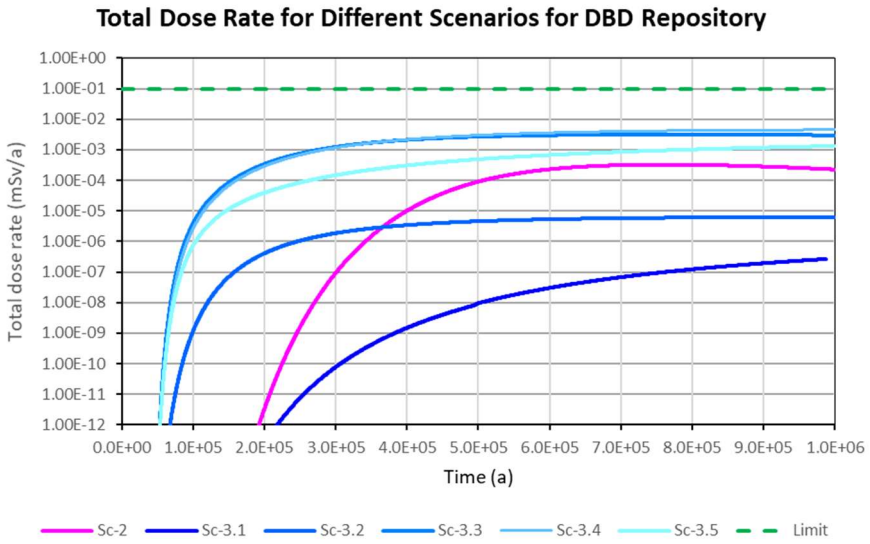

Figure 10-1. Total dose rates for the reference cases of the alternative scenario Sc-2 and the variants Sc-3.1–Sc-3.5 of the alternative scenario Sc-3 (Sc-3.3 and Sc-3.4 have nearly identical dose rate).

Summary of LILW calculations

The results from the generic safety assessment for the LILW repository indicate a potential radiological impact that is about 4 orders of magnitude below the expected regulatory limit of 0.1 mSv/a. The rather pessimistic reference scenario leads to a total dose rate that is characterized by two maxima. The first maximum occurs at 620 years and is mainly dominated by the radionuclides Ag-108m, U-238 and Tc-99. The second maximum occurs significantly later at 339,000 years, and the dominant radionuclides are Ac-227, Pb-210, Pa-231 and Ra-226. Radionuclides with a rather short half-life such as Cs-137, Sr-90 or Co-60 are no major contributors due to the retardation in the EBS and the duration of travel in the geosphere.

Comparison of long-term calculations considering only the inventory of either ILW or LLW showed that more than 95 % of the combined maximum dose rate for the reference scenario is originating from the LLW part.

The alternative human activity (HA) scenario differs from the reference scenario in the assumed existence of a fast transport pathway towards the surface. Due to the already very pessimistic nature of the reference assumptions, calculated dose rates remain in the same order of magnitude as the reference scenario and are even smaller. Figure 10-2 shows the total dose rate curves for the two scenarios.

The third scenario that has been assessed, the HI scenario, is a what-if scenario assuming that a drilling event hits a waste package with high specific activity and some of its content is brought to the surface. The scenario has been specifically implemented to evaluate the potential consequences from disposing certain waste packages with high activity content in the ILW disposal chamber. This scenario leads partly to significantly increased total dose rates. Due to the small likelihood of this scenario, resulting dose rates can mostly be accepted or even used as an argument for the robustness of the facility. Only one of the special waste packages leads to unacceptable dose rates of more than 1,000 mSv/a even after a period of institutional control, during which no human intrusion is assumed to occur.

The sensitivity analyses based on the reference scenario showed that the annual resulting dose is highly sensitive to the amount of concrete in and around the waste and the sorption properties of that concrete. In the ILW chamber, the results are more sensitive to these parameters than to the hydraulic properties of the concrete in vault. The results indicate the importance of the sorption capacity of the concrete surrounding the waste. But this only remains true for as long as the hydrogeological properties in the host rock remain as expected. The host rock quality and the resulting groundwater flow through the facility are, therefore, also of very high importance for the long-term containment of LILW.

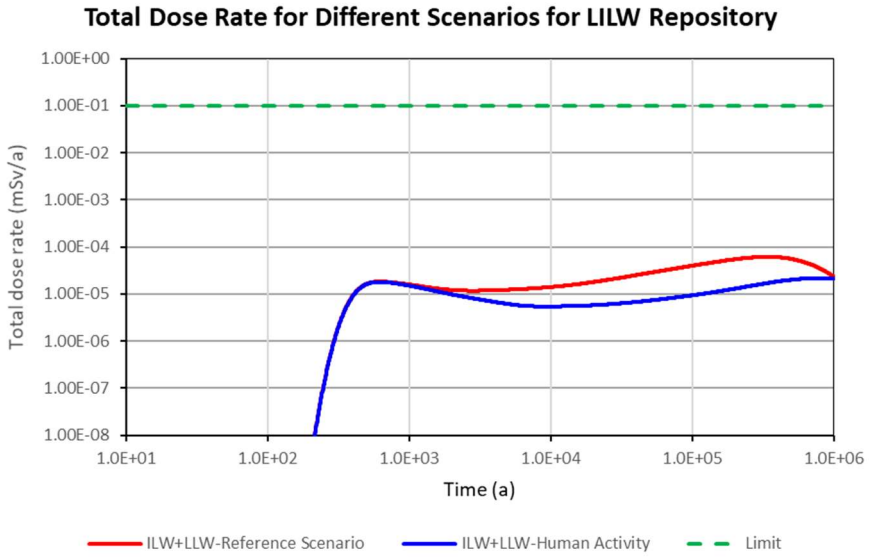

Figure 10-2. Total dose rate curves for the Reference Scenario and the human activity scenario for the LILW repository.

10.3 Compliance of results with assumed regulatory limits

For evaluating the safety of the assessed disposal concept, the results of this generic safety assessment have been compared with the assumed regulatory limit of 0.1 mSv/a. For the intermediate depth repository for LLW and ILW, the results of the reference scenario are more than three orders of magnitude below this level. Considering the rather pessimistic assumptions of this scenario this indicates that the ILW and LLW of Norway can be safely disposed of at the proposed intermediate depth repository without causing unacceptable harm to human beings or the environment.

It needs to be kept in mind that at this stage of the project, there are still uncertainties concerning the disposal concept, the inventory, and especially the properties of the host rock formation. However, the large safety margin of three orders of magnitude plus the conservatism built into the model makes it seem very unlikely that future reduction of these uncertainties through an improved database and advanced level of technical planning will change the general statement of this safety assessment.

For the deep borehole disposal, the calculated results for the normal evolution scenario are far below the limit of 0.1 mSv/a even for the pessimistic calculation cases. Significant dose rates are measured only in the two alternative scenarios, i.e., if either advective upwards directed flow along the borehole takes place or if some highly transmissive fracture network exists between the disposal zone and the surface. Both alternative scenarios are considered to have been included as a kind of worst-case scenarios. Despite the pessimistic assumptions, the calculated maximum dose rates are between 1.5 and 2.5 orders of magnitude below the 0.1 mSv/a limit. Also, further pessimistic assumptions applied in the sensitivity analysis or special calculation cases do not lead to dose rates exceeding the regulatory limit.

10.4 Identified uncertainties and their treatment

The main uncertainties that have been identified and which have a significant impact on the results of the long-term safety calculations are the:

- hydrogeological conditions in the host rock and the geosphere,
- physical/chemical properties such as sorption and solubility limits of radionuclides in the appropriate environments, and
- waste characteristics (inventory).

The hydrogeological conditions of the host rock and the wider geosphere are decisive for the release pathways from the near field to the biosphere. The assumptions concerning advective flow in this area have a significant impact on the release of radionuclides and potential radiological impact. In this safety assessment, the attempt has been made to choose pessimistic conditions, especially concerning the vertical transport from the disposal depth towards the surface, and to assess even more pessimistic conditions through the sensitivity analysis.

Assumptions regarding solubility limits and sorption are also important parameters for both repositories. Especially for the DBD model, the database for selecting suitable values for sorption of radionuclides and solubility limits is scarce. There are no DBD projects anywhere that have reached the level of technical feasibility and scientific exploration that mined geological repositories have. Accordingly, little research has been done to explore the solubility and sorption conditions under the chemical thermal and physical conditions that are to be expected in the significantly larger depths of a disposal borehole. So far, databases have been used that were gathered for the conditions to be expected for the two repositories, but the kd-values, which define the sorption capacity of solids to radionuclides, need to be re-evaluated to comply with the conditions at the actual repository site. So far, these uncertainties have been treated by using suitable data sources for these parameters. In addition, pessimistic values have been assumed for calculation cases and sensitivity analyses to assess their influence on the potential radiological impact, should site-specific data prove to be less favourable.

The projected inventory is also subject to major uncertainty for both repositories. These uncertainties have been treated by deriving reasonable inventory vectors based on available information data from similar waste streams. The potential impact of possible changes of the assumed inventory has been addressed in the framework of the sensitivity analysis.

Other uncertainties identified in this safety assessment, are related to the final technical concept and its implementation and have been addressed by using simplified model components and varying parameters to analyse the sensitivity of the model. In addition, uncertainties concerning general material properties such as degradation of concrete or corrosion of metal have been approached in the same way. Parameter values have been selected that are assumed to be realistic or pessimistic and, subsequently, sensitivity calculations have been carried out to analyse the sensitivity of the system to the parameters. The same approach has usually been used here.

10.5 R&D needs

The summary of uncertainties given above directly leads to the fields of future R&D work on technical issues and/or knowledge gaps that have the largest potential to improve and enhance the confidence of future safety assessments.

For both repository models, the level of uncertainty would be significantly decreased by an improved characterization of the existing waste and/or estimate of future waste streams. In addition, site-specific data for the host rock conditions would be very important, but it is acknowledged that time is needed before a site can be selected and site-specific data, e.g., on the hydrogeological conditions, are made available. However, also before a site has been selected, research on chemical, thermal and physical conditions at depths typical for DBD disposal zones and their impact on important parameters such as solubility limits, kd-values or corrosion rates could be carried out and be helpful.

Additional studies are needed to improve the selection of normal and alternative scenarios that are realistic for a repository in crystalline rock, particularly for a deep borehole repository, and the associated conceptual and mathematical models for the radionuclide release pathways.

For the LILW model, further development on the technical concept and the planned conditioning of the waste would give important input to the simulated release of radionuclides from the waste form and the amount of concrete inside the repository, which acts as a chemical barrier for radionuclide transport. Also, underground dimensions could be better adjusted to the expected waste volumes.

In addition to these fields of R&D also those FEPs that have not been addressed so far in the generic safety assessment, e.g., climate change/glaciation, earthquakes and the production and transport of gas are areas for future R&D. It would be important to gain a better evaluation of their potential impact on the repository evolution and to develop models to implement these events and processes in the simulation models.

10.6 Potential of assessed disposal concepts for future development

One of the main objectives of this generic safety assessment was to provide a first evaluation on the safety and the general suitability of the considered concepts. In addition, NND had some general open questions related to the implementation of the assessed repository concepts, for which the results of this generic safety assessment could provide some clarification. Such questions are:

- Question about the potential of the assessed repository concepts for the Norwegian needs (mainly DBD, as lots of practical experience exits for the intermediate depth repository),
- Question of one site or separate sites ILW – LLW,
- Acceptability of special waste packages mainly containing sealed sources,
- Question of one site or separate sites LILW – DBD, and
- Question about the importance of depth.

As far as the estimated potential radiological impact is concerned, the results of this safety assessment summarized in the statement of confidence above strongly suggest that deep borehole disposal is a potentially suitable solution for the disposal of the Norwegian HLW. Similarly, the assessed intermediate depth disposal repository would be well suited for the disposal of the expected amounts of LLW and ILW.

For the intermediate depth LILW repository the existing extensive practical experience proves that the safe technical implementation and operation of such a repository is possible.

For deep borehole disposal, the situation is different. While from the radiological point the concept promises very high potential, significantly less research has been done regarding the conditions at respective depths of the crystalline basement and the related impact these conditions may have on the evolution of the repository. In addition, up to now, no comparable project has been realized so that several aspects concerning the technical implementation are still to be solved. However, the potential of deep borehole disposal is considered high despite the lacking technical experience.

The existing intermediate depth repositories often contain specific disposal areas for both LLW and ILW. The co-location of these different waste streams is, therefore, obviously no problem in general. Based on the current concept for the Norwegian case, the main release of radionuclides would originate from the LLW. Whether the intermediate depth repository includes an additional module for ILW or not, no significant changes in the estimated radiological impact of the repository are caused by it. Consequently, from the long-term safety aspect, there is no reason to have separate repositories for these waste streams in the Norwegian case.

The acceptability of certain existing waste packages containing waste with high specific activity in the ILW part of the intermediate depth repository has been addresses in detail within this safety assessment. According to the results (Section 9.3.3 and Appendix IV), their disposal in the ILW chamber does not present significant changes in the potential radiological impact from the repository for the release scenarios. However, human intrusion by a drilling event hitting one of these waste packages leads to very high doses to exposed persons. The assumption for this case is that, with the excavated material or core samples from the borehole, part of the waste package content will be brought to the surface, and during treatment and subsequent

inspection, drillers or geologists might be exposed to the material. While the related dose rates are within tolerable limits for most of the waste packages – considering the likelihood of the scenario – for one of the packages it would be too high.

As the scenario is considered a very improbable one, measures that would be suited to reduce even further the probability for this scenario to occur or the specific activity of the waste package, might be considered sufficient to also accept the disposal of the waste package in question.

To evaluate the consequences of a combined facility with a deep borehole repository and an intermediate depth repository, it is assumed that they would be separated one from each other far enough to prevent mutual geotechnical interference or the probability that excavated areas of one repository can be used as fast pathway for radionuclide transport from the other repository. If this is the case, the calculated dose rate curves for both repositories can be superimposed accounting for the timing of release and that contaminated fluid from both repositories enter the same aquifer, from which the drinking water well draws water.

The maximum dose rates caused by the LILW repository are expected to be approximately three orders of magnitude lower in the reference scenario than the assumed regulatory limit. Consequently, its situation with another repository should be no problem from the long-term safety point of view if the potential radiological impact from the other repository is not extremely near to the regulatory limit.

For the normal evolution scenario of the deep borehole repository, practically no significant radiological impact is to be expected. Accordingly, for the deep borehole repository, combination with another repository is even less problematic from the point of view of summing up dose rates. Consequently, the combination of the two repositories in one facility is acceptable.

Even if the unlikely deep borehole scenarios Sc-2 and Sc-3, which assume advective transport through the host rock, were taken as a yardstick to evaluate the co-location with the LILW repository, this would still be acceptable. However, as discussed above, Sc-2 and Sc-3 are considered as a kind of worst-case scenarios and not aimed to render realistic values for the potential radiological impact from the deep borehole repository.

About the open question concerning the required or optimized depth of the two repositories, the generic safety assessment does not provide quantitative answers. It is quite clear that the depth is decisive for the thermal, hydraulic, chemical, and mechanical conditions in the host rock. It is also clear that, in general, groundwater movement and host rock permeability will decrease with depth. Therefore, in principle a larger depth of a repository will in general lead to reduced transport from the disposal area towards the biosphere.

In the GoldSim models developed for this first generic safety assessment, the transport of radionuclides through the geosphere has been largely simplified and pessimistic assumptions have been used regarding transport velocities, retardation of radionuclides etc. Consequently, the exact depth of the repositories has very little influence on the dose rate results. Determination of depth-depending results that allow quantitative evaluation of different repository depths would require more sophisticated models for transport through crystalline rocks and site-specific information on hydrogeological conditions. At this stage of the project this is not possible.

In conclusion, the concept of a National Facility for Norwegian radioactive waste consisting of a deep borehole repository for high level waste and a LILW repository at an intermediate depth is considered to have potential to be further developed into a suitable technical solution.

References

Anttila, M. 2005. Radioactive characteristics of the spent fuel of the Finnish nuclear power plants. Olkiluoto, Finland: Posiva Oy. Working Report 2005-71. 310 p. Link: https://www.posiva.fi/en/index/media/reports.html

Bennett, P. 2020. Summary of Norway's Research Reactor Spent Fuel. Presentation on 20.-21.2.2020, Espoo, Finland.

Bennett, P. 2020a. Personal communication to Henri Loukusa. 11.3.2020.

Brady, P.V., Arnold, B. W., Freeze, G.A., Swift, P.N., Bauer, S.J., Kanney, J.L., Rechard, R.P., Stein, J.S. 2009. Deep borehole disposal of high-level radioactive waste. Technical Report SAND2009-4401, Sandia National Laboratories, Albuquerque, NM, USA, 2009.

Engelhardt, H.-J. & Fischer T. 2021. COO9 Borehole sealing concept. Task CoO9 for Norwegian Nuclear Decommissioning by BGE TECHNOLOGY GmbH and AINS Group, 2021.

Fischer, T., Engelhardt, H.-J. & T. Wanne, T. 2020. Deep Borehole Disposal Concept. Technical Report Task CoO3 for Norwegian Nuclear Decommissioning by BGE TECHNOLOGY GmbH and AINS Group, 2020.

Freeze, G., Voegele, M., Vaughn, P., Prouty, J., Nutt, W.M., Hardin, E. & Sevougian, S.D. 2013. Generic Deep Geologic Disposal Safety Case – Fuel Cycle Research & Development. Report for US Department of Energy, FCRD-UFD-2012-000146, SAND2013-0974P, Revision 1, August, 2013.

Hagros, A., Engelhardt, H-J., Fischer, T., Gharbieh H., Hautojärvi A., Hellä, P., Häkkinen, I., Ikonen A., Karvonen T., Keto, P., Rinta-Hiiro, V., Schatz, T., Wanne, T., Ärväs-Tuovinen, T. 2021. Host Rock Target Properties for Norwegian National Facility. AINS Group Technical Report. June 2021.

Hjerpe, T., Marcos, N., Ikonen, A.T.K., Reijonen, H. & Åstrand, P-G. 2021. Safety Case for the Operating Licence Application: FEP database description. Working Report 2020-19. Eurajoki, Finland: Posiva Oy. 76 p.

IAEA 2006. Fundamental Safety Principles. IAEA Safety Standards, Safety Fundamentals No. SF-1, Vienna, Austria, 2006.

IAEA 2009. Borehole Disposal Facilities for Radioactive Waste. IAEA Safety Standards for protecting people and the environment. Vienna: International Atomic Energy Agency (IAEA). Specific Safety Guide No. SSG-1.

IAEA, 2011. Disposal of radioactive waste. Vienna, Austria: International Atomic Energy Agency (IAEA). IAEA Safety Standard Series Specific Safety Requirements, No. SSR-5. 62 p. ISBN 978-92-0- 103010-8.

IAEA 2015. Site survey and site selection for nuclear installations –Specific safety guide. Vienna, Austria: International Atomic Energy Agency (IAEA). IAEA Safety Standard Series No. SSG-35.

IAEA 2018. IAEA Safety Glossary 2018.
Link: https://www-pub.iaea.org/MTCD/Publications/PDF/PUB1830_web.pdf

ICRP 1998. Radiation Protection Recommendations as Applied to the Disposal of Long-lived Solid Radioactive Waste. International Commission on Radiological Protection, ICRP Publication 81, Pergamon Press, 1998.

ICRP 2013. ICRP: Radiological Protection in Geological Disposal of Long-lived Solid Radioactive Waste. ICRP (International Commission on Radiological Protection) Publication 122, Ann. ICRP 42 (3), Elsevier, Amsterdam, 2013.

Ikonen, A., Engelhardt, J., Fischer, T., Gardemeister, A. Karvonen, S., Keto, P., Rasilainen, K., Saanio, T. & Wanne, T. 2020. Concept description for Norwegian national disposal facility for radioactive waste. AINS

Group, Technical Report. Link:
https://www.norskdekommisjonering.no/wpcontent/uploads/2020/10/Technical-report-Concept-Description-for-Norwegian-National-DisposalFacility-for-Radioactive-Waste.pdf

Loukusa, H. & Nordman, H. 2020. Feasibility of KBS-3 spent fuel disposal concept for Norwegian spent fuel. May 2020

McKinley, I.G. & A. Scholtis, A. 1993. A comparison of radionuclide sorption databases used in recent performance assessments. Upper Saddle River, NJ, Prentice-Hall. Journal of Contaminant Hydrology 13: 347-363, 1993.

NEA 2004. Post-Closure Safety Case for Geological Repositories – Nature and Purpose, NEA No. 3679, OECD/NEA, Paris.

Nummi, O. 2018. Safety case for Loviisa LILW repository 2018 – Main report. Fortum LO1-T3552-00023.

Saanio, T., Hagros, A. & Wanne, T. 2021a. Site selection criteria and site selection process for Norwegian National Facility, NND. AINS Group Technical Memorandum. June 30th, 2021.

Saanio, T., Seppälä, T, Wanne, T. & Lundby, I.M. 2021b. Siting strategy, criteria, and related legal framework for Norwegian National Facility. AINS Group memorandum. July 2021.

SKB 2010. Data report for the safety assessment SR-Site. Updated 2014-01. SKB TR-10-52. Swedish Nuclear Fuel and Waste Management Co. (SKB).

Schweizer, V.J. & Kurniawan, J.H. 2016. Systematically linking qualitative elements of scenarios across levels, scales, and sectors. Environmental Modelling & Software 79, 322-333.

Walke, R., Watson, S., Metcalfe, R., Newson, R., Wilson, J., Thorne, M. & Wood, P. 2018. Disposability Assessment for Norwegian Research Reactor Fuel – Post closure Safety Assessment Report. Quintessa Report QRS-1924A-1, Version 2.0 for Norwegian Radiation Protection Authority (NRPA), 2018.

Wunderlich, A., Seidel, D., Herold, P., Wanne, T. 2021. Deep Borehole Disposal Canister. Technical Report Task COO10 for Norwegian Nuclear Decommissioning by BGE TECHNOLOGY GmbH and AINS GROUP, 2021.

Appendix I – Inventories of Norwegian spent nuclear fuel

Derivation of MU/SNF inventory by H. Nordman: Henrik Nordman. AINS Group. 8th October 2021. Inventories of Norwegian spent fuel.

CONTENTS of Appendix I

I.1 Introduction

This memorandum presents a proposal for the spent nuclear fuel inventory to be used in the work package COO11 for the generic safety assessment. This proposal includes a simplified approach to account for the metallic uranium. The accuracy of fission product inventories is pretty good within per cents. The inventory of transuranic is more uncertain, but in this work a reasonable estimate is made and discussed. The LILW inventory is not discussed in this memorandum.

It is emphasised that the approach presented in this memorandum is a simplified approach considered applicable for the generic safety case. However, in the future, when preparing safety cases for the licensing purposes, more detailed calculations on the inventories are needed, e.g., more detailed information on the fuel is needed and some reactor physicist should carry out a simulation with, e.g., SERPENT or SCALE 5 codes. SFCOMPO is a database of nuclide compositions of spent nuclear fuel by OECD/NEA (see Michel-Sendis et al. (2014, 2017), Gauld et al. (2017)). Information can be found also:
https://www.oecd-nea.org/jcms/pl_21515/sfcompo-2-0-spent-fuel-isotopic-composition

I.2 Uranium in fuel elements

Commercial power plants with UO_2 fuel have typically a burnup in range 40-60 MWd/kg. But in Halden there is both UO_2 (slow corrosion and 15 MWd/kg-80 MWd/kg) and metallic U (fast corrosion, but very low burnup of less than 0.4 MWd/kg).

The fuel types are presented in Table I.2-1, which is a modified table from Loukusa & Nordman (2020).

*Table I.2-1. Fuel types and some properties (Loukusa & Nordman (2020) based on data from Bennett 2020). *: Bennett (2020a), **: calculated based on other values in the table). HBWR = Halden Boiling Water Reactor.*

Reactor	**JEEP I**	**HBWR 1st charge**	**JEEP II**	**HBWR 2nd to 4th charge / + 5th**	**HBWR Booster/ +experimental**
Fuel	U metal	U metal	UO_2	UO_2	UO_2 /+ MOX, ThO_2
^{235}U enrichment (%)	0.72	0.72	3.5	≤ 10	≤ 20/ + higher
Cladding material	Al	Al	Al	Zircaloy	Zircaloy/ +various
U mass per rod (kg)	19	22	1	0.6 – 0.9	0.2 – 0.9
Burn-up (MWd/kg_U)	≤ 1	≤ 0.021	≤ 15	≤ 79.4	≤ 79.4 / + higher
Rod length (m)	2.4	2.8	1.5	~ 1.8/1.1	≤ 1.1
Rod diameter (mm)	25	40	15	12.25 – 14.3	6.25 – 9.5/+ 14.3
Number of rods (ca.)	170	300	1500	700/4500	2000
Assembly or single rods*	Assembly	Rods	Assembly	Assembly/rods	Rods and assemblies/ + mostly rods
Assembly length (m)	2.8	2.8	1.5	2nd charge: 2.83, 3rd & 4th charge: 3.66, 5th charge 1.1	1.2
Assembly diameter (mm)	70	40	90	≤ 70	≤ 70
Number of rods per assembly	2*	1*	11*	7*	
Number of assemblies (ca.)	85**	300**	136**	100**	
Mass (kg)	3000	7000.0	1500	3600	1400
Mass per assembly (kg)	35.29	23.3	11.03	4.2 - 6.3/0.4-0.9	0.2 – 0.9

I.2.1 Methodology and background for fuel

For the approximation of inventory, the following assumptions have been used.

a) JEEP I: Waste generated is aluminium cladded rods, 3 tonnes of metallic uranium with typical burnup of 0.2–0.4 MWd/kg according to Bennet & Larsen (2013). 0.3 MWd/kg is a chosen value for this work.
b) HBWR 1st charge: Waste generated is aluminium cladded rods, 7 tonnes of metallic uranium with burnup of only 0.012 MWd/kgU according to Bennet & Larsen (2013).
c) JEEP II: Waste generated is 1.5 tonnes of UO_2 with aluminium cladding and burnup 15 MWd/kgU.
d) HBWR 2nd to 5th charge: Waste generated is 3.6 tonnes of UO_2 experimental fuel with zirconium cladding. Burnup is assumed to be 40 MWd/tU.
e) HBWR booster/experimental: Waste generated is Zircalloy cladding 1.4 tonnes of UO_2 experimental with zirconium cladding. Burnup is assumed to be 80 MWd/tU.

For future studies, the burnup for cases d) and e) is recommended to be clarified.

Fission products

An inventory in a commercial spent fuel with certain burnup is assumed to be known, like those presented by Posiva (Anttila 2005) or SKB (2010). The inventory for lower burnup from NND can be estimated from simple linear extrapolation according to Equation I-1 below.

$$INV_{NND} = INV_{comm} \cdot BU_{NND} / BU_{comm} \cdot M_{NND} / M_{comm} \qquad \textit{(Equation I-1)}$$

where

INV_{comm} is activity inventory of commercial fuel (Bq) per a given amount of charged U,
M_NND is the mass of relevant NND fuel and isotopes with burnup of BU_{NND}
M_{comm} is the given amount of charged U (tU or kgU),
BU_{comm} is the burnup of the commercial fuel (MWd/kgU), and
BU_{NND} is the burnup of the NND fuel (MWd/kgU).

The linear approximation is good for most important fission product nuclides. Some deviations may take place if the nuclide has a large neutron capture cross-section or produced additionally by neutron activation of a high yield fission product. Such processes can be accounted for in final reactor physical calculations to a needed accuracy.

As a background process for this work, a rough comparison between some results has been made in Table I.2-2.

Table I.2-2. Comparison of fission product inventories (GBq/tU) by Anttila (2005) and SKB (2010). Burnup 40 MWd/kgU. The inventory by SKB (2010) is calculated based on 47637 BWR assemblies and assuming 195 kg uranium per assembly.

Nuclide	Inventory Anttila (2005)	Inventory SKB (2010)
Cs-135	1.99E+01	1.91E+01
Cs-137	2.36E+06	1.83E+06
I-129	1.16E+00	1.09E+00
Pd-107	4.65E+00	4.60E+00
Se-79	3.27E+00	2.91E+00
Tc-99	6.06E+02	5.36E+02

From Anttila 2005 (Table 2.1.1.4), fission product I-129 activity after 30 years is 1.115 Bq/tU with burnup of 40 MWd/kgU. JEEP I inventory for I-129 is calculated by multiplying this activity by the mass of JEEP I fuel, 3 tonnes, and the ratio between burnups of the two fuels, 0.3 MWd/40MWd, and resulting in 0.025 GBq.

U-234 inventory critical

U-234 is important as the daughter nuclide Ra-226 forms a radiological risk. As the fuel is natural low burnup fuel, U-234 can be estimated to be in balance with parent U-238. So, in 3 tonnes there is about 36 GB of uranium and thus same amount of U-234, and also same amount of Ra-226 in the later times.

For U-234 the situation, is a bit uncertain with high enrichment of U-235. According to NRC (2012), “the 4 times enrichment in U-235 from 0.711 % to 2.96 % results in five times enrichment of U-234” resulting U-234 percentage to rise from the natural 0.0055 % to 0.028 %. This means roughly an additional 4 to 16 times increase in U-235 to 11.84 % and results in about 25 times increase in U-234 activity rising from natural 12 GBq/tU to 300 GBq/tU in 11.84 % enriched fuel. Production from Pu-238 is also added when burnup is higher. In an old report, a smaller increase factor of 30 was estimated for U-234 with enrichment of 20 % for U-235.

One can write an equation for the enrichment of U-234, Rich234 (%), when the number of 4-fold enrichments of U-235 from the natural concentration 0.711 % is known:

$$Rich234 = Nat234 \cdot 5^{N_4} \qquad \textit{(Equation I-2)}$$

where

Nat234 is the natural concentration of U-234 (0.0055 % or 12 GBq/ton),
N_4 is the number of times of the 4-fold enrichment of U-235 has taken place, and
N_4 is $\log_4$(enrichment 235/0.711).

But at high burnups, the enriched U-234 will be transformed partly to other isotopes, so the situation is not straightforward. A real modelling with a reactor physics code is needed for accurate assessments, although for the generic safety case, this simplified estimation is considered to be sufficient.

Pu-239 and other actinides in JEEP I and HBWR 1st

The inventories are explained in Annex I.A2. There are uncertainties for low burnup fuels as accumulation and consumption of, e.g., Pu-239, cause a nonlinear behaviour contrary to most fission products.

I.2.2 Summary for metallic uranium fuel

The inventories are summarized in Table I.2-3 for JEEP I and HBWR 1st. In Section I.5.1, the corrosion and gas generation aspect is analysed.

Table I.2-3. JEEP I and HBWR 1st charge. See Annex I.A2 for plutonium. Others extrapolated with Equation I-1.

Nuclide	**JEEP I 3 ton.** **0.3 MWd/kgU natural (GBq)**	**$H^{BW}R$ 1st 7 ton.** **0.012 MWd/kgU natural (GBq)**	**Sum metallic uranium** **(GBq)**
Ag-108m	2.0E-05	1.8E-06	2.1E-05
Am-241	From Pu-241	From Pu-241	From Pu-241
C-14	1.7E+00	1.6E-01	1.8E+00
Cl-36	2.0E-01	1.8E-02	2.1E-01
Cs-135	6.1E-01	5.7E-02	6.7E-01
Cs-137	5.9E+04	5.5E+03	6.5E+04
I-129	2.8E-02	2.6E-03	3.1E-02
Mo-93	2.7E-08	2.5E-09	3.0E-08
Nb-93m	1.6E+00	1.5E-01	1.8E+00
Nb-94	1.2E-04	1.1E-05	1.3E-04
Ni-59	4.6E-02	4.3E-03	5.0E-02
Ni-63	4.7E+00	4.3E-01	5.1E+00
Pa-231	1.7E-04	1.6E-05	1.9E-04

Nuclide	JEEP I 3 ton. 0.3 MWd/kgU natural (GBq)	$H^{BW}R$ 1st 7 ton. 0.012 MWd/kgU natural (GBq)	Sum metallic uranium (GBq)
Pd-107	4.7E-02	4.4E-03	5.2E-02
Pu-239	1.6E+03	9.2E+01	1.6E+03
Pu-240	2.1E+02	0	2.1E+02
Pu-241	4.3E+03	0	4.3E+03
Se-79	7.4E-02	6.9E-03	8.1E-02
Sm-151	7.0E+02	6.6E+01	7.7E+02
Sn-126	2.3E-01	2.2E-02	2.5E-01
Sr-90	5.0E+04	4.7E+03	5.5E+04
Tc-99	1.6E+01	1.5E+00	1.8E+01
U-234	3.6E+01	8.4E+01	1.2E+01
U-235 (*	4E-2	9E-02	1.3E-01
U-238	3.6E+1	8.4E+1	1.2E+01
Zr-93	2.3E+00	2.2E-01	2.5E+00

Comparison to Quintessa results

In Quintessa (2018, Table 3-1), the inventories are higher: E.g. I-129 inventory is 0.144 GBq with burnup 400 MWd/tU which does not explain the difference. Perhaps they have included the 6.7 tonnes of HBWR fuel with very low burnup but using (400 MWd/tU). The inventory is based on the report by Smith & Thorne (2018), which is not available for the author.

Table I.2-4. Comparison of the approximated metallic U inventory to STUK's release rate limits (STUK 2018).

Nuclide	Half-life	Metallic U inventory (GBq)	STUK release rate limit (GBq/yr)
C-14 (*	5.70E+03	1.8E+00	0.3
Cl-36	3.01E+05	2.1E-01	0.3
Cs-135	2.30E+06	6.7E-01	0.3
I-129	1.57E+07	3.1E-02	0.1
Se-79	3.27E+05	8.1E-01	0.1
Tc-99	2.11E+05	1.80E+01	3
Ra-226	1.60E+03	(0.05 GBq/yr produced from U)	0.03
Pu-239	2.30E+4	1.1E+03	0.03

I.2.3 Uranium oxide fuel

Table I.2-5 below is based on extrapolation from Equation I-1. The U-234 inventory is based on enrichment of U-235. But from results, e.g., Anttila (2005) it is seen that with a high burnup majority of enriched U-234 is burned away but on the other hand, more U-234 is later produced from Pu-238 decay after removal from the reactor.

So, the final inventory of important U-234 is a bit open.

Table I.2-5. Extrapolated from existing results. See Annex I.A1.

Nuclide	JEEP II 1.5 ton. 15 MWd/kgU UO_2 (GBq)	HBWR 2st to 5th 3.6 ton ~40 MWd/kgU (GBq)	HBWR Booster 1.4 t. ~80 MWd/kgU UO_2 (GBq)	Sum UO_2. total 6,5 ton (GBq)
Assumed Enrichment (%)	3.5	6	11.84	
Ac227	1.5E-03	2.4E-03	1.3E-03	5.2E-03
Ag108m	4.4E-04	7.5E-03	9.1E-03	1.7E-02
Am241	2.9E+04	4.6E+05	2.0E+05	6.9E+05
Am242m	9.9E+00	1.2E+03	2.4E+02	1.4E+03
Am243	6.1E+00	3.7E+03	6.5E+03	1.0E+04
C14 (*	4.5E+01	3.0E+02	2.3E+02	5.8E+02
Cl36 (*	4.5E+00	3.0E+01	2.3E+01	5.8E+01
Cm245	3.7E-03	4.9E+01	3.0E+02	3.5E+02
Cm246	1.0E-04	1.0E+01	2.2E+02	2.3E+02
Cs135	1.4E+01	6.9E+01	5.6E+01	1.4E+02
Cs137	1.4E+06	6.6E+06	6.2E+06	1.4E+07
I129	6.4E-01	3.9E+00	3.7E+00	8.3E+00
Mo93	6.1E-07	3.9E-05	1.0E-04	1.4E-04
Nb93m	3.7E+01	2.2E+02	1.5E+02	4.0E+02
Nb94	2.7E-03	1.8E-02	3.3E-02	5.3E-02
Ni59	1.0E+00	3.3E+00	6.3E+00	1.1E+01
Ni63	1.1E+02	3.7E+02	8.3E+02	1.3E+02
Np237	3.9E+00	4.8E+01	3.2E+01	8.4E+01
Pa231	3.9E-03	4.1E-03	1.9E-03	9.9E-03
Pb210	7.6E-05	1.2E-04	3.8E-05	2.3E-04
Pd107	1.1E+00	1.7E+01	1.9E+01	3.6E+01
Pu238	5.4E+03	3.7E+05	4.4E+05	8.1E+05
Pu239	1.5E+04	3.9E+04	1.4E+04	6.8E+04
Pu240	7.7E+03	7.2E+04	4.4E+04	1.2E+05
Pu241	2.7E+05	2.9E+06	1.9E+06	5.0E+06
Pu242	3.2E+00	3.1E+02	4.2E+02	7.3E+02
Ra226	3.0E-04	4.0E-04	1.1E-04	8.1E-04
Ra228	8.5E-09	0.0E+00	2.0E-08	2.9E-08
Se79	1.7E+00	1.1E+01	7.5E+00	2.0E+01
Sm151	1.6E+04	3.8E+04	1.5E+04	6.9E+04
Sn126	5.2E+00	7.6E+01	5.4E+01	1.4E+02
Sr90	1.1E+06	4.4E+06	3.5E+06	9.0E+06
Tc99	3.7E+02	1.9E+03	1.4E+03	3.7E+03
Th229	4.8E-06	4.2E-05	7.1E-05	1.2E-04
Th230	4.4E-02	4.9E-02	1.6E-02	1.1E-01
Th232	1.5E-08	7.3E-08	3.3E-08	1.2E-07
U233	1.8E-03	9.6E-03	5.1E-03	1.7E-02
U234 (*	1.4E+02	3.2E+02	1.3E+02	5.9E+02 (*
U235	5.6E+00	1.9E+00	9.7E-02	7.6E+00
U236	1.0E+01	3.8E+01	1.9E+01	6.7E+01
U238	2.7E+01	3.8E+01	1.6E+01	8.0E+01
Zr93	5.2E+01	2.6E+02	2.0E+02	5.1E+02

(* For HBRW fuels a bit arbitrary based on enrichment

For JEEP II with lower burnup the data from Mertyurek et al. (2010) below have been used.

For the samples with about 15 MWd/kgU and t for JEEP II actinide inventory data have from Radulescu et al. (2010) have been used.

I.3 Cladding and other parts

The dimensions and properties of materials should be clarified. E.g., if there is niobium in zircalloy claddings as activation product, Nb-94 may be an important nuclide. In zirconium cladding of Loviisa nuclear power plant fuel there is more than 1 % niobium.

I.3.1 Aluminium

In Section I.5.2, the corrosion and gas generation aspect is analysed.

Carlsson et al (2014) present an approximation of the inventory in irradiated aluminium.

In Table 2.3 in Carlsson et al. (2014), there are inventories for aluminium.; The inventories are based on 0.76 mm of aluminium cladding in a reflector for FIR-1, which is a very small reactor and low burnup compared to NND fuel cladding (JEEP II).

Table I.3-1. Approximation for inventory in irradiated aluminium Carlsson et al. (2014, Table 2.3).

Nuclide	Half-life	Activity (Bq)	Fraction of total
Sc-46	83.9 d	1.11E+08	1.74E-04
Mn-54	312.5 d	4.43E+09	6.93E-03
Fe-55	2.6 a	3.15E+11	0.493
Co-60	5.263 a	1.55E+08	2.42E-04
Ni-63	100 a	4.90E+07	7.67E-05
Zn-65	243.8 d	3.19E+11	0.5
Total		6.39E+11	1

I.3.2 Zirconium alloys

The zirconium masses should be clarified by NND.

The inventories of zircalloys are given by Posiva (2012, Table 6-5). The burnup is quite high (50-60 MWd/kgU) and the choice is conservative 752 GBq/tU for Nb-94. Inventories of zircalloys are also given by Anttila (2005). In Anttila (2005, Table 3.1.1.4), the Nb-94 inventory is 500 GBq/tU for Loviisa fuel where there is some added niobium in cladding. In Quintessa 2018, the total inventory is 42.8 GBq for 5 tonU in zirconium cladding. The total inventory is significantly smaller compared to the inventory based on the other sources mentioned above.

According to experiences Cl-36 in zircalloys is the only important nuclide. Assuming 1 GBq/tU and 5 tonnes of zirconium cladding, there would be 5 GBq total in Zr cladding of HBWR fuels. (Not HBWR 1st charge with aluminium cladding)

I.3.3 Other metal parts, e.g., spacers and end plates

This is an open question as there is no info about the materials. They may be, e.g., Inconel, or zircalloys as in commercial fuel.

I.4 Conclusions for inventory

Source term for a safety analysis:

In Table I.4-1, the idea how to use the data as source term for NND's spent fuel waste is presented.

Table I.4-1. Source term for the safety analyses.

Waste	Inventory based on this work	Example of degradation time
Metallic uranium	Table I.2-3 Sum column	100 years or more
UO_2 fuel	Table I.2-5 Sum column	1E+6 yr
IRF from uranium	to be evaluated	0 yr
Zircalloys Cl-36	5 GBq	1E+4 yr
Other metal parts	unknown	unknown

I.5 Issues

I.5.1 Issues to be considered in safety considering metallic uranium

Finally, it is noted that compared to oxidised fuel, including metallic uranium in the generic safety assessment has implications for the scenarios to be considered.

Data on uranium metal reaction behaviour is to be found in Delegard & Scmidt (2008).

From Table 2.1 Delegard & Schmidt (2008). i. At temperature 15 °C predicted corrosion rate is 0.0021 µm/h and at 30 °C rate is 0.00861 µm/h (Temperature at 1 km could be estimated from a common gradient of 1.1 – 1.5 °C / 100 m and mean annual temperature at the surface being about +4 °C. This results in a temperature of about 15 – 20 °C). The given values of 15 °C and 30 °C correspond to 0.0184 mm/yr and 0.075 mm/yr, respectively. The metallic rods from JEEP 1 and HBWR have a diameter of 25.4 mm and 40 mm from Table I.2-1.

The corrosion of 50 % of mass of the cylindrical surface (~ 8 mm deep) would take at least 100 years. In the repository or in the geological formation, there should be some material to retain nuclides like Pu-239 and Ra-226. Other nuclides seem to have a marginal effect (comparison in Table I.2-4).

The 10 tonnes of metallic uranium are about 4.2E+4 moles. Total corrosion of this to UO_2 will produce 1900 m^3 of hydrogen at NTP. But at depth of 0.5 km or more this is only 38 m^3. So, the rate of gas generation will be less than 0.4 m^3 /yr assuming total corrosion would take at least 100 years.

Heat generation will be moderate: maximally few tens of watts.

I.5.2 Aluminium cladding risk

From Table I.3-1, it is seen that the only long-lived nuclide is Ni-63. If this is the case in Norwegian aluminium cladding the risk is quite low. N-B. In JEEP II fuel with aluminium cladding, the burnups are 15 MWd/kgU.

In JEEP I, there is perhaps 400 kg, in HBWR first ~1100 kg and in JEEP II ~800 kg of aluminium. This is 2300 kg total = 8.5E+4 moles total. Corrosion of it at pH range 4-8.5 produces Al_2O_3 and the result is passivation perhaps if chlorides are not present. So potentially there is 1.27E+5 moles of produced hydrogen H_2, which in NTP conditions has volume of 2850 m^3. At depth of 500 m the corresponding volume is 57 m^3.

JEEP II: The H_2 share of higher burnup fuel JEEP II is 20 m^3 at 500 m depth. This may be a problem in a single borehole with some higher activity aluminium.

According to Adams et al. (2021): "*Considering the rate of corrosion of the alloys in both solutions, alloy AA8011 had corrosion rate of 0.0873 mm/yr, which was the highest in acetic acid solution, while alloy AA1200 had the least corrosion rate of 0.0045 mm/yr in the solution. Meanwhile, alloy AA4017 exhibited the highest corrosion rate of 0.0552 mm/yr and alloy AA1200 had the least corrosion rate of 0.0126 mm/yr in nitric acid solution.*"

And according to Schrieber et al. (1979): *"In ambient temperature seawater, pretreated aluminum alloy 5052 has a final interval corrosion rate of'0.01'5 mm/yr. (0.59 mpy) a.s opposed to a final interval corrosion rate of 0.056-0.065 mm/yr. (2.20-2.57 mpy) for untreated aluminum alloys 3003, 5052, and 5086."*

Conclusion: The above links indicate that the gas production rate would be moderate enough.

Recommendation

When aluminium or metallic uranium is in a borehole, the **upper part should NOT** be gas tight, e.g. compacted bentonite, as then gas can expel contaminated water (or C-14 as gas) to a fracture at high velocity and further to biosphere.

I.6 Recommendations for deep borehole disposal

Based on the preliminary analysis, the following features of the design of the disposal system would improve long-term safety:

- Use a narrow 200 mm diameter borehole. Distance from most of the waste to a fracture intersecting the borehole will be long and area for diffusion in backfill of hole is small.
- Risk of criticality (chain reaction) is smaller than with larger borehole. There are high enrichment fuels. How much and what enrichment need to be known.
- Put several boreholes around a shallow hill of granite. Groundwater and potential gas flows going to different directions; no interaction.
- Where there is aluminium or metallic uranium, do not use compacted bentonite in upper parts of borehole. Gas expelling a water pulse is a risk.
- Last but not least: Use bronze as canister material. Corrosion resistance is good and there is enough strength. Welding technology, etc., must be evaluated by experts.

References Appendix I

Adams, F. V., Akinwamide, S.O., Obadele, B & Olubambi, P. A. 2021. Comparison study on the corrosion behavior of aluminium alloys in different acidic media. Elsevier. Ltd: Materials Today: Proceedings: Special Issue: 2020 International Symposium on Nanostructured and Advanced Materials. Volume 38, part 2, 2021, pages 1040-1043. Link: https://www.sciencedirect.com/science/article/pii/S2214785320343947#

Anttila, M. 2005. Radioactive characteristics of the spent fuel of the Finnish nuclear power plants. Olkiluoto, Finland: Posiva Oy. Working Report 2005-71. 310 p. Link: https://www.posiva.fi/en/index/media/reports.html

Bennett, P & Larsen E. 2013. Storage of Spent Nuclear Fuel in Norway: Status and Prospects. NEA/CSNI/R(2013)10. Link: https://inis.iaea.org/collection/NCLCollectionStore/_Public/45/107/45107537.pdf

Bennett, P. (2020). Summary of Norway's Research Reactor Spent Fuel. Presentation on 20.-21.2.2020, Espoo, Finland.

Bennett, P. (2020a). Personal communication to Henri Loukusa. 11.3.2020.

Carlsson, T., Kotiluoto, P., Vilkamo, O., Kekki, T., Auterinen, I. & Rasilainen, K. 2014. Chemical aspects on the final disposal of irradiated graphite and aluminium. A literature survey. Espoo, Finland: VTT. VTT Technology 156. 57 p + App. 1 p.

Delegard, CH & Schmidt AJ. 2008. Uranium Metal Reaction Behavior in Water, Sludge, and Grout Matrices. Pacific Northwest National Laboratory, Richland, Washington, USA. PNNL-17815. Link: https://www.pnnl.gov/main/publications/external/technical_reports/PNNL-17815.pdf.

Gauld, I., Williams, M.L, Michel-Sendis, F. & Martinez, J.S. 2017. Integral Nuclear Data Validation Using Experimental Spent Nuclear Fuel Compositions. Journal of Nuclear Engineering and Technology. Volume 49, Issue 6, pp. 1226-1233. Link: www.sciencedirect.com/science/article/pii/S1738573317303054.

Loukusa, H & Nordman, H., 2020. Feasibility of KBS-3 spent fuel disposal concept for Norwegian spent fuel. AINS Group May 2020

Mertyurek, U., Francis, M.W. &, Gauld, I.C. 2010. SCALE 5 Analysis of BWR Spent Nuclear Fuel Isotopic Compositions for Safety Studies. Oak Ridge, Tennessee, USA: Oak Ridge National Laboratory. ORNL/TM-2010/286. Link: http://info.ornl.gov/sites/publications/Files/Pub27046.pdf

Michel-Sendis, F., Gauld, I., Bossant, M. & Soppera, N. 2014. A New OECD/NEA Database of nuclide compositions of spent nuclear fuel. Proceedings of the PHYSOR 2014 International Conference, Kyoto, Japan, October 2014. Link: dx.doi.org/10.11484/jaea-conf-2014-003.

Michel-Sendis, F., Gauld, I., Martinez, J.S., Alejano, C., Bossant, M., Boulanger, D., Cabellos, O., Chrapciak, V., Condef, J., Fast, I., Gren, M., Govers, K., Gysemans, M., Hannstein, V., Havlůj, F., Hennebach, M., Hordosy, G. Ilas, G., Kilger, R., Mills, R., Mountford, D., Ortego, P., Radulescu, G., Rahimi, M., Ranta-Aho, A., Rantamäki, K., Ruprecht, B., Soppera, N., Stuke, M., Suyama, K., Tittelbach, S., Tore, C., VanWinckel, S., Vasiliev, A., Watanabe, T., Yamamoto, T., Yamamoto, T. 2017. SFCOMPO-2.0: An OECD NEA Database of Spent Nuclear Fuel isotopic Assays, Reactor Design Specifications and Operating Data. Annals of Nuclear Energy. Volume 110, pp. 779-788. Link: www.sciencedirect.com/science/article/pii/S0306454917302104.

NRC 2012. Module 1.0 Introduction to uranium enrichment. Directed self Study. USNRC Technical Training Center 9/08 (rev3). Link: https://www.nrc.gov/docs/ML1204/ML12045A049.pdf

Posiva. 2012. Safety Case for the Disposal of Spent Nuclear Fuel at Olkil–oto - Assessment of Radionuclide Release Scenarios for the Repository System 2012. Posiva Oy, Eurajoki, Finland. Report Posiva 2012-09. Link https://www.posiva.fi/en/index/media/reports.html

Quintessa. 2018. Disposability Assessment for Norwegian Research Reactor Fuel Post-closure Safety Assessment Report. QRS-1924A-1, Version 2.0. Received from NND 6th June 2021.

Radulescu, G., Gauld, I.C.& Ilas, I. 2010. SCALE 5.1 predictions of PWR Spent Nuclear Fuel Isotopic Compositions. Oak Ridge, Tennessee, USA: Oak Ridge National Laboratory. ORNL/TM-2010/44. Link:.http://info.ornl.gov/sites/publications/files/Pub23359.pdf

Schrieber, C. F., Grimes, W.D. & McIlhenny, W.F. 1979. A Study of the corrosive effect on aluminum and CP titanium of mixtures of ammonia and seawater that may be encounters in OTEC heat exchangers. Argonne, Illinois, USA: Argonne National Laboratory. ANL/OTEC-BCM-004. Link: https://www.osti.gov/servlets/purl/6204870

SKB 2010. Spent nuclear fuel for disposal in the KBS-3 repository. Stockholm, Sweden: Svensk Kärnbränslehantering AB. Technical report TR-2010-13. 97 p.

Post-closure Safety Assessment Report. QRS-1924A-1, Version 2.0. Received from NND 6th June 2021.

Smith G M and Thorne M C (2018). SF Inventory Assumptions for Use in Preliminary Disposability Assessments. GMS Abingdon Ltd. and Mike Thorne and Associates Ltd. document, draft 27 June 2018.

STUK 2018. YVL guide D-5. Link: https://www.stuklex.fi/en/ohje/YVLD-5

ANNEX I.A1 Tables from SKB (2010) and Anttila (2005)

The data used is from a public SKB TR-2010-13 report.

For nitrogen (C-14 is a neutron reaction product) and chlorine (Cl-36 is an activation product) concentrations seem to be low in SKB 2010. Also, for nickel and niobium assumed concentrations in fuel matrix are very low so they have been increased.

On the other hand, Mo-93 and Ag-108m inventories in SKB (2010) are very high.

Based on information in JENDL-4.0 and NuDat 2.8 (by NNDC) databases, see links below, the inventories have been decreased.

Mo-93

https://wwwndc.jaea.go.jp/cgi-bin/nuclinfo2014?42,93

https://www.nndc.bnl.gov/nudat2/reCenter.jsp?z=42&n=51

Am-108m

https://wwwndc.jaea.go.jp/cgi-bin/nuclinfo2014?47,108

https://www.nndc.bnl.gov/nudat2/reCenter.jsp?z=47&n=61

The cumulative fission yields are of about 1E-10 per fission of Ag-108m and for Mo-93 1E-13 in JENDL-4.0 reactor physics database (see link above).

Also, in table F.1.f of Guenther et al. (1991), the same thing can be seen for Ag-108m. according to this reference, the inventory of

Ag-108m is 1.5E-3 GBq/tU so 100 times lower than in SKB (2010). Guenther et al. (1991) do not even include Mo-93.

For higher burnup, data have been adopted from Table B3 in Naegeli (2004), where activity of Ag-108m is 8.6E-3 GBq/tU so 50 times lower than in SKB 2010 and Mo-93 is not even included.

The source data are from the first column of Table C-2 in SKB (2010) with 47,637 BWR assemblies each 195 kg of uranium. So, the total mass of uranium is 9289 tonnes. The SKB table values are divided by the total mass to get values per ton in table I.A1-1.

Table I.A1-1 Activities per ton of uranium 40 MWd/tU. Modified from SKB (2010) according to arguments above.

Nuclide	Inventory SKB (2010) (GBq/tU)	Inventory Multiplied by 3.6 tU (GBq)	Inventory Modified to Table I.2-5 (GBq)
Ac-227	6.72E-04	2.4E-03	
Ag-108m	2.14E-01	7.7E-01	7.5E-03
Am-241	1.27E+05	4.6E+05	
Am-242	3.20E+02	1.2E+03	
Am-243	1.02E+03	3.7E+03	
C-14	1.22E+01	4.4E+01	3.0E+02 (*
Cl-36	1.94E-01	7.0E-01	3.0E+01 (*
Cm-245	1.37E+01	4.9E+01	
Cm-246	2.77E+00	1.0E+01	
Cs-135	1.91E+01	6.9E+01	
Cs-137	1.83E+06	6.6E+06	
I-129	1.09E+00	3.9E+00	
Mo-93	2.78E-02	1.0E-01	3.9E-05
Nb-93m	5.76E+01	2.1E+02	
Nb-94	4.97E-03	1.8E-02	
Ni-59	1.05E-01	3.8E-01	3.3E+00
Ni-63	1.11E+01	4.0E+01	3.7E+02
Np-237	1.35E+01	4.8E+01	
Pa-231	1.13E-03	4.1E-03	
Pb-210	3.37E-05	1.2E-04	
Pd-107	4.60E+00	1.7E+01	
Pu-238	1.02E+05	3.7E+05	
Pu-239	1.08E+04	3.9E+04	
Pu-240	1.99E+04	7.2E+04	
Pu-241	7.96E+05	2.9E+06	
Pu-242	8.48E+01	3.1E+02	
Ra-226	1.11E-04	4.0E-04	
Ra-228	0.00E+00	0.0E+00	
Se-79	2.91E+00	1.1E+01	
Sm-151	1.06E+04	3.8E+04	
Sn-126	2.12E+01	7.6E+01	
Sr-90	1.22E+06	4.4E+06	
Tc-99	5.36E+02	1.9E+03	
Th-229	1.16E-05	4.2E-05	
Th-230	1.36E-02	4.9E-02	
Th-232	2.03E-08	7.3E-08	
U-233	2.66E-03	9.6E-03	
U-234	4.34E+01	1.6E+02	3.2E+02 enrichment to 6 %!
U-235	5.16E-01	1.9E+00	
U-236	1.06E+01	3.8E+01	
U-238	1.04E+01	3.8E+01	
Zr-93	7.12E+01	2.6E+02	

Below a snapshot from Anttila (2005, Table 1.2.1.4.)

Compare to Table I.2-5 with 40 MWd/tU

Table I.A1-2. So called light elements from Anttila (2005). Burnup 40 MWd/tU.

Nuclide	Inventory GBq/tU	Inventory multiplied by 3.6tU GBq
c14	3.02E+01	1.09E+02
cl36	1.15E+00	4.15E+00
ni63	1.57E+04	5.64E+04
zr93	8.71E+00	3.13E+01
nb93m	3.64E+02	1.31E+03
nb94	3.15E+01	1.13E+02
mo93	1.18E+01	4.24E+01

Compare to Table I.2-5 with 40 MWd/tU

Table I.A1-3. Fission products from Anttila 2005. Burnup 40 MWd/tU.

Nuclide	Inventory GBq/tU	Inventory multiplied by 3.6tU GBq
se79	3.27E+00	1.18E+01
sr90	1.65E+06	5.95E+06
zr93	8.11E+01	2.92E+02
nb93m	6.06E+01	2.18E+02
tc99	6.06E+02	2.18E+03
pd107	4.65E+00	1.67E+01
cd113m	3.60E+00	1.29E+01
sn126	2.26E+01	8.13E+01
sb126	3.16E+00	1.14E+01
sb126m	2.26E+01	8.13E+01
i129	1.16E+00	4.18E+00
cs134	2.58E+02	9.30E+02
cs135	1.99E+01	7.17E+01
cs137	2.36E+06	8.49E+06
sm151	1.03E+04	3.70E+04

Compare to Table I.2-5 with 40 MWd/tU

Table I.A1-4. Actinides from Anttila (2005). Burnup 40 MWd/kgU.

Nuclide	GBq/tU	Multiplied by 3.6tU (GBq)
u234	5.00E+01	1.80E+02
u236	1.20E+01	4.33E+01
u238	1.17E+01	4.19E+01
np237	1.28E+01	4.60E+01
np239	9.05E+02	3.26E+03
pu238	9.09E+04	3.27E+05
pu239	1.02E+04	3.65E+04
pu240	2.08E+04	7.47E+04
pu241	9.97E+05	3.59E+06
pu242	8.74E+01	3.15E+02
am241	1.10E+05	3.95E+05
am242m	2.47E+02	8.88E+02
am242	2.46E+02	8.84E+02
am243	9.05E+02	3.26E+03
cm242	2.03E+02	7.31E+02
cm243	3.33E+02	1.20E+03
cm244	3.47E+04	1.25E+05
cm245	7.83E+00	2.82E+01
cm246	1.73E+00	6.22E+00

References Annex I.A1

Anttila, M. 2005. Radioactive Characteristics of the Spent Fuel of the Finnish Nuclear Power Plants. Olkiluoto, Finland: Posiva Oy. Working Report 2005-71. 310 p.

Guenther, R.J., Blahnik, D.E., Campbell, T.K., Jenquin, U.P., Mnedel, J.E., Thomas, L.E. & Thornhill, C.K. 1991. Characterisation of Spent Fuel Approved Testing Material – ATM-105. Pacific Northwest National Laboratory, Richland, Washington, USA. PNL-5109-105. Link: https://www.oecd-nea.org/science/wpncs/ADSNF/reports/CalvertCliffs/PNL-5109-105.pdf

Naegeli, R.E. 2004. Calculation of the Radionuclides in PWR Spent Fuel Samples for SFR Experimental Planning. Sandia Report SAND2004-2757, Sandia National Laboratories, Albuquerque, NM, USA, Link: https://digital.library.unt.edu/ark:/67531/metadc889278/m2/1/high_res_d/919122.pdf

SKB 2010. Data report for the safety assessment SR-Site. Updated 2014-01. SKB TR-10-52. Swedish Nuclear Fuel and Waste Management Co. (SKB).

ANNEX I.A2 Plutonium in very low burnup JEEP I and HBWR 1st charge

In production of weapons grade plutonium the fuel has burnup of 600-1000 MWd/tU according (Sublette, 2021).

In in Table 1.1 of van Rooijen (2006), as n Sublette (2021) for weapons grade plutonium, the isotopic composition is

- Pu-239 93.6 %,
- Pu-240 6 %, and
- Pu-241 0.3 %.

Ilas et al. (2014) present data from measurements of Hanford reactor.

In Table 6 of Ilas et al. (2014), the burnups are mentioned. The burnups for first two samples are 350 MWd/tU so very near JEEP I burnup 200-400 MWd/tU. (PY number 1079 fuel element 11 and 12 in Hanford reactor).

In Table 8 of Ilas et al. (2014), the amount of produced plutonium is 343 and 464 g/tU in the first two samples with burnup 350 MWd/tU. But in sample 6 with burnups 720 MWd/tU the produced plutonium is only 677 g/tU

In Table 7 of Ilas et al. (2014), the isotopic composition of the plutonium by weight is given:

- Pu-239 96.5 %,
- Pu-240 3.3 %, and
- Pu-241 0.17 %.

This is in line with the data by van Rooijen (2006) and Sublette (2021) as the burnup is lower than in the weapons grade.

But according to Coles (2014), a bundle with weight of 13.4 kg produces 760 g/ton plutonium with burnup of 1 GWd/tU. With burnup 2 GWd/tU the production is 1640 g/tU.

Thus it could be chosen that at burnup of 300 MWd/tU in JEEP I the Pu produced is 230 grams per tonne. Also, in table at page 18 in Rozon (1997) for CANDU heavy water reactor the value of about 200 g/U is supported. (In table burnup 8.69 MWh/kg ~360 MFa/tU producing 225 grams Pu-239 per ton)

Thus, the following data will be used for 3 tonnes of JEEP I fuel assuming 230 grams of Pu per ton

- Pu-239 = 96.5 w% = 666 grams = 1.6E+3 GBq ($T_{½}$ = 2.41E+4 yr)
- Pu-240 = 3.3 w% = 22.8 grams = 2.1E+2 GBq ($T_{½}$ = 6.56E+3 yr)
- Pu-241 = 0.17 w% = 1.17 grams = 4.8 E+3 GBq ($T_{½}$ = 14.3 yr)

For HBWR 1st charge, only Pu-239 will be included by multiplying the JEEP I inventory by the ratio of burnups 0.012 / 0.3 and masses 7 ton / 3 ton so 150 GBq will be the used inventory.

An illustrative example of the Pu-239 mass in the assembly as a function of burnup is shown below (source: https://serpent.vtt.fi/mediawiki/index.php/Tutorial)

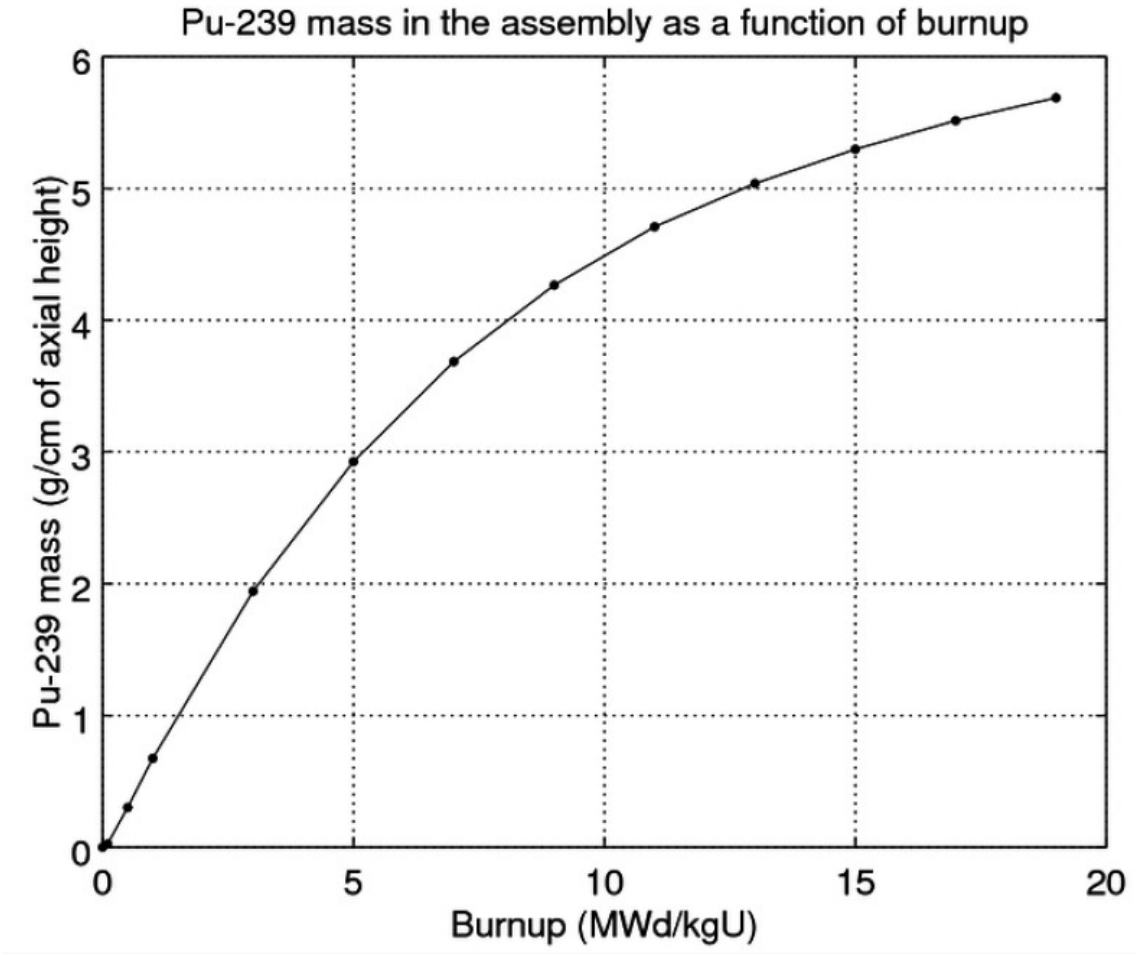

References Annex I.A2

Coles, T. M. 2014. Computional Nuclear Forensic Analysis of Weapon-grade Plutonium Separated from Fuel Irradiated in a Thermal reactor. Texas A&M University. Thesis for Master of Science degree. Link: http://oaktrust.library.tamu.edu/bitstream/handle/1969.1/152706/COLES-THESIS-2014.pdf?sequence=1

Ilas, G., Gauld, I., Westfall, R.M. & Pigni, M. 2014. Evaluation of Hanford B Reactor Experiments (PTA-069 and PTA -084) for Code and Data Benchmarking. Oak Ridge, Tennessee, USA: Oak Ridge National Laboratory. ORNL/TM-2014/53. Link: https://info.ornl.gov/sites/publications/files/Pub48555.pdf

van Rooijen, W.F.G. 2006. Improving Fuel Cycle Design and Dafety Characteristics of a Gas Cooled Fast Reactor. Amsterdam, The Netherlands: IOS Press. 144 p.
Link: https://inis.iaea.org/collection/NCLCollectionStore/_Public/44/098/44098617.pdf

Rozon, D. 1997. Introduction to Nuclear reactor kinetics. Course presented at Chulalongkorn University, Bangok, Thailand. Ecole Polytechnique.
Link: https://canteach.candu.org/Content%20Library/20041804.pdf

Sublette, C. 2021. Nuclear wepapons Frequently Asked Questions.
Link: http://nuclearweaponarchive.org/Nwfaq/Nfaq4-1.html. (8.10.2021)

Appendix II – Low and intermediate level waste (LILW) inventory estimations for Norway

Derivation of the ILW/LILW inventory; memo by HNOR dated 15-3-2022, as received from HKR on 21.3.2022: For use in the project final report.

II.1 Introduction

Even in a generic safety analysis, the used inventories could be as realistic and credible as possible. This is the purpose of this memo. Especially the relationship of different isotopes should be as correct as possible. This is an important factor in risk and dose evaluation as dose potential differs between isotopes.

Norwegian low and intermediate level nuclear waste consists of different sources as:

1) Operational waste from HBWR and JEEP. Contamination of materials and activity in, e.g., ion exchange resins.
2) Other waste from hospitals and industry.
3) Decommissioning waste of research reactors and associated facilities.
4) Reprocessing waste from a former pilot reprocessing plant at Kjeller, currently stored at Himdalen.

For 1) Operational waste and 2) Other waste, the Swedish SFR 1 repository data in Almkvist & Gordon (2007) have been selected and a conservative approach has been used by scaling up the SFR inventories relative to spent uranium fuel. The repository SFR 1 (Almkvist & Gordon 2007) is designed for the disposal of low and intermediate level radioactive waste from the Swedish nuclear power plants and the Central Interim Storage for Spent Nuclear Fuel (Clab) and for similar waste from other industries, research, and medical care. In Almkvist & Gordon (2007), the radionuclide inventory is based on actual measurements: measurements of gamma emitters Co-60 and Cs-137 in waste packages and on measurements of Pu-239 and Pu-240 in reactor water. Other nuclides in the inventory are calculated using correlation factors. One must keep in mind that the inventories are anyway approximations with uncertainties of one order of magnitude.

For 3) Decommissioning waste, the data for Oskarshamn 2 power plant in Larsson et al. (2013) have been used. The data are quite exact for Oskarshamn 2 and the inventories have been scaled with the much less total burnup and thus neutron bombardment in HBWR. But in the future the materials, geometry, and operation history data of HBWR should be used in an exact way to get a better approximation.

4) Reprocessing waste used the data given in Norwegian Radiation Protection Authority (NRPA, 2018, page 19).

Some points of interesting nuclides.

- Co-60 is an activation product from stainless steel parts where there is nickel about 10 % and cobalt as trace max 0.2 % which then becomes Co-60.
- Ca-41 is an activation product from concrete in the biological shield.
- C-14 is an activation product from nitrogen which is in, e.g., stainless steels and its dose potential is important.
- Mo-93 is an activation product and important contributor to doses in SFR 1 safety analyses via drained-mire farmland (SKB, TR-14-01, Table-9-1). It is important to know if in Halden there has been molybdenum rich alloys like Inconel-718 or stainless steel SIS316.
- Cs-137, I-129 etc. are fission products and found, e.g., in ion exchange resins.

II.2 Discussion on the findings in Avila (2021)

It has been found that in the inventory provided in Avila (2021), there are large discrepancies or errors. The most notable as examples are those concerning Co-60 and Ca-41 as follows:

The material and quantities considered in Avila (2021) are concrete and reinforcement with a total mass of 405 tonnes (TN), metal from components (pipes, structural steel, ventilation, cabling and chutes) with a total mass of 509 tonnes, and other materials (Section 3.5 after equation 1 in Avila 2021) with a total mass of 64 tonnes. For the ILW, the Scaling Factors method (see Section 3.4 in Avila 2021) was used to derive a maximum inventory for each radionuclide. From the Co-60 inventory in Table 2.5 (Avila 2021):

$$Inv_i = conc_{Co-60} * SF_i * M * UF \qquad \textit{(Equation II-1)}$$

where

Inv_i is inventory of nuclide i (Bq),
SF_i is the maximum value of Scaling Factor for the ***i-th*** radionuclide across all material types (unitless),
M is the total mass of the disposed material (g), and
UF is an Uncertainty Factor (unitless).

For the total mass (M), a value of 1000 TN was used, which is the rounded-up value of 978 TN shown in Table 2.1 (Avila 2021).

Assuming 1000 TN of disposed waste, and the Co-60 concentration in the disposed waste of 100,000 Bq/g. Uncertainty factor of 4 is mentioned in the text. Thus, in Appendix B, Table B1 of Avila (2021), the Ca-41 inventory is 5E+13 Bq. This is the result for Ca-41 as:

- 500 tonnes of concrete material,
- scaling factor to Co-60 one text “The maximum values of the SF found in the literature for each of these material types were used in the calculations”
- and a Co-60 concentration of 100,000 Bq/g.

In the final Table 4.3 (Avila 2021), the reported Ca-41 inventory is 5E+14 Bq for unknown reasons.

A comparison with reliable inventories (see below) shows that for Ca-41 and Co-60, a too high concentration of 100,000 Bq/g is given in Avila (2021), as it is the relation Ca-41/Co-60 = 1.

In Table 4-8 in Larsson et al. (2013), the total Ca-41 inventory in 547 TN of concrete from a 600 MW(electric) boiling water reactor (BWR) after 48 years of operation is only 3.6E+9 Bq (i.e. concentration 6.6 Bq/g compared to 100,000 Bq/g). The Co-60 amount in concrete is 1.1E+11 Bq and 1.8E+11 in concrete reinforcement (168 tonnes, one year decay time) so the average concentration is 400 Bq/g and not 100,000 Bq/g as reported in Avila (2021).

In IAEA (1998, IAEA 1998. Table XI. 10 years after shutdown), although the concentration is not reported, a total of Ca-41 2.6E+8 Bq is reported for in a reactor of 90 MW(thermal) operated for 13 years.

In IAEA (1993, page 46, Figure 2 by Anttila.), for a BWR, the maximum Ca-41 concentration in concrete is about 6 Bq/g, which is in line with the concentration value reported in Larsson et al. (2013). The Co-60 concentration (one year cooling time) in concrete is about 5E+8 Bq/ton equivalent to 500 Bq/g, which is also in line with Table 4-8 of Larsson et al. (2013). In Avila (2021), the too high Co-60 concentration up to 100,000 Bq/gram is assumed.

Given the large discrepancies in the values found in Avila (2021) as compared to other reliable sources, a better reliable inventory estimate is needed and proposed below.

II.3 Revised estimate of LLW and ILW waste

The revised estimate of ILW and LLW inventory is based on the Swedish low and intermediate level waste repository SFR data (SKB Report R-07-17). In addition, for the ILW inventory, an estimate of the decommissioning waste is based on data from Oskarshamn 2 (https://www.okg.se/oskarshamn-2) with an impact especially on Ca-41 inventory, and on reprocessing waste data at Himdalen Norwegian Radiation Protection Authority (NRPA) 2018) that affects especially the Pu-inventory.

The closed Oskarshamn 2 (O2) is a 638 MW(electric) BWR nuclear power plant and it has produced a total of 154 TWh of electricity (https://www.okg.se/oskarshamn-2). Thus, the thermal energy produced with an efficiency of 0.35 % is 440 TWh thermal. The 6.5 tonnes of spent fuel UO_2 in Halden has an average burnup of about, e.g., 50 GWd/tU so the total thermal energy produced is 6.5 t · 50 GWd/tU · 24 h/d = 7.8 TWh. To note that the effect of metallic uranium has not been evaluated as it has a total burnup of only 1/300 compared to UO_2.

Approach for decommissioning waste

Now the approach is to use the sum of the decommissioning inventories for Oskarshamn 2 in Table 4-8 in Larsson et al. (2013) multiplied by the ratio of produced thermal energies 7.8 TWh /440 TWh = 0.018, which is about the correlation to neutron bombardment of materials. Oskarshamn 2 (a light-water BWR) is a good example of a power plant for which there exist public data (Larsson et al. 2013). The Halden BWR is a heavy-water reactor and therefore, inventory estimates based on data from a light-water reactor need to be re-evaluated. Same kind of analyses of Ca-41 for Maine Yankee NPP leads to a similar scale of estimates for the radionuclide inventory. Ca-41 measurements (in Lee et al. (2021), 6 Bq/gram in concrete) and history of NPP (lifetime in MAINE2 ~330 TWh thermal). Multiplied by 7.8 TWh /330TWh and 6 Bq/gram in 500 tonnes of concrete, one gets a Ca-41 inventory of $7.1 \cdot 10^7$ Bq, which leads to about the same results as by using the Oskarshamn 2 data.

Reprocessing waste inventories from Himdalen with plutonium are not scaled.

Weaknesses of the approach

The neutron bombardment depends on the total burnup in the reactor. But the, e.g., Halden reactors geometry, materials and neutron spectre certainly differ from Oskarshamn 2 BWR. Therefore, it is recommendable that a detailed analysis of activation products is carried out in the future. A top expert on reactor physics in this topic should be involved, e.g., from the Finnish National Technology research centre (VTT). It would also be recommendable to do a spent fuel inventory evaluation in the future. (Link: https://www.vttresearch.com/en).

Regarding the comment about that waste from decommissioning hot cell and laboratories will differ from waste from decommissioning research reactors remarking that the former will have higher actinide and contamination-type radionuclide content, the proposed method does not affect it, as the actinide contents have been taken from Himdalen data (Norwegian Radiation Protection Authority (NRPA 2018). See also column B in the Excel file and text about this column below.

Reading the results in the Table II-1 with both operational and decommissioning waste:

In the Table II-1 (original Excel file = revisedinputHnord3CC.xlsx), a proposal for the LLW and ILW inventories to be used in the current generic safety case calculations is given:

- Column A: nuclide
- Column B: The estimated inventory for LLW. These values are modified from Table 7-4 in Almkvist & Gordon (2007, R-07-17, page 44), Table 7-4. These are values given in for the value for low level waste “BLA” divided by 100. The ratio of used UO_2 fuel masses in Norway and Sweden is 6.5/12,000 (tonnes of UO_2) = 1/1850. But as uncertainties exist, e.g., regarding the amount of waste from hospitals and laboratories, the division by 100 is chosen as a conservative approximation.
- Column C: Inventory for ILW. Sum of column E (operational waste based on Almkvist & Gordon 2007), column G (decommissioning waste based on Larsson et al. (2013)) and column F reprocessing waste at Himdalen (Norwegian Radiation Protection Authority (NRPA) 2018).

- Column E: Operational ILW waste. Modified from Table 7-4 in Almkvist & Gordon (2007; pages 44-45). ILW inventory is based on the total inventory in SFR scaled by the amount of waste (in column “total”) and multiplied by 10·6.5ton/12,000ton. The ratio of amounts of used spent fuel is multiplied by a factor of 10 to account for uncertainties. Halden HBWR is a test reactor and thus there might potentially be, e.g., leaching fuel rods leading to increase in ILW inventory. Inventory is estimated at year 2040.
- Column F: Reprocessing waste at Himdalen (Norwegian Radiation Protection Authority (NRPA) 2018).
- Column G: Decommissioning waste inventory. For decommissioning waste 20 years decay period is assumed. In Column I, inventory at closure of Oskarshamn 2 is given.
- Column I: Decommissioning waste inventory for Oskarshamn 2 at the time of closure. Data from Table 4-8 in Larsson et al. (2013) total multiplied by 7.8 TWh /440 TWh. This is the ratio of neutron bombardment of Halden and Oskarshamn 2.
- Column K: Half-lives.
- Column L: Decay time of nuclides in decommissioning waste in column I and the 20 years decayed inventories in column G.

Some observations:

- Ca-41 is only present in the decommissioning waste as there is none in SFR.
- Short lived H-3 from concrete has 12.6 times higher inventory in decommissioning waste. Very irrelevant short-lived Eu, Fe-55 and Co-60 isotopes are also dominating in decommissioning waste.
- The significant nuclides which have higher inventory in decommissioning waste are: Mo-93 (3.4 times), Nb-93m (2.3 times) and Ni-59 (1.02 times).

Mo-93 (T½ = 4000 yr) was safety relevant for SFR analyses (TR-14-01), but in decommissioning waste it is in stainless steel or INCONEL, so the release rate is slow and decays quite fast.

Table II-1. LLW and ILW inventory derived based on the Swedish low and intermediate level waste repository SFR data and the decommissioning waste from Oskarsharmn.

column	B	C	E	F	G	I	K	L
	SFR BLA /100	**SUM E and G**	**SFRtotal* 10*6.5/12 000**		**Oskars-hamn2**	**Oskars-hamn2deco*0.018**		**time**
	LLW	**ILW**	**year 2040**	**Himdalen**	**20 years decay time**	**1 year decay**	**T½**	**decay**
Nuclide	**(Bq)**	**(Bq)**	**(Bq)**	**(Bq)**	**(Bq)**	**(Bq)**	**(y)**	**(y)**
H-3*	1.50E+06	1.99E+10	1.46E+09	0.00E+00	1.85E+10	6.30E+10	1.13E+01	2.00E+01
Be-10	5.60E+01	4.55E+04	4.55E+04	0.00E+00	1.49E+01	1.49E+01	1.50E+06	2.00E+01
C-14 org	8.00E+07	6.50E+10	6.50E+10	0.00E+00	0.00E+00	0.00E+00	5.73E+03	2.00E+01
C-14 inorg	1.90E+08	2.06E+11	1.57E+11	0.00E+00	4.87E+10	4.89E+10	5.73E+03	2.00E+01
C-14 tot	2.70E+08	2.71E+11	2.22E+11	0.00E+00	4.87E+10	4.89E+10	5.73E+03	2.00E+01
Cl-36	7.20E+04	6.80E+07	5.09E+07	0.00E+00	1.71E+07	1.71E+07	3.00E+05	2.00E+01
Ca-41	0.00E+00	7.02E+07	0.00E+00	0.00E+00	7.02E+07	7.02E+07	1.00E+05	2.00E+01
Fe-55	2.90E+08	2.32E+12	8.13E+11	0.00E+00	1.51E+12	2.42E+14	2.73E+00	2.00E+01
Ni-59	3.70E+08	7.22E+11	3.58E+11	0.00E+00	3.64E+11	3.64E+11	7.60E+04	2.00E+01
Co-60	2.50E+09	6.26E+12	3.52E+12	6.60E+08	2.74E+12	3.80E+13	5.27E+00	2.00E+01
Ni-63	4.60E+10	7.83E+13	4.33E+13	0.00E+00	3.50E+13	4.02E+13	1.00E+02	2.00E+01
Se-79	3.40E+04	4.77E+07	4.77E+07	0.00E+00	7.20E+01	7.20E+01	3.27E+05	2.00E+01
Sr-90	3.30E+08	6.12E+11	4.82E+11	1.30E+11	1.23E+08	1.98E+08	2.90E+01	2.00E+01
Mo-93	1.40E+06	6.16E+08	1.41E+08	0.00E+00	4.75E+08	4.77E+08	4.00E+03	2.00E+01
Nb-93m	2.20E+07	6.86E+10	2.06E+10	0.00E+00	4.81E+10	1.14E+11	1.60E+01	2.00E+01
Zr-93	3.00E+05	8.67E+07	8.67E+07	0.00E+00	4.59E+03	4.59E+03	1.53E+06	2.00E+01
Nb-94	9.20E+05	1.19E+09	7.58E+08	0.00E+00	4.31E+08	4.32E+08	2.00E+04	2.00E+01
Tc-99	3.50E+07	1.58E+10	1.57E+10	0.00E+00	7.49E+07	7.49E+07	2.10E+05	2.00E+01
Ru-106	2.20E+02	5.96E+07	5.96E+07	0.00E+00	2.49E+02	7.38E+07	1.10E+00	2.00E+01
Pd-107	8.60E+03	1.19E+07	1.19E+07	0.00E+00	3.42E+01	3.42E+01	6.50E+06	2.00E+01
Ag-108m	2.90E+07	4.35E+09	4.33E+09	0.00E+00	1.22E+07	1.26E+07	4.38E+02	2.00E+01
Cd-113m	7.40E+05	1.30E+09	1.30E+09	0.00E+00	1.96E+04	5.25E+04	1.41E+01	2.00E+01
Sb-125	2.10E+07	8.67E+10	8.67E+10	0.00E+00	2.75E+07	4.40E+09	2.73E+00	2.00E+01
Sn-126	4.30E+03	5.96E+06	5.96E+06	0.00E+00	4.50E+02	4.50E+02	1.00E+05	2.00E+01
I-129	2.20E+04	3.79E+07	3.79E+07	0.00E+00	5.76E+01	5.76E+01	1.57E+07	2.00E+01
Ba-133	1.20E+05	1.21E+08	1.19E+08	0.00E+00	1.68E+06	6.30E+06	1.05E+01	2.00E+01
Cs-134	1.70E+06	3.63E+10	3.63E+10	0.00E+00	5.62E+05	4.69E+08	2.06E+00	2.00E+01
Cs-135	1.40E+05	1.95E+08	1.95E+08	0.00E+00	6.84E+02	6.84E+02	2.30E+06	2.00E+01
Cs-137	3.40E+09	5.23E+12	5.09E+12	1.40E+11	1.25E+08	1.98E+08	3.00E+01	2.00E+01
Pm-147	7.00E+06	7.04E+10	7.04E+10	0.00E+00	8.83E+05	1.75E+08	2.62E+00	2.00E+01
Sm-151	1.90E+07	2.67E+10	2.65E+10	0.00E+00	1.28E+08	1.50E+08	9.00E+01	2.00E+01
Eu-152	7.50E+07	1.81E+09	2.00E+08	0.00E+00	1.61E+09	4.50E+09	1.35E+01	2.00E+01
Eu-154	5.20E+07	1.03E+11	1.03E+11	0.00E+00	4.10E+07	2.06E+08	8.59E+00	2.00E+01
Eu-155	5.60E+06	2.28E+10	2.28E+10	0.00E+00	5.18E+06	9.52E+07	4.76E+00	2.00E+01
Ho-166m	1.20E+06	3.37E+08	3.36E+08	0.00E+00	1.57E+06	1.58E+06	1.20E+03	2.00E+01

column	B	C	E	F	G	I	K	L
	SFR BLA /100	**SUM E and G**	**SFRtotal* 10*6.5/12 000**		**Oskars-hamn2**	**Oskars-hamn2deco*0.018**		**time**
	LLW	**ILW**	**year 2040**	**Himdalen**	**20 years decay time**	**1 year decay**	**T½**	**decay**
Nuclide	**(Bq)**	**(Bq)**	**(Bq)**	**(Bq)**	**(Bq)**	**(Bq)**	**(y)**	**(y)**
U-232	4.10E+01	3.18E+04	2.82E+04	0.00E+00	3.68E+03	4.50E+03	6.89E+01	2.00E+01
U-234	2.10E+03	1.30E+06	1.30E+06	0.00E+00	0.00E+00	0.00E+00	2.45E+05	2.00E+01
U-235	3.00E+07	1.73E+07	1.73E+07	0.00E+00	0.00E+00	0.00E+00	7.00E+08	2.00E+01
U-236	6.20E+02	5.26E+05	5.25E+05	0.00E+00	8.28E+02	8.28E+02	2.30E+07	2.00E+01
Np-237	1.90E+03	5.96E+06	5.96E+06	0.00E+00	1.12E+03	1.12E+03	2.14E+06	2.00E+01
Pu-238	3.30E+06	5.02E+11	1.84E+09	5.00E+11	7.69E+06	9.00E+06	8.80E+01	2.00E+01
U-238	9.90E+07	2.24E+08	5.42E+07	1.70E+08	0.00E+00	0.00E+00	4.50E+09	2.00E+01
Pu-239	9.10E+05	3.14E+10	4.23E+08	3.10E+10	5.94E+04	5.94E+04	2.40E+04	2.00E+01
Pu-240	1.80E+06	1.21E+11	8.67E+08	1.20E+11	1.13E+04	1.13E+04	6.56E+03	2.00E+01
Pu-241	3.40E+07	1.60E+13	3.09E+10	1.60E+13	1.91E+06	5.04E+06	1.43E+01	2.00E+01
Am-241	3.50E+06	1.90E+10	1.90E+10	0.00E+00	1.53E+04	1.58E+04	4.32E+02	2.00E+01
Am-242m	1.70E+04	1.14E+07	1.14E+07	0.00E+00	1.79E+02	1.98E+02	1.41E+02	2.00E+01
Pu-242	6.20E+03	3.34E+08	3.95E+06	3.30E+08	1.44E+02	1.44E+02	3.73E+05	2.00E+01
Am-243	6.20E+04	4.12E+07	4.12E+07	0.00E+00	1.80E+03	1.80E+03	7.37E+03	2.00E+01
Cm-243	1.60E+04	1.08E+07	1.08E+07	0.00E+00	6.59E+02	1.06E+03	2.90E+01	2.00E+01
Cm-244	1.50E+06	3.79E+08	3.79E+08	0.00E+00	1.59E+05	3.42E+05	1.81E+01	2.00E+01
Cm-245	6.20E+02	3.95E+05	3.95E+05	0.00E+00	4.13E+01	4.14E+01	8.50E+03	2.00E+01
Cm-246	1.70E+02	1.03E+05	1.03E+05	0.00E+00	1.63E+01	1.64E+01	4.73E+03	2.00E+01
Tot	**5.30E+10**	**1.11E+14**	**5.42E+13**	**1.69E+13**	**3.98E+13**	**3.14E+14**	**1.00E+10**	**2.00E+01**

*HBWR in Halden is a heavy water reactor so the inventory of H-3 is relatively higher than in light water reactors. Thus the inventory of H-3 in above table should be re-evaluated.

References Appendix II

Almkvist, L. & Gordon, A. 2007. Low and intermediate level waste in SFR 1 Reference waste inventory 2007. Stockholm, Sweden: Svensk Kärnbränslehantering AB. R-07-17. 270 p.

Avila 2021. Technical Note Estimation of the Radionuclide Inventory for different decommissioning waste categories 21 August 2021- AFRY

IAEA 1993. Decontamination and decommissioning of nuclear facilities Results of a Co-ordinated Research Programme, Phase II: 1989-1993 Vienna, Austria: International Atomic Energy Agency. IAEA-TECDOC-716. 205 p.
Link: https://inis.iaea.org/collection/NCLCollectionStore/_Public/24/070/24070041.pdf

IAEA 1998. Radiological Characterization of Shut Down Nuclear Reactors for Decommissioning Purposes. Vienna, Austria: International Atomic Energy Agency. Technical Reports Series No. 389. 184 p. Link: https://www-pub.iaea.org/MTCD/publications/PDF/TRS389_scr.pdf

Larsson, H., Anunti, Å. & Edelborg, M. 2013. Decommissioning study of Oskarshamn NPP. Stockholm, Sweden: Svensk Kärnbränslehantering AB. R-13-04. 196 p.
Link: https://www.skb.com/publication/2625263/R-13-04.pdf

Lee, Y.-J., Lim, J.-M., Lee, J.-H., Hong, S.-B. & Kim, H. 2021 Analytical method for determination of 41Ca in radioactive concrete. Nuclear Engineering and Technology. Volume 53, Issue 4, pp 1210-1217. Link: https://www.sciencedirect.com/science/article/pii/S1738573320308822

MAINE2:
https://en.wikipedia.org/wiki/Maine_Yankee_Nuclear_Power_Plant

Norwegian Radiation Protection Authority (NRPA), 2018. Joint Convention on the Safety of Spent Fuel Management and on the Safety of Radioactive Waste Management National Report from Norway to the sixth review meeting, 21 May – 1 June 2018.
Link: https://www.iaea.org/sites/default/files/national_report_of_norway_for_the_6th_review_meeting_-_english.pdf

Appendix III – Brief overview of GoldSim simulation environment

III.1 Introduction

GoldSim is a flexible and powerful Windows-based computer program to carry out probabilistic simulations of complex systems to support management and decision-making in engineering, science and business. The program is highly graphical, highly extensible, able to directly represent uncertainty, and supports the creation of presentations of developed models to third parties.

The following paragraphs are excerpts from the handbooks for GoldSim computer code for probabilistic simulations [A1] and its expansion module for radionuclide transport [A2] and are only aimed to give an overview of the main software features and provide understanding for the description of the GoldSim model developed for this project. For more detailed explanations especially regarding the mathematical equations and formulas used within GoldSim, please refer to the respective GoldSim manuals, available from www.goldsim.com.

Although GoldSim is suited to solve a wide variety of complex problems, it is particularly well suited (and was originally developed) to support evaluation of existing or planned radioactive waste management facilities.

For such evaluations or performance of operational safety analyses the basic GoldSim software must be expanded by the GoldSim Radionuclide Transport (RT) Module, which includes specified features to facilitate simulation of radionuclide transport within a range of environmental media.

The RT module can accurately and efficiently model complex processes such as decay and ingrowth of reaction/decay products, solubility constraints, sorption onto porous media, release from engineered barriers, diffusive and advective transport, and transport of contaminants on particulates.

III.2 GoldSim general information

The software version used for simulating the long-term evolution of the NDF and to calculate the potential radiological consequences in the long-term is GoldSim, release 14.0 dating from October, 04, 2021. The handbooks for GoldSim computer code for probabilistic simulations [A1] and its expansion module for radionuclide transport [A2] give an overview of the main software features and provide understanding for the description of the GoldSim model developed for this project. For detailed explanations especially regarding the mathematical equations and formulas used within GoldSim, please refer to the respective GoldSim Manuals, generally available from www.goldsim.com.

The internationally accepted suitability of the GoldSim software is evident, confirmed by its development and use over a period of almost 25 years (see www.GoldSim.com). GoldSim has been used by and for a diverse set of customers and clients, including government agencies in over ten countries (such as the US Department of Energy, NASA, the Nuclear Regulatory Commission), research laboratories (including Sandia National Laboratories, Los Alamos National Laboratory, the Paul Scherrer Institute, and Massachusetts Institute of Technology), and commercial organizations worldwide. It has become a standard code for repository calculations.

It has also been used for respective purpose in various IAEA projects on safety assessments for radioactive waste repositories, e.g., [A3] and [A4].

Released versions of GoldSim are verified by the program developers. During verification, many test problems are executed and the results compared with expected values. Extensive documentation and user guides are available for the software. The following paragraphs quote the official statement of GoldSim Group regarding the quality assurance procedures followed during the further development of the software:

Overview of GoldSim Software Development Quality Assurance Procedures

GoldSim is developed and maintained according to a rigorous set of Software Configuration Management Procedures to ensure quality. These procedures include requirements for the following:

Source Code Revision Control: Each time a file (e.g., a source code module) is modified, a new revision (or version) of the file is created. Revision control provides a mechanism for saving and managing all the revisions of a file in an archive (i.e., a database), dating from the time the file was first entered into the revision control system.

Change Control and Tracking: Change tracking is the act of managing software problem reports and change requests submitted by users and/or members of the software development team. A problem report is associated with an apparent or actual defect (i.e., a bug) in the code or documentation. A change request is associated with a suggested modification or improvement to the software or documentation. A change tracking system is a database of all reported defects and requests. This database describes all changes made to the software.

Testing and Verification: All code modifications are thoroughly tested by the software development team. Prior to release of a new version, the program also undergoes an extensive set of verification tests to ensure that the changes work as intended and have not introduced any new problems. The tests are described in a Verification Plan, and the results of the verification are documented in a Verification Report.

Documentation: Throughout the process of addressing a modification to the source code, requirements and design specifications are produced (if the change is significant). Typically, the requirements and design evolve somewhat as the task is evaluated in more detail. As such, these documents (which may be formal documents or simply descriptions in the change tracking system), are temporary tools for communication, and cease to be used or referred to after the changes are made. The final requirements and design details are integrated into the User Documentation, which becomes the "as built" and definitive statement of the new functionality.

However, GoldSim is just a programming language, which allows the programming of well-working or less well-working models. It is, therefore, of importance that the user takes adequate QA/QC precautions to ensure that the developed model is simulating the evolution of the system in question in the intended way.

To that purpose, during model development a wide range of test runs is being carried out with artificial parameters that allow an easy control of intermediate results. GoldSim supports these kinds of scoping calculations by offering features like the possibility to switch off radioactive decay during the calculation to enable an easy control of radionuclide masses that are transported through the system. It also provides the possibility to view the time history of any of the parameters used in the model.

At the safety assessment group at BGE TECHNOLOGY there is a continuous discussion of intermediate results and internal review of the modules developed for the simulation of certain subsystems as well as a review of the completed model.

For more detailed explanations especially regarding the mathematical equations and formulas used within GoldSim, please refer to the respective GoldSim Manuals, generally available from https://www.goldsim.com/Web/Customers/Education/Documentation/.

III.3 Modelling contaminant transport using GoldSim – Basic concepts

The GoldSim Contaminant Transport Module is a mass transport model. A mass transport model is a mathematical representation of an actual system (e.g., the subsurface environment near a waste disposal site) which can be used to simulate (and hence predict) the release, transport (movement) and ultimate fate of mass within the system. The "mass" that is typically simulated is that of chemical contaminants that have been accidentally released or intentionally disposed of within the system.

Contaminant species: GoldSim allows simulating the transport of an unlimited number of species (types of chemical constituents) within an environmental system. The species can undergo complex user-specified chemical reactions as they are transported through the system. The species can be defined to behave independently or can be coupled by either being specified as part of a reaction (decay) chain or as isotopes of the same chemical element.

Modelling transport pathways: The GoldSim Contaminant Transport Module allows simulating the transport of mass through an environmental system by providing a number of specialized GoldSim elements. The most important of these is the ***transport pathway*** (of which there are several types):

Figure III-1. Transport pathway types used by GoldSim

Transport pathways represent physical components through which contaminant species can move and/or be stored, such as aquifers, lakes, sediments, surface soil compartments, and the atmosphere. The properties of the pathways, such as their geometry and which environmental media (e.g., water, soil, air) they contain are defined individually. All pathways contain one or more environmental media.

For each medium, the general properties (e.g., its density) are also defined individually as well as the properties of each species in each medium (e.g., solubility and partition coefficients).

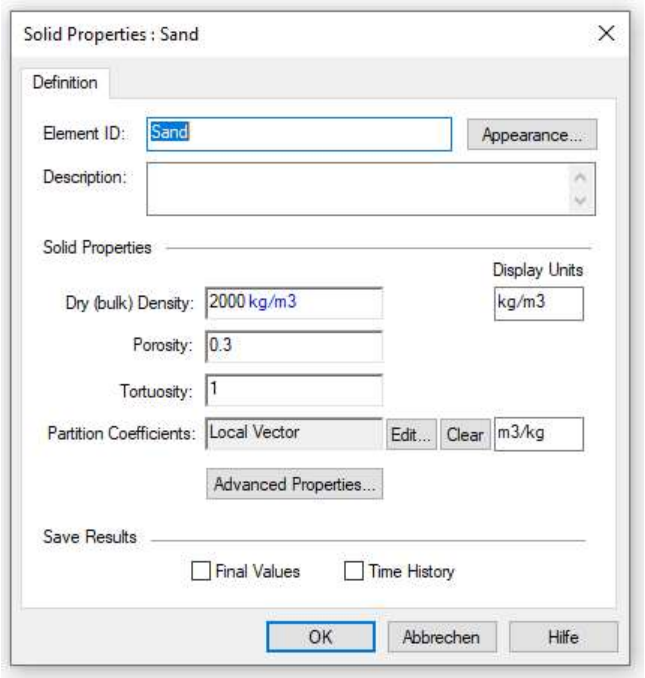

Figure III-2. User Interface for input of medium properties.

An environmental system is created by defining a network of transport pathways, as shown in Figure III-3. below.

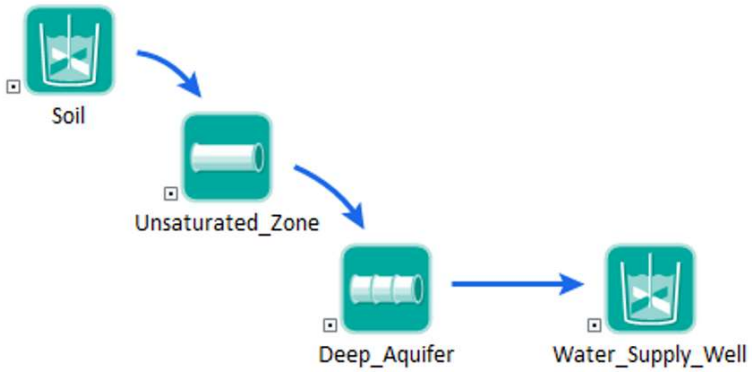

Figure III-3. Simple model of environmental pathway network.

To create such a network, individual pathways are connected via mass flux links. A mass flux link defines the mechanisms by which species move between pathways. It represents a vector by species (i.e., it has one item for each species), since the flux will differ for each species being simulated and has dimensions of mass/time.

Two major types of mass flux links and three special purpose mass flux links can be defined in GoldSim. In an advective mass flux link, a quantity of a medium is specified to flow from one pathway to another, carrying dissolved, sorbed, and/or suspended species with it. In a diffusive mass flux link, species diffuse between pathways according to a concentration gradient.

Three special purpose mass flux links allow modelling processes that cannot be represented as using advection or diffusion. In a direct transfer mass flux link, species are moved from one pathway to another based on a user-specified transfer rate. In a precipitate removal mass flux link, species present as precipitated mass are moved from one pathway to another based on a specified transfer rate. In a treatment mass flux link, species are treated or filtered and are moved to from one pathway to another based on a specified treatment efficiency (a fraction).

It must be noted that the Contaminant Transport Module is a mass transport model, not a flow model. That is, it does not directly solve for the movement of media through the environmental system being modelled. Hence, the media flow rates associated with an advective flux link must be entered directly.

Based on the properties of each pathway, the media in each pathway, the species, and the specified mass flux links, GoldSim computes the temporally varying concentrations in each pathway's media, as well as the mass fluxes between pathways. Hence, the fundamental output of a pathway element is a series of vectors:

- the mass (of each species) in the pathway,
- the concentration (of each species) within each environmental medium in the pathway; and
- the mass flux (of each species) to each of the pathways to which it is connected via mass flux links.

Modelling contaminant sources: Within GoldSim, there are two ways to introduce mass into the system:

- An initial mass or a rate of addition of mass can be directly specified for one or more pathways in the system; and
- When using the RT Module, the user can define the properties of one or more sources, and based on their properties, GoldSim will compute rates of release of mass from the source(s) to specified pathways.

Often, you can use the former method to introduce mass into your model. In many cases, however, direct specification of an initial mass or rate of release at various locations is not possible or appropriate, and explicit modelling of the source is necessary.

In this respect the definition of what is meant by a “source” is completely determined by the user. A “source” may represent an entire disposal facility, or a single buried drum. a group of leaking underground tanks or a complex engineered facility. The key point is that the source provides mass input to the pathways that then transport the mass through the system, as illustrated below.

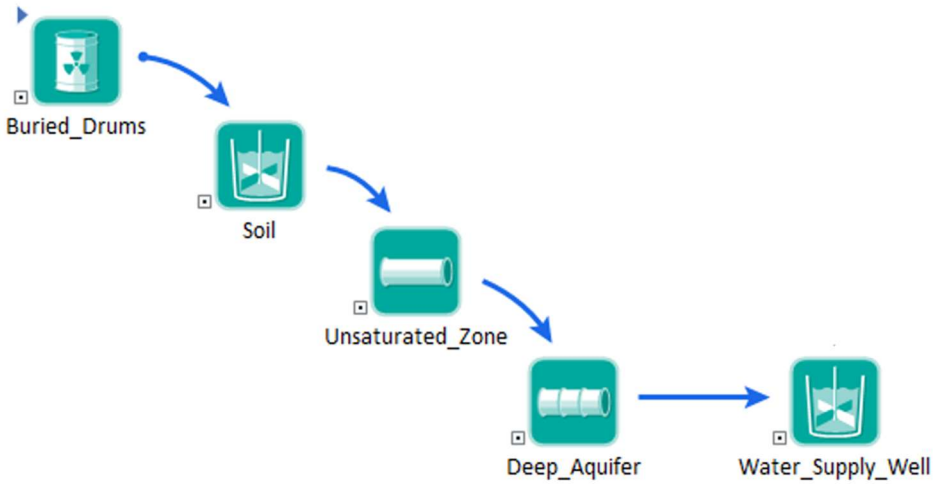

Figure III.4. Simple model of pathway network including a contaminant source.

The properties of a source define by the user consist of 1) the failure rate of any barriers (e.g., drums, boxes) which must fail before the species are released; and 2) the degradation rate of any matrix (e.g., cement, grout) in which the species are bound, which must degrade before the species are released.

Uncertainty in processes, parameters, and future events: One of the large advantages of GoldSim compared to other computer codes for simulating contaminant transport is its use of probabilistic elements. Uncertainty in processes and parameters can be represented by specifying model inputs as probabilistic distributions. The impact of uncertain events (e.g., earthquakes, floods, sabotage) can also be directly represented by specifying the occurrence rates and consequences of such “disruptive events”.

However, as useful as these capabilities are for assessing probabilistic effects and the correlation between certain model parameters and the resulting radiological impacts, the execution of deterministic calculations combined with a sensitivity analysis is of prime importance for safety assessments. Only deterministic calculations render comprehensible results with clearly defined boundary conditions which allow the investigation of the relative importance of individual parameters and independent review by third parties.

References Appendix III

[A1] GTG 2021a: “User's Guide: GoldSim - Probabilistic Simulation Environment”. Version 14.0 (October 2021) GoldSim Technology Group, Seattle, WA, USA. Available from: https://www.goldsim.com/Web/Customers/Education/Documentation/.

[A2] GTG 2021b: “User's Guide: GoldSim Contaminant Transport Module”. GoldSim Version 14.0 (October 2021) GoldSim Technology Group, Seattle, WA, USA. Available from: https://www.goldsim.com/Web/Customers/Education/Documentation/.

[A3] Neerdael, B., Finsterle, S., Chen, W., De Lemos, F., Hossain, S., Hwang, Y.-S., Ilie, P., Ionescu, A., Kang, C.-H., Mallants, D., Narayan, P., Poskas, P., Poskas, R., Rakesh, R., Seetharam, S., Shybetskyi, I., Sillen, X., Rui, S., Thomas, H. & Vardon, P. 2013. The use of numerical models in support of site characterization and performance assessment studies of geological repositories. Vienna, Austria: International Atomic energy Agency. IAEA-TECDOC-1717. 119 p. Link:

https://www.researchgate.net/publication/259923736_IAEA-TECDOC-1717_The_use_of_numerical_models_in_support_of_site_characterization_and_performance_assessment_studies_of_geological_repositories

[A4] IAEA. 2004. Safety Assessment Methodologies for Near Surface Disposal Facilities (ISAM) - Results of a co-ordinated research project - Vol.2: Test Cases". Vienna, Austria: International Atomic energy Agency. Link:

https://www.iaea.org/publications/6971/safety-assessment-methodologies-for-near-surface-disposal-facilities

Appendix IV – Acceptability of special waste packages (WPs)

The list of special WPs containing (un)sealed sources is in Table -1 (see also Table 2-4). It becomes apparent that the list is incomplete, especially regarding drum weights. Moreover, the line for WP with “Depleted uranium 210 litres (approx. 400 kg)” does not contain any radionuclides. For modelling purposes, relevant WPs, for which data were available, were selected for the analysis presented in Chapter 9. The respective lines are colour-coded (as in Figure 9-11) in the table and serially enumerated. Since several WPs only contained Ra-226, as a representative of these, the WP with the highest Ra-226 activity was selected (WP1) for the HI scenario.

- WP1: Lead containers with Ra-226 sources from Radium Hospital.
- WP2: Ra source used for calibration from Rikshospitalet.
- WP3: Probable Ra sources (needles), further description probable on drum. Reported to contain 240 mg Pu (9.6 GBq assuming Pu-239).
- WP4: Many Ra-226 sources. One strong source at 370 MBq. 2 packages under designation needles.
- WP5: Uranium, many smaller packages with various salts from various labs - external remediation.
- WP6: Industrial source from Hydro.
- WP7: Strong Co-60 source protected in depleted uranium and lead container total 185 kg.
- WP8: Coal on flint from NTNU, 2 Am-241 sources.

If a drum weight was not available, 300 kg were used as a conservative assumption. This rather low weight is conservative since a low weight will lead to a higher specific activity of the waste material. Consequently, the resulting radiological dose is higher.

The column with U, Pu, Fr as denomination for radionuclides is not precise enough to assign activities to a specific radionuclide. It was conservatively assumed that the corresponding activity belongs to U-238 since this radionuclide has shown to be directly relevant for the resulting doses in the reference scenario. Radioactive Fr isotopes, on the other hand, only have a half-life of several minutes and should not occur in the waste at the time of disposal.

Table IV-1: List of special WPs with radionuclide inventory and other attributes

					Nuclide; MBq	Ra-226	Co-60	Cs-137	Ba-133	Pu-239	Cm-244	U-238	U-234	U, Pu, Fr	Th-232	Th-228	Am-241
Contents of containers/barrels		Drum		Date	Emitter Type	α	β-	β-	E, C	α	α	α, SF	α	α	α, SF	α	α
Special Storage - all drums toppstopt (?)	Container ID	No	weight (kg)		Half-life (a)	1.60E+03	5.27E+00	3.01E+01	1.05E+01	2.44E+04	1.81E+01	4.47E+09	2.34E+05	*	1.41E+10	1.91E+00	4.33E+02
Lead containers with Ra-226 sources from Radium Hospital	4945	2410	850	14.11.1985		2.82E+04											
Ra source used for calibration from Rikshospitalet	4956	4112		19.06.2000		1.48E+02	1.33E+02	2.00E+00	3.70E+01								
Ra sources from different suppliers; FFITOX (Phillips radium standard), small sources from Sweden, higher school, CERBERUS	4957	2610	466	15.08.1996		2.46E+02											

					Nuclide; MBq	Ra-226	Co-60	Cs-137	Ba-133	Pu-239	Cm-244	U-238	U-234	U, Pu, Fr	Th-232	Th-228	Am-241
Contents of containers/barrels		Drum		Date	Emitter Type	α	β-	β-	E, C	α	α	α, SF	α	α	α, SF	α	α
(smoke detector)																	
Probable Ra sources (needles), further description probable on drum	4958	3251	240	07.03.2001		1.11E+03											
Probable Ra sources (needles), further description probable on drum	4959	4083	320	09.12.1999		2.55E+03											
Probable Ra sources (needles), further description probable on drum. Reported to contain 240 mg Pu (9.6 GBq	4960	2409		12.06.1997		143E+03				9.60E+03							

					Nuclide; MBq	Ra-226	Co-60	Cs-137	Ba-133	Pu-239	Cm-244	U-238	U-234	U, Pu, Fr	Th-232	Th-228	Am-241
Contents of containers/barrels		Drum		Date	Emitter Type	α	β-	β-	E, C	α	α	α, SF	α	α	α, SF	α	α
assuming Pu-239)																	
Stored for Algeta/Bayer by Harald Dugstad. De probably want to get rid of this source	5114	45 12		30.05. 2007		1.11E +02											
PONDEN (Warehouse 2 from 15 August)																	
Many Ra-226 sources. One strong source at 370 MBq. 2 packages under designation needles		26 56				3.89E +02	4.00E +00	4.00E +00		3.00E +00							
Uranium, many smaller packages with various salts from various labs - external remediation		43 64										1.92E +02	4.00E +00	1.35E +02	1.08E +03	2.00E +00	

					Nuclide; MBq	Ra-226	Co-60	Cs-137	Ba-133	Pu-239	Cm-244	U-238	U-234	U, Pu, Fr	Th-232	Th-228	Am-241
Contents of containers/barrels		Drum		Date	Emitter Type	α	β-	β-	E, C	α	α	α, SF	α	α	α, SF	α	α
Industrial source from Hydro		4364		31.12.1984							1.85E+04						
Depleted uranium 210 litres (approx 400 kg)		4892															
Strong Co-60 source protected in depleted uranium and lead container total 185 kg		7076		16.07.2013			1.00E+05										
Coal on flint from NTNU, 2 Am-241 sources		7114		18.03.2014													7.40E+03

Assessment of acceptability of the waste(s)

The assessment of acceptability of the special waste was carried out in two ways: First, a general assessment of whether the additional waste belongs to the ILW category and can be disposed of in its respective facility. The second step was the assessment of the radiological impact of the special waste if disposed in the ILW chamber of the LILW facility.

The general assessment is based on IAEA (2005a), which allows to assign so-called D-values to the occurring radionuclides. These can be summed up for all WPs to estimate the radiological hazard of each one (Table IV-2). All WPs result in category 4 or 5, except for WP7. However, the activity in WP7 is exclusively caused by Co-60, which has a half-life of ca. 5 years. It is, therefore, reasonable to assume that the waste in WP7 will have sufficiently decayed until disposal to be at least in category 4. For category 4, IAEA (2005a) states that being close to such an individual source is "unlikely to be dangerous to a person". For category 5, this assessment changes to "most unlikely".

In addition, IAEA (2005b) allows a visual estimation of waste categories for radioactive sources depending on their half-life and the source strength (Figure IV-1) Integrating the range for both attributes of all sources in the special waste results in the red rectangle. As a result, increased depth and enhanced engineering are required to contain the waste. To require as a significant depth as for high level waste, the overall activities remain too low.

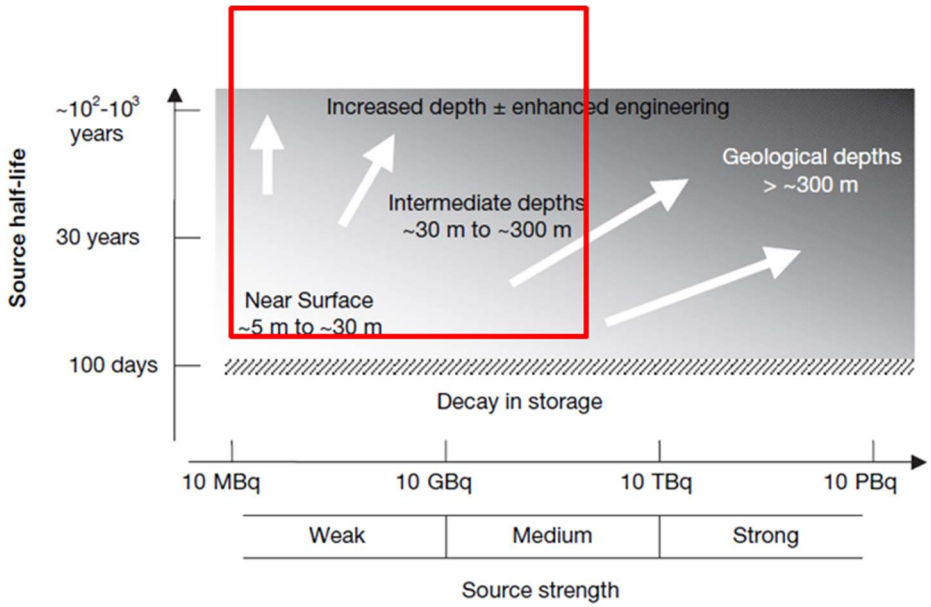

Figure IV-1. Graph to classify radioactive waste based on half-life and activity (IAEA 2005b)

As a preliminary result, the special waste seems to be acceptable in an underground ILW facility with EBS.

Table IV-2: Calculation of D-values for all WPs and resulting category (is assumed to have decayed to 4 by now)*

WP-ID		Nuclide; A/D-value	Ra-226	Co-60	Cs-137	Ba-133	Pu-239	Cm-244	U-238	U-234	U, Pu, Fr	Th-232	Th-228	Am-241	Sum for WP	Category
	Date	Emitter Type	α	β-	β-	E, C	α	α	α, SF	α	α	α, SF	α	α		
		Half-life (a)	1.60E+03	5.27E+00	3.01E+01	1.05E+01	2.44E+04	1.81E+01	4.47E+09	2.34E+05	*	1.41E+10	1.91E+00	4.33E+02		
4945	14.11.1985		7.05E-01												7.05E-01	4
4956	19.06.2000		3.70E-03	4.43E-03	2.00E-05	1.85E-04									8.34E-03	5
4957	15.08.1996		6.15E-03												6.15E-03	5
4958	07.03.2001		2.78E-02												2.78E-02	4
4959	09.12.1999		6.38E-02												6.38E-02	4
4960	12.06.1997		3.58E+00				1.60E-01								3.74E+00	4
5114	30.05.2007		2.78E-03												2.78E-03	5
AX1			9.73E-03	1.33E-04	4.00E-05		5.00E-05								9.95E-03	5
AX2											2.25 E-03		?		2.25E-03	5
AX3	31.12.1984							3.70E-01							3.70E-01	4
AX4																-
AX5	16.07.2013			3.33E+00											3.33E+00	3*
AX6	18.03.2014													1.23E-01	1.23E-01	4

The potential radiological impact of the special WPs was investigated in two different scenarios.

The first scenario was the HI scenario as part of Chapter 9 in this report. This choice was made as a conservative assumption for human intrusion. Since the specific activity of the special WPs is generally higher than that of the initial ILW waste inventory, choosing the special WPs as those compromised by human intrusion leads to higher radiological results (Section 9.3.3) than selecting a WP from the initial waste inventory. In this scenario, WPs were investigated individually.

The second scenario assumes that the waste inventory from the special waste is emplaced into the ILW vault in addition to the other ILW waste. The number of WPs, the vault volume and corresponding attributes like concrete volume and vault size were adjusted. The sum of activity per radionuclide from the special waste was added to the ILW inventory. Apart from these adjustments, the reference case was applied. The addition to the inventory vector by the special WPs is shown in Table IV-3.

Table IV-3: Inventory vector for special waste added to ILW inventory (activity for "U, Pu, Fr" is included in U-238)*

Radionuclide	MBq
Ra-226	1.76E+05
Co-60	1.00E+05
Cs-137	6.00E+00
Ba-133	3.70E+01
Pu-239	9.60E+03
Cm-244	1.85E+04
U-238	3.27E+02
U-234	4.00E+00
U, Pu, Fr*	1.35E+02
Th-232	1.08E+03
Th-228	2.00E+00
Am-241	7.40E+03

Radiological impact from special WPs

The radiological impact from the Human Intrusion Scenario was demonstrated in Section 9.3.3. The results from the reference case including the special waste inventory from Table IV-3 in the ILW inventory vector are shown in Figure IV-2.

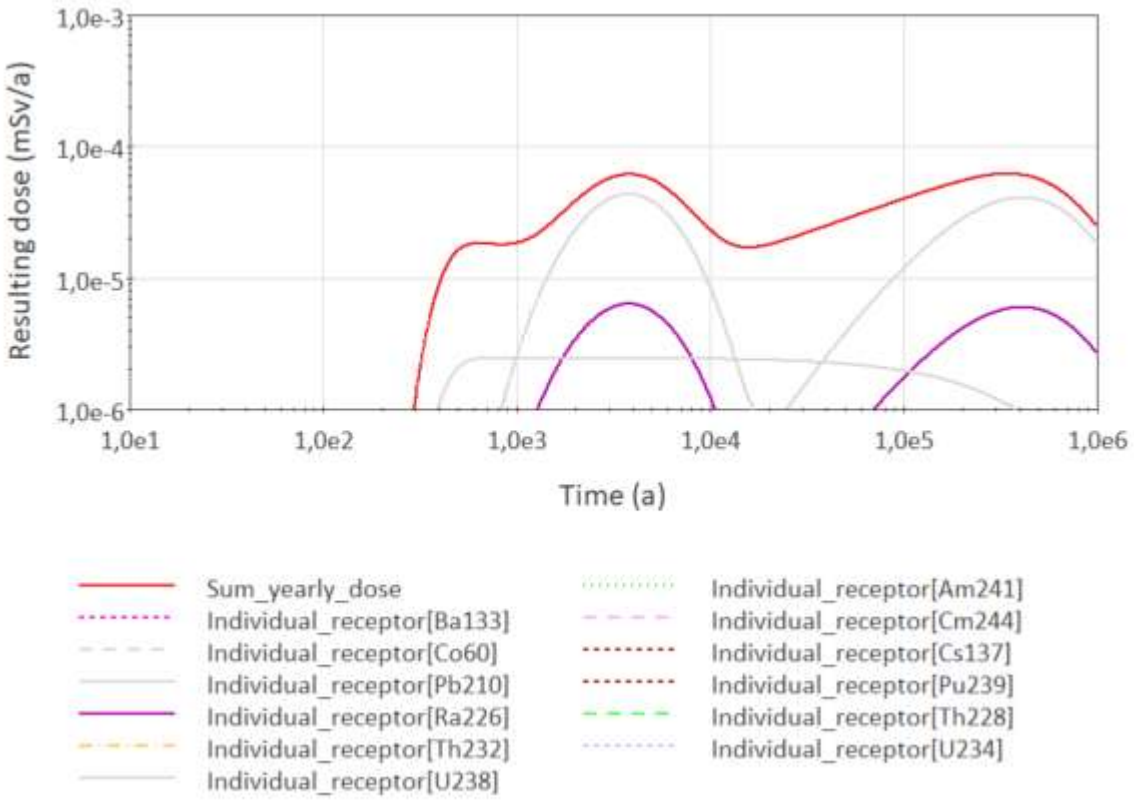

Figure IV-2. Resulting annual dose for individual and with radionuclides from special waste.

Compared to the reference scenario, the maximum peak is only 1.3% higher and comes 3,833 years later. The most notable difference, though, is the occurrence of a second peak at around 3,800 years after closure, which is dominated by the additional Ra-226 and its decay product, Pb-210.

Conclusions

As to the acceptability of the special waste for the LILW disposal facility, the radiological impact on the resulting annual dose is of primary concern. Including the respective waste inventory in the reference case does not lead to a significantly higher total dose. However, a second peak of similar magnitude occurs as soon as 3,800 years after closure. Due to the general low level of resulting annual doses, this is not generally problematic. For future updates of the safety assessment and repository design, this additional peak needs to be checked.

Regarding the HI Scenario, drilling into WP3 results in critical doses. As a countermeasure, several measures could be taken to reduce the probability of this scenario to occur even further or to reduce the specific activity. For instance, the WP could be emplaced in the lowest level inside the ILW vault. In that way, core samples or borehole cuttings from the area above would indicate to the drilling crew that some kind of man-made technical construction has been hit to alert their risk awareness. Reconditioning of the waste into several waste packages could reduce the specific activity and thereby the severeness of potential radiological exposure should part of the material be retrieved through drilling operations.

References in Appendix IV

IAEA 2005a. Categorization of Radioactive Sources. Safety Guide No. RS-G-1.9, Publication 1227, Vienna, 2005.

IAEA 2005b. Disposal options for disused radioactive sources. IAEA Technical reports series no. 436, Vienna, 2005.

Appendix V – Input data DBD GoldSim model

V.1 Normal evolution scenario Sc-1

The list of parameters below contains all parameters that have been used for the deterministic calculations presented in this report. The associated GoldSim model contains a number of additional parameters that could be used for probabilistic calculations, or which simplify the change of parameters for calculation cases or sensitivity calculations. These parameters have not been included in the tables below.

Material properties

Aquifer properties				
Name of Parameter	Value	Unit	Description	Source
Aquifer_Porosity_mean	10	%	Porosity of aquifer	Model assumption for aquifer (or fracture zone) near to surface
Aquifer_Density_Intrinsic	2800	kg/m³	Intrinsic density of crystalline rock	Typical value for crystalline rock, compare Clayton et al. (2011)
Aquifer_Saturation	100	%	Water saturation of aquifer	Expected value in aquifer
Aquifer_Tortuosity	1		Tortuosity of aquifer pathway	Conservative assumption
Kd_Vector_Aquifer	0	m³/kg	Partition coefficient for aquifer	Conservatively set to zero m³/kg
Zero_kd	0	m³/kg	Zero vector for partition coefficient	

Backfill properties				
Name of Parameter	Value	Unit	Description	Source
Backfill_Porosity_mean	30	%	Porosity of backfill in borehole backfill zone	Educated guess
Backfill _Density_Intrinsic	2800	kg/m³	Intrinsic density of crystalline rock (fractured for backfilling)	Typical value for crystalline rock, compare Clayton et al. (2011)
Backfill _Saturation	100	%	Water saturation of backfill in upper borehole zone	Expected value in water filled borehole
Backfill _Tortuosity	1		Tortuosity of backfill for calculation of diffusion	Conservative assumption

Backfill properties				
Name of Parameter	Value	Unit	Description	Source
Kd_Vector_Backfill	See extra Table below	m³/kg	Partition coefficient for backfill in upper borehole zone	See extra Table below

Bentonite buffer properties				
Name of Parameter	Value	Unit	Description	Source
Buffer_Porosity_mean	50	%	Achievable porosity of bentonite in bentonite buffer	Educated guess
Buffer_Density_Intrinsic	2500	kg/m³	Intrinsic density of bentonite	Typical value for bentonite, compare Ahonen et al. (2008)
Buffer_Saturation	100	%	Water saturation of buffer around canisters	Expected value in water filled borehole
Buffer_Tortuosity	1		Tortuosity of buffer for calculation of diffusion	Conservative assumption
Kd_Vector_Bentonite	See extra Table below	m³/kg	Partition coefficient for bentonite	See extra Table below

EDZ properties				
Name of Parameter	Value	Unit	Description	Source
EDZ_Porosity_mean	4.5	%	Porosity of EDZ	Model assumption for EDZ (or fracture zone) . (Porosity probably too high, see porosity of fractured rock below)
EDZ_Density_Intrinsic	2800	kg/m³	Intrinsic density of crystalline rock	Typical value for crystalline rock, compare Clayton et al. (2011)
EDZ_Saturation	100	%	Water saturation of EDZ	Expected value in EDZ
EDZ_Tortuosity	1		Tortuosity of EDZ pathway	Conservative assumption
Kd_Vector_EDZ	0	m³/kg	Partition coefficient for EDZ	Conservatively set to zero m³/kg
EDZ_Thickness	0.35	m	Thickness of EDZ around borehole	Conservatively chosen according to Engelhardt & Fischer, 2021*

*EDZ parameters were chosen very pessimistically, thickness of seriously affected EDZ probably significantly smaller (few centimetres) and porosity probably similar to expected porosity of host rock (1% or less)

Fractured Rock properties				
Name of Parameter	Value	Unit	Description	Source
Frac_Rock_Porosity_mean	0.2	%	Porosity of fractured rock	Model assumption (see SKB, 2010
Frac_Rock_Density_Intrinsic	2800	kg/m³	Intrinsic density of crystalline rock	Typical value for crystalline rock, compare Clayton et al. (2011)
Frac_Rock_Saturation	100	%	Water saturation of fractured rock	Expected value in fractured rock
Frac_Rock_Tortuosity	1		Tortuosity of fractured rock pathway	Conservative assumption
Kd_Vector_Frac_Rock	0	m³/kg	Partition coefficient for fractured rock	Conservatively set to zero m³/kg

Sealing Bentonite properties				
Name of Parameter	Value	Unit	Description	Source
Sealing_Porosity_mean	35	%	Porosity of sealing	Educated guess
Sealing_Density_Intrinsic	2500	kg/m³	Intrinsic density of bentonite	Typical value for bentonite, compare Ahonen et al. (2008)
Sealing_Saturation	100	%	Water saturation of sealing	Expected value in sealing
Sealing_Tortuosity	1		Tortuosity of sealing pathway	Conservative assumption
Kd_Vector_Sealing	See extra Table below	m³/kg	Partition coefficient for bentonite	See extra Table below

Kd-values for bentonite in the disposal and sealing zones and backfill

There are a number of sources for kd-values from safety assessment documentations of other geological disposal projects in granite or other crystalline environment, which are partly based on detailed site-specific investigations. For this generic safety assessment, data for the planned deep borehole disposal have been chosen from Freeze et al. (2013).

This source has been chosen because their generic safety assessment for different disposal concepts gives specific values for a deep borehole facility. The authors have specifically adjusted kd-values from other sources to the expected conditions in a deep borehole. It is, therefore, assumed that these data will be best suited for the assessment of the planned Norwegian facility, and they have been taken for the bentonite in the disposal zone and the sealing zone.

The values for the backfill have been also taken from Freeze et al. (2013) from their model for a geological disposal facility in crystalline, because their deep borehole concept expected crushed sediments as backfill material, while we expect crushed crystalline rock.

Deterministic kd-values used for bentonite and backfill			
Element	Bentonite disposal zone (high saline)	Bentonite sealing zone (low saline)	Backfill
	mL/g	**mL/g**	**mL/g**
Actinum	1.07E+02	6.35E+03	2.49E+03
Silver*			
Americium	1.07E+02	6.35E+03	2.49E+03
Carbon	3.00E-01	5.00E+00	1.10E+00
Chlorine	0.00E+00	0.00E+00	0.00E+00
Curium	1.07E+02	6.35E+03	2.49E+03
Cesium	2.25E+01	4.15E+02	3.91E+01
Iodine	0.00E+00	0.00E+00	0.00E+00
Molybdenum*			
Niobium	1.00E+00	1.00E+01	1.40E+03
Nickel*			
Neptunium	8.03E+01	2.77E+02	3.91E+03
Protactinium	8.03E+01	2.77E+02	1.95E+03
Lead	0.00E+00	0.00E+00	0.00E+00
Palladium	1.00E+00	8.50E+00	1.25E+01
Plutonium	8.03E+01	3.53E+03	3.91E+03
Radium	1.70E+00	7.21E+02	3.91E+01
Selenium	3.50E-01	1.20E+01	2.00E+00
Samarium*			
Tin	6.00E+00	3.25E+01	1.60E-01
Strontium	1.70E+00	7.21E+02	3.90E-01
Technetium	1.70E+00	4.51E+01	1.17E+03
Thorium	9.71E+01	3.96E+03	3.91E+03
Uranium	7.01E+01	3.78E+02	3.91E+03
Zirconium	9.71E+01	1.25E+03	1.40E+03

* Elements marked in light blue: No values were given in Freeze et al. (2013). For model calculations, kd-values for these elements have been set to 0 mL/g.

Water properties				
Name of Parameter	Value	Unit	Description	Source
RefDiffusivity_Water	1.0 E-09	m²/s	Reference molecular diffusivity	Standard value chosen for modelling purposes. Ion-specific values range typically from 5E-10 to 2E-9 m²/s for 25 °C (see e.g. Schwartz & Zhang, 2003).

Water properties				
Name of Parameter	Value	Unit	Description	Source
Solubility	See extra Table below	mg/L	Solubility limit for elements	See extra Table below

Solubility limits for disposal and sealing zone

The values for solubility limits for the different elements have also been taken from Freeze et al. (2013), for the same reasons as mentioned in relation to the kd-values, as they have been adjusted to expected conditions in deep boreholes.

Although under other environmental conditions, solubility limits are expected to change, the same values have been kept also for other parts of the model like the backfilling zone. The reason is that outside of the disposal zone concentration of radionuclides decrease very fast so that solubility limits do not play any role for the further transport calculations. Accordingly, for simplification of the model, the solubility limits have not been changed for other areas of the deep borehole model.

Solubility limits for brine and deep borehole conditions *	
Element	Bentonite disposal zone (high saline)
	mg/L
Actinum	1.48E-03
Silver**	-1.00E+00
Americium	4.12E-03
Carbon	-1.00E+00
Chlorine	1.51E+05
Curium	1.59E-03
Cesium	-1.00E+00
Iodine	-1.00E+00
Molybdenum**	-1.00E+00
Niobium	1.49E+00
Nickel**	-1.00E+00
Neptunium	6.70E-01
Protactinium	4.39E-01
Lead**	-1.00E+00
Palladium	4.28E+01
Plutonium	3.56E-08
Radium	-1.00E+00
Selenium	1.58E+00
Samarium**	-1.00E+00
Tin	4.53E-03
Strontium	-1.00E+00
Technetium	3.20E-03
Thorium	9.19E-03

Solubility limits for brine and deep borehole conditions *	
Element	Bentonite disposal zone (high saline)
	mg/L
Uranium	2.81E-07
Zirconium	9.30E-06

* If solubility is unlimited, for GoldSim, the maximum solubility must be set to -1.

** Elements marked in light blue: No values were given in Freeze et al. (2013). For model calculations, no solubility limits have been defined for these elements.

V.2 Source term and near field

The following table lists all radionuclides included in the long-term calculations. Alpha-emitting radionuclides have been colour-coded in light blue.

Short-lived progeny of radionuclides listed below are considered to exist in secular equilibrium in the waste. Their presence is considered by using dose coefficients for the parent radionuclides, which include the effect of the short-lived progeny.

Radionuclide vector for DBD GoldSim model		
Radio-nuclide	Half-life (a)	Daughter radionuclides
Ac227	2.18E+01	
Ag108m	1.27E+02	
Am241	4.32E+02	Np237 – 82.7%, Pu-242 – 17.3%
Am242m	1.41E+02	Pu238
Am243	7.37E+03	Pu239
C14	5.73E+03	
Cl36	3.01E+05	
Cm245	8.50E+03	Pu241
Cm246	4.73E+03	Pu242
Cs135	2.30E+06	
Cs137	3.01E+01	
I129	1.57E+07	
Mo93	4.00E+03	Nb93m
Nb93m	1.61E+01	
Nb94	2.03E+04	
Ni59	7.50E+04	
Ni63	1.00E+02	
Np237	2.14E+06	U233
Pa231	3.28E+04	Ac227
Pb210	2.23E+01	
Pd107	6.50E+06	
Pu238	8.77E+01	U234
Pu239	2.41E+04	U235

Radionuclide vector for DBD GoldSim model		
Radio-nuclide	Half-life (a)	Daughter radionuclides
Pu240	6.56E+03	U236
Pu241	1.44E+01	Am241
Pu242	3.76E+05	U238
Ra226	1.60E+06	Pb210
Ra228	5.75E+00	Th228
Se79	1.13E+06	
Sm151	9.00E+01	
Sn126	1.00E+05	
Sr90	2.88E+01	
Tc99	2.11E+05	
Th228	1.91E+00	
Th229	7.34E+03	
Th230	7.54E+04	Ra226
Th232	1.41E+10	Ra228
U233	1.59E+05	Th229
U234	2.45E+05	Th230
U235	7.04E+08	Pa231
U236	2.34E+07	Th232
U238	4.47E+09	U234
Zr93	1.53E+06	Nb93m

Inventory

For the Normal Evolution Scenario, the inventory of the different waste streams expected to be disposed of in the deep borehole have been taken according to the methodology in Appendix I and presented in Chapter 2.

In general, waste canisters are expected to contain either metallic uranium spent fuel or a mixture of UO_2 SNF, zircalloy waste, other metals. A certain part of the UO_2 SNF is expected to be instantaneously released from the waste form.

For the model calculations, it has been assumed that the canisters will contain either metallic uranium SNF or an equally distributed mixture of the other three waste forms. The total inventory listed in the table below is expected to be conditioned in 52 canisters with metallic uranium SNF and 36 canisters with UO_2 SNF, zircalloy and other metal waste. For simplicity, the latter group is referred as "UO_2 SNF" canisters.

Estimated inventory of waste to be disposed of in the deep borehole					
Species ID	Expected Inventory Metallic U	Expected Inventory UO_2	Expected Inventory Zircalloy	Expected Inventory other Metal	IRF part of Inventory UO_2
	Bq	**Bq**	**Bq**	**Bq**	**Bq**
Ac227	0.00E+00	5.20E+06	0.00E+00	0.00E+00	0.00E+00
Ag108m	2.10E+04	1.70E+07	0.00E+00	0.00E+00	0.00E+00

Estimated inventory of waste to be disposed of in the deep borehole					
Species ID	Expected Inventory Metallic U	Expected Inventory UO_2	Expected Inventory Zircalloy	Expected Inventory other Metal	IRF part of Inventory UO_2
	Bq	**Bq**	**Bq**	**Bq**	**Bq**
Am241	0.00E+00	6.90E+14	0.00E+00	0.00E+00	0.00E+00
Am242m	0.00E+00	1.40E+12	0.00E+00	0.00E+00	0.00E+00
Am243	0.00E+00	1.00E+13	0.00E+00	0.00E+00	0.00E+00
C14	1.80E+09	5.80E+11	3.02E+11	1.80E+11	6.65E+10
Cl36	2.10E+08	5.80E+10	1.29E+10	7.46E+08	1.03E+10
Cm245	0.00E+00	3.50E+11	0.00E+00	0.00E+00	0.00E+00
Cm246	0.00E+00	2.30E+11	0.00E+00	0.00E+00	0.00E+00
Cs135	6.70E+08	1.40E+11	0.00E+00	0.00E+00	4.33E+09
Cs137	6.50E+13	1.40E+16	0.00E+00	0.00E+00	4.33E+14
I129	3.10E+07	8.30E+09	3.47E-04	0.00E+00	4.37E+08
Mo93	3.00E+01	1.40E+05	8.33E+08	1.10E+10	4.20E+01
Nb93m	1.80E+09	4.00E+11	5.10E+10	8.28E+09	0.00E+00
Nb94	1.30E+05	5.30E+07	1.68E+12	1.64E+11	0.00E+00
Ni59	5.00E+07	1.10E+10	1.48E+10	4.08E+11	2.52E+10
Ni63	5.10E+09	1.30E+11	1.83E+11	4.95E+12	2.90E+11
Np237	0.00E+00	8.40E+10	0.00E+00	0.00E+00	0.00E+00
Pa231	1.90E+05	9.90E+06	0.00E+00	0.00E+00	0.00E+00
Pb210	0.00E+00	2.30E+05	0.00E+00	0.00E+00	0.00E+00
Pd107	5.20E+07	3.60E+10	0.00E+00	0.00E+00	0.00E+00
Pu238	0.00E+00	8.10E+14	0.00E+00	0.00E+00	0.00E+00
Pu239	1.60E+12	6.80E+13	0.00E+00	0.00E+00	0.00E+00
Pu240	2.10E+11	1.20E+14	0.00E+00	0.00E+00	0.00E+00
Pu241	4.30E+12	5.00E+15	0.00E+00	0.00E+00	0.00E+00
Pu242	0.00E+00	7.30E+11	0.00E+00	0.00E+00	0.00E+00
Ra226	0.00E+00	8.10E+05	0.00E+00	0.00E+00	0.00E+00
Ra228	0.00E+00	2.90E+01	0.00E+00	0.00E+00	0.00E+00
Se79	8.10E+07	2.00E+10	0.00E+00	0.00E+00	6.02E+07
Sm151	7.70E+11	6.90E+13	0.00E+00	0.00E+00	0.00E+00
Sn126	2.50E+08	1.40E+11	7.85E+04	0.00E+00	1.40E+08
Sr90	5.50E+13	9.00E+15	5.75E+09	2.62E+03	1.80E+13
Tc99	1.80E+10	3.70E+12	1.32E+08	1.59E+09	1.11E+09
Th228	0.00E+00	0.00E+00	0.00E+00	0.00E+00	0.00E+00
Th229	0.00E+00	1.20E+05	0.00E+00	0.00E+00	0.00E+00
Th230	0.00E+00	1.10E+08	0.00E+00	0.00E+00	0.00E+00
Th232	0.00E+00	1.20E+02	0.00E+00	0.00E+00	0.00E+00
U233	0.00E+00	1.70E+07	0.00E+00	0.00E+00	0.00E+00
U234	1.20E+11	5.90E+11	0.00E+00	0.00E+00	0.00E+00
U235	5.70E+09	7.60E+09	0.00E+00	0.00E+00	0.00E+00

Estimated inventory of waste to be disposed of in the deep borehole					
Species ID	Expected Inventory Metallic U	Expected Inventory UO_2	Expected Inventory Zircalloy	Expected Inventory other Metal	IRF part of Inventory UO_2
	Bq	**Bq**	**Bq**	**Bq**	**Bq**
U236	0.00E+00	6.70E+10	0.00E+00	0.00E+00	0.00E+00
U238	1.20E+11	8.00E+10	0.00E+00	0.00E+00	0.00E+00
Zr93	2.50E+09	5.10E+11	6.53E+10	6.43E+05	0.00E+00
Total	**1.27E+14**	**2.98E+16**	**2.32E+12**	**5.73E+12**	**4.51E+14**
Total alpha	**2.06E+12**	**1.70E+15**	**0.00E+00**	**0.00E+00**	**0.00E+00**

Waste parameters

Waste Parameters				
Name of Parameter	Value	Unit	Description	Source
Waste_Density	8000	kg/m³	Assumed density of waste	Estimate, based on effective density of fuel (10-11,000 kg/m³)) and additional material for positioning of material inside canister.
Metallic_U_SF_Waste	10000	kg	Total mass of metallic uranium SNF	Nordman, 2021
UO2_SF_Waste	6500	kg	Total mass of UO_2 SNF	dito
Metallic_U_Fract_Release	1 E-02	1/a	Fractional release factor for metallic uranium SNF	dito
UO2_Fract_Release	2 E-05	1/a	Fractional release factor for UO_2 SNF	dito
Zircalloy_Fract_Release	4 E-05	1/a	Fractional release factor for Zircalloy	dito
Other_Met_Fract_Release	1 E-03	1/a	Fractional release factor for other metal waste	dito

Waste package/Canister properties

Below the properties of the canisters are listed that are foreseen to be used for borehole disposal. Within this report and the associated GoldSim model, they are also referred to as waste packages (WP).

WP Parameters				
Name of Parameter	Value	Unit	Description	Source
WP_Weight_Empty	4600	kg	Weight of empty WP	Conceptual Design*

WP Parameters				
Name of Parameter	Value	Unit	Description	Source
Initial_Water_WP	25	L	Initial volume of water inside WP	Model parameter - no influence on corrosion etc. required to reduce percentual increase of water inside exposed waste cell
WP_Waste_Percentage	35	%	Assumption on waste volume inside canister.	Based on assumed density of waste and maximum load of 1600 kg
WP_Diameter_Inner	0.44	m	Inner diameter of WP	Conceptual Design*
WP_Diameter_Outer	0.60	m	Outer diameter of WP	dito
WP_Length_Inner	3.67	m	Inner length of WP	dito
WP_Length_Outer	4.23	m	Outer length of WP	dito
WP_Wall_Thickness	0.08	m	Thickness of WP wall	dito
WP_Wall_Thickness_min	0.05	m	Minimum thickness of WP wall to withstand in situ pressure	dito
WP_total_Number	88		Total number of WPs	dito
WP_Number_per_Cell	4		Number of WPs modelled as one disposal zone segment	Model parameter to restrict calculation steps within model
WP_Corrosion_Rate_planar	1 E-06	m/a	Rate of planar corrosion for stainless steel of WP	dito
WP_Failure_Period	200	a	Assumed period during which waste inside source cell is exposed. Number of WPs contained in source cell will fail equally distributed over period.	Model assumption to smooth out sudden release of activity from WP
Failure_Delay	10		Factor to distribute exposure over certain period of time to prevent too large changes within short periods and to improve simulation of natural evolution. Factor leads to fragmentation of waste cell into that number of sub-cells that will fail accordingly	Model assumption to smooth out sudden release of activity from WP
Pit_Hole_Corrosion_Rate	5 E-04	m/a	Rate of pit-hole corrosion for stainless steel of WP	dito
Pit_Hole_Size	1 E-04	m²	Final cross section of pit hole	Model assumption
Hole_Increase_Period	20	a	Time pit hole increases from 0 to final cross section	Model assumption to smooth out sudden release of activity from WP
Pit_Hole_Failure_Period	10	a	Period over which pit holes at packages within one common disposal segment occur.	Model assumption to smooth out sudden release of activity from WP

WP Parameters				
Name of Parameter	Value	Unit	Description	Source
Pit_Hole_Data	See table below		Defines occurrence of pit-hole corrosion in disposal zone segments	Model assumption for simulation of pit-hole corrosion. For Sc-1 assumed to be 0 for all source cells
Source_Cell_Parameters	See table below		Defines occurrence of container failure and emplacement sequence of WPs inside disposal zone	Failure time based on planar corrosion rate and canister wall thickness

* Conceptual design of canister described in Wunderlich et al. (2021).

Source cell parameters and pit-hole data				
Disposal zone segment number	Average depth m	Canister failure time* a	SNF Type Metallic U = 1 UO_2 = 2	No of canisters with pit hole corrosion (1-4)
1	3450	30000	1	0
2	3429	30100	1	0
3	3408	30200	1	0
4	3387	30300	1	0
5	3366	30400	1	0
6	3345	30500	1	0
7	3324	30600	1	0
8	3303	30700	1	0
9	3282	30800	1	0
10	3261	30900	1	0
11	3241	31000	1	0
12	3220	31100	1	0
13	3199	31200	1	0
14	3178	31300	2	0
15	3157	31400	2	0
16	3136	31500	2	0
17	3115	31600	2	0
18	3094	31700	2	0
19	3073	31800	2	0
20	3052	31900	2	0
21	3031	32000	2	0
22	3010	32100	2	0

* For definition of failure times for canisters in disposal zone segments a delay of 100 years has been assumed to account for generally less critical corrosion and failure conditions with decreasing depth and to smooth out the sudden release of activity from the canisters.

V.3 Borehole and geosphere parameters

Borehole Parameters				
Name of Parameter	Value	Unit	Description	Source
Disposal_Zone_Plug_Length	1	m	Thickness of plugs between successive canisters	Conceptual Design*
Borehole_Diameter	0.70	m	Initial volume of water inside WP	dito
Sealing_Zone_Length	500	m	Length of sealing zone	dito
Backfill_Zone_Length	2500	m	Length of backfill zone	dito
Sealing_Segment_Length	20	m	Length of sealing zone	Model parameter
Backfill_Segment_Length	100	m	Length of backfill zone	dito

* Fischer et al., 2020

Aquifer Parameters				
Name of Parameter	Value	Unit	Description	Source
Distance_Well_Aquifer	100	m	Distance between disposal borehole and drinking water well	Model assumption
Intersection_Aquifer	true		Switch set to true if top part of disposal borehole is intersected by aquifer	Model assumption for Sc-1
Thickness_Aquifer	5	m	Length of sealing zone	Model assumption
Width_Aquifer	10	m	Assumed width of aquifer, through which all contaminated water is transported towards well	Model assumption
Flow_Aquifer	36.5	m/a	Groundwater velocity	Model assumption 10 cm/day

Borehole Parameters				
Name of Parameter	Value	Unit	Description	Source
Disposal_Zone_Plug_Length	1	m	Thickness of plugs between successive canisters	Conceptual Design*
Borehole_Diameter	0.70	m	Initial volume of water inside WP	dito
Sealing_Zone_Length	500	m	Length of sealing zone	dito
Backfill_Zone_Length	2500	m	Length of backfill zone	dito
Sealing_Segment_Length	20	m	Length of sealing zone	Model parameter
Backfill_Segment_Length	100	m	Length of backfill zone	dito

Aquifer Parameters				
Name of Parameter	Value	Unit	Description	Source
Distance_Well_Aquifer	100	m	Distance between disposal borehole and drinking water well	Model assumption
Intersection_Aquifer	true		Switch set to true if top part of disposal borehole is intersected by aquifer	Model assumption for Sc-1
Thickness_Aquifer	5	m	Length of sealing zone	Model assumption
Width_Aquifer	10	m	Assumed width of aquifer, through which all contaminated water is transported towards well	Model assumption
Flow_Aquifer	36.5	m/a	Groundwater velocity	Model assumption 10 cm/day

Vertical Borehole Flow Parameters				
Name of Parameter	Value	Unit	Description	Source
Occurrence_Variable_Vert_Flow	false		Switch set to true if variable vertical flow through borehole is assumed to take place	Scenario selection parameter for Sc-2
Variable_Vert_Flow_Strat	50	L/a	Start value of variable vertical flow	Model assumption based on Clayton et al. (2011)
Variable_Vert_Flow_End	5 E-04	L/a	End value of variable vertical flow	Model assumption based on Clayton et al. (2011)
Variable_Vert_Flow_Start_Time	50	a	Start time for variable vertical flow	Model assumption based on Clayton et al. (2011)
Variable_Vert_Flow_End_Time	1 E+06			Model assumption based on Clayton et al. (2011)
Occurrence_Constant_Vert_Flow	false		Switch set to true if variable vertical flow through borehole is assumed to take place	Scenario selection parameter for Sc-2r
Vert_Flow_Const	1	L/a	Constant vertical flowrate	Model assumption (see Section 8.3.1)
Hydr_Cond_EDZ_DZ	1 E-09	m/s	Hydraulic conductivity of EDZ in disposal zone	Model Assumption
Hydr_Cond_BH_DZ	1 E-08	m/s	Hydraulic conductivity of borehole in disposal zone	Model Assumption
Hydr_Cond_EDZ_SZ	1 E-09	m/s	Hydraulic conductivity of EDZ in sealing zone	Model Assumption
Hydr_Cond_BH_SZ	1 E-09	m/s	Hydraulic conductivity of borehole in sealing zone	Model Assumption
Hydr_Cond_EDZ_BZ	1 E-09	m/s	Hydraulic conductivity of EDZ in backfilling zone	Model Assumption
Hydr_Cond_BH_BZ	1 E-07	m/s	Hydraulic conductivity of borehole in backfilling zone	Model Assumption

Fracture Pathway Parameters				
Name of Parameter	Value	Unit	Description	Source
Fracture_Lower_Backfill	false		Switch set to true if fracture is intersecting lower part of backfilling zone	Scenario selection parameter
FR_Lower_Backfill	1.0	L/a	Flowrate assumed to pass through lower backfill zone of borehole	Model assumption for Sc-3.1
Fracture_Middle_Sealing	false		Switch set to true if fracture is intersecting middle part of sealing zone	Scenario selection parameter
FR_ Middle_Sealing	1.0	L/a	Flowrate assumed to pass through middle sealing zone of borehole	Model assumption for Sc-3.2
Fracture_Upper_Disp_Zone	false		Switch set to true if fracture is intersecting upper part of disposal zone	Scenario selection parameter
FR_Upper_Disp	0.1	L/a	Flowrate assumed to pass through upper disposal zone of borehole	Model assumption for Sc-3.3
Fracture_Middle_Disp_Zone	false		Switch set to true if fracture is intersecting middle part of disposal zone	Scenario selection parameter
FR_Middle_Disp	0.1	L/a	Flowrate assumed to pass through middle disposal zone of borehole	Model assumption for Sc-3.4
Fracture_Lower_Disp_Zone	false		Switch set to true if fracture is intersecting lower part of disposal zone	Scenario selection parameter
FR_Lower_Disp	0.1	L/a	Flowrate assumed to pass through lower disposal zone of borehole	Model assumption for Sc-3.5
Matrix_Diff_takes_Place	true		Switch set to true if matrix diffusion is considered in model calculation of fracture transport	Scenario selection parameter
Min_Depth_Matrix_Diff	5	mm	Assumed minimum Depth of Matrix Diffusion	Model Assumption
Max_Depth_Matrix_Diff	5	mm	Assumed maximum Depth of Matrix Diffusion	Model Assumption
Aperture_Fracture	0.15	mm	Aperture of fractures assumed to intersect disposal borehole and vertical fracture system	Model assumption (see Section 8.3.2)
Fraction_Perimeter	1		Fraction of perimeter of fracture where matrix diffusion takes place	Model assumption
Length_Horiz_Frac_Part	50	m	Length of sub-horizontal fracture intersecting disposal borehole	Model assumption
Width_Horiz_Frac_Part	1.4	m	Width of sub-horizontal fracture intersecting disposal borehole	Model assumption, set equal to borehole+EDZ diameter
Width_Vert_Frac_Part	5	m	Width of sub-vertical fractures connecting horizontal fracture with aquifer	Model assumption
Number_Vert_Frac	10		Number of individual fractures forming the vertical fracture system	Model assumption (see Section 8.3.2)
Tortuosity_Vert_Frac_Part	5		Tortuosity of vertical fracture system	Model assumption (see Section 8.3.2)

V.4 Scenario Parameters

Scenario Parameters				
Name of Parameter	Value	Unit	Description	Source
Sorption	true		Switch set to true if sorption is considered for bentonite and backfill	Parameter for selecting scenarios and calculation cases
Solubility_Limits	true		Switch set to true if solubility limits are considered	Parameter for selecting scenarios and calculation cases
Instant_Failure	false		Switch set to true if instant failure of all canisters is assumed to take place	Parameter for selecting scenarios and calculation cases
Water_Consumption	3	L	Assumed consumption of water from well by person	Model assumption for drinking water biosphere scenario
Well_Production	600	L/h	Well production rate	Model assumption based on minimum production rate for typical drinking water well (see Section 8.2.2)

Data for dose rate calculations

Dose conversion factors[1)] used for calculation of annual dose for adult members of the public		
Species ID	Value	Unit
Ac227	1.21E-06	Sv/Bq
Ag108m	2.3E-09	Sv/Bq
Am241	2.00E-07	Sv/Bq
Am242m	2.94E-07	Sv/Bq
Am243	2.13E-07	Sv/Bq
C14	5.80E-10	Sv/Bq
Cl36	9.30E-10	Sv/Bq
Cm245	2.10E-07	Sv/Bq
Cm246	2.10E-07	Sv/Bq
Cs135	2.00E-09	Sv/Bq
Cs137	1.30E-08	Sv/Bq
I129	1.10E-07	Sv/Bq
Mo93	3.10E-09	Sv/Bq
Nb93m	1.20E-10	Sv/Bq
Nb94	1.70E-09	Sv/Bq
Ni59	6.30E-11	Sv/Bq
Ni63	1.50E-10	Sv/Bq
Np237	1.11E-07	Sv/Bq
Pa231	7.10E-07	Sv/Bq
Pb210	1.89E-06	Sv/Bq
Pd107	3.70E-11	Sv/Bq
Pu238	2.30E-07	Sv/Bq
Pu239	2.50E-07	Sv/Bq

Dose conversion factors[1)] used for calculation of annual dose for adult members of the public		
Species ID	Value	Unit
Pu240	2.50E-07	Sv/Bq
Pu241	4.80E-09	Sv/Bq
Pu242	2.40E-07	Sv/Bq
Ra226	2.80E-07	Sv/Bq
Ra228	6.90E-07	Sv/Bq
Se79	2.90E-09	Sv/Bq
Sm151	9.80E-11	Sv/Bq
Sn126	4.55E-08	Sv/Bq
Sr90	3.07E-08	Sv/Bq
Tc99	6.40E-10	Sv/Bq
Th228	1.43E-07	Sv/Bq
Th229	6.13E-07	
Th230	2.10E-07	
Th232	2.30E-07	
U233	5.10E-08	
U234	4.90E-08	
U235	4.73E-08	
U236	4.70E-08	
U238	4.84E-08	
Zr93	1.10E-09	

1) Values colour-coded in light yellow include effects of short-lived daughters (half-life < 1 yr) not explicitly listed, assuming secular equilibrium at time of intake.

2) Data from ICRP (1998) for adults.

References in Appendix V

Ahonen, L., Korkeakoski, P., Tiljander, M., Kivikoski, H., Laaksonen, R. 2008. Quality assurance of the bentonite material. Posiva Working Report 2008-33. Eurajoki, Finland: Posiva Oy. Link: https://cris.vtt.fi/en/publications/quality-assurance-of-the-bentonite-material

Clayton, D., G. Freeze, T. Hadgu, E. Hardin, J. Lee, J. Prouty, R. Rogers, W. M. Nutt, J. Birkholzer, H. H. Liu, L. Zheng & Chu, S. 2011. Generic Disposal System Modeling - Fiscal Year 2011 Progress Report. SAND 2011-5828P; FCRD-USED-2011-000184. Sandia National Laboratories, Albuquerque, NM.

Engelhardt, H., & Fischer, T. 2021. COO9 Borehole sealing concept. Task CoO9 for Norwegian Nuclear Decommissioning by BGE TECHNOLOGY GmbH and AINS Group,.

Fischer, T., Engelhardt, H.-J. & T. Wanne, T. 2020. Deep Borehole Disposal Concept. Technical Report Task CoO3 for Norwegian Nuclear Decommissioning by BGE TECHNOLOGY GmbH and AINS Group, 2020.

Freeze, G., M. Voegele, P. Vaughn, J. Prouty, W.M. Nutt, E. Hardin, & S.D. Sevougian: " Generic Deep Geologic Disposal Safety Case - Fuel Cycle Research & Development". Report for US Department of Energy, FCRD-UFD-2012-000146, SAND2013-0974P, Revision 1, August, 2013

ICRP (International Commission on Radiological Protection). 1998. ICRP Database of Dose Coefficients: Workers and Members of the Public, CDROM, Ver.1. Elsevier Science Ltd. 1998. Data taken from “Beilage 160 a und b zum Bundesanzeiger vom 28. August 2001.

Schwartz, F.W. & Zhang, H. 2003. Fundamentals of Groundwater. John Wiley & Sons, New York.

SKB 2010. Data report for the safety assessment SR-Site. Stockholm, Sweden: Svensk Kärnbränslehantering AB. Technical report TR-2010-52.

Wunderlich, A., D. Seidel, P. Herold and T. Wanne: "Deep Borehole Disposal Canister". Technical Report Task CoO10 for Norwegian Nuclear Decommissioning by BGE TECHNOLOGY GmbH and AINS GROUP, 2021.

Appendix VI – Input data LILW disposal GoldSim model

List of Input Data for lLLW

General				
Name of Parameter	Value	Unit	Description	Source
Depth_Repository	100	m	Depth of disposal chambers	Ikonen et al. 2020
DFC_ingestion_vector	s. table below	Sv/Bq	Vector with dose conversion factors for RN	ICRP database of dose coefficients
Flowswitch_ILW_LLW	1		Switch to separate flow through ILW and LLW; if set to 1: no separation; if set to 0: separation	-
Flowswitch_ILWLLW_to_infrastr	0		Defines whether flow through ILW backfill and LLW chamber goes through infrastructure before entering host rock and well; set 0 or 1; 0 means no flow	-
Flowswitch_Well_near_Shaft	0		Switch for scenario that drinking water well near to upper shaft area would draw inflow into infrastructure. If set to 1, all inflow to shaft, if 0 normal horizontal flow out of Infrastructural area. area.	-
Infrastructure_area_in_flow	1,000	m²	Area of infrastructure perpendicular to flow	Estimation based on Ikonen et al. 2020
Infrastructure_volume	14,000	m³	Volume of underground openings except vaults	Estimation based on Ikonen et al. 2020
Large_Value	1e30		In some cases, values defined in GoldSim have to be positive or be very large etc. In that cases very small or large values are selected to fulfil requirement but without causing any impact on the results.	-
Length_Shaft	7	m	Length of personnel shaft from concept description	Ikonen et al. 2020
Pathway_distance_to_well	100	m	Distance of travel from vault to well	Conservative assumption
Small_Value	1e-20		In some cases, values defined in GoldSim must be positive or be very large etc. In that cases very small or large values are selected to fulfil requirement but without causing any impact on the results.	-
Switch_ILW_sorption_on_off	1		Switch for sorption to waste. Assuming that part of waste will be concrete, a certain percentage of concrete_kd could be applied. 0 is off, 1 is on.	-

General				
Name of Parameter	Value	Unit	Description	Source
Switch_LLW_sorption_on_off	1		Switch for sorption to waste. Assuming that part of waste will be concrete, a certain percentage of concrete_kd could be applied. 0 is off, 1 is on.	-
Switch_Matrix_Diff_Conn_Frac	true		To b set to true if diffusion takes place in connecting fracture	-
Switch_special_waste	0		Switches on and off, whether special waste taken into account in ILW inventory	-
Width_Shaft	5.2	m	width of personnel shaft from concept description	Ikonen et al. 2020
Zero_kd	0	m³/kg	Zero vector for kd values	-

Inventory				
Name of Parameter	Value	Unit	Description	Source
ILW_inventory_activity_vector	s. table below	Bq	Activity per RN according to H. Norsman based on data from SFR, Oscarshamn and Himdalen	based on data from SFR, Oscarshamn and Himdalen
ILW_Inventory_factor	1		Factor to increase or decrease total ILW inventory activity	-
LLW_activity_SFR_vector	s. table below	Bq	Activity per RN according to H. Norsman based on data from SFR, Oscarshamn and Himdalen	based on data from SFR, Oscarshamn and Himdalen
LLW_inventory_factor	1		Factor to modify LLW inventory activities	-

Chamber and plug Parameters				
Name of Parameter	Value	Unit	Description	Source
Concrete_plug_thickness	10	m	Thickness/Length of the concrete plug in the access to the ILW and LLW vault	Assumption
ILW_chamber_height	17.4	m	Inner height of chamber	Ikonen et al. 2020
ILW_chamber_width	17.7	m	Inner width of chamber	-"-
ILW_chamber_length	63.0	m	Inner length of chamber	-"-
ILW_Concrete_plug_area	30	m²	cross-sectional area of the concrete plug/former access drift to vault	Assumption
LLW_chamber_height	5.5	m	Height of an LLW chamber	Ikonen et al. 2020
LLW_chamber_length	105	m	Length of individual LLW chamber for waste	Ikonen et al. 2020
LLW_chamber_width	6	m	width of an individual LLW chamber	Ikonen et al. 2020
LLW_chambers_nr	8		Number of LLW chambers	Ikonen et al. 2020
Plug_End_Degradation	10,000	a	End of plug concrete degradation	Reference evolution assumption

Chamber and plug Parameters				
Name of Parameter	Value	Unit	Description	Source
Plug_final_hydr_Cond	1e-7	m/s	Plug final hydraulic conductivity	Reference evolution assumption
Plug_initial_hydr_Cond	1e-10	m/s	initial hydraulic conductivity	Reference evolution assumption
Plug_Start_Degradation	1	a	Start of plug concrete degradation	Reference evolution assumption

ILW Concrete Vault Parameters				
Name of Parameter	Value	Unit	Description	Source
Vault_wall_thickness	1	m	Thickness of the concrete vault around the WP stack	Estimation based on Ikonen et al. 2020.
Concrete_vault_conductivity	1e-07	m/s	Hydraulic conductivity of concrete vault	Reference assumption for vault concrete
WP_horiz_gap	0.05	m	horizontal gap between stacked WPs	Ikonen et al. 2020
WP_no_across_vault	6	WP	Width of the WP stack	Ikonen et al. 2020
WP_no_stacked_vert	10	WP	Number of WPs stacked above each other/height of the WP stack in WP	Ikonen et al. 2020

WP and waste Parameters				
Name of Parameter	Value	Unit	Description	Source
Concrete_contam_ILW	0		share of ILW material that is basically contaminated concrete - not concrete from conditioning.	Conservative assumption
Concrete_contam_LLW	0		share of LLW material that is basically contaminated concrete - not concrete from conditioning.	Conservative assumption
Drum_diameter	0.565	m	diameter of waste drum	Ikonen et al. 2020
Drum_height	0.875	m	Height of the waste drum	Ikonen et al. 2020
Drum_steel_thickness	0.1	cm	Thickness of steel of the drum walls, bottom and lid	Ikonen et al. 2020
Drums_per_WP	6	drum	Number of drums in one ILW WP	Ikonen et al. 2020
ILW_WP_failed_at_closure	10	%	Percentage of ILW WP assumed to have failed directly after closure	Conservative Assumption
ILW_WP_failure_period	100	years	Period, over which those ILW WPs fail that have not failed directly at closure.	Conservative Assumption
ILW_Concr_Frac_def	0.75		Percentage of concrete in ILW waste including the concrete WPs	Estimation based on Ikonen et al. 2020.

WP and waste Parameters				
Name of Parameter	Value	Unit	Description	Source
ILW_Concr_to_be_defined	false		To be selected, if concrete share of ILW not to be calculated but to be defined. In reference case, share ca. 73% combined from concrete Box, concrete backfill of voids inside box, concrete share of waste inside ILW drums and backfill.	-
ILW_Drum_Concr_Frac	0.3		Percentage of backfill concrete in ILW waste within the waste drums	Assumption
ILW_drybulkdensity	1,000	kg/m³	Density of pure ILW material within drums	Estimation based on waste type
ILW_Porosity	0.5		Porosity of ILW material	Estimation based on waste type
ILW_Saturation	1		Water saturation of ILW material	Conservative assumption
ILW_Tortuosity	1		Tortuosity for ILW, conservatively set to 1	Conservative assumption
ILW_WP_No	663	WP	The total number of WP with ILW	Inventory data provided by NND
LLW_Drum_Concr_Frac	0.3		Percentage of backfill concrete in LLW waste within the waste drums	Assumption
LLW_drum_total_No	51,000		Number of steel drums with LLW	Ikonen et al. 2020
LLW_drybulkdensity	1,000	kg/m³	Density of pure waste material within drums	Estimation based on waste type
LLW_Porosity	0.5		Porosity of LLW material	Estimation based on waste type
LLW_Saturation	1		Water saturation of LLW material	Conservative assumption
LLW_Tortuosity	1		Tortuosity for LLW material, conservatively set to 1	Conservative assumption
LLW_WP_failed_at_closure	30	%	percentage of WPs that fail to provide containment directly after closure	Conservative assumption
LLW_WP_failure_period	50	a	Duration until all WPs have lost containment	Conservative assumption
WP_height	1.1	m	Outside height of a concrete box	Ikonen et al. 2020
WP_inner_height	0.88	m	Height on the inside of the concrete box	Ikonen et al. 2020
WP_width	1.55	m	Outside width of an individual concrete box	Ikonen et al. 2020
WP_inner_width	1.35	m	Width of the concrete box on the inside	Ikonen et al. 2020
WP_length	2.2	m	Outside length of an individual concrete box	Ikonen et al. 2020
WP_inner_length	2.0	m	Length of concrete box on the inside	Ikonen et al. 2020

ILW Special Waste parameters				
Name of Parameter	Value	Unit	Description	Source
AW_WP1_activity_vector	s. Appendix A	MBq	s. Appendix A	NND
AW_WP2_activity_vector				
AW_WP3_activity_vector				
AW_WP4_activity_vector				
AW_WP5_activity_vector				
AW_WP6_activity_vector				
AW_WP7_activity_vector				
AW_WP8_activity_vector				
Breathing_rate	1.2	m³/hr	Breathing rate of individual at surface	IAEA TecDoc1380
DCF_inhalation	s. table below	Sv/Bq	Vector with dose conversion factors for exposure by inhalation	ICRP database of dose coefficients
DCF_irradiation	s. table below	(Sv-m3)/(s-Bq)	Vector with dose conversion factors for exposure by irradiation	ICRP database of dose coefficients
Dilution_waste	0.33		Dilution of waste with drilllings	Conservative assumption
Drilling_time	15	hr/a	Drilling time during penetration of WP and transport of waste material to surface	Assumption
Drilling_time_of_presence	24	hr/a	Drilling time during penetration of WP and transport of waste material to surface	Assumption
Dust	1e-6	kg/m3	Concentration of dust in air	IAEA TecDoc1380
Mass_WP1	850	kg	Mass of WP1	NND
Mass_WP7	185	kg	Mass of WP 7	NND
Mass_WP_guess	300	kg	Assumed mass of other WPs for special waste for which a mass was not available	Conservative assumption
Soil_ingestion	3.4E-05	kg/hr		IAEA TecDoc1380
Special_waste_activity_vector	s. Appendix A	Bq	Activity vector with all radioactive nuclides present in special waste	NND
WPs_special_waste	13		Number of WP containing special waste	NND

Backfill parameters in ILW, LLW chambers and infrastructure				
Name of Parameter	Value	Unit	Description	Source
Backfill_conductivity	2e-2	m/s	conductivity of crushed rock backfill	Estimation based on Toumpanou et al. (2021)

Backfill parameters in ILW, LLW chambers and infrastructure				
Name of Parameter	Value	Unit	Description	Source
Backfill_Diff_Length_Plug	5	m	Diffusive length for backfill in front of entrance (plug). Assumption that there will be some 10 m distance between plug and concrete vault.	Assumption
Backfill_diffusive_length	0.5	m	Estimated diffusive length in backfill around concrete vault. For three sides ca. 1 m distance, roof 4.4 m and towards entrance 40 m. Conservatively set to 0.5 m.	Assumption
Backfill_Saturation	1		Water saturation of backfill; conservatively set to 100%	Conservative assumption
Backfill_Turtuosity	1		Tortuosity for water through backfill, conservatively set to 1	Conservative assumption
Infrastructure_diff_length	5	m	Diffusive length of infrastructure area	Assumption

Concrete parameters				
Name of Parameter	Value	Unit	Description	Source
Concrete_kd	s. table below	m³/kg	Kd values for concrete	s. table below
Concrete_Kd_factor	1		Factor to adjust Kd values for sensitivity analyses	-
Concrete_kd_switch	1		Switch to switch concrete sorption on (1) or off (0)	-
Concrete_Saturation	1		Water saturation of concrete (and Waste/Concrete) conservatively set to 1	Conservative assumption
Concrete_Turtuosity	1		Tortuosity for water through concrete, conservatively set to 1	Conservative assumption

Water parameters				
Name of Parameter	Value	Unit	Description	Source
Water_RefDiffusivity	1e-6	m²/s	Reference diffusivity in water	Estimated general value usually chosen in similar calculations, actual values generally in the order of magnitude from 1 E-8 m²/s to 1 E-10 m²/s
Water_Solubility_Radionuclides	-1	g/l	Solubility of radionuclide species in water; conservatively set to infinite	Conservative assumption

Hydraulic parameters for geosphere				
Name of Parameter	Value	Unit	Description	Source
Aperture_Connect_Frac	0.15	mm	Assumed aperture for the connecting fracture	Assumption
Aquifer_Density_intrinsic	2,800	kg/m³	Expected intrinsic density of upper aquifer rocks (assumed to be fractured crystalline)	Assumption
Aquifer_Density_SD	100	kg/m³	SD for expected bulk density of upper aquifer	Assumption
Aquifer_Porosity_SD	0.01		SD for expected porosity of upper aquifer inside upper borehole zone	Assumption
Aquifer_Saturation	1		Saturation of backfill in upper aquifer	Conservative assumption
Aquifer_Tortuosity	1		Tortuosity of upper aquifer	Conservative assumption
Aquifer_Porosity_mean	10	%	expected porosity of assumed aquifer near surface	Assumption
Avg_hydr_conductivity	1e-08	m/s	Target property IDR-3a: avg hydraulic conductivity < 10^-8 m/s	Hagros et al. 2021
Depth_Aquifer	20	m	Assumed depth of aquifer crossing uppermost cell of shaft backfilling zone.	Assumption
Dist_Waste_Level_Aquifer	80	m	Distance between waste level and near surface aquifer.	Assumption
Fraction_Perimeter	1		assumed fraction of perimeter of fracture where matrix diffusion takes place	Assumption
Fracture_transmissivity	1e-7	m²/s	Target property IDR-3b: highest transmissivity of a fracture intersecting the waste halls should be less than 10^-7 m²/s	Hagros et al. 2021
Host_rock_Saturation	1		Water saturation of host rock conservatively set to 100%	Conservative assumption
Host_rock_Turtuosity	10		Tortuosity for water through host rock set to 10, educated guess	Assumption
Hydraulic_gradient	0.01		Target property IDR-3a and IDR-3b: hydraulic gradient of 0.01 or less	Hagros et al. 2021
Max_Depth_Matrix_Diff	50	mm	assumed maximum depth of Matrix Diffusion	Assumption
Min_Depth_Matrix_Diff	50	mm	assumed minimum Depth of Matrix Diffusion	Assumption
Nr_of_fractures	100		arbitrary value that influences surface area in fractures for matrix diffusion etc.	Assumption
Number_connect_Frac	40		Number of vertical fractures assumed to connect horizontal fractures in downstream from waste chambers with aquifer near surface.	Assumption

Hydraulic parameters for geosphere				
Name of Parameter	Value	Unit	Description	Source
Number_frac_from_Infra	20		number of fractures between infrastructure area and vertical connecting fractures.	Assumption
Thickness_Upper_Aquifer	5	m	Assumed Thickness of aquifer near surface around repository site.	Assumption
Tortuosity_connect_frac	5		Assumed tortuosity of vertical fracture connecting groundwater flow with near surface aquifer	Assumption
Travel_Distance_Aquifer	50	m	Distance of intersection of vertical fracture with aquifer from intersection of aquifer and drinking water well.	Assumption
Width_Connect_Frac	100	m	Assumed width of the connecting fracture	Assumption

Biosphere parameters				
Name of Parameter	Value	Unit	Description	Source
median_well_yield	600	l/hr	Median yield of a well in Scandinavia	Banks et al., 2010
Water_daily_consumption	3	l/d	daily consumption of drinking water from well	Assumption

The following Table VI-1 lists all nuclides modelled with their respective activities in ILW and LLW as well as all used dose conversion factors and Kd values. When multiple Kd values were available, the more pessimistic option was selected.

Table VI-1: Data used in the model, radionuclides, Kd values for concrete and relevant dose conversion factors. (Kd values are from 1: NAGRA, 2: IAEA (2004) and 3: Krupka & Serne (1998); DCF values were from ICRP database (ICRP 2013).

Species ID	Half-life (years)	Daughter 1	Stoichiometry1	Daughter 2	Stoichiometry2	Description	Kd concrete degraded	Origin of Kd value	DCF Ingestion	DCF Inhalation	DCF Irradiation
Ac227	21.772					Actinium 227	2.0E-01	2	1.21E-06		
Ag108m	418					Silver 108	1.0E-03	1	3.70E-08		
Am241	432.2	Np237	1			Americium 241	2.0E-01	2	2.00E-07	1.60E-05	2.34E-19
Am243	7370	Pu239	1			Americium 243	2.0E-01	2	2.13E-07		
Ba133	10.52					Barium 133	0.0E+00	1	1.50E-09	1.00E-08	1.06E-17
C14	5700					Carbon 14	1.0E-02	3	5.80E-10		
Ca41	1.02e+05					Calcium 41	2.0E-03	1	1.90E-10		
Cl36	3.01e+05					Chlorine 36	0.0E+00	1	7.30E-09		
Cm243	29.1	Pu239	0.9976	Am243	0.0024	Curium 243	2.0E-01	2	1.50E-07		
Cm244	18.1	Pu240	1			Curium 244	2.0E-01	2	5.70E-05	1.30E-05	6.74E-22
Co60	5.2713					Cobalt 60	1.0E-02	2	3.10E-08	3.10E-08	8.68E-17
Cs137	30.167					Caesium 137	2.0E-02	2	1.30E-08	3.90E-08	1.93E-17
Eu152	13.537					Europium 152	5.0E-01	3	1.40E-09		
Eu154	8.593					Europium 154	5.0E-01	3	2.00E-09		
Eu155	4.7611					Europium 155	5.0E-01	3	3.20E-10		
H3	12.32					Hydrogen 3	1.0E-04	1	1.80E-11		
Ho166m	1200					Holmium 166	0.0E+00	1	1.40E-09		
I129	1.57e+07					Iodine 129	1.0E-03	2	1.1E-07		
Mo93	4000	Nb93m	0.88			Molybdenum 93	4.0E-04	1	3.1E-09		

Species ID	Half-life (years)	Daughter 1	Stoichiometry1	Daughter 2	Stoichiometry2	Description	Kd concrete degraded	Origin of Kd value	DCF Ingestion	DCF Inhalation	DCF Irradiation
Nb93m	16.13					Niobium 93	1.0E-01	2	1.2E-10		
Nb94	20300					Niobium 94	1.0E-01	2	1.70E-09		
Ni59	1.01e+05					Nickel 59	1.0E-02	2	6.30E-11		
Ni63	100.1					Nickel 63	1.0E-02	2	1.50E-10		
Np237	2.144e+06	U233	1			Neptunium 237	1.0E-01	2	1.11E-07		
Pa231	32760	Ac227	1			Protactinium 231	1.0E-01	2	7.10E-07		
Pb210	22.2					Lead 210	5.0E-02	2	1.89E-06		
Pu238	87.7	U234	1			Plutonium 238	1.0E+00	2	2.30E-07		
Pu239	24110	U235	1			Plutonium 239	1.0E+00	2	2.50E-07	1.60E-05	1.58E-21
Pu240	6564	U236	1			Plutonium 240	1.0E+00	2	2.50E-07		
Pu241	14.35	Am241	0.99998	Np237	2.45E-05	Plutonium 241	1.0E+00	2	2.30E-06		
Pu242	3.75e+05	U238	1			Plutonium 242	1.0E+00	2	2.40E-07		
Ra226	1600	Pb210	0.9998			Radium 226	5.0E-02	2	2.80E-07	9.50E-06	5.99E-17
Ra228	5.75	Th228	1			Radium 228	5.0E-02	2	6.90E-07		
Sm151	90					Samarium 151	1.0E-03	1	9.80E-11		
Sr90	28.79					Strontium 90	1.0E-03	2	3.07E-08		
Tc99	2.111e+05					Technetium 99	4.0E-04	1	6.40E-10		
Th228	1.9116					Thorium 228	1.0E+00	2	1.43E-07	4.00E-05	1.04E-17
Th229	7340					Thorium 229	1.0E+00	2	6.13E-07		
Th230	75380	Ra226	1			Thorium 230	1.0E+00	2	2.10E-07		

Species ID	Half-life (years)	Daughter 1	Stoichiometry1	Daughter 2	Stoichiometry2	Description	Kd concrete degraded	Origin of Kd value	DCF Ingestion	DCF Inhalation	DCF Irradiation
Th232	1.405e+10	Ra228	1			Thorium 232	1.0E+00	2	2.30E-07	2.50E-05	2.79E-21
U233	1.592e+05	Th229	1			Uranium 233	1.0E-01	2	5.10E-08		
U234	2.455e+05	Th230	1			Uranium 234	1.0E-01	2	4.90E-08	9.40E-06	2.15E-21
U235	7.04e+08	Pa231	1			Uranium 235	1.0E-01	2	4.73E-08		
U236	2.342e+07	Th232	1			Uranium 236	1.0E-01	2	4.70E-08		
U238	4.468e+09	U234	1			Uranium 238	1.0E-01	2	4.84E-08	8.00E-06	6.10E-19
Zr93	1.53e+06	Nb93m	0.975			Zirconium 93	2.0E-03	1	1.10E-09		

References in Appendix V

Banks, D., Gundersen, P., Gustafson, G., Mäkelä, J. and Morland, G. 2010. Regional similarities in the distributions of well yield from crystalline rocks in Fennoscandia. *Norges geologiske undersøkelse Bulletin,* 450, 33–47.

Hagros, A., Engelhardt, H-J., Fischer, T., Gharbieh H., Hautojärvi A., Hellä, P., Häkkinen, I., Ikonen A., Karvonen T., Keto, P., Rinta-Hiiro, V., Schatz, T., Wanne, T., Ärväs-Tuovinen, T. 2021. Host Rock Target Properties for Norwegian National Facility. AINS Group Technical Report. June 2021.

IAEA 2004. Safety Assessment Methodologies for Near Surface Disposal Facilities (ISAM) - Results of a co-ordinated research project - Vol.1: Review and Enhancement of Safety Assessment Approaches and Tools". IAEA, Vienna, 2004.

Ikonen, A., Engelhardt, J., Fischer, T., Gardemeister, A. Karvonen, S., Keto, P., Rasilainen, K., Saanio, T. & Wanne, T., 2020. Concept description for Norwegian national disposal facility for radioactive waste. AINS Group, Technical Report. Link: https://www.norskdekommisjonering.no/wpcontent/uploads/2020/10/Technical-report-Concept-Description-for-Norwegian-National-DisposalFacility-for-Radioactive-Waste.pdf

Krupka, K. M. & Serne. R. J. Effects on Radionuclide Concentrations by Cement/Ground-Water Interactions to Support Performance Assessment of Low-Level Radioactive Waste Disposal Facilities. NUREG/CR-6377, Pacific Northwest National Laboratory, Richland, Washington, 1998.

NAGRA: Mckinley, I. G. & Scholtis, A. 1993. Compilation and comparison of radionuclide sorption databases used in recent performance assessments. Nagra, Nationale Genossenschaft furdie Lagerung radioaktiver Abfalle. Hardstrasse 73, CH 5430 Wettingen,. Switzerland.

Toumpanou, I.C., Pantazopoulos, I.A., Markou, I.N. et al. 2021. Predicted and measured hydraulic conductivity of sand-sized crushed limestone. Bull. Eng. Geol. Environ., 80, 1875–1890. Link: https://doi.org/10.1007/s10064-020-02032-1

Mitta Engineering Oy

Riihimiehentie 3

FI-01720 Vantaa

www.mitta.fi